eman ta zabal zazu

Universidad del País Vasco

Euskal Herriko Unibertsitatea

SMOOTH MUSCLE CELL CHARACTERIZATION AND TRANSCRIPTOMIC ANALYSIS IN HUMAN CAROTID ATHEROSCLEROTIC PLAQUES

HAIZE GOICURIA

2018

UNIVERSIDAD DEL PAÍS VASCO (UPV / EHU)

Departamento de Neurociencias

SMOOTH MUSCLE CELL CHARACTERIZATION AND TRANSCRIPTOMIC ANALYSIS IN HUMAN CAROTID ATHEROSCLEROTIC PLAQUES

TESIS DOCTORAL

Haize Goicuria

Directores:

Dra. Iraide Alloza y Dr. Koen Vandenbroeck

Leioa, 2018

AKNOWLEDGEMENTS

I would like to thank all those people who have participated so much and who have made this thesis possible.

First, thanks to the directors of this thesis Koen Vandenbreock and Iraide Alloza, for their direction, support and enthusiasm during these years of thesis in the laboratory of Neurogenomiks.

Also thanks to the University of the Basque Country (UPV / EHU) as well as ACHUCARRO center which have facilitated the development of this thesis.

I would also like to thank all the members of the laboratory for their support during all these years. In one way, to the colleagues of the past as Aitzkoa, Pepe and Ianire and, in another way, to those of the present as Nerea, Jorge, Cristina and Andoni, and especially to Paloma, my laboratory partner, for her unconditional help and because the fun moments with her helped me to get here.

I am immensely grateful to my parents and relatives for their support and especially to my mother for her motivation, empathy and patience during these years, her understanding has been very important to me. I would like also give thanks to my friends Bea and Ana for their understanding during my PhD and to Alberto, for be my breath and bring me a piece of happiness to my life every day.

And finally I wish to thank patients of this study for their sample donation without whom this study would be impossible.

TABLE OF CONTENTS

LIST OF PUBLICATIONS

Goikuria H., Freijo Guerrero M. del M., Vega R., Sastre M., Elizagary E., Lorenzo A., Vandenbroeck K., Alloza I., Characterization of Carotid Smooth Muscle Cells during Phenotypic Transition, Cells, 7 (2018) 23. doi: 10.3390/cells7030023.

Goikuria H., Vandenbroeck K., Alloza I., Inflammation in human carotid atheroma plaques, Cytokine Growth Factor Rev. 39 (2018) 62-70. doi: 10.1016/j.cytogfr.2018.01.006

Alloza Moral I., **Goikuria H**., Idro J.L., Triviño J.C., Férnandez Velasco J.M., Elizagaray E., García Barcina M., Montoya G., Sarasola E., Vega R., Freijo Guerrero M. del M., Vandenbroeck K., RNAseq based transcriptomics study of SMCs from carotid atherosclerotic plaque: BMP2 and IDs proteins are crucial regulators of plaque stability, Sci. Rep. 7 (2017) 3470. doi: 10.1038/s41598-017-03687-9.

Alloza Moral I., **Goikuria H**., Freijo Guerrero M. del M., Vandenbroeck K., A role for autophagy in carotid atherosclerosis, European stroke journal 1 (2016) 255 - 263. doi: 10.1177/2396987316674085.

Swaminathan B., **Goikuria H**., Rodríguez-Antigüedad A., López Medina A., Freijo Guerrero M. del M., Vandenbroeck K., Alloza I, Autophagic marker MAP1LC3B expression levels are associated with carotid atherosclerosis symptomatology, Plos One (2014) 12 - 9. doi: 10.1371/journal.pone.0115176.

ABBREVIATIONS

SMC	smooth muscle cells
EC	endothelial cells
CV	cardiovascular disease
ROS	reactive oxygen species
ECM	extracellular matrix
ICAM-1	intracellular adhesion molecule 1
VCAM-1	vascular cell adhesion molecule 1
MCP-1	monocyte chemoattractant protein 1
CCL2	C-C motif chemokine ligand 2
LDL	low density lipoprotein
oxLDL	oxidized low density lipoprotein
IFN-γ	interferon-gamma
TNF-α	tumor necrosis factor-alpha
HDL	high density lipoprotein
PDGF	platelet-derived growth factor
EGF	endothelial growth factor
NFκβ	nuclear factor kappa beta
IL	interleukin
G-CSF	granulocyte colony-stimulating factor
M-CSF	macrophage colony-stimulating factor
GM-CSF	granulocyte-macrophage colony-stimulating factor
VEGF	vascular endothelial growth factor
VLDL	very low density lipoprotein
DC	dendritic cell
TIA	transient ischemic attack
eNOS	endothelial nitric oxide synthase
IMT	intima-media thickness

CRP	C-reactive protein
MIP-1b	macrophage inflammatory protein 1 beta
CX3CL1	C-X3-C motif chemokine ligand 1
MMP	matrix metalloproteinase
APC	antigen-presenting cells
MHC-II	major histocompatibility complex II
suPAR	soluble urokinase-type plasminogen activator receptor
TIMP	tissue inhibitor of metalloproteinase
ADAM	a disintegrin and metalloproteinase
PKC	protein kinase C
PAPP-A	pregnancy-associated plasma protein A
OPN	osteopontin
OPG	osteoprotegerin
ABCA1	ATP-binding cassette subfamily A receptor 1
miRNA	microRNA
KLF4	Kruppel-like factor 4
SRF	serum response factor
RANKL	receptor activator nuclear factor-kappa beta ligand
α-SMA	alpha smooth muscle actin
ACTA2	actin, alpha 2, smooth muscle, aorta
MYH11	myosin heavy chain 11
TAGLN	transgelin
CALD1	caldesmon
ERK	extracellular signal regulated kinase
CNN	calponin
MYH10	myosin heavy chain 10 (smemb)
PLQ	plaque
MIT	macroscopically intact tissue
ASYMPT	asymptomatic

SYMPT	symptomatic
IGF	insulin like growth factor
FGFb	fibroblast growth factor beta
BSA	bovine serum albumin
HIASMC	human iliac arterial smooth muscle cells
ECGS	endothelial cell growth supplement
FBS	fetal bovine serum
PBS	phosphate-buffered saline
PECAM-1	platelet and endothelial cell adhesion molecule 1
RIN	RNA integrity
SPP1	secreted phosphoprotein 1
MAP1LC3B	microtubule-associated protein 1 ligth chain 3 beta
MKL2	MKL1/Myocardin like-2 falta
LGALS3	galectin 3
CXCL9	C-X-C motif chemokine ligand 9
CD5L	CD5 molecule like
BMP2	bone morphogenetic protein 2
GAPDH	glyceraldehydes-3-phosphate dehydrogenase
RPL41	ribosomal protein L41
ACTB	beta actin
MMSE	minimental state examination test
FDR	false discovery rate
P_{adj}	*P* adjusted value
G3BP2	G3BP stress granule assembly factor 2
MKLN1	muskelin 1
EML3	echinoderm microtubule associated protein like 3
ADCK5	Aarf domain containing kinase 5
HBSS	Hank’s balanced salt solution
LPS	lipopolysaacharide

FC	fold change
7-KC	7-ketocholesterol
SBS	sequencing by synthesis
PCA	principal component analysis
DEG	differentially expressed genes
DEI	differentially expressed isoforms
GO	gene ontology
KEGG	Kyoto encyclopedia of genes and genomes
DO	disease ontology
OMIM	online mendelian inheritance in man
TGF-β	transforming growth factor beta
ALK1	activin receptor-like kinase 1
GeneMANIA	gene multiple associations network integration algorithm
MCODE	molecular complex detection
SMAD9	smad family member 9
ID1	inhibitor of DNA binding 1
ID4	inhibitor of DNA bindig 4
CHODL	chondrolectin
TNFRSF11B	TNF receptor superfamily 11b
TNFAIP8L3	TNF- alpha-induced protein 8-like 3
SOCS3	suppressor of cytokine signaling 3
KCNE4	potassium voltage-gated channel subfamily E regulatory subunit 4
HAPLN1	hyaluronan and proteoglycan link protein 1
TBX18	T-box 18
LILR	leukocyte immunoglobulin-like receptor
IL6ST	interleukin 6 signal transducer
JAK	Janus kinase
STAT	signal transducers and activator of transcription
OSM	oncostatin M

IL6R	interleukin 6 recpetor
TWEAK	TNF-like weak inducer of apoptosis
TRAIL	TNF-related apoptosis-inducing ligand
TNFSF10	TNF superfamily member 10
TNFRSF10D	TNF receptor superfamily member 10d
TNFRSF10B	TNF receptor superfamily member 10b
DR5	death receptor 5
DCR2	decoy receptor 2
SDF-1	stromal cell-derived factor 1
IL1RAP	interleukin 1 receptor accessory protein
IL1RL1	interleukin 1 receptor like 1
IFNAR1/2	interferon alpha receptor 1 and 2
IFNGR1/2	interferon gamma receptor 1 and 2
IL17RD	interleukin 17 receptor D
IL20RB	interleukin 20 receptor beta subunit
CCL5	C-C motif chemokine ligand 5
IL11	interleukin 11
LIFR	leukemia inhibitory factor receptor
OSMR	oncostatin M receptor
IGF1R	insulin-like growth factor 1 receptor
LEPR	leptin receptor
GHR	growth hormone receptor
EPOR	eritropoyetin receptor
IL-12Rβ2	IL-12 receptor beta 2
TNFRSF1A	TNF receptor superfamily 1A
CCR	C-C motif chemokine receptor
TIPE	TNF-alpha induce protein 8-like
GDF	growth differentiation factor
GDF5	growth and differentiation factor 5

CA12	carbonic anhydrase 12
PTHLH	parathyroid hormone-like hormone
NPPC	natriuretic peptide C
Th	lymphocyte T helper cell
NFKBIZ	NFKB inhibitor zeta
TNFRSF12A	TNF receptor superfamily 12A
EGFR	epidermal growth factor receptor
TLR	Toll-like receptor
IL20RA	interleukin 20 receptor subunit alpha
IL22RA1	interleukin 22 receptor subunit alpha 1
HHT-1	hemorrhagic telangiectasia type 1
PAH	Loeys-Dietz syndrome

1. INTRODUCTION

1.1. ATHEROSCLEROSIS DISEASE

Atherosclerosis is a slow and progressive disease that belongs to arteriosclerosis diseases which consist of hardening of large and medium-size arteries [1]. Atherosclerosis is a degenerative disease that may start in childhood and is characterized by thickening of the inner lining of the arterial wall, caused by deposits of fatty material in the subendothelial space (intima) at regions of disturbed blood flow. It is usually triggered by an interplay between endothelial dysfunction and subendothelial lipoprotein retention [2], that eventually forms an atheromatous plaque composed of infiltrating inflammatory cells (e.g. monocytes/macrophages, T cells and dendritic cells), smooth muscle cells (SMCs), endothelial cells (ECs) and lipids [3]. This plaque gradually narrows the arteries and reduces the blood flow to the tissues, resulting in pain or limited function of the arteries. As well, rupture of the plaque can suddenly occur and produce distal thrombus propagation, and hence, vessel occlusion causing an ischemic event [4].

Atherosclerosis can affect arteries anywhere in the body, however, it often develops in blood vessels supplying heart, brain, pelvis, legs, arms and kidneys [1]. Thus, atherosclerotic vascular disease can be the underlying cause of myocardial infarction (coronary heart disease), stroke (carotid artery disease), peripheral artery disease (legs and arms) and chronic kidney disease [1,3], which together are responsible for approximately half of the deaths in developed nations [4].

1.1.1. Epidemiology

Cardiovascular diseases (CV) are one of the most important causes of disability and premature death worldwide. One of the underlying causes of CVs is atherosclerosis, which is considered as chronic progressive disease that clinically appears at middle age [5] as ischemic heart disease, cerebrovascular disease or peripheral arterial disease [6]. Cerebrovascular disease remains a leading cause of death from the 1990s. In 2016, the World Health Organization estimated that cerebrovascular disease (i.e. stroke) accounted for 6.7 million deaths worldwide [7]. There are two types of stroke, hemorrhagic ones which account for about 13% of stroke cases and ischemic strokes covering the remaining 87%. Approximately 20% to 30% of ischemic strokes are caused by a carotid atherosclerotic plaque [8–10]. In fact, the most common extra-cranial cause of ischemic stroke is the thromboembolism from unstable atherosclerotic plaque in the carotid bifurcation [11]. Thereby, stroke is one of the main cerebrovascular events related to atheroma plaques [12]. Patients with cerebrovascular symptoms of carotid origin are at high risk of a subsequent imminent life-threatening stroke [13]. The population at risk for atherosclerosis

is extremely large, and it continues to grow in response to the epidemic of obesity and metabolic disease [2].

1.1.2. Carotid atherosclerosis

Carotid artery wall configuration at bends and bifurcations is associated to and altered by local modifications in blood flow pattern and velocity [14]. Blood flow generates a physical force on the vessel wall that can be divided into wall shear stress and wall tensile stress (Figure 1). Shear stress is the stress exerted parallel to vessel wall producing frictional force on the endothelial surface, whereas tensile stress is defined as the stress produced by forces perpendicular to the vessel wall causing dilatation force by blood flow over the vessel wall. The absolute shear stress has temporal and spatial variations because cardiac cycle is pulsatile, and therefore, endothelium is able to discriminate these variations and respond differently through mechanochemical transduction pathways [15]. In this way, chronic exposure to high levels of shear stress with little temporal oscillations promotes athero-protective mechanisms involving ECs from carotid wall [16,17]. In these regions, ECs show ellipsoidal morphology and coaxial alignment in the flow direction [2].

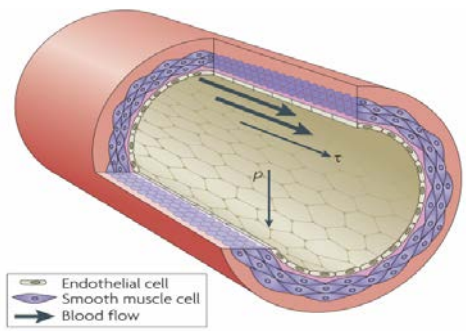

Figure 1. **Wall stresses in healthy artery vessel.** ρ, is tensile stress exerting perpendicular forces to the vessel wall. τ, is shear stress and produced forces parallel to the vessel wall. Endothelial cells and smooth muscle cells are aligned longitudinally and circumferentially, respectively [4].

However, as common carotid flow enters the bifurcation, changes appear in flow direction, and thus, laminar flow is localized to the inner wall of the internal carotid artery while the outer wall is a zone of stasis and recirculation of blood flow with relatively low wall shear stress (Figure 2) [14]. In this region of recirculating flow usually also temporal and spatial gradients of shear stress exist [18]. Thus, regions of low flow, flow separation, gradients and reversal flow are often grouped under the term ‘disturbed flow’ [19].

Under conditions of flow disturbances ECs fail to align in the direction of flow and display cuboidal morphology [2], and also, are associated with high rates of both EC proliferation and apoptosis as well as higher permeability to solutes, increased production of reactive oxygen species (ROS) and extracellular matrix (ECM) proteins, in addition to increased expression of inflammatory mediators such as cytokines and chemokines [2,20,21]. These atherogenic flow patterns, in consequence, impair endothelial barrier formation, initiating a local proatherogenic environment [2].

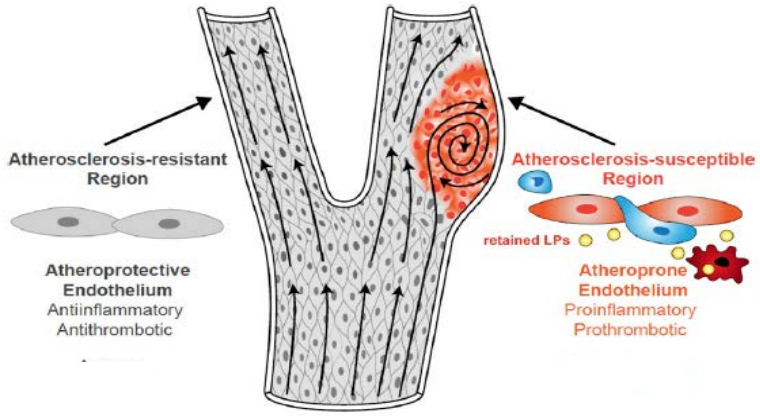

Figure 2. **Blood flow pattern in human carotid bifurcation.** Early lesions of atherosclerosis develop in carotid sinus where artery wall is exposed to low shear stress, high oscillatory shear index, and temporal and spatial gradients. Endothelial cells at this site (in orange) display an athero-prone phenotype, which promotes a proinflammatory milieu. Blood-borne monocytes (in blue) enter into the intima and differentiate into macrophages (in red) due to lipoproteins (LP) retained in the endothelium. In contrast, atherosclerosis-resistant region maintains an athero-protective endothelium with a decrease in LP retention, promoting antiinflammatory and anti-thrombotic environment [2].

The mechanisms underlying this process remain unclear [22]. It has suggested that low shear stress could interfere with turnover of essential substances at the endothelial surface for optimal endothelial metabolic function whereas has also been proposed that a retarded transport of circulating particles away from the wall may results in lipids accumulation in the intima [14]. More recent studies have suggested that global DNA methylation [23]and mRNA splicing [24] happening in the endothelium may also be affected by the athero-prone flow.

Therefore, atherosclerotic plaques are localized mainly in the outer wall of the bifurcation of the carotid artery where laminar flow is absent and stasis is predominant[15]. Furthermore, it is suggested that atherosclerosis develops in such static zones which have been noted at the outer wall of the carotid sinus in patients with cerebrovascular symptoms [14].

1.1.3. Biology of atherosclerotic plaque

The arterial wall is composed of three layers. The innermost layer is the intima, is in contact with the lumen of the arteries and consist of ECs, fibronectin and type IV collagen. In the media are mainly vascular SMCs (SMCs) embedded in collagen (types I, III, V and XVIII), fibronectin and proteoglycans, whereas adventitia composes the outer layer of the arterial wall and is rich in fibroblasts, collagen (types I and III) and elastin [25].

The American Heart Association Committee on Vascular Lesions suggested the following international histological atherosclerotic plaque classification system [26]:

- Type I lesion: it is the **initial** lesion and consist of isolated foam cells. Sufficient amount of lipoprotein can be found here to promote the conversion of macrophages to foam cells. Intimal thickening will be present during every stage of atheroma plaque development as everyone can develop it from birth as adaptive thickening in order to adapt to local mechanical forces.

- Type II lesion: the main characteristic of this stage is multifocal accumulation of lipid-laden macrophages and smooth muscle cells. In this lesions begin to appear **fatty streaks**.

- Type III lesion: it corresponds to the preatheroma stage. In addition to lipid-laden cells there are present **extracellular lipid droplets** and some smooth muscle cells lack their characteristic contractile morphology.

- Type IV lesion: extracellular lipids droplets become in a large and confluent **lipid core** of atheroma.

- Type V lesion: or **fibroatheroma**, consist of a lipid core below thick layers of fibrous connective tissue.

- Type VI lesion: it is a complex plaque with possible **surface defects** as fissure or appear hemorrhage and/or thrombus.

- Type VII lesion: it is a plaque that is predominantly **calcified**.

- Type VIII lesion: **fibrotic** plaque consisting in collagen and smooth muscle cell accumulation without lipid core.

Although the exact mechanism underlying atherosclerosis remains unknown, plaque development process has been tried to describe precisely for a better understanding.

1- Initiation of atheroma plaque formation:

Atherosclerosis starts in the endothelium of the intimal layer at the site of artery bifurcations, arteries and regions of high curvature that result in complex blood flow patterns [4]. At these susceptible sites, the endothelium supports greater hemodynamic stress as compensatory response in order to maintain normal homeostatic properties [27]. Thus, when endothelial dysfunction occurs, endothelium increases its permeability through expression of adhesion receptors such as intracellular adhesion-molecule-1 (ICAM-1) and vascular cell adhesionmolecule- 1 (VCAM-1), and chemokines such as monocyte chemoattractant protein-1 (MCP-1/CCL2) [28]. Therefore, endothelium allows blood low density lipoproteins (LDL) to enter and accumulate within the arterial wall reinforcing susceptible sites of rupture [29]. However, there may be an excess of LDL accumulation within the intima that is retained by proteoglycans and glycosaminoglycans [30] and which will be oxidized (oxLDL) by surrounding cells and molecules that are trying to digest it [29]. This oxLDL will act as chemotaxis/chemoattractant agent for monocytes, that acquire highly activated inflammatory phenotype and produce additional inflammatory mediators [3]. In addition, injured endothelium forms vasoactive molecules, cytokines and growth factors, and also modifies its properties toward procoagulant rather than anticoagulant processes [27], with the consequent adhesion of leukocytes and platelets to the intima and hence, the reaction of the innate inflammatory system [31].

2- Fatty streaks:

During atheroma plaque formation complex interactions are taken place between resident (arterial wall cells) and attracted cells (mostly immune cells) to the injury as well as between all of these cells with platelets and lipoproteins found in the damaged area. At this stage, cells in the subendothelial space are involved in the vascular remodeling process [32]. ECs are able to bind to and activate antithrombin III due to expression of heparan sulfate in their membranes, and thus thrombin (coagulation factor II) remains inactivated. However, when endothelium becomes dysfunctional heparan sulfate expression is reduced and hence, thrombin is activated with subsequent platelet adhesion to the endothelium. As aforementioned, ECs also express specific adhesion receptors for monocytes and T lymphocytes. The latter ones produce interferon-γ (IFN-γ) and tumor necrosis factor-α (TNF-α), activating monocytes and stimulating macrophage proliferation [30]. Monocytes within the intima take up lipids and differentiate first into macrophages and then are transformed into specialized cells, called foam cells. These foam cells express the main enzymes involved in LDL oxidation, myeloperoxidase and lipoxygenase. Additionally, macrophages can take up aggregated LDL by phagocytosis and oxLDL by scavenger receptors, both processes regulated independently of intracellular cholesterol levels. Thus, LDL will accumulate within the cells [30].

Clearing of the oxLDL excess is carried out by high density lipoprotein (HDL) particles [29] that are responsible for cholesterol reverse transport, and thus, oppose the effects of LDL since HDL carry lipids away from these cells [4].

Platelets are also attracted to the site of the lesion and release molecules such as platelet-derived growth factor (PDGF) and endothelial growth factor (EGF) [30] that initiate SMC migration from the tunica layer to the intima. Once SMCs reach the intimal layer, they proliferate and produce connective tissue accumulation, and hence, develop the intimal hyperplasia and consequent thickening of the arterial wall [29]. This newly formed intima layer is called neointima. In order to compensate arterial wall thickening, there is a gradual dilation of the vessel while the lumen remains unaltered, a phenomenon termed “positive remodeling” (Figure 3) [27]. These intimal SMCs may also accumulate fat droplets in the cytoplasm such as macrophages do and become also foam cells [33,34], and therefore, promote further lesion [31]. Thus, foam cell population within atherosclerotic plaques may be originated by SMCs or by macrophages. The excess of oxLDL phagocytized by foam cells and extracellular lipids retained in the vessel wall produce macroscopic changes called fatty streaks [29].

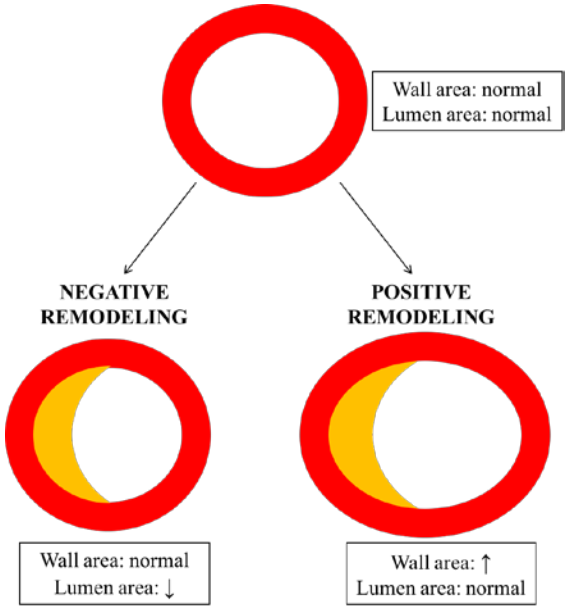

Figure 3. **Artery remodeling** when atherosclerotic plaque is formed [29].

3- Early fibroatheroma:

Fatty streaks can progress to larger, more inflamed lesions called atherosclerotic plaques [4]. At this stage of development of the atherosclerotic plaque, foam cells, activated inflammatory cells (mainly T lymphocytes) and resident cells of arteries are accumulated within the intima [31] in a highly focal way [4].

LDL uptake by macrophages/SMCs and HDL cholesterol reverse transport are the main cleaning system for removal of cholesterol excess. Both cleaning systems are ultimately exceeded because LDL accumulation is excessive and foam cell ability to accumulate cholesterol is limited [30]. Lipid loaded cells are finally induced to enter in apoptosis and consequently, multinucleated cells appear in order to phagocytose apoptotic cells in an attempt not to worsen the lesion [29]. However, at this point, the inflammation within the plaque becomes uncrontollable due to the accumulation of oxLDL, apoptotic cells and immune cells. Lipid filled apoptotic cells (mostly foam cells), multinucleated cells, cell debris and extracellular lipids pools form the lipid-rich necrotic core, which is encapsulated by a fibrous tissue called "fibrous cap". SMCs secreting collagen, elastic fibers and proteoglycans are responsible for producing fibrous cap, which is formed over the lipid-rich necrotic core and under the endothelium. Once atheroma plaque has been developed, normal architecture of the artery wall is already disrupted [31].

4- Advanced atheroma/Complicated lesion:

OxLDL regulates the production of nuclear factor (NF)-κβ molecule by macrophages that activates gene expression of TNF-α, interleukin (IL)-1, -6 and -8, colony-stimulating factors (G-CSF, M-CSF, GM-CSF), MCP-1/CCL2, the tissue factor, adhesion molecules (ICAM-1, VACM-1) and *c-myc* [30] among others, increasing inflammatory response within the atheroma plaque. In this context, ECs are unable to adapt to these events, resulting in sustained activation of pathways associated with inflammation, tissue remodeling and increased production of reactive oxygen species (ROS) [4]. Vascular SMC-derived ECM exacerbates oxLDL effects because facilitates the retention of LDL lipoproteins within subendothelial space, increasing their susceptibility to modification toward oxLDL as well as their uptake by intimal cells [35].

In advanced atheroma plaques, local O_2 diffusion from the arterial lumen may be insufficient because of intimal thickening and inflammation. Hypoxia promotes vascular endothelial growth factor (VEGF) expression, mainly secreted by phagocytic cells and cholesterol loaded SMCs, promoting angiogenesis through EC proliferation and migration within the lesion [36,37]. This neoangiogenesis decreases ischemic situation within plaque protecting tissue for hypoxia, however, is also a source of leukocyte infiltration and atherogenic lipid entry, resulting in plaque worsening [38].

Then, new vessels are formed from vasa vasorum within the intima (Figure 4) [30], but due to their thin wall and discontinuities in the endothelial lining, they are fragile and are prone to leakage, which may produce a hemorrhage within the arterial wall [31,37].

Figure 4. Neovascularization in the arterial wall. A. Healthy artery with reduced neovasculartization.

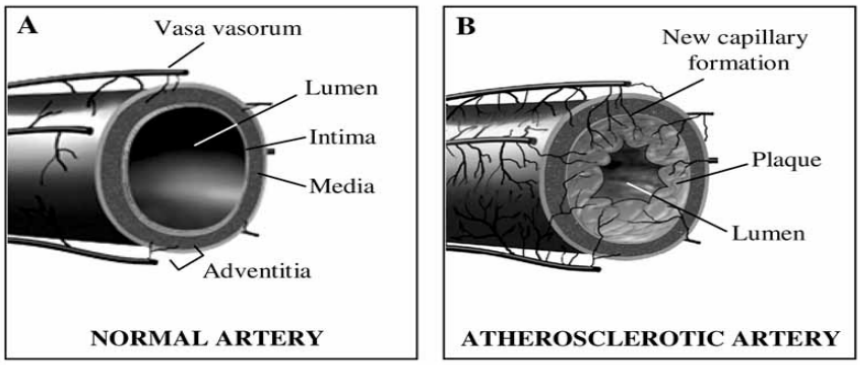

B. Atherosclerotic artery with extended neovascularization from adventitia to inside intima [36].

If the fibrous cap is ruptured because any new formed vessel is broken, there is an activation of coagulation factors and platelet that eventually leads to a thrombus formation in the lumen of the vessel [29]. Furthermore, lipid-rich necrotic core has important thrombogenic ability due to a high tissue factor and plasmin content produced by apoptotic cells [29] and activated by ECs [30]. This thrombus that can be formed, will block vascular flow [29]. In consequence, plaque continues growing and artery could no longer compensate intimal thickening by dilation [27]. Any further plaque enlargement will reduce the arterial lumen and vascular hemodynamic (blood flow) may be affected [31].

Plaque´s morphology or characteristics can vary substantially among individuals and within any given individual [31]. For instance, plaque composition can vary considerable in the size of lipid-rich necrotic core, foam cell accumulation or fibrous cap thickness [4]. The latter is one of the most conditioning factors to promote plaque rupture since a thin fibrotic cap is more susceptible to rupture than a thicker one [31]. The mechanisms responsible for plaque rupture are not known yet. However, the reason why the areas in which fibrous cap is attached to the vascular wall are prone to rupture is related with the fact that this region of the plaque contains few SMC and is abundant in macrophages and T lymphocytes secreting TNF-α and IL-1β. These factors induce increased metalloproteinase expression by SMCs and macrophages [30]. To date, the excessive activity of matrix metalloproteinases is one of the most supported mechanisms associated to plaque rupture [39–42] due to fibrous cap disruption, which causes atheroma plaque destabilization [43], and for that, this lesion usually is classified as vulnerable plaque [31].

5- Fibrotic plaque:

30% of the plaques are usually totally fibrotic plaques with thick fibrous cap and low risk to be ruptured [29]. This kind of plaques is formed because some ruptures of thin fibrous cap are healed by plaque itself forming fibrous tissue over the thrombus. The repeated cycles of rupture

and healing result in multiple layers of healed tissue increasing the whole mass of the plaque [31]. Fibrotic plaques are more stable plaques because do not tend to rupture [31]; however, they also enhance the risk to develop a cerebrovascular event depending on the degree of stenosis they cause [29]. Thus, this type of plaque alone may be sufficient to cause ischemic stroke simply through flow restriction [31], and if they rupture, given that the thrombus is a reservoir of thrombin [30], its release can trigger a new thrombus formation [44].

Fibrotic plaques usually become calcified due to calcium deposits accumulation that occurs during all stages of atherosclerotic plaque development [29]. They accumulate first in small aggregates and then in large nodules [31]. It is believed to be originated from apoptotic cells or from released molecules by their matrix vesicles [45]. When plaque is ruptured, calcium nodules are released from lipid-rich necrotic core, which are also a source of thrombosis [31]. Therefore, any stable plaque can become in an unstable plaque [46].

1.1.4. Unstable vs Stable plaque – Symptomatic vs. Asymptomatic patients

Carotid artery stenosis is considered severe when lumen stenosis exceeds 70%. Stenosis degree is associated with a significant risk of stroke [47]; however, in the general population 0% to 3% of carotid atherosclerotic lesions [48] have >70% of stenosis and remain asymptomatic, while only among 1%-3% culminate with stroke [49,50] . Hence, many strokes occur even with carotid plaques not displaying high degrees of narrowing [47].

The appearance of symptoms depends on multiple characteristics such as severity of the carotid stenosis, but also atherosclerotic plaque morphology/composition and the presence of other risk factors [51]. Patients with similar characteristics such as hypertension, smoking, diabetes, hypercholesterolemia and with carotid stenosis caused by atherosclerotic plaques have been found to have different risk of stroke, which has led to suggest that the degree of artery stenosis alone would not be the best estimation of stroke risk [52].

Asymptomatic plaques have relatively stable features with low risk for rupture and consequent event [53]; however, clinical stability does not always indicate biologic stability [54]. In advanced atherosclerosis, where is a complex interplay of variables in and outside the plaque [54], minor alterations in plaque biology may disrupt the clinically asymptomatic and stable condition to unstable and symptomatic disease [55]. Clinically asymptomatic carotid plaques frequently progress over time to produce symptoms [56] because a conversion of stable plaques to unstable ones may occur [46]. However, not all plaques become symptomatic and some may remain asymptomatic for life [57].

Although the mechanism underlying plaque rupture and subsequent symptomatology is largely unknown there are some histological characteristics that are widely used to classify plaques as stable or unstable. Unstable atherosclerotic plaques are those that are vulnerable to rupture and usually contain large lipid pools, infiltration of inflammatory cells (lymphocytes and macrophages), hemorrhage and a thin or virtually absent fibrous cap with low vascular SMC density [44]. The size of the lipid core has been associated with rupture events by van der Wal & Becker [54]. It was estimated that necrotic core occupying more than 30% of the total plaque may be a risk factor to produce an ischemic event [44]. Moreover, lipid-rich lesions have shown high content of inflammatory cells in the attenuated cap and shoulders of the lesion, and for this reason, active plaque inflammation has also been associated with the initiation of plaque rupture [54]. Local differences in macrophage and SMC densities have been found along the plaque and its distal side. Thus, carotid plaques show large SMC-rich areas in the downstream areas of the stenosis which are under low flow. In contrast, in upstream shoulder that is under high flow, macrophage-rich areas are predominant (Figure 5) [58]. Furthermore, the upstream area is associated with cap rupture, intra-plaque hemorrhage and a thin fibrous cap [59]. Actually, 70% of ruptured plaques experience a rupture at the site of the upstream shoulder [54].

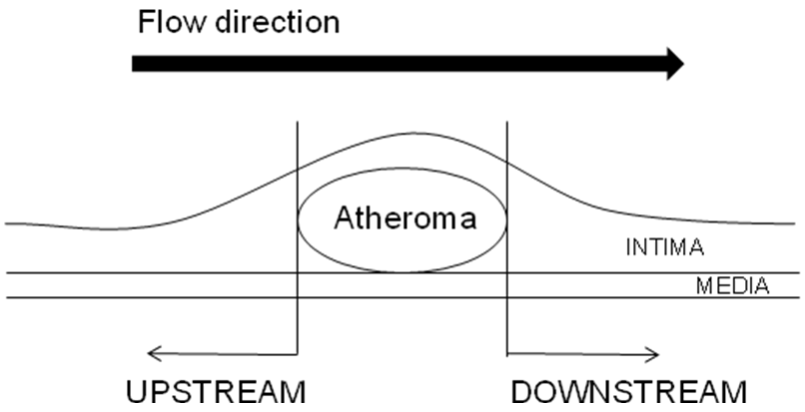

Figure 5. Diagram of carotid atherosclerotic plaque sites [58].

Several studies have demonstrated that smaller amounts of collagen and calcium, and more neoformed vessels (neovascularization) are also determinants of plaque instability and are characteristic of rupture-prone plaques (Figure 5) [52,60,61]. Indeed, asymptomatic patients usually show increased prevalence of collagen-rich stable plaques [62], composed of solid fibrous or fibrocellular tissue and only small amounts of extracellular lipid [54]. However, fissures also appear in fibrotic and calcified plaques that can make them vulnerable to rupture [60]. Fissures can vary in depth, but they may be limited to the plaque surface or may reach up to the intimal layer and lipid core [54]. When this kind of plaque surface irregularity becomes

gross ulceration, an opening accompanied by disintegration of tissue occurs, and subsequently, this may trigger hemorrhage as consequence of intimal neovessel leakages (Figure 6) [63,64].

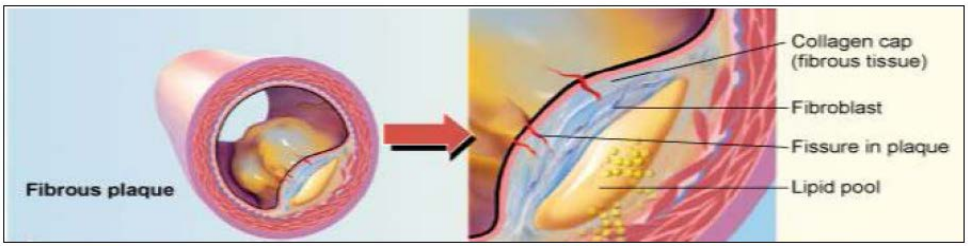

Figure 6. Fissures are formed from the vessel lumen inside the intima and toward lipid pool.

Because ulceration implies exposure of highly thrombogenic plaque constituents (lipids, tissue factor, collagens) to the blood flow, it can result in activation of the coagulation system and hence, thrombus formation [54]. Recent studies suggest that intra-plaque hemorrhage could be a trigger of plaque instability because it activates red blood cells and iron phagocytosis [64]. Hemorrhage also plays a role in releasing free heme, which is a strong activator of reactive oxygen species, and in cholesterol crystal production and retention. Thus, it develops further enlargement of necrotic cores [65]. The presence of fresh thrombus exposed to the vessel lumen has been correlated with the production of neurological symptoms [66]; in fact, ulceration is present in 51% of the transiently symptomatic patients compared to 36% of the asymptomatic patients [63].

Flow dynamics may also influence plaque stability in a mechanical manner through a physical impact that may trigger plaque rupture as well as affect cellular composition of the plaque. Fully stable or unstable plaques are the minority and most patients have mixtures in varying proportions of characteristics concerning stable/unstable plaque types [54]. This makes it more difficult to identify factors determining plaque vulnerability and healing [55].

1.1.5. Risk factors

It is unknown the exact cause of atherosclerosis, however, there are certain features and habits that maybe provoke the development of the disease. These conditions that increase disease progression are known as risk factors and include:

- Physiological characteristics
  - Hyperlipidemia

It is among the major risk factors for atherosclerosis [4], however, whether serum cholesterol levels are related to stroke and carotid arterial disease incidence is not yet established.

Lipidemic risk factors include elevated levels of total cholesterol, very low- (VLDL) and LDL, triglycerides, and lipoprotein (a) [67]. These are the responsible factors for bringing cholesterol to the tissues [68]. When endothelium permeability is increased in athero-prone regions, the lipoproteins enter into the vessel wall and will be retained by matrix components involved in remodeling if atherosclerosis has started to develop [69]. Additionally, oxidant stress together with LDL presence generates oxLDL molecules [68], which act as chronic stimulators of innate and adaptive immune response. OxLDL also induce ECs and vascular SMCs to express adhesion molecules, chemoattractants and growth factors that interact with receptors on monocytes and stimulate their migration and differentiation into macrophages and dendritic cells (DCs) [70].

On the contrary, elevated levels of HDL and apolipoprotein A1, the major protein component of HDL, seem to confer a protective effect. The capacity for cholesterol efflux through HDL is inversely correlated with carotid stenosis and plaque instability. For instance, patients with fibroatheroma plaques have lower cholesterol efflux than those of calcified or fibrous plaques [71].

However, an increased blood concentration of apolipoprotein B-containing lipoproteins — of which LDL usually is the most prevalent form — can be a sufficient cause of atherosclerosis, such as in familial hypercholesterolemia and other genetic hyperlipidemias (monogenic diseases) [70].

- Hypertension

High blood pressure leads to the deposition of cholesterol in the arteries [72] and promotes oxidative stress[73], which increases the risk of atherosclerotic plaque rupture and consequent stroke [72]. For that, hypertension has been identified as a significant risk factor for atherosclerotic plaque formation and/or progression [74]. Recent observational studies concluded that risk of death caused by ischemic stroke increases progressively and linearly as systolic and diastolic blood pressure levels increase from 115 and 75 mmHg, respectively [75,76]. Moreover, in patients with known cerebrovascular disease a direct and continuous relationship has been found between blood pressure and recurrent strokes (The United Kingdom-transient ischemic attack (TIA) trial) [76].

- Diabetes

Both in human and animal models, diabetes leads to broader, more diffuse and complex lesion although how this accelerates the disease is largely a mystery [77]. The risk of carotid disease and stroke is 4 times higher in diabetics than in people without diabetes [72]. Furthermore,

diabetes increases post-stroke mortality [78] and it is known that hyperglycemia extends the ischemic penumbra and has an adverse effect on neurologic outcome[79].

Diabetic patients usually have high blood pressure, high cholesterol and are more likely to develop cholesterol blockages in the artery [72]. Pathologic processes related to diabetes can enhance LDL oxidation because increased levels of glucose promote glycosylation and accelerate oxidative activities [80]. Thus, increased ROS production and oxidative stress may occur in diabetes that accelerate atherosclerosis [81].

- Behaviors

  - Smoking

Smoking is an independent stroke risk factor, increasing the risk of stroke by about two- to fourfold [82]. Smoking damages the lining of the blood vessels and makes cholesterol deposits more likely to be formed [72], thus, smokers have more lipids in their plaques, particularly oxidized lipoproteins, than non-smokers [83]. Being an ex-smoker or current smoker carries more than 6-fold risk of atherosclerotic carotid stenosis than in non-smokers [84]. Furthermore, the risk for stroke increases proportionally with the number of cigarettes smoked per day [76] and there is a dose-response relationship so that heavy smokers are at a higher risk of stroke than light smokers [85]. In consequence, stopping smoking is extremely important to keep carotid artery blockages from worsening and to prevent stroke [72].

  - Obesity

Associated risk factors such as hypertension, diabetes and hyperlipidemia are more prevalent in obese individuals than in healthy ones [86]. The risk of ischemic stroke also increases with obesity, being about three times higher for obese people than the normal population [87]. In addition, Suk's study [87] suggests that distribution of fat in the body could be associated to the risk of stroke, particularly, abdominal fat accumulation in men. Thus, current guidelines recommend targeting body mass index of 18.5 to 24.9 kg/m2 and waist circumference lower than 90cm and 100cm for women and men, respectively [86].

  - Physical inactivity

Sedentary lifestyle is also a significant risk factor for cerebrovascular disease. Physical activity has beneficial effects on blood pressure, glucose and lipoprotein levels [88]. Increased cardiac output during exercise increases fluid shear stress within the arteries until athero-protective levels of shear [89]. Additionally, this may increase endothelial nitric oxide synthase (eNOS) expression and hence, reduce the inflammatory status of these regions [4]. Epidemiologic and case-control studies have suggested that physical activity could decrease stroke incidence with a

dose-dependent relationship for both intensity and duration [90–92]. It is suggested that exercise before ischemia induces neuroprotection, reducing cerebral infarct size to levels that are not symptomatic [93,94].

- Inherent biological traits

  - Sex

Age specific stroke incidence rates are generally higher among men compared with women [85]. Multiple studies [85,95] have shown an increased incidence of stroke in men compared with women with moderate-severe carotid stenosis. For instance, there is a progressive increase in thickness equal to 0.0034mm per year in men and 0.0018mm in women[96]. The male-to-female ratio in carotid vascular disease prevalence has the maximum peak at age of 45-49 years [97] but in the extremes of old age, >75 years old, gender-related prevalence differences are less noticeable [98]. These prevalence changes according to age have been related to events linked to menopause that may promote atherosclerosis in women [97]. The authors speculated that estrogens might act not only on risk factor reduction, but also directly on plaque morphology and arterial remodeling [99]. Then, sex-related differences in the type of plaque rupture may be the result of differences in plaque composition [54].

Men have softer plaques, with a necrotic core more rich in lipids [100] and more erosions with subsequent healing than plaques from women [99]. On the contrary, plaques in women are likely to be fibro-calcified with less inflammatory features such as concentration of foam cells and lymphocytes in the cap [99,101]. This may suggest that sex hormones related to menopause such as estrogens play an athero-protective role giving stabilizing properties to the plaque [99]. Additionally, men have also greater carotid plaque area than women; in spite of women have greater stenosis [102]. Several studies have shown that women have significantly smaller carotid arteries than men, which predisposes women to higher velocity for any given blood pressure, reducing therefore biological risk to develop the lesion [100]. Nevertheless, women have worse recovery from stroke than men [103].

  - Age

Although the relation between advancing age and atherosclerotic plaque composition is unclear, there are structural changes with aging in large arteries such as carotid and aorta arteries [104]. These changes include arterial dilation, arterial compliance reduction, increased stiffening, endothelial dysfunction and intima-media thickness (IMT), considered to reflect early stages of atherosclerotic disease [104]. Increased IMT is a physiological effect of aging that corresponds to diffuse intimal thickening, especially in very elderly people. It has found that aging is the primary determinant of IMT [96]; during the sixth decade of life advanced lesions began to

appear, thus, in the seventh and eighth decades of life IMT and plaque prevalence are closely associated [105]. Moreover, plaques seem to become more atheromatous with aging, containing less SMCs and increased macrophage content. SMC apoptosis has been reported to be increased with age and additionally, in an inflammatory environment, SMC apoptosis may become impaired worsening the lesion [104,106].

Other risk factors are also affected with aging such as hypertension and hypercholesterolemia that increase their prevalence with age. Hypertension has been associated with increased prevalence of preclinical atherosclerosis in the older population [107] while arterial wall of aged people is more susceptible to hypercholesterolemia [104].

Therefore, the rate of progression is determined by various risk factors such as hyperlipidemia, levels of oxidants from smoking or other sources, elevated blood glucose, circulating inflammatory mediators and exercise among the previously aforementioned [4]. For example, at regions of arteries where athero-protective flow patterns are lost, there is an activation of proinflammatory pathways through ECs. Thus, the local chronic inflammation synergizes with additional risk factors such as hypertension, high plasma cholesterol, diabetes, etc, leading to more severe inflammation and atherosclerosis [4]. In addition, medical factors including previous transient ischemic attack (TIA) or stroke, ischemic heart disease, atrial fibrillation, and glucose intolerance, all increase the risk of stroke [85].

1.1.6. Biomarkers of carotid atherosclerotic plaque rupture

There is a need to identify biomarkers with the aim to select patients with carotid plaque and to be associated with the degree of stenosis or with features of plaque vulnerability, with the purpose of distinguish patients with higher risk of developing CV accidents [108]. Although during last decade there has been an advance in stroke risk detection from carotid artery stenosis degree measurement toward characterization of biological processes occurring within plaque [52], to date the standard diagnostic imaging tools still focus more on arterial luminal narrowing and less on plaque characteristics, and hence, it makes it difficult to estimate the vulnerability of a plaque. Therefore, plaque rupture remains complicated to predict [109]. For instance, plaque echolucency —lipid-rich necrotic core or intraplaque hemorrhage based on ultrasound technique—, total plaque area and plaque surface irregularities have been suggested as ultrasound markers of unstable plaque and risk of stroke, independent of the degree of artery stenosis However, the association between these variables is not fully understood [52].

An alternative to the use of imaging methods to identify vulnerable plaques could be the use of circulating or plaque in situ biomarkers such as molecules or specific cell types that may be able to define subjects with high-risk carotid plaques. Therefore, the identification of plaque

instability biomarkers has been focused on finding a molecule detectable either in serum or tissue. This molecule must be specific of carotid atherosclerotic plaques and be different expressed in unstable and stable plaques, and its increase/decrease should mean that plaque is prone to rupture [110]. For that reason, this biomarker must be present in atherosclerotic plaques and be released into circulation before rupture of the plaque to facilitate efforts to prevent it, or after rupture and remain increased since rupture might occur up to several days before the patient presents symptoms [111]. This biomarker would be intended to be used for risk prediction instead of just diagnosis. Thus, the biomarker may be also predictor of the risk of flow-limiting thrombus formation after plaque rupture and then, avoid a new event [110].

The following are the most widely distributed biomarkers:

- Inflammatory markers

Inflammation in the atherosclerotic lesion is considered to play a role in the events that lead to plaque rupture [104]. Changes in arterial inflammation have shown to be higher in patients with the highest rates of atherosclerosis progression, and could therefore be considered as a local marker for advanced plaque development [104]. The arterial regions where flow patterns develop disturbances are more susceptible to activate proinflammatory signaling pathways [4] and plaques prone to rupture show a high grade of inflammation [112]. In fact, arterial inflammation has been correlated with macrophage infiltration within the plaque [113] and it has been shown that inflammatory cells co-localize with plaque rupture sites [104]. Furthermore, there is a probable association between plaque echolucency (associated to vulnerable plaque) and inflammatory burden, with macrophages contributing to plaque destabilization in lipid-rich lesions [114].

- C-reactive protein (CRP)

CRP is an acute phase protein and is considered representative of the inflammatory status of an individual [104]. CRP is a well-established biomarker of cardiovascular risk and specially, a well-known circulating marker of atherosclerosis [115]. Its circulating levels have been shown to correlate with carotid IMT [116] and may reflect a systemic inflammatory response coming from inflamed atherosclerotic plaque [115].

CRP is probably directly involved in atherogenesis; it binds to a modified form of LDL, and when aggregated, CRP can also bind to native LDL [117]. However, CRP is a much less specific indicator of vessel wall inflammation than other inflammatory molecules such as interleukins (ILs). The exact role of CRP in the inflammatory process is uncertain, and in addition to several studies that have demonstrated elevated CRP concentration to be an independent prognostic factor in patients with stroke [118], there are also recent studies, which

have shown there is no association between plasma CRP levels and carotid plaque inflammation [119]. Then, the role of the CRP assay for treatment decisions has not been fully established, and CRP is not broadly applied as a risk marker for the prediction of plaque rupture [120].

- Cytokines:

Cytokines, and especially proinflammatory cytokines, have been found in plasma of atherosclerosis patients as well as within carotid atheroma plaques. The abundance of these cytokines has been associated with plaque vulnerability. Example of these are the high plasma levels of macrophage inflammatory protein 1beta (MIP-1b), tumor necrosis factor alpha (TNF-α) and C-X3-C motif chemokine ligand 1 (CX3CL1 or fractalkine), that have been found to be associated with high content of proinflammatory cytokines within the plaque, and hence, may serve to identify plaques with high inflammatory activity, and moreover, as markers predicting future TIA [121]. Nevertheless, the association between cytokines found into the plaques and in plasma appeared to be stronger in asymptomatic patients than in symptomatic ones, maybe because a recent event would have induced a systemic inflammatory response but unstable carotid plaques remodel and stabilize over time after stroke [122].

High levels of IL-6 have been shown to be associated with low echogenicity of carotid plaques, which means low content in fibrotic tissue and calcification, suggesting a link between inflammation and the potential risk of plaque rupture [114]. Indeed, large amounts of IL-6 have been found in human atherosclerotic plaque, in particular within the shoulder region of stable and unstable plaque[123], as well as in serum from patients with vulnerable plaques. Furthermore, IL-6, MIP-1b and C-C motif chemokine ligand (CCL) 2 plaque levels have been significantly correlated with plaque lipid staining [121]. However, increased IL-6 level is non-specific because IL-6 is also secreted by T cells during infection, therefore, could not be used as a marker of plaque instability [124].

IL-6 modulates lipid homeostasis, vascular remodeling, and plaque inflammation in atherogenesis, and together with IL-18 and IL-1β has been identified to play a role in the late stages of atherosclerotic lesion development [125]. IL-1β and IL-18 are present predominantly in advanced atherosclerotic lesions of unstable plaques, located in the lipid core in macrophages and foam cells. They are detected at higher levels in carotid atherosclerotic patients than in control groups (without atherosclerotic lesions), therefore, plasma levels of IL-1β and IL-18 might be candidates to be used as predictors for carotid atherosclerosis [126].

In addition, IL-18 acts directly as a proinflammatory cytokine by inducing IL-1β, IL-8 and expression of adhesion molecules. It is produced mainly by monocytes/macrophages and is involved in the induction of IFN-γ production, which greatly affects collagen content through

inhibition of collagen synthesis by SMCs from plaques and enhances expression of matrix metalloproteinases (MMPs) [127]. As a result, plaque destabilization is encouraged. However, even though IFN-γ plays an important role in atherosclerosis, its use as a circulating biomarker has been limited by the rapid metabolization that occurs following its release [121].

In a health condition, legumain, a cysteine protease localized in the endolysosomal system, can be expressed by different antigen-presenting cells (APCs) through generation of T-cell epitopes on major histocompatibility complex-II (MHC-II). Legumain protein and pro-legumain mRNA levels are increased in symptomatic human carotid plaques, as well as in unstable regions of plaques compared to stable ones. Legumain is co-localized with macrophages in foam-cells rich areas within the plaques. On the contrary, it has not been possible to discriminate between symptomatic and asymptomatic patients at systemic level [108].

CCL19, small cytokine belonging to the CC chemokine family, is found to be significantly upregulated in clinically and histologically unstable plaques. Serum CCL19 levels are also higher in patients who were recently symptomatic compared with those who were not. CCL19 is involved in the chemokine signaling pathways regulating cytokine production, cellular growth and differentiation, and apoptosis, as well as in transendothelial migration and activation of leukocytes, lipid uptake of macrophages, and foam cell formation within atherosclerotic plaques. CCL19 is strongly expressed around the core and cap region where it is co-localized with CD3-positive T-cell lymphocytes of recently symptomatic plaques [128]. Moreover, plaque T-cell accumulation appears increased in patients with carotid plaque and ischemic symptoms compared to those in patients with carotid plaque but without ischemic symptoms. Additionally, interleukin (IL)- 17A, - 21, - 23 and vascular cell adhesion molecule-1 (VCAM-1) expression were also found significantly increased [129].

Apart from the molecules already mentioned, several other inflammatory markers have been associated with atherosclerosis and cardiovascular disease. Serum amyloid A [67], YKL-40[130], CD146 [131], high white blood cell count [62], P-selectin, soluble urokinase-type plasminogen activator receptor (suPAR) [132], IL-23 [133], visfatin [134], granzyme B [135] and S100A12 [136] have been all associated with carotid plaque instability and stroke [67], as well as with the progression of asymptomatic to symptomatic plaques [46].

Measurement of circulating markers after 1–2 years after the endarterectomy surgery showed that the levels of most of the inflammatory markers were not significantly different compared with the pre-operative period [115], which may suggest that there could be influenced by other concomitant conditions [121].

- Extracellular matrix markers

- Metalloproteinases (MMPs) and their inhibitors (TIMPs):

MMPs are calcium-dependent zinc-containing endopeptidases capable of degrading extracellular matrix proteins. They are known to be involved in the cleavage of cell surface receptors, release of apoptotic ligands and chemokine/cytokine inactivation. MMPs are also thought to play a role in cell behaviors such as cell proliferation, migration, differentiation, angiogenesis, apoptosis and host defense [137].

MMPs are detected in atherosclerotic plaques and are particularly important in plaque stability due to their presence in areas of plaques prone to rupture [138]. Some MMP such as MMP-2, -3 and 9 can facilitate vascular SMC migration from the media into the developing atherosclerotic plaque where they participate in fibrous cap formation and maintenance, thus promoting plaque stability. On the contrary, MMP-1, -8, -12, -13 and -14 can degrade fibrous cap and prompt the recruitment and accumulation of monocytes and macrophages, resulting in thinning of the fibrous cap and lipid core expansion, respectively [139]. Indeed, gene expression of MMP-1, -12, and -14 is found increased in vulnerable carotid plaques compared to stable carotid plaques [41].

MMP-8 and -9 levels were found to be increased in plaques with histological evidence of carotid plaque instability [140,141]. In fact, macrophage-derived MMP-9 has demonstrated to be a trigger of intra-plaque hemorrhage, which is considered a destabilizing factor [139]. Also, high levels of MMP -9, together with MMP-7, are found to be associated with symptomatic carotid plaques obtained from patients undergoing carotid endarterectomy [142]. MMP-7, secreted by macrophages, can induce vascular SMC apoptosis, and therefore, compromise also plaque stability [143]. The activity of these three MMPs has been detected in macrophage-rich carotid atherosclerotic lesions whereas increased MMP-2 activity is associated with SMC-rich lesions [144]. Plaques seem to become more atheromatous with the aging, containing less SMCs and increased macrophage content and higher MMP-9 levels [104]. In fact, stroke incidence (ipsilateral) is significantly increased in patients with ≥50% of carotid stenosis and elevated plasma MMP-9 levels compared to that in patients with carotid stenosis ≥50% but without elevated plasma MMP-9 levels [145].

- A disintegrin and metalloproteinases (ADAMs) and ADAM with thrombospondin motifs (ADAMTSs):

ADAM proteases are a family of transmembrane and secreted metalloendopeptidases that are involved in the cleavage of cell-surface molecules such as adhesion molecules, growth factors and receptors for cytokines/chemokines [139]. ADAMs are found in carotid atherosclerotic plaques at high levels compared to health arteries. For instance, ADAM-10 is expressed in both

early and advanced atherosclerotic carotid lesions and its expression is markedly increased in unstable plaques compared to stable lesions [9,146]. This protein possesses a proteolytic function and activates various inflammatory factors [147]. ADAM-10 participates in protein kinase C (PKC)-alpha-ADAM-10 cascade regulating N-cadherin cleavage in atherosclerotic plaque. Soluble form of N-cadherin provides a pro-survival signal to vascular SMCs, macrophages and foam cells attenuating their own apoptosis. Therefore, during apoptosis in atherosclerotic plaques ADAM-10 appeared to be upregulated, and its increase has been correlated with decreased N-cadherin expression due to its cleavage, and hence, an augmented apoptosis [148].

ADAM-9, -15 and -17 are localized to foam cell-rich regions and are found upregulated in advanced carotid atherosclerosis at transcriptional and protein levels. It is suggested that these ADAMs may play a role in monocyte homing, migration and proliferation in carotid plaque [146]. Similarly, ADAMTS-4 and -8, inflammatory regulated enzymes, have been detected in foam cell-rich areas of human carotid atherosclerotic plaques and moreover, their expression increases during lesion progression [149]. ADAMTS-7, also, is associated with plaque vulnerability due to its higher expression in plaques of symptomatic patients than asymptomatic, and its association with plaques rich in foam cells and lipid content [150]. ADAMTS have been implicated in atherosclerosis due to their ability to processing pro-collagens and von Willebrand factor as well as remodeling ECM. In general, ADAMTS have been related to roles such as coagulation, inflammation, angiogenesis and cell migration. Thus, ADAMTS1 can promote vascular SMC migration in culture and is found to be expressed by SMCs within human atherosclerotic lesions suggesting a role in plaque stability [151].

- Tissue inhibitor metalloproteinases (TIMPs)

TIMPs play a homeostatic role in regulating the activity of MMPs and ADAMS. TIMPs are commonly increased where MMP activity is prevalent with the aim to inhibit them. TIMPs comprise a family of four protease inhibitors TIMP-1, -2, -3 and -4. TIMP-1 has shown decreased serum levels in stroke patients compared to those in asymptomatic patients [152]. Symptomatic patients with carotid stenosis ≥50% have demonstrated to have decreased levels of TIMP-1 in addition to HDL, while blood IL-6 and triglycerides were found significantly increased compared to asymptomatic patients with carotid stenosis ≥50% [153]. TIMP-3, however, is associated with stable carotid plaques due to its abundant presence in foam cells within the fibrous cap of human plaques [42], and additionally, it has shown the highest expression levels of all TIMPs in stable carotid plaques [41]. TIMP-3 is also expressed by medial SMCs within advanced lesions albeit at lesser amounts than foam cells [154]. Accordingly, TIMP-3 positive foam cells are associated with stable plaques rich in SMCs and

small necrotic core [42]. Macrophages can express TIMP-4 as demonstrated in human atherosclerotic plaque lesions, in which TIMP-4 activity has been detected in macrophages around the necrotic core [155]. Nevertheless, the role of TIMP-4 in atherosclerosis remains unclear [139].

- Pregnancy-associated plasma protein A (PAPP-A):

This is a high-molecular-weight zinc-binding matrix metalloproteinase which is secreted by vascular EC and SMCs within atherosclerotic plaques. There is an association between the high level of serological PAPP-A and its detection in plaques, also between the PAPP-A expression and fibrous cap thickness [156], as well as with rupture-prone plaques [157]. Based on this correlation, it is suggested that circulating high levels of PAPP-A may reflect the risk of developing unstable plaque [156].

- Fibrinogen

Fibrinogen blood levels are associated with a specific histological composition of carotid atherosclerotic plaques that predispose them to rupture and thrombosis. Thus, an increase in the presence of blood fibrinogen is related to macrophage cap infiltration and decrease in plaque cap thickness, which are characteristics of vulnerable plaque. Moreover, plaques of patients with the highest fibrinogen levels are usually characterized by a high incidence of thrombosis compared with plaques of subjects with lower levels of fibrinogen. Therefore, plaque rupture has been associated with hiperfibrinogemia [158].

- Vascular calcification markers

The risk of vascular disease increases with increasing burden of calcified plaque [104]. The bone matrix proteins osteopontin (OPN) and osteoprotegerin (OPG) have emerged as novel markers of calcified atherosclerotic plaque. OPN has a role anchoring osteoclasts in the ECM facilitating bone resorption whereas OPG functions by inhibiting osteoclast differentiation. High levels of OPN and OPG are found in symptomatic carotid plaques with possible implications for plaque stability [159]. Although OPN expression, in carotid plaques and blood, has displayed to be predictive for athero-thrombotic events [160], it does not correlate with vulnerability features of the plaques [161]. An increase of OPG together with lipoprotein-associated phospholipase A_2, however, may indicate the symptomatic transformation of the carotid atherosclerotic plaque [153].

- Lipid-related markers

Lipid core in thickened carotid walls is strongly associated with total plasma cholesterol [162]. Symptomatic carotid plaques trended toward more cholesterol deposition than asymptomatic

plaque as immunohistochemical analysis of carotid atherosclerotic plaques have shown. A strong correlation between increased total cholesterol staining and characteristics of vulnerable carotid plaque such as high content of foam cells, calcification and low SMCs have been demonstrated [163].

Pathologic studies have showed accumulation of oxLDL in rupture-prone atherosclerotic plaques, suggesting that high concentrations of oxLDL in plasma and plaque could play a role in the transition from stable to vulnerable plaques [164]. Elevated plasma oxLDL concentrations are also associated with moderate ischemic damage in stroke patients and a persistent increase in plasma oxLDL may represent a predictor of enlargement of the ischemic lesion after [165].

The vascular wall can be considered as a major source of circulating oxLDL [165]. Oxysterols arise through enzymatic reactions of cholesterol oxidation as well as non-enzymatic reactions such as free radical mediated processes. They are involved in advance atherosclerotic plaque formation [166] as demonstrated by elevated levels of oxysterols in patients with advanced carotid atherosclerosis [167].

Myeloperoxidase is one of the main enzymes responsible for oxidizing LDL molecules. It is a heme protein secreted by activated macrophages that has been detected in human atherosclerotic lesions [168] and is associated with the progression of the disease in patients with low levels of HDL cholesterol [169]. In human atherosclerotic tissue, myeloperoxidase catalyzes oxidative modification of HDL producing dysfunctional proinflammatory and proatherogenic HDL and influencing ATP binding cassette subfamily A receptor 1 (ABCA1) affinity with HDL, which results in an impaired reverse cholesterol transport [170]. In addition, myeloperoxidase activates metalloproteinases and hence facilitates destabilization and rupture of the vulnerable plaque [169].

- MicroRNA deregulation

MicroRNAs (miRNAs) are non-coding small RNAs that regulate gene expression by degradation or translational repression of target mRNAs. A group of miRNAs contributing to plaque instability development has been detected. Within atherosclerotic plaque miR-100, miR-125a, miR-127, miR-133a, miR-145, andmiR-221 levels are found to be markedly increased in symptomatic plaques compared to asymptomatic plaques [171]. At serum level, a recent study of miRNA trafficking by exosomes has shown that miR-199b-3p, miR-24-3p, miR-221-3p, miR-27b-3p and miR-130a-3p were increased in patients with asymptomatic carotid artery stenosis with progression toward symptomatic stenosis. These miRNAs had previously been related with processes such as inflammation, angiogenesis, or endothelial and vascular smooth muscle cell differentiation, leading to atherosclerotic plaque growth, instability, rupture, and

possible subsequent cerebrovascular events. It is suggested that this subclinical miRNA profile may serve as a biomarker for stenosis progression toward ischemic event [172].

More recently, some miRNAs have been identified which can regulate MMP and TIMP expression, exerting direct effects on plaque progression. MiR-181b has been involved in TIMP-3 expression by foam cells whereas miR-24 can regulate MMP-14 protein expression on macrophages [139].

However, thus far no single biomarker has been found to be able to reliably predict ischemic stroke or cardiovascular disease. There is a need to carry out additional studies for the identification of biomarkers since microarrays, qPCR and/or immunohistochemical techniques have not been able to find reliable biomarkers for use in the clinic [52].

1.2. VASCULAR SMOOTH MUSCLE CELLS

One of the main cellular components in carotid atherosclerosis are vascular smooth muscle cells. These cells are highly specialized in their main function; contraction, which is used to provide support and contractility to the vascular system [173]. During vascular development, SMCs are in a dedifferentiated state and display a high rate of proliferation, migration and production of extracellular matrix components (collagen, elastin, proteoglycans, cadherins and integrins) that comprise a major portion of the arterial wall mass and they formed abundant gap junctions with ECs for the right vascular maturation [174]. At the end of the development, SMCs became differentiated into contractile-state cells to perform their contractile function and show low rates of proliferation and synthetic activity [173].

SMCs are highly specialized cells in adult blood vessels that have developed a complex contractile system and maintain a quiescent state of proliferation. Their main function is to maintain vessel tone and diameter, and thus control blood pressure, but they also participate in vessel homeostasis and development. To carry out their functions they express a unique repertoire of contractile proteins that give them these contractile properties that differentiate SMCs from other muscle cell types [175].

Both, ECs and SMCs, are involved in blood pressure maintenance by responding to mechanical forces to modulate arterial diameter. The mechanism, called the myogenic effect, makes SMCs responsive to acute changes in blood pressure in these vessels, as myosin activation through voltage-dependent calcium channels results in activation of cell contraction [176]. During increased blood flow ECs respond to it causing relaxation of the surrounding smooth muscle [177]. SMC relaxation consists in increase the arterial diameter to restore wall shear stresses to basal levels [178]. Thus, elasticity of large arteries, such as the aorta, softens the periodic

variation in blood pressure expanding and deflating as pressure increase or decrease during the cardiac cycle. Therefore, the resultant cyclic stretch of artery walls promotes a quiescent and contractile state where SMCs express a full range of differentiation markers [179].

1.2.1. SMC phenotypic switching

The major characteristic in the differentiation of SMC is that this cell can exhibit a wide range of different phenotypes at different stages of development, and even in adult organisms the cell is not terminally differentiated [180]. SMCs are able to suffer phenotypic modulation to ensure local adaptation to chronic changes in the vessel, and consequently, SMCs provide the vessel with the necessary flexibility to address physiological and pathological situations [181]. "Phenotypic modulation" is a descriptive term coined by Julie Chamley-Campbell et al. in 1979 [182]. This term refers to the full range of possible alterations in functional and structural properties that can be exhibited by the SMCs in response to changing environmental cues, including changes in gene expression patterns, signaling mechanisms, contractility, etc. [180].

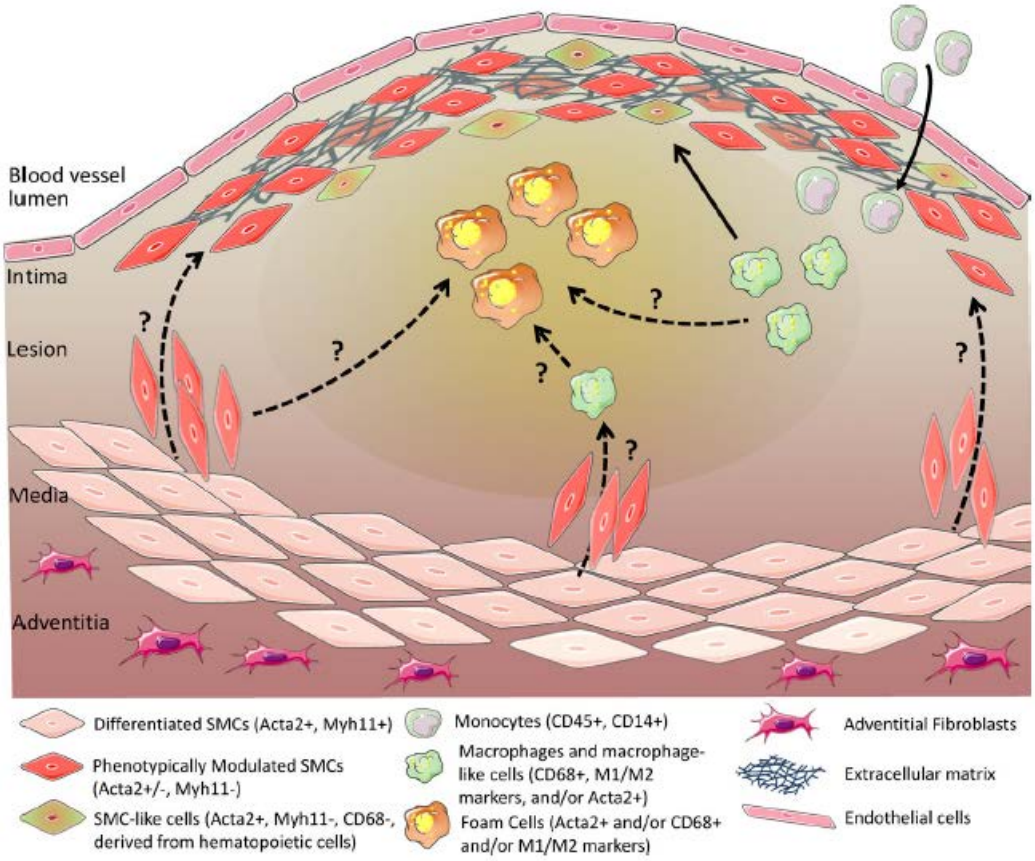

Figure 7. SMC phenotypic modulation in atherosclerosis disease [183].

In general, SMC phenotypic switching is characterized by markedly reduced expression of SMC-selective differentiation marker genes [180] originated by Krüppel-like factor 4 (KLF4)-dependent myocardin downregulation [184]. Although KLF4 is a molecular regulator of phenotypic switch of SMCs towards hyperplasia [185], it is normally not expressed in SMCs and its activation leads to downregulation of myocardin and myocardin target genes, and hence, modulation of these cells [184]. The only cells in the vasculature that express myocardin are SMCs [183]. Myocardin is the principal regulator of smooth muscle development and is necessary for SMC differentiation through interactions with serum response factor (SRF) [184]. Myocardin activates smooth muscle gene expression [186], and thus, genes like smooth muscle specific α-actin, calponin, h-daldesmon, transgelin and myosin heavy chain 11, that are SMC-selective differentiation marker genes, are regulated by SRF [187].

Once phenotypic switching is accomplished, the function of SMC can vary dramatically depending on the nature of the phenotypic transitions [183]. Several phenotypes have been described for SMCs (Figure 7) [180]:

- Synthetic phenotype:

The most studied one is the synthetic phenotype; in which cells acquire characteristics such as an increased rate of proliferation, migration, and synthesis of ECM [180]. Synthetic SMCs have a lack of myofibrils and hence they lose contractile ability [188] but in contrast, they have increased content of rough endoplasmic reticulum, Golgi and free ribosomes used for ECM components production [182]. The characteristics of these two phenotypes, contractile and synthetic, represent the two ends of spectrum of SMCs with intermediate phenotypes [189]. Due to different signals, SMCs can switch in both directions, synthetic- or contractile-state, thus, proliferative SMCs can reacquire some of the contractile SMC characteristics when surrounding signals drive the cells towards it [190].

- Macrophage-like phenotype

Another phenotype that SMCs can acquire is the macrophage-like phenotype (or foam cells). Cells with this phenotype are able to express macrophage markers such as scavenger receptor CD68, and gain properties such as the uptake of cholesterol. Then, after cholesterol loading, SMCs are able to transform into foam cells [191]; however, gene expression patterns of these SMC-derived macrophage-like cells seems to be distinctly different from classical monocytes, macrophages, and DCs. For instance, SMC-derived macrophage-like cells have reduced phagocytic capacity compared with activated macrophages [192].

- Osteoblast-like phenotype

It is demonstrated that high concentration of phosphate induces KLF4 expression contributing to transition of SMCs to osteoblast-like cells and hence, suppressing SMC contractile genes [193]. Pro-osteogenic factors such as the bone morphogenetic proteins and inflammatory mediators increase expression of the bone-related proteins osteocalcin, sclerostin, and receptor activator of nuclear factor-kappa β ligand (RANKL). These cells are the main responsible for generating matrix vesicles that serve as a nidus for bone matrix deposition in the vessel wall and thus, they mediate vessel calcification [194].

1.2.2. SMCs in carotid atherosclerosis

Atherosclerosis is one of the best-known example in which SMC phenotypic switching plays a key role in the development of the disease, a disease currently responsible for >40% of all deaths in Western civilization [195].

The role of the SMC in the pathogenesis of atherosclerosis appears to vary, depending on the stage of the disease. The SMC has a maladaptive role in lesion development and progression; it is estimated that up to 70% of the lesion mass is occupied by SMCs or is SMC-derived (e.g. ECM). At the same time intimal SMCs within atherosclerotic lesions are contributing to luminal narrowing, medial SMCs play a key role in adaptive positive remodeling, a process beneficial in maintaining blood flow [195].

In the context of atherosclerosis, there is a pathological environment with mechanical forces, endocytosis of specific molecules, chemokines and growth factors that regulate SMC-specific genes [196]. These signals induce contractile SMCs to undergo transient modification of their phenotype toward a highly synthetic phenotype [180], and consequently, these cells proliferate and migrate from the media to the intima [196]. Thus, SMCs contribute to the healing of the damaged wall; 1) in long periods of elevated pressure, intimal thickening reinforces the arterial wall avoiding its rupture[4]; 2) SMCs maintain plaque stability by producing a protective fibrous cap overlying encapsulated lipid core to avoid proinflammatory response [191]. Upon resolution of the injury, the local environmental cues within the vessel return to normal, and SMCs reacquire their contractile phenotype/properties [180]. Thus, this ability to adapt to distinct functions indicates mature SMCs which are not fully differentiated and may retain significant plasticity [175].

In the firsts stages of plaque development adaptive intimal thickening takes place, which implies a change in their phenotype from contractile- to synthetic-state. This phenotypic switching is considered a pre-requisite in the initiation of the plaque formation [189]. However, SMC accumulation can become aberrantly regulated leading to increased switched cells and

extracellular matrix formation [197], that forwards the progression of the plaque from moderate to advanced stage [189].

Exposition of SMCs to oxidized phospholipids induce SMC phenotypic switch from the contractile to the synthetic phenotype and increased expression of chemokines by SMCs. Oxidized phospholipids also increased nuclear translocation of KLF4, a known repressor of SMC marker genes [198]. In this way, in the process of plaque formation where there is a prolonged exposure to oxLDL, the retention of blood lipoproteins is facilitated by SMC-derived ECM, increasing the susceptibly of oxLDL modification and therefore, their uptake by SMCs [35]. The presence of excessive oxLDL promotes over-expression of scavenger proteins involved in LDL phagocytosis leading to the formation of foam cells. Nevertheless, SMC-derived foam cells have less affinity for LDLs than cells specialized in phagocytosis and also, they have reduced ability to clear dying cells and necrotic debris [189]. As a result, SMC-derived foam cells do not contribute to produce fibrous cap components but promote necrotic core formation and enlargement as well as neointima formation [183]. SMC-derived foam cells end up transforming into apoptotic cells, promoting adjacent SMC proliferation, plaque calcification, and increasing plaque size with reduced fibrous cap area and plaque stability [199].

Since inflammation may become unchecked and excessive, some factors can promote death of macrophages and SMCs, and together with the reduced phagocytosis of debris by SMC-derived cells and macrophages [200], the atherosclerotic plaque evolves toward an advanced stage. Dead cells begin to form the lipid-rich necrotic core in the central part of the intima covered by collagen-rich fibrous cap that is produced by migrated SMCs [31].

Apoptotic SMCs or matrix vesicles released by these cells originate micro-calcifications in the neointima of atherosclerotic plaques. These matrix vesicles are the mineral nucleation sites for the initial deposition of calcium and phosphate in blood vessel and are originated from de-differentiated or calcifying SMCs as a mechanism to decrease high levels of intracellular calcium [201]. Oxidant stress and endoplasmic reticulum stress are implicated in vascular calcification and have shown to promote differentiation of SMCs to osteoblast-like cells, however, other mechanisms such as calcification inhibitors, DNA damage response signaling, lipid deposition and inflammation are also involved. The presence of these matrix vesicles derived from SMCs have been shown to be one of the responsible of disruption of normal vessel architecture [194].

Within the fibrous cap, SMCs may play either a beneficial adaptive role or a detrimental role in determining plaque stability, depending on the phenotypic state of these cells. Synthetic-state cells are the responsible for stabilizing fibrous cap, but on the contrary, in response to

environmental cues these cells may undergo apoptosis and/or activate expression of various matrix metalloproteinases and/or inflammatory mediators that may contribute to events such as plaque rupture and thrombosis, and subsequently may lead to stroke [195]. The possibility of the plaque to rupture increases as the cap becomes thinner, promoted by death of SMCs and breakdown of collagen and ECM. Thus, thickness of the fibrous cap and the degree of cap inflammation are factors determining the stability of the atherosclerotic plaque. However, SMCs can repair the rupture. For this, synthetic SMCs proliferate and synthesize ECM resulting in subclinical plaque rupture but with luminal narrowing produced by a thick atherosclerotic plaque. These SMCs properties, i.e. proliferation, migration and ECM synthesis, are affected by cell death in the necrotic core and cellular senescence within the plaque in advanced stage. Hence, the balance between both conditions is going to determine the population of SMCs present in the atherosclerotic plaque and its stability [183].

Therefore, as aforementioned, SMCs are able to show their plasticity and give rise to a considerable diversity of SMC responses during atherosclerosis plaque development [191]. For instance, intimal thickening, a hallmark of development from moderate stage to advanced atheroma plaque, is considered a SMC phenotypic response to cope with vascular wall damage [202].

1.2.3. SMC-specific markers

The expression patterns of a wide range of protein markers have been characterized to describe the phenotypic state of SMCs. At the contractile extreme, and in healthy adult blood vessel, are SMCs with a fully functional contractile apparatus [203] which includes the expression of smooth muscle α-actin (α-SMA or ACTA2), smooth muscle myosin heavy chains (e.g. MYH11), h_1-calponin, SM-22α or transgelin (TAGLN), h-caldesmon (CALD1), smoothelin, desmin and metavinculin among others. In the other extreme it can be found synthetic, macrophage or osteogenic-like phenotype SMCs [180].

Myocardin is one of the central regulators of most, but not all, SMC-specific contractile marker genes that directly interacts with transcriptional cofactor SRF, which is involved in the regulation of cell programs such as proliferation and differentiation of SMCs and is also active in the promoters of muscle-specific genes during differentiation [203]. SRF binds to a CArG box DNA sequence of genes such as α-SMA, calponin, SM-22α and MYH11 [187] inducing their transcription and maintaining the contractile state [204].

Functional contractility is the most robust indicator of contractile SMC phenotype [203]. Contraction occurs through cyclic interaction between thin and thick contractile filaments, composed of the SMC-specific isoforms of α-SMA and myosin heavy chain, respectively [204].

α-SMA is the first known protein expressed during differentiation of the SMC and is the most widely used SMC marker because is the most abundant protein in differentiated SMCs reaching the 40% of total protein content [174]. Additionally, it is highly selective for SMC or SMC-like cells in adult animals under normal conditions [180], however, in atherosclerosis is also expressed in many non-SMC cells like ECs or fibroblasts [205].

The following are the most used SMC markers:

- TRANSGELIN (SM22α or TAGLN)

SM22α is one of the earliest markers of contractile vascular SMCs and is, together with α-SMA, the most widely used markers for SMC identification [204]. Overexpression of SM22α inhibits SMC proliferation and neointima formation via blockade of the Ras-extracellular signal regulated kinase (ERK) 1/2 pathway [206]. SM22α co-localized with F-actin and participates in the organization of the cytoskeleton facilitating the assembly of actin filaments into bundles in differentiated vascular SMCs. Thus, SM22α facilitates the activities of migration and contraction in contractile vascular SMCs [207]. Its disruption is known to increase atherosclerotic lesions [208] due to the blockade of SM22α expression that lead to the thinning and dispersion of actin filaments and consequently, the cell contractility and mobility are lost [207].

- MYOSIN HEAVY CHAIN 11 (MYH11 OR SM-MHC)

It is the most specific SM-marker known up to date and its absence or reduction is the result of phenotypic switching [204]. MYH11 can be expressed transiently under certain circumstances in other non-vascular SMCs *in vivo*, however, there is no conclusive evidence of this and at present is considered the most discriminating marker of differentiated SMCs [195]. The signal transduction pathways that are activated by stretch and shear stress have been shown to increase expression of MYH11 [181]. Cells which stain for MYH11 exhibit the elongated morphology and, the electrical and contractile behavior expected from SMCs [205].

- CALDESMON

This protein is additional thin filament protein whose function is thought to be in regulation of calcium activation of the myofilaments. There are multiple isoforms of caldesmon which are classified as high (h) and low (l) molecular weight caldesmon proteins [209]. The expression ratio of h- and l-caldesmon are closely associated with phenotypic modulation of SMCs. Thus, mRNA and protein levels of h-form are primarily found in differentiated vascular SMCs and l-form is found in modulated phenotypes [210].

- CALPONIN

It is a thin filament-associated protein that inhibits actin-activated myosin ATPase activity [209]. Calponin has the ability to stabilize actin filaments in living cells and to reduce actin remodeling, thus, acquiring a structural role [211]. There is some evidence for differential expression of three calponin isoforms (i.e. CNN1, CNN2 and CNN3) in SM and non-muscle tissues [209]. CNN1 is specifically expressed in SMCs and plays a role in SM contractility, while CNN2 is expressed in both SMCs and non-muscle cells, and CNN3 appeared to be expressed in embryonic development and myogenesis contributing to actin cytoskeleton-based functions [212].

- SMOOTHELIN

Smoothelin is a structural component of the contractile apparatus. It increases the contractile potential of SMCs and contributes to the maintenance of the contractile phenotype. In atherosclerotic lesions, the neointima contains little smoothelin until the plaque stops growing and smoothelin appears to be expressed in SMCs present at the cap. There is a co-localization of smoothelin and α-SMA as demonstrated in primary SMCs. Smoothelin decreases together with myosin heavy chain and partly α-SMA, but smoothelin downregulation is more rapid as compared to these other SMC contractile proteins. The lack of smoothelin leads to a decreased contractile potential of SMCs [213].

- DESMIN

Desmin is a muscle-specific protein that functions as subunit of intermediate filament in cardiac, skeletal and smooth muscle. It plays a role in cell-matrix interactions via its anchorage on dense bodies and membrane-associated dense bands, and thus, is involved in the correct transmission of contractile force to the cell surface. Desmin has been postulated to be essential for maintaining the structure and mechanical strength of the vascular wall [214]. The pre-atheroma stage revealed a lack of expression of desmin by SMCs and the switch to a synthetic phenotype [215].

Although many markers of contractile phenotype can be found (Figure 8), those previously discussed are the most widely used due to their specificity, sensitivity or abundance.

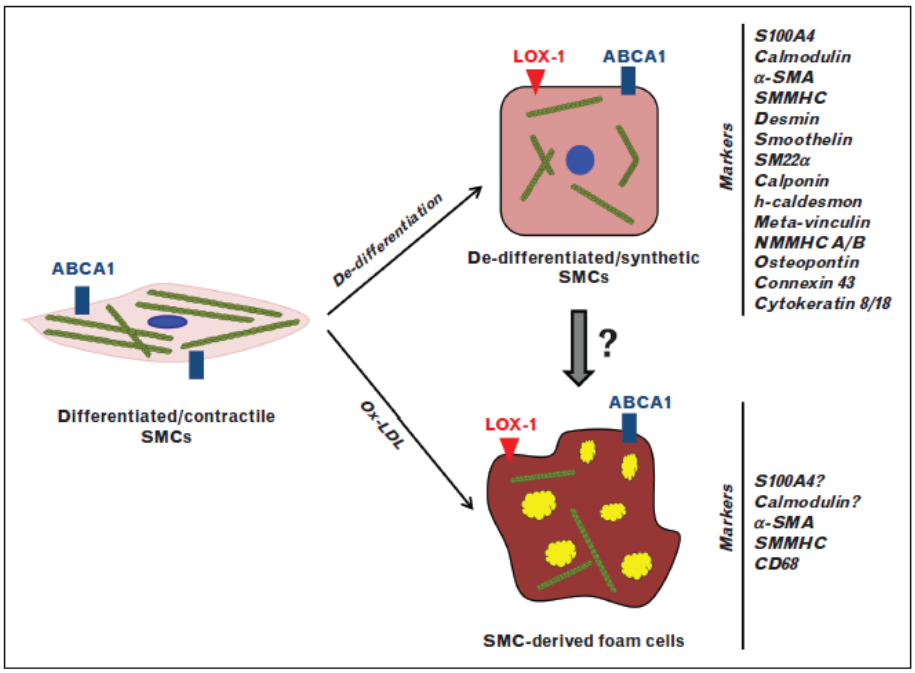

Figure 8. SMC phenotype markers [196]

There are also several markers of synthetic SMC phenotype, but these have been utilized less widely because, generally, they display less SMC specificity [203]. Myosin heavy chain 10 (MYH10 or SMemb) and vimentin are example of synthetic phenotype markers. The first is the non-muscle myosin heavy chain isoform and is expressed in SMCs undergoing growth and/or cell division, such as proliferating vascular SMCs in atherosclerotic neointima [216]. And the second is an intermediary filament that can be found in differentiated SMCs but it is co-expressed there with MYH11, desmin and α-SMA, while SMCs of synthetic phenotype expressed α-SMA and vimentin [215].

The recognition of the synthetic phenotype mostly relies upon the reduced expression, or the absence, of cytoskeletal markers of the mature or differentiated phenotype [196]. Relative expression of these and other marker proteins can be used to localize vascular SMCs on the contractile-synthetic state; however, during tissue repair there is a continuum process that give cells diverse functions [203]. Thus, the rigorous identification of mature SMC requires examination of multiple marker genes and if tested in tissues, appropriate localization within the medial layer of blood vessels or other SMC tissues is needed [175].

2. OBJECTIVES

SMCs are central players in carotid atherosclerosis plaque development. Although the precise mechanisms involved in plaque destabilization are not completely understood, it is known that SMC differentiation, proliferation and migration participate in plaque stabilization. The two

aims of this study are: first, to analyze expression patterns of genes involved in carotid atherosclerosis development (e.g., transcription factors of regulation of SMC genes) of SMCs located inside (PLQ: plaque) and outside (MIT: macroscopically intact tissue) the plaque lesion that may give clues about changes in phenotypic plasticity during atherosclerosis. And second, to perform a comparative transcriptomic analysis between the two groups, asymptomatic (Asympt) and symptomatic (Sympt), by applying RNAseq technology to understand the role of SMCs in symptomatology of carotid atherosclerosis.

3. SUBJECTS & METHODS

3.1. SMC CHARACTERIZATION

3.1.1. Patient selection

Patients who underwent carotid endarterectomy at Basurto University Hospital were selected to be included in the current study on the bases of clinical parameters (age, symptoms and no other clinical manifestations such as cardioembolic origin stroke). 39 patients were selected who were proposed for carotid endarterectomy by the committee of medical experts from Basurto University Hospital, who evaluated the clinical data of patients. MRI and cervical duplex was performed in all patients by the radiology service at the hospital. Patients with >70% stenosis and diagnosed cerebrovascular event were selected as Sympt patients (n=20), while patients with stenosis of >80% and no events were included as Asympt (n=19) in the study. Demographic and clinical data for the selected patients are summarized in Table 1. Carotid tissue sample was collected after surgery and transported immediately to the lab for cell isolation.

Patient Characteristics	**Asymptomatic**	**Symptomatic**	***p*-Value**
n	19	20	
Age	68 ± 9	71 ± 8	ns (0.5)
Sex	14 male/5 female	16 male/4 female	ns (0.6)
Risk Factor (%)			
Contralateral occlusion	66	61	ns (1.0)
Hypertension	66	69	ns (1.0)
Diabetes mellitus	51	8	ns (0.09)
Augmented cholesterol	83	62	ns (0.3)
Cardiopathy	0	23	ns (0.2)
Ischemic cardiopathy	41	46	ns (1.0)
Atrial fibrillation	9	23	ns (0.6)
Intermitent claudication	26	24	ns (1.0)
Tobacco	16	8	ns (0.6)
Medications (%)			

Statins	100	70	ns (0.1)
Anticoagulant	8	23	ns (0.2)

Table 1. Demographic and clinical data from asymptomatic and symptomatic patients. Statistical analysis was performed with the chi-square test for all parameters except age, for which the non-parametric Mann–Whitney U test was used. p-value ≤0.05 was considered significant.

This study was approved by the local ethical committee (Ethical committee of clinical research, Basurto University Hospital) and all carotid atheroma plaques were collected from patients who had signed written informed consent. This research was performed in agreement with the principles outlined in the Declaration of Helsinki.

3.1.2. Isolation of human vascular smooth muscle cells

SMCs were extracted from 39 carotid arterial atherosclerotic tissue samples. SMCs from plaque site area (PLQ-SMCs) and tissue from neighboring area (macroscopically intact tissue (MIT)-SMCs) were isolated for each sample. PLQ-SMCs were extracted from central site of atheroma plaque where maximum of the lesion is presented while MIT-SMCs come from furthest area from the center of the atheroma plaque. An enzymatic tissue digestion method was used to isolate and culture SMCs from atherosclerotic tissue samples in two consecutive digestions. First, tissue was digested by 3 hours incubation at 5% CO_2 and 37ºC with 300U/mL of Collagenase type I (ColI, 17018029, Thermo Fisher Scientific, Waltham, MA, USA) followed by a second digestion over night with 220U/mL of ColI at 5% CO_2 and 37ºC. Digested tissue was filtered by a 100 µm nylon Falcon™ Cell Strainer (CLS431752-50EA, Sigma-Aldrich, St Louis, MO, USA) to remove undigested tissue and then cells were plated in selective medium, which consist in:

- 2ng/ml FGFb (130-093-839, Miltenyi Biotec, Bergisch Gladbach, Germany)
- 20ng/ml IGF-1 (130-093-885, Miltenyi Biotec, Bergisch Gladbach, Germany)
- 0.5ng/ml EGF (130-0997-749 Miltenyi Biotec, Bergisch Gladbach, Germany)
- 5ng/ml Heparin (H3149, Sigma-Aldrich (St Louis, MO, USA)
- 5% newborn calf serum (N4762, Sigma-Aldrich, St Louis, MO, USA)
- 0.2µg/ml bovine serum albumin (BSA) (A9418, Sigma-Aldrich, St Louis, MO, USA)
- 2mM L-glutamin (G7513, Sigma-Aldrich, St Louis, MO, USA)
- 100µg/ml Streptomycin and 100U/ml Penicillin (P4458, Sigma-Aldrich, St Louis, MO, USA)
- Gibco's 231 medium (M231500, Thermo Fisher Scientific, Waltham, MA, USA).

This medium promotes selective SMC growth. All the experiments were carried out with cells in passage zero to reach a situation as close as possible to the real one.

Human iliac arterial smooth muscle cells (HIASMCs) were obtained from the Coriell Cell Repositories (Coriell AG11545, N.J., USA). These cells were obtained by explantation of iliac arterial tissue. The culture was grown on flasks coated with 0.1 % gelatin (G8090, Sigma-Aldrich, St. Louis, MO, USA) and with the medium 199 (11150059, Thermo Fisher Scientific, Waltham, MA, USA) supplemented with:

- 0.02 mg/ml endothelial cell growth supplement (ECGS; 02-102, Millipore, Billerica, MA, USA)
- 0.05 mg/ml heparin (H3149, Sigma-Aldrich, St Louis, MO, USA)
- 10% fetal bovine serum (FBS) (F7524, Sigma-Aldrich, St Louis, MO, USA)
- 2mM L-glutamin (G7513, Sigma-Aldrich, St Louis, MO, USA)
- 100µg/ml Streptomycin and 100U/ml Penicillin (P4458, Sigma-Aldrich, St Louis, MO, USA).

3.1.3. Flow cytometry

SMC cultures were trypsinized (11581861, Thermo Fisher Scientific, Waltham, MA, USA) and then fixed with 4% paraformaldehyde during 10 min at room temperature. SMCs were permeabilized with 0.5% saponin (S7900, Sigma-Aldrich St Louis, MO, USA) in phosphate-buffered saline (PBS) for 5 min and blocked with 1% BSA (A6003, Sigma-Aldrich St Louis, MO, USA) for 30 min. Primary antibodies used were anti-α SMA at 1/100 (ab66133, Abcam, Cambridge, UK), transgelin/SM22 monoclonal antibody at 1/100 (TAGLN) (60213-1-Ig, ProteinTech, Manchester, UK) and anti-CD31 (also called platelet and endothelial cell adhesion molecule 1, PECAM1) [EPR3094] antibody at 1/50 (ab76533, Abcam, Cambridge, UK) during 1h in shaking at room temperature. SMCs were washed with 5mM EDTA (E7889, Sigma-Aldrich St Louis, MO, USA) and 0.5% BSA in PBS and were incubated with secondary antibodies Alexa Fluor®488 goat anti-mouse IgG (H+L) (A-11001, Invitrogen, Thermofisher, Carlsbad, CA, USA) and Alex Fluor®647goat anti-rabbit IgG (H+L) (A-21244, Invitrogen, Thermofisher, Carlsbad, CA, USA) at 1/500 for 30 min in shaking and darkness. After washing cells, they were resuspended in 5mM EDTA and 0.5% BSA in PBS. Cells were analyzed using a Miltenyi MACS Quant flow cytometer (Miltenyi Biotec, Bergisch Gladbach, Germany).

3.1.4. Gene expression analysis

RNA was extracted from SMCs with PureLink® RNA mini kit (1218308A, Thermo Fisher Scientific, Waltham, MA, USA) followed by DNaseI treatment (12185010, Thermo Fisher

Scientific, Waltham, MA, USA). RNA integrity (RIN > 9) was analyzed by using RNA 6000 Nano Chips on the Bioanalyzer Agilent 2100 (Agilent Technologies, Palo Alto, CA, USA), and then, RNA was retrotranscribed with High-Capacity cDNA Reverse Transcription Kit (4368814, Thermo Fisher Scientific, Waltham, MA, USA) using 160ng. Gene expression analysis was carried out using Fast SYBR® Green Master Mix (4385614, Thermo Fisher Scientific, Waltham, MA, USA) in ABI7500 Fast Real-Time PCR instrument (Applied Biosystems™, CA, USA). Primers for genes related with contractile phenotype were *ACTA2*, *MYH11*, caldesmon (*CALD1*), calponin 1 (*CNN1*) and *TAGLN*; for synthetic phenotype were *MYH10*, intercellular adhesion molecule 1 (*ICAM1*), secreted phosphoprotein 1 *(SPP1*), *MMP3*, *7*, *9*, *TIMP1* and microtubule-associated protein 1 light chain 3 B (*MAP1LC3B*); primers for transcription factors related with specific SMCs differentiation were MKL1/Myocardin like 2 (*MKL2*), serum response factor (*SRF*), kruppel like factor (*KLF*) 4 and 5; primers for genes related with macrophage-like phenotype were CD68 molecule (*CD68*) and galectin 3 (*LGALS3*) (Table 2). Additionally, SYBRgreen technology was used for gene expression of C-X-C motif chemokine ligand 9 (*CXCL9*) and *CXCL10*, CD5 molecule like (*CD5L*) and bone morphogenetic protein 2 (*BMP2*) for quality control of pure SMCs used for RNAseq analysis. Glyceraldehyde-3-phosphate dehydrogenase (*GAPDH*), ribosomal protein L41 (*RPL41*) and β-actin (*ACTB*) were tested as housekeeping genes. The geometric mean of *GAPDH* and *RPL41* was used for data analysis due to their stable gene expression values across samples [217]. PCR amplification efficiencies were in all cases close to 100%. Results were analyzed using ΔΔCt method [218]. We analyzed gene expression by taking into account the localization of SMCs, PLQ-SMCs (n = 39), or MIT-SMCs (n = 39) using the Wilcoxon matched-pairs signed rank test. The Mann–Whitney U test was used to analyze gene expression patterns between plaque SMCs from Asympt (n = 20) and Sympt (n = 19) patients, as well as the expression levels of 15 μM 7-ketocholesterol (7-KC)-treated HIASMCs versus not-treated HIASMCs. Statistical analysis was performed with GraphPad Prism 5 software. *p*-value < 0.05 was considered significant.

Gene symbol	Gene name	Accesion number	Assay code
ACTA2	α-smooth muscle actin	NM_001613	Hs.PT.56a.2542642
ACTB	Actin β	NM_001101	QT00095431
BMP2	Bone morphogenetic protein 2	NM_001200	Hs.PT.56a.28076895
CALD1	H-caldesmon	NM033138	QT00997899
CD5L	CD 5 molecule like	NM_005894	Hs.PT.56a.2816096
CD68	CD68 molecule	NM_001040059	Hs.PT.58.2488447.g
CNN1	Calponin 1	NM_001229	Hs.PT.58.38799164
CXCL9	C-X-C motif chemokine ligand 9	NM_002416	Hs.PT.56a.27316119
CXCL10	C-X-C motif chemokine ligand 10	NM_001565	Hs.PT.56a.3790956.g
GAPDH	Glyceraldehyde-3-phosphate dehydrogenase	NM_002046	Hs.PT.39a.22214836

ICAM1	Intercellular adhesion molecule-1	NM_000201	Hs.PT.56a.4746364
KLF4	Kruppel like factor 4	NM_004235	Hs.PT.58.45542593
KLF5	Kruppel like factor 5	NM_001730	Hs.PT.56a.40282397
LGALS3	Galectin 3	NM_001177388	Hs.PT.58.1435723
MAP1LC3B	Microtubule associated protein 1 light chain 3 beta	NM_022818	QT00055069
MKL2	MKL1/myocarkin like 2	NM_002446	Hs.PT.85.19760686
MMP3	Matrix metallopeptidase 3	NM_002422	QT00060025
MMP7	Matrix metallopeptidase 7	NM_002423	QT00001456
MMP9	Matrix metallopeptidase 9	NM_004994	QT00040040
MYH10	Myosin heavy chain 10	NM_001256012 NM_001256095 NM_005964	QT00005117
MYH11	Myosin heavy chain 11	NM_002474	Hs.PT.58.2909933
RPL41	Ribosomal prtein L41	NM_001035267	Hs.PT.58.38804367
SPP1	Secreted phosphoprotein 1	NM_001040058	Hs.PT.58.19252426
SRF	Serum response factor	NM_003131	Hs.PT.58.4857809
TAGLN	Transgelin	NM_001001522 NM_003186	QT01678516
TIMP1	Tissue inhibitor of metallopeptidase 1	NM_003254	QT00084168

Table 2. List of primers used in gene expression analysis for SMC phenotypic characterization.

3.1.5. Western blot

Cell lysis was performed with RIPA lysis buffer (150 mM TrisHCL, 150 mM NaCl, 0.5% Deoxycholate, 0.1% SDS, 1% NP-40) for 30 min at 4 °C followed by centrifugation at 20,000*xg* for 10 min. Cell lysates were quantified by Pierce™ BCA Protein Assay Kit (23225, Thermo Scientific) and 12µg protein were loaded into 6%- or 12% SDS-PAGE gels with reducing loading buffer. Then, proteins were transferred from SDS-PAGE gel to 0.45 µm-pore PVDF membrane, which was blocked with 2% casein solution. Inmunodetections were done by incubation with following primary antibodies: anti-smooth muscle MYH11 (ab82541, Abcam, Cambridge, UK), ACTA2 (23081-1-AP, ProteinTech, Manchester, UK), TAGLN (60213-1-Ig, ProteinTech, Manchester, UK) and anti-CD31 antibody [EPR3094] antibody (ab76533, Abcam, Cambridge, UK) and then washed 3 times with TBS-Tween. The secondary antibodies were anti-rabbit IgG, horseradish peroxidase linked (#7074, Cell Signaling Technology, MA, USA) and anti-mouse IgG, horseradish peroxidase linked and anti-ACTIN antibody (A2066, Sigma-Aldrich, St Louis, MO, USA) as well as anti-GAPDH antibody (MAB374, Millipore, Billerica, MA, USA) as housekeeping were used for normalization. Proteins were detected with Immobilon™ Western Chemiluminescence HRP Substrate detection reagent (WBKLS0500, Millipore, Billerica, MA, USA) and were visualized with the ChemiDoc™XRS Imaging System (Bio-Rad, Richmond, CA, USA). Data analysis was done by densitometry scanning by

comparing MIT and PLQ cells and additionally, between A and S plaque SMCs, both using Image Lab™ Software (Bio-Rad, Hercules, CA, USA).

3.1.6. Confocal microscopy

Cells were grown on 24 well plates with 144mm round glass coverslips, fixed in ice-cold methanol for 10 min at room temperature and then blocked in PBS/3% w/v BSA (A6003, Sigma-Aldrich St Louis, MO, USA) for 30 min and stained with anti-smooth muscle myosin heavy chain 11 antibody (ab82541, Abcam, Cambridge, UK) for 1h at room temperature. Cells were washed with PBS and incubated with Alexa FluorR 488 goat anti-rabbit IgG (H + L) secondary antibody (A-11008, Invitrogen, Thermofisher, Carlsbad, CA, USA) for 45 min at room temperature in darkness and DNA was counterstained with 4′,6-diamino-2-fenilindol (DAPI). After three washes, coverslips were mounted in Fluoromount™ Aqueous Mounting Medium (F4680, Sigma-Aldrich, St Louis, MO, USA). Image acquisition was performed with Leica TCS STED CW SP8 super-resolution microscope with a 40x or 10x lenses and recording optical sections every 0.3 μm. Image analysis was done using ImageJ software (National Institute of Health, USA). Image analysis was done analyzing staining fluorescence of each cell per cell area in MIT and PLQ SMCs with ImageJ software (National Institute of Health, Bethesda, MD, USA).

3.2. RNA-SEQ TECHNOLOGY

3.2.1. Patient selection for SMCs isolation from Sympt and Asymptc carotid plaques

Sympt patients (n=7) were identified as those with >70% stenosis and presenting symptoms of transient ischemic attack or ipsilateral stroke within the past 6 months, while Asympt patients (n=7) were those with stenosis >80% without any presence of cerebrovascular disease. Degree of stenosis was evaluated with carotid cervical Eco-Doppler ultrasound and tomographic angiography according to established criteria [219]. Brain MRI was performed in all patients before and after the surgery to monitor potential complications. All patients were evaluated before and after the operation by a specialized neuropsychologist. The analysis carried out by the neuropsychologist were Mini Mental State Examination (MMSE) to evaluate the general state of the patient; WMS-III that evaluates memory; the subtests of matrices and cubes of the WAIS-III to analyze executive functions; and the speed of processing was evaluated through the number key subsets of the WAIS-III. Neuropsychiatric disorders were evaluated through the Neuropsychiatric Inventory (NPI), and assessment of impairment and disability were measured through the Blessed Scale, The Informant's test and with the interview for the impairment of activities of daily living in the dementia.

Only patients who fulfill all the required parameters were finally included in the study (Table 3).

Other required parameters for selection of eligible patients to be included in this study were defined as: (1) age (70 years±12); (2) no other medical conditions and (3) no previous contralateral endarterectomy and (4) no other cause of stroke, such us cardioembolic. During the recruitment period several patients were excluded from the study because they presented at least one of the following problems: (1) patients showing sign of dementia according to the minimental state examination test (MMSE); (2) patients with psychological alterations due to drugs or cerebral surgery intervention; (3) patients who presented medical or surgery complications that may alter the intellectual capacity and/or the neuroimaging test and (4) patients who were not able to perform the neuropsychological test due to difficulty of communication (i.e. vision impairment).

Patient Selection	**All**	**Symptomatic**	**Asymptomatic**
Number, n	14	7	7
Years	68	68 ± 8	68 ± 8
Sex M/F, n	11/3	4/3	7/0
Treatment with statins	14	7	7
Risk factors (%)			
Diabetes Mellitus	100	43 (3)	57 (4)
Dyslipidemia	100	100 (7)	100 (7)
Arterial hypertension	100	100 (7)	100 (7)
Tobacco	100	57 (4)	43 (3)

Table 3. Demographic data of cohort of samples from Basurto University Hospital

3.2.2. RNA library assembly

Ribosomal RNA removal was performed with the Ribo-Zero rRNA removal kit (MRZH11124, Illumina Inc, San Diego, CA, USA). Generation of libraries was performed with the TruSeq Stranded Total RNA library Prep kit (20020596, Illumina Inc, San Diego, CA, USA) following manufacture's recommendations. We started from 2 μg of total RNA (RIN > 9) libraries, which were sequenced using a HiSeq2000 instrument (Illumina Inc, San Diego, CA, USA). Sequencing readings were paired-end with a length of about 100 bp reading performed in 14 samples. The estimated coverage was around 60 million reads per sample (3 lanes). Library generation and RNA sequencing was done at Sistemas Genómicos S.L. (Valencia, Spain) following manufacturer´s instructions.

3.2.3. RNA transcriptomics analysis

The quality control of the raw data was performed using the FastQC tool. Then, the raw paired-end reads were mapped against the human genome provided by Ensembl database (version

GRchr37/hg19) using tophat2 algorithm [220]. Insufficient quality reads (Phred score < 10; quality of the identification of the nucleobases generated) were eliminated using the Picard Tools software (version 1.129) (http://picard.sourceforge.net). Gene predictions were estimated using the Cufflinks method [221] and the expression levels were calculated using the HT Seq software (version 0.6.0, http://www-huber.embl.de/users/anders/HTSeq/). This method employs unique reads for the estimation of gene expression and eliminates the multimapped reads. Differential expression of genes (DEG) and isoforms (DEI) analysis between Sympt and Asympt was done by using statistical packages designed by Python and R, i.e. DESeq2 method (version 3.4) [222]. Finally, we selected differentially expressed genes with a *p*-value adjusted (P_{adj}) by false discovery rate (FDR) < 0.05 [223] to avoid identification of false positives across the differential expression data and, a fold change (FC) of at least 1.5.

3.2.4. Gene Set functional enrichment analysis and network analysis

Differentially expressed sets were processed using ClusterProfiler [224], a bioconductor package, to search for biological processes involved in plaque instability. This tool screens for genes in specific databases (i.e. Gene Ontology – GO, Kyoto Encyclopedia of Genes and Genomes – KEGG, DRUG, etc.) to evaluate biological annotations that rise as over-represented with respect to the whole genome. A *p*-value of 0.05 adjusted by FDR, called *q*-value, was used to determine a functional category as statistically significant or over-represented [223]. Gene networks were generated using GeneMANIA software (http://www.genemania.org/). GeneMANIA uses functional interconnections among genes from published data to generate a global view of interactions of genes. MCODE tool (http://apps.cytoscape.org/apps/mcode) was used to identify highly interconnected clusters in a network.

3.2.5. Digital PCR on Fluidigm Biomark platform

Assays for 41 genes identified in our RNAseq DEG analysis and 4 housekeeping genes chosen from our own DEG as those showing no variability between samples (G3BP stress granule assembly factor 2 (*G3BP2*), muskelin1 (*MKLN1*), echinoderm microtubule associated protein like 3 (*EML3*) and AarF domain containing kinase 5 (*ADCK5*)) were use for validation (Table 4).

Gene Symbol	Gene name	Accesion number	Assay ID
ANXA10	Annexin A10	NM_007193	Hs.PT.58.258700
ANXA3	Annexin A3	NM_005139	Hs.PT.56a.103535
BMP2	Bone morphogenetic protein 2	NM_001200	Hs.PT.56a.28076895
DEPP1	DEPP1, autophagy regulator	NM_007021	Hs.PT.58.40344222

CA12	Carbonic anhydrase 12	NM_001218	Hs.PT.56a.24934240
DIRAS3	DIRAS family GTPase 3	NM_004675	Hs.PT.58.971668
GULP	GULP, Enguylfment adaptor PTB domain conatining 1	NM_001252668	Hs.PT.58.26109032
ID1	Inhibitor of DNA binding 1	NM_002165	Hs.PT.58.45682625.g
ID4	Inhibitor of DNA binding 4	NM_001546	Hs.PT.58.26292654.g
ITGA7	Integrin subunit alpha 7	NM_001144997	Hs.PT.58.19415929
KCNE4	Potassium Voltage-Gated Channel Subfamily E Regulatory Subunit 4	NM_080671	Hs.PT.58.46324308
KLF5	Kruppel like factor 5	NM_001730	Hs.PT.56a.40282397
MGST1	Microsomal glutathione S-transferase 1	NM_001260511	Hs.PT.58.38644776
MOCOS	Molybdenum cofactor sulfurase	NM_017947	Hs.PT.58.3583296
NPPC	Natriuretic peptide C	NM_024409	Hs.PT.58.40078220
PTHLH	Parathyroid hormone like hormone	NM_002820	Hs.PT.58.41054442
SMAD9	SMAD family member 9	NM_001127217	Hs.PT.58.18749479
ST6GALNAC5	ST6 N-Acetylgalactosaminide Alpha-2,6-Sialyltransferase 5	NM_030965	Hs.PT.58.27746012
TMTC2	Transmembrane And Tetratricopeptide Repeat Containing 2	NM_152588	Hs.PT.58.2079491
RGS2	Regulator of G protein signaling 2	NM_002923	Hs.PT.58.22488494
TMEM35A	Transmembrane protein 35A	NM_021637	Hs.PT.58.2938658
CHODL	Chondrolectin	NM_024944	Hs.PT.58.5002738
ABCG2	ATP Binding Cassette Subfamily G Member 2	NM_001257386	Hs.PT.58.39633789
ADAMTS7	ADAM Metallopeptidase With Thrombospondin Type 1 Motif 7	NM_014272	Hs.PT.58.20739942
DHRS3	Dehydrogenase/Reductase 3	NM_004753	Hs.PT.58.21163170
EPHA4	EPH receptor A4	NM_004438	Hs.PT.58.40080791
EPHB2	EPH receptor B2	NM_017449	Hs.PT.58.19695111
ESM1	Endothelial cell specific molecule 1	NM_001135604	Hs.PT.58.19279572
FRMD3	FERM Domain Containing 3	NM_001244960	Hs.PT.58.25637022
HAPLN1	Hyaluronan And Proteoglycan Link Protein 1	NM_001884	Hs.PT.58.39802081
IL17RD	Interleukin 17 receptor D	NM_017563	Hs.PT.58.15565560
MYO18B	Myosin XVIIIB	NM_032608	Hs.PT.58.947408
PDK1	Pyruvate Dehydrogenase Kinase 1	NM_002610	Hs.PT.58.19794808
PFKFB4	6-Phosphofructo-2-Kinase/Fructose-2,6-Biphosphatase 4	NM_004567	Hs.PT.58.2331520

SOCS3	Suppressor Of Cytokine Signaling 3	NM_003955	Hs.PT.58.4303529
SYNE3	Spectrin Repeat Containing Nuclear Envelope Family Member 3	NM_152592	Hs.PT.58.21438299
TBX18	T-box 18	NM_001080508	Hs.PT.58.20293106
TNFAIP8L3	TNF alpha induced protein 8 like 3	NM_207381	Hs.PT.58.549257
DDR2	Discoidin Domain Receptor Tyrosine Kinase 2	NM_001014796	Hs.PT.58.26536814
RDH10	Retinol Dehydrogenase 10	NM_172037	Hs.PT.58.4062554
ZSCAN31	Zinc Finger And SCAN Domain Containing 31	NM_001243241	Hs.PT.58.39448911
G3BP2	G3BP Stress Granule Assembly Factor 2	NM_012297	Hs.PT.58.1944755
MKLN1	Muskelin 1	NM_001145354	Hs.PT.58.2002335
EML3	Echinoderm microtubule associated protein like 3	NM_153265	Hs.PT.58.3509596
ADCK5	AarF Domain Containing Kinase 5	NM_174922	Hs.PT.58.786984

Table 4. List of primers used in gene expression analysis for RNAseq results validation.

RNA was converted into cDNA using the AffinityScript Multiple Temperature cDNA Synthesis kit (200436, Agilent, Technologies, Santa Clara, CA, USA) following manufacturer's instructions. Gene expression analysis was performed with the Fluidigm Biomark 48.48 dynamic arrays (Fluidigm Corp., South San Francisco, CA, USA) and pre-designed PrimeTime qPCR assays (IDT, Leuven, Belgium) in 24 samples in duplicates; 13 samples were corresponding to those used in RNAseq and 11 new extra samples for RNAseq result validation. Patient characteristics for the additional 11 samples are giving in Table 5. Gene expression levels of housekeeping genes were used as endogenous control to normalize our samples. Relative expression was calculated using the ΔΔCt method [218]. The statistical significance of gene expression levels between Sympt and Asympt was analyzed with the GraphPad Prism 5 (GraphPad Software, La Jolla, CA, USA) using the non-parametric Mann-Whitney U-test (one-tailed) and level of significance was defined at $p < 0.05$. All PrimeTime qPCR assays showed amplification efficiencies close to 100%.

Patient Selection	All	Symptomatic	Asymptomatic
Number, n	11	4	7
Years	68	68 ± 8	68 ± 8
Sex M/F, n	7/4	1/3	6/1
Treatment with statins	10	3	7
Risk factors (%)			
Diabetes Mellitus	54 (6)	75 (3)	43 (3)
Dyslipidemia	90 (10)	100 (4)	86 (6)

Arterial hypertension	81 (9)	75 (3)	86 (6)
Tobacco	46 (5)	75 (3)	29 (2)

Table 5. Demographic data of cohort of samples from Basurto University Hospital.

4. RESULTS

4.1. SMC ANALYSIS

4.1.1. Selection of SMC culture method

There are multiple isolation methods for SMC purification including enzyme-dispersed cells method, reaggregation, free-floating explants and substrate-attached explants. The choice of one technique or enzyme over another is arbitrary and based on experience rather than scientific theory [225]. We have chosen substrate-attached explants method because is recommended if large quantity of cells is required and starting material is small tissue such as carotid artery [226]. For that, immediately after extraction, the specimens were transported to Neurogenomiks lab (University of Basque Country and Achucarro Basque Center for Neuroscience). Fresh carotid artery tissue samples were processed on a sterile dissection board and were washed with Hank`s balanced salt solution (HBSS + 100µg/mL gentamycin + 0,025M HEPES + 20mM Bicarbonate) to clear of peripheral blood and of any thrombotic material. First, the artery was cut longitudinally with the luminal surface upward and endothelium was removed along the whole length of the artery by scraping the cell layer off with a sterile scalpel blade. Then, artery was cut into 2mm3 pieces and placed on the surface of a 25cm2 culture flask ensuring that the luminal surface was in contact with the flask wall. 12-16 cubes were distributed evenly on the surface of 25cm2 flask and a small drop of serum-containing medium was placed on each cube. To facilitate adherence of the explanted tissue to the culture plastic substrate, the flask was kept upright for 2-4h in the incubator at 37ºC and 5%CO2 with 5 mL serum containing medium in the bottom of the flask. After, the flask was carefully placed horizontal, such that the medium completely covered the attached explants, and was maintained in the incubator. Every 4 days, any unattached explants were removed and half of the medium was replaced with fresh pre-warmed serum-containing medium. It is assumed that cells will initially migrate out from the explants within 1 to 2 weeks, and after 3 to 4 weeks, there should be sufficient density of SMCs around the explants for removal of the tissue. However, cell density was not enough to carry out expected gene expression analysis.

Although the ultimate goal of cell isolation is to yield viable and functional dissociated cells [225], the cell density of cultures is also conditioning factor for experiments that will be carry out. In this context, we decided to try enzyme-dispersed cell method. For that, after wash carotid atherosclerotic human plaques, they were digested with collagenase type I enzyme. First, we

decided to cut the tissue as small as possible, instead of cut tissue into 2mm3 as in explants method, and then, we performed 3 hours digestion at 300 U/mL concentration of collagenase type I. Digested tissue was submitted to another digestion, in this case overnight, with 220 U/mL collagenase type I and afterwards was filtered by a 100 μm nylon Falcon™ Cell Strainer for removing undigested material. Second digestion yielded higher amount of cells. Therefore, this method allowed us to obtain the number of cells necessary to carry out the designed experiments. 200.000 cells were plated in selective medium for human SMC growth (see Materials and Methods). All the experiments were carried out with cells in passage zero to reach a situation as close as possible to the real one.

From here on, when processing the sample, it was separated into two parts, MIT and PLQ. Division in these two parts was performed as Figure 9 shows.

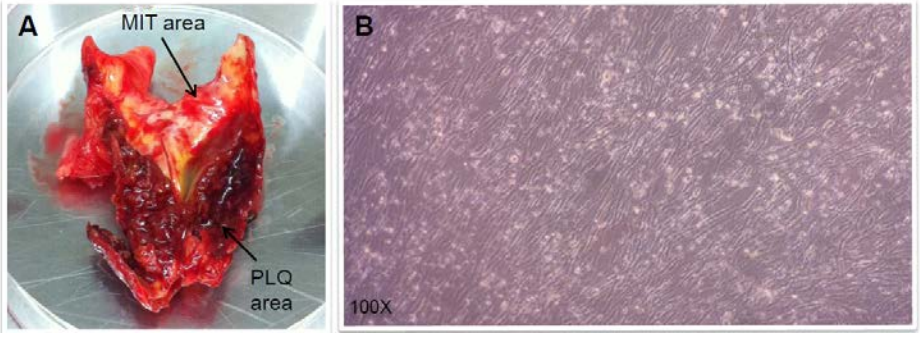

Figure 9. (A) Illustrative photo of a carotid endarterectomy specimen. Macroscopically intact tissue and atherosclerotic tissue is visualized on sample. **(B)** SMC in culture medium attached to the culture flask.

4.1.2. Purity control

We have done some/several control tests with the aim to confirm the purity of our SMC cultures and discard any contamination with another cell type (i.e. ECs and fibroblasts).

Human carotid atherosclerotic plaque tissues obtained by carotid endarterectomy surgery were enzymatically digested and once cells were totally disaggregated from tissue, we routinely analyzed the presence of two specific markers of SMCs i.e., ACTA2 and TAGLN, together with that of endothelial cell marker PECAM-1 by flow cytometry in 39 PLQ-SMCs and 39 MIT-SMCs. SMC suspension was 90% ACTA2+ and almost 100% of SMCs isolated from carotid tissue were TAGLN+, whereas endothelial cell marker PECAM-1 was nearly absent with just 2% of cells expressing it, together indicative for SMCs cultures devoid of endothelial cells following cultivation in SMC-selective culture medium. Figure 10 shows an illustration of flow cytometry detection of those markers in one representative cell culture.

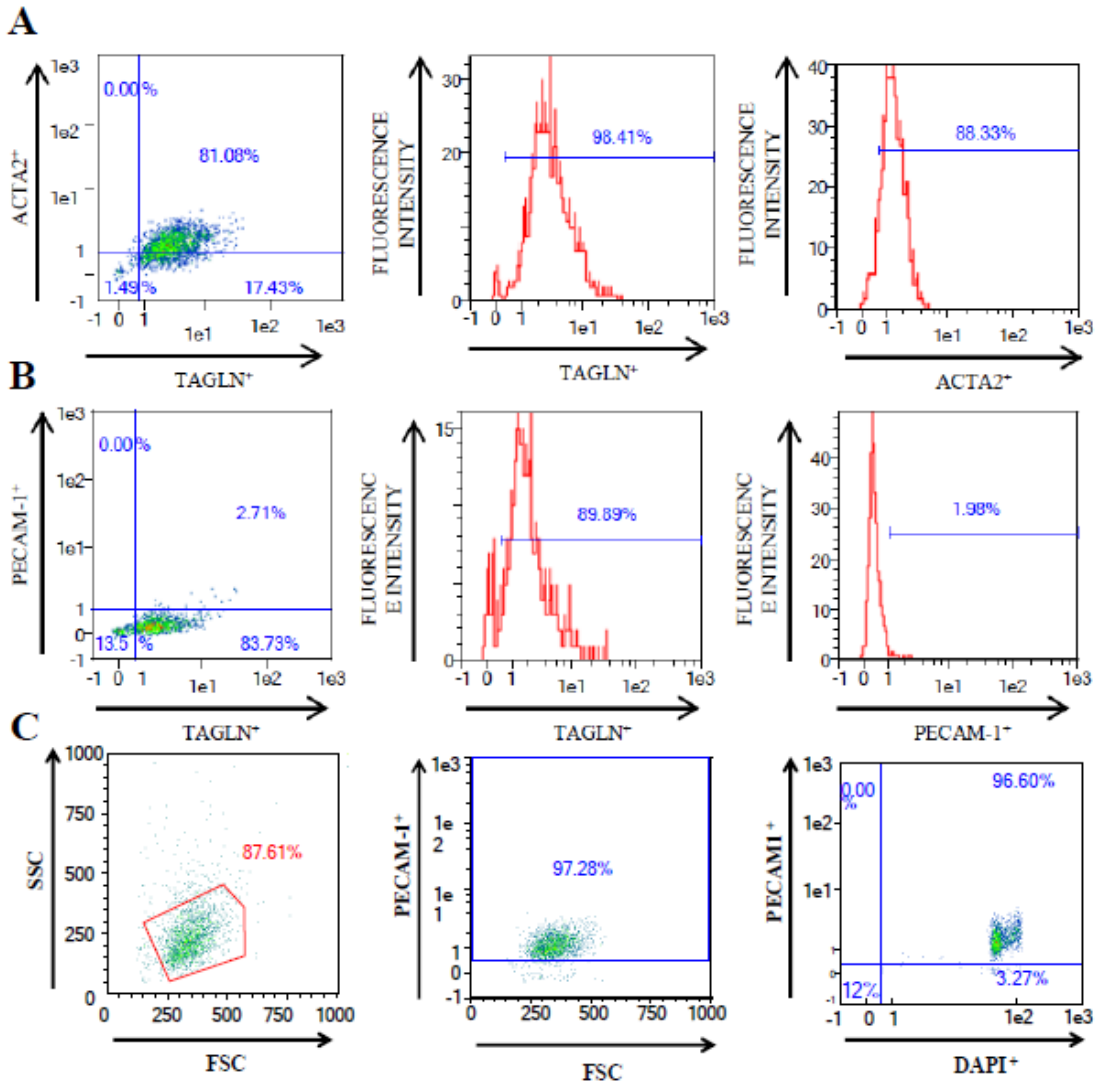

Figure 10. Flow cytometry graphs indicating staining of SMC and EC markers in SMC cultures. **(A)** panel shows ACTA2$^+$ and TAGLN$^+$ staining in culture SMCs. **(B)** panel demonstrates absence of PECAM-1$^+$ staining in SMC population. **(C)** panel shows PECAM-1$^+$ detection in U937 cell line as positive control.

In addition to flow cytometry, quality control of pure SMC culture was also performed by identification of the presence of SMC-specific marker MYH11 by microscopy. Additionally, cells were stained with DAPI with the aim to detect MYH11 not-expressing cells. Figure 11A shows representative images of four cultures of SMCs isolated from carotid plaques with positive staining for MYH11, DAPI-stained nuclei and merged. The number of MYH11-positive cells in our cultures was identified by comparing the total number of cells (DAPI-stained nuclei) with the MYH11 positive stained cells (Figure 11B) and this revealed absence of contaminating cells (i.e. fibroblast, endothelial cells, etc.).

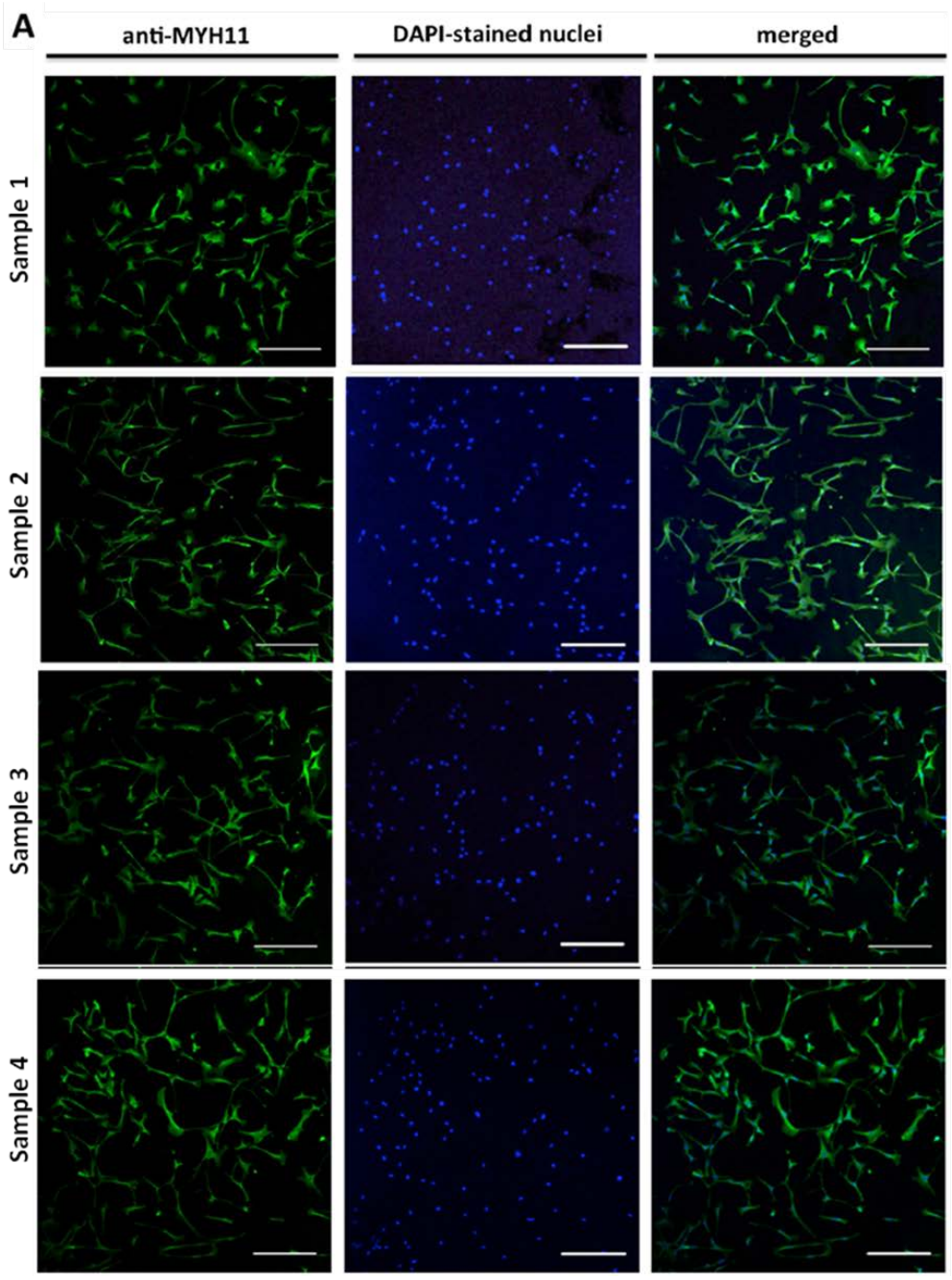
A
anti-MYH11
DAPI-stained nuclei
merged
Sample 1
Sample 2
Sample 3
Sample 4

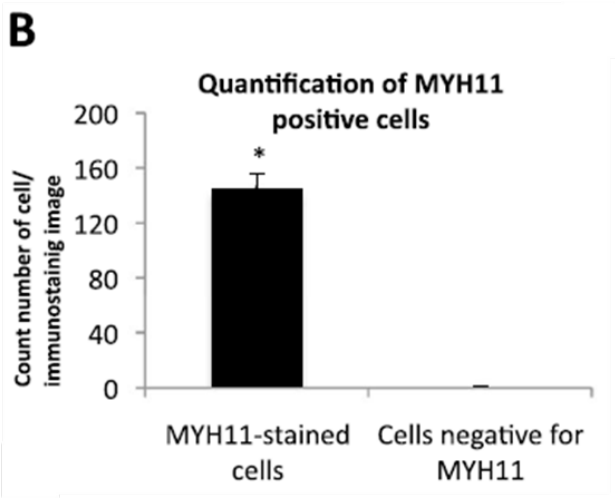
B
Quantification of MYH11 positive cells
Count number of cell/ immunostainig image
200
160
120
80
40
0
*
MYH11-stained cells
Cells negative for MYH11

Figure 11. Immunolocalization of MYH11 in primary carotid SMCs. (A) Representative confocal images of MYH11-positive cells (left panel), DAPI-stained cells (central panel) and merged (right panel). Magnification: the horizontal bars represent a scale of 250µm. **(B)** Quantification of MYH11-positive cells versus total number of cells (DAPI-stained nuclei). Data are mean ± SD. *p< 0.05.

Then, we analyzed intracellular expression of SMC specific protein MYH11, ACTA2 and TAGLN, and endothelial specific protein PECAM-1. Western blot analysis showed that isolated SMC cultures all expressed SMC markers, while they were negative for endothelial marker PECAM-1 (Figure 11). Cell lysates from different cell lines showed in Figure 12A are part of the purity control of our SMC cultures. SMC markers are not expressed by cells that are not SMCs, since they are negative controls for SMCs and/or positive controls for EC marker. GAPDH was used as loading control as in Figure 12B, where a set of SMC cultures expressing ACTA2 and TAGLN proteins are shown. Figure 12C shows protein identification by western blot using α-ACTIN, α-MYH11 and α-PECAM1 antibodies in cell lysates extracted from all SMC cultures used for RNAseq analysis. Jurkat and U937 cell lysates were used as positive control of PECAM1 detection. There is a positive detection of PECAM1 and negative detection of MYH11 in Jurkat and U937 cells.

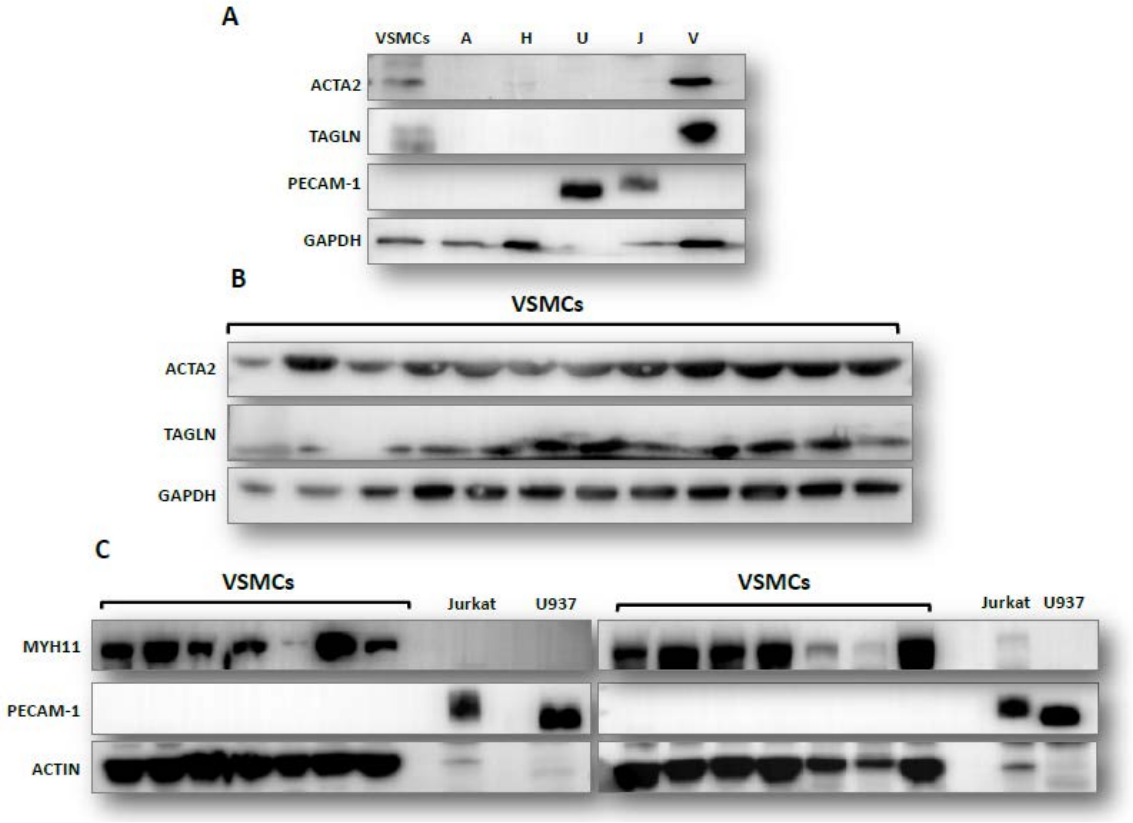

Figure 12. Western blot detection of SMC markers in SMC cultures. (A) Detection of ACTA2, TAGLN and EC marker PECAM-1 in different cell lines. **(B)** Example of ACTA2 and TAGLN detection

in SMC cultures. GAPDH was used as loading control. **(C)** MYH11 and PECAM1 in our SMCs cultures. ACTIN was used as loading control. A: A549 cell line, H: HEK293T cell line, U: U937 cell line, J: Jurkat cell line. V: HIASMCs.

CXCL9 and *CXCL10* along with *CD5L* specific markers for macrophages were tested in the 14 samples used for RNAseq analysis. CXCL9 is a chemotactic molecule for lymphocytes T and CXCL10 stimulates migration of monocytes, natural killers and T lymphocytes, while CD5L is a secreted molecule involved in lipid synthesis regulation [227–229] and has been shown to be expressed in foam cells induced by oxLDL [230]. As positive control for *CXCL9, 10* and *CD5L* we used RNA extracted from monocytic cell line U937 induced with lipopolysaccharide (LPS: 100 ng/ml) during 6 hours and $CD14^+$ monocyte-derived DCs treated with LPS (100 ng/ml) for 6 hours.

RNA extracted from SMCs of Asympt and Sympt patients showed no expression of *CXCL9*, *CXCL10* and *CD5L*. In contrast, carotid atheroma plaques, expected to contain macrophages, exhibited high expression of *CXCL9*, *CXCL10* and *CD5L*, similar to positive controls including human LPS-induced DCs and LPS-induced U937 monocytic cell line (Figure 13). For these quality control analyses we routinely used passage 0–2 cell cultures.

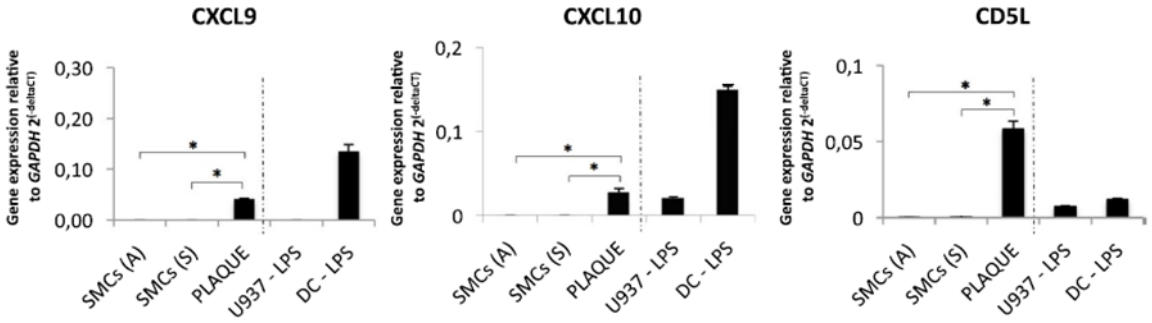

Figure 13. Gene expression quantification of macrophages markers *CXCL9, CXCL10* and *CD5L* performed by qPCR using RNA extracted from: (i) SMCs from asymptomatic patients (average of 7 samples); (ii) SMCs from symptomatic patients (average of 7 samples); (iii) atheroma plaque (average of 3 samples); (iv) Monocyte cell line U937 treated with LPS; (v) CD14+ monocyte-derived dendritic cells treated with LPS. The analysis was performed using the ΔCt method and expressed as $2(-\Delta Ct)$. The statistical significance was calculated using the non-parametric Mann-Whitney U-test (one-tailed) and level of significance was defined at $p < 0.05$.

4.1.3. SMC characterization

SMC-Specific Gene Expression Pattern Shows Phenotypic Modulation in SMCs Isolated from Human Carotid Plaques.

Gene expression levels of contractile and synthetic phenotype markers were analyzed in SMCs isolated from both the lesion and MIT areas of carotid atherosclerosis plaques. Although *ACTA2*

expression did not show any differences, *MYH11*, *CALD1*, and *CNN1* appeared to be downregulated in the lesion area compared to the MIT area (Figure 14A). *MYH11* displayed decreased expression levels (*p*-value= 0.03) in PLQ-SMCs compared to MIT-SMCs with a FC of -30.67, and similarly, *CALD1* (*p*-value = 0.001) was decreased with an FC value of -10.59. In contrast, *TAGLN*, M*YH10*, and *ICAM1* expression was similar between PLQ-SMCs and MIT-SMCs (Figure 14A). The synthetic indicator *SPP1* was upregulated in PLQ-SMCs (*p*-value = 0.009). Furthermore, *MAP1LC3B*, which is related to phenotype switching by playing a role in contractile protein removal, was also significantly over-expressed in PLQ-SMCs vs. MIT-SMCs (*p*-value = 0.0181) (Figure 14A).

Human iliac arterial smooth muscle cells (HIASMCs), from a healthy donor treated with 7-ketocholesterol (7-KC), an oxysterol which is abundant in the plaque, were used to mimic the physiological environment to which SMCs are exposed during atherosclerosis development. HIASMCs showed also a marked decrease of contractile biomarkers when treated during 24 h with 15 µM 7-KC (Figure 14B).

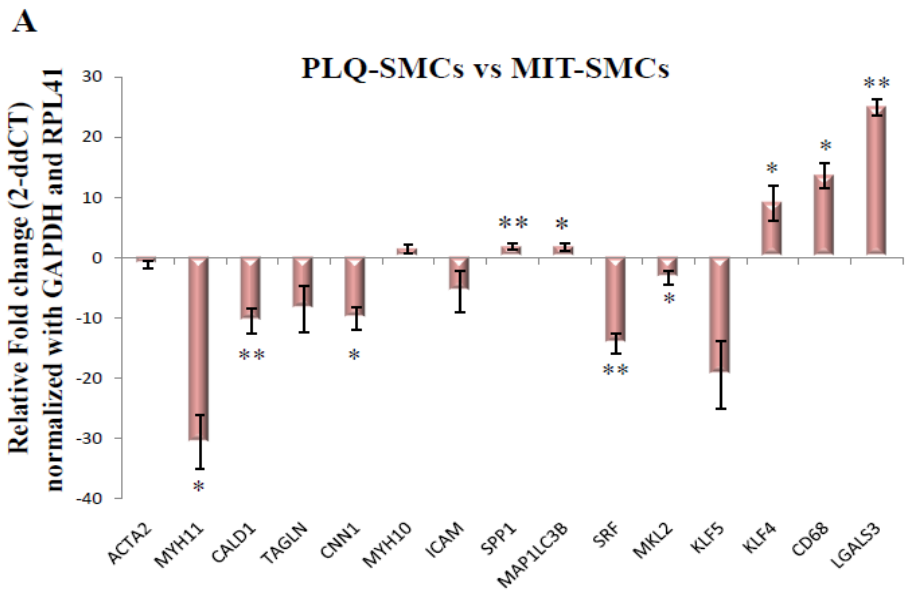

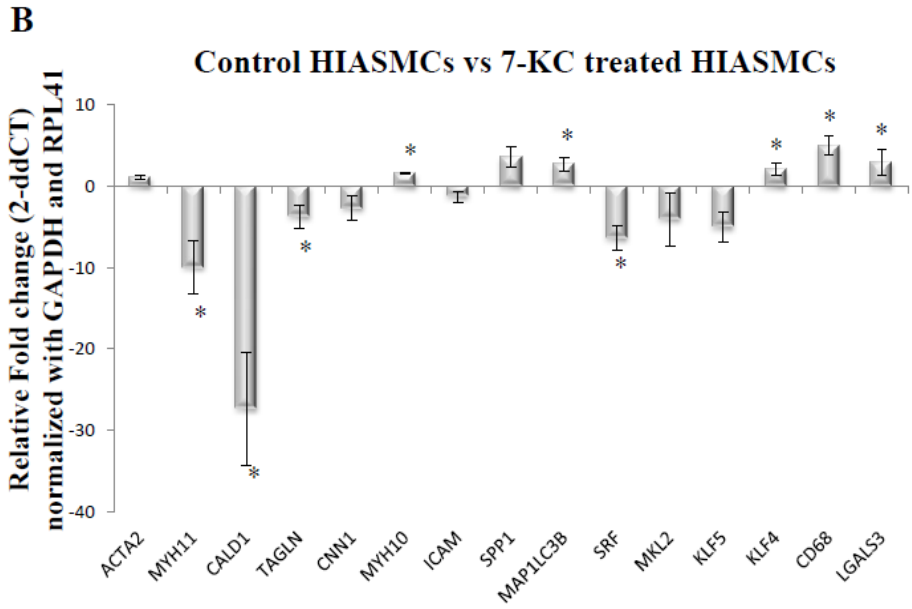

Figure 14. SMC specific marker expression analyzed by quantitative PCR. (**A**) Fold change differences of contractile and synthetic marker expression in 39 plaque SMCs (PLQ-SMCs) versus 39 macroscopically intact tissue area SMCs (MIT-SMCs) analyzed by quantitative PCR (error bars represent ± SEM, n = 39). Data was normalized with *GAPDH* and *RPL41*. Wilcoxon matched-pairs signed rank test ($p < 0.05$ * and $p < 0.01$ **); (**B**) Fold change differences of contractile and synthetic marker expression in 7-KC treated (15 µM) HIASMCs versus not treated HIASMCs analyzed by quantitative PCR (error bars represent ± SEM, n = 3). Non-parametric Mann–Whitney U test was used ($p < 0.05$ *).

Transcriptional regulatory pathways control the expression of SMC markers and are governed by the transcription factors SRF, MKL2, KLF4, and KLF5. *SRF* and *MKL2* were both downregulated in PLQ-SMCs (Figure 14A). *KLF4*, which has been reported to suppress expression of SMCs markers, at least in part by disrupting SRF–myocardin interaction, showed higher levels of expression in PLQ-SMCs [199]. On the other hand, *KLF5* expression, involved in phenotypic modulation, did not differ significantly between PLQ-SMCs and MIT-SMCS (Figure 14A) [184]. HIASMCs treated with 7-KC also showed a similar pattern of transcription factor expression levels as SMC isolated from carotid plaques (Figure 14B) with *SRF* diminished and *KLF4* enhanced upon 7-KC treatment.

In a recent study, we have found SMCs isolated from carotid atherosclerotic plaques to express a series of macrophage markers [231], concomitant with a macrophage-like phenotype [232]. Analysis of the expression levels of *CD68* and *LGALS3* showed that both macrophage markers were significantly augmented in PLQ compared to MIT-SMCs (Figure 14A). Similarly, when HIASMCs were treated with 7KC, both genes were clearly upregulated (Figure 14B). Thus, SMCs in the lesion have been driven towards a phenotype with partial characteristics of macrophages.

To verify that these differences in gene expression were not due to patient symptomatology caused by the plaque, we analyzed the gene expression data separately using either only symptomatic samples (20 PLQ-SMCS vs. 20MIT-SMCs) (Figure 15A) or only asymptomatic samples (19 PLQ-SMCS vs. 19 MIT-SMCs) (Figure 15B). As similar patterns of expression were observed in both cases, the differences in gene expression found (Figure 15A) are independent of symptomatology and due to the location within the excised carotid area.

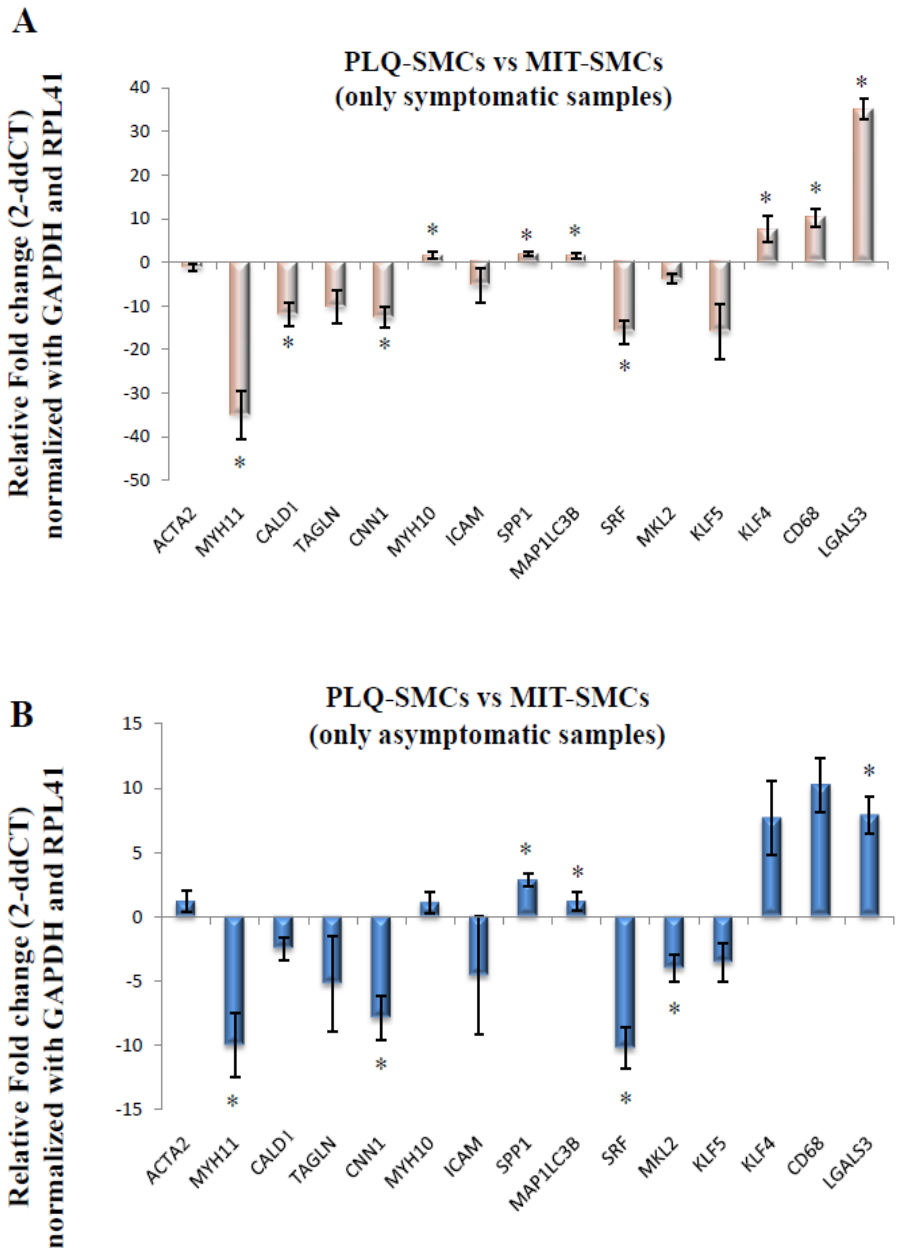

Figure 15. Fold change differences of contractile and synthetic markers in plaque SMCs (PLQ-SMCs) versus macroscopically intact area SMCs (MIT-SMCs) analyzed by quantitative PCR. **(A)** 20 PLQSMCs versus MIT-SMCs. **(B)** 19 PLQ-SMCs versus 19 MIT-SMCs (error bars represent ± SEM, n=20 Sympt and n=19 Asympt). Wilcoxon matched-pairs signed rank test ($p<0.05$*).

Then, we decided to analyze the gene expression pattern in atheroma PLQ-SMCs isolated from both Sympt and Asympt patients and compare between them. We found *MYH11* and *KLF5* to be significantly under-expressed in SMCs from Sympt patients compared with those from Asympt patients (*p*-value= 0.045 and p = 0.01 respectively, Table 6), while *SPP1* was upregulated (*p*-value = 0.05). The rest of the genes analyzed were found to be statistically similarly expressed in Asympt and Sympt PLQ-SMCs.

Gene Symbol	FC (Asympt vs. Sympt)	*p* Value
Actin, alpha 2, smooth muscle, aorta (*ACTA2*)	1.3	ns
CD68 molecule (*CD68*)	−1.01	ns
Caldesmon 1 (*CALD1*)	−1.17	ns
Calponin 1 (*CNN1*)	1.14	ns
Galectin 3 (*LGALS3*)	1.05	ns
Intercellular adhesion molecule 1 (*ICAM1*)	−1.30	ns
Kruppel like factor 4(*KLF4*)	1.04	ns
Kruppel like factor 5 (*KLF5*)	−1.89	0.01
Microtubule associated protein 1 light chain 3 beta	−1.09	ns
MKL1/myocardin like 2 (*MKL2*)	−1.17	ns
Myosin heavy chain 10 *(MYH10)*	−1.31	ns
Myosin heavy chain 11 (*MYH11*)	−4.53	0.045
Secreted phosphoprotein 1 (*SPP1*)	2.08	0.05
Serum response factor (*SRF*)	−1.38	ns
Transgelin (*TAGLN*)	−1.01	ns

Table 6. Relative gene expression analysis between 20 Sympt and 19 Asympt SMCs. Gene expression was normalized with the housekeeping genes *GAPDH* and *RPL41*. Differences between the two groups were analyzed with Mann–Whitney U Test. p-value ≤ 0.05 was considered significant. (FC: fold change).

The balance between the matrix accumulation and degradation determines plaque stability and for that reason we analyzed matrix metallopeptidase (*MMP*) 3, 7, 9 and *TIMP1* expression levels in our SMC samples (Figure 16). Our results did not identify any significant association between gene expression of *MMP*s and type of SMCs, both Asympt/Sympt and MIT/PLQ. Therefore, *MMP3, 7, 9* and *TIMP1* do not emerge as differentially expressed in SMCs between asymptomatic and symptomatic and neither do between plaque and MIT cells.

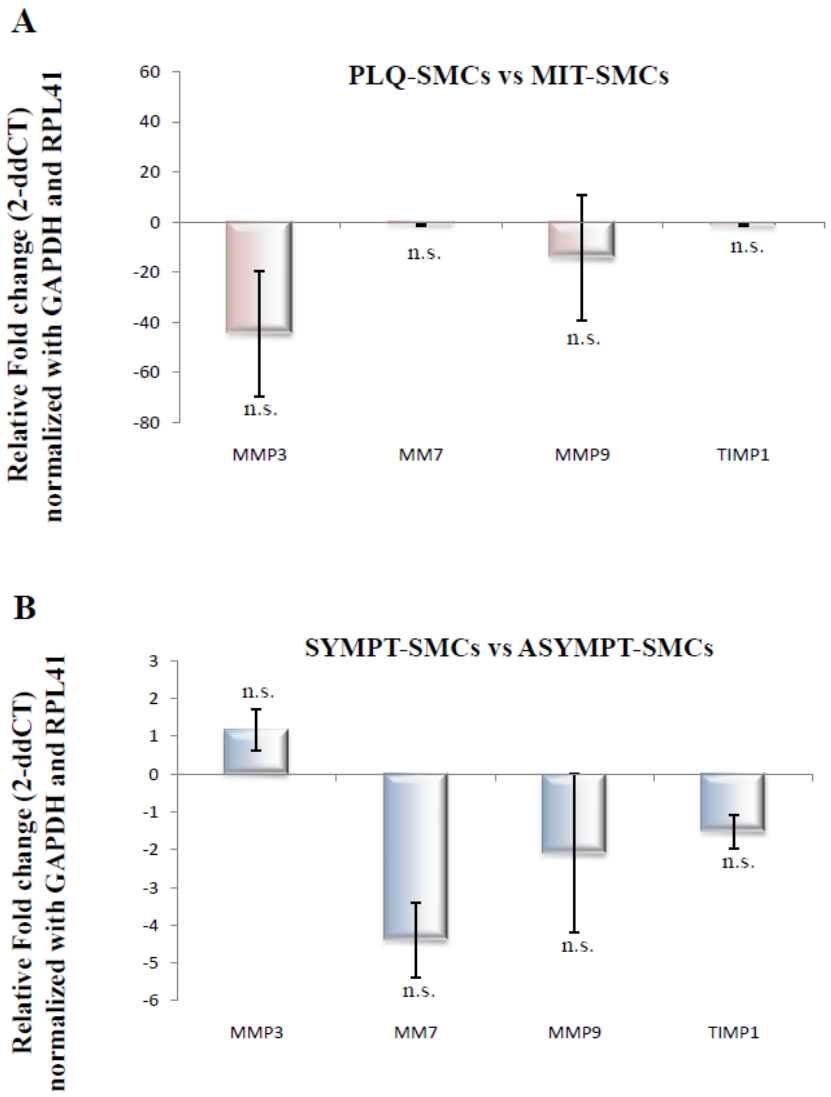

Figure 16. MMP3, 7, 9, tissue inhibitor MMP 1 mRNA expression quantified by qPCR in SMCs. (A) PLQ-SMCs versus MIT-SMCs. **(B)** Sympt-SMCs versus Asympt-SMCs. Wilcoxon matched-pairs signed rank test was used ($p<0.05$ was considered statistically significant). (n.s. no significant).

MYH11 Protein Level in SMCs from Sympt vs. Asympt Patients and from PLQ vs. MIT Region

Due to the high differences in gene expression of *MYH11* we wanted to analyze MYH11 at protein level in carotid atheroma plaque-derived SMCs. For that, we choose Western blot and immunoflourescence techniques to carry out the analysis.

In immunoblot analysis, MYH11 levels were under-expressed both in PLQ-SMCs compared to MIT-SMCs (Figure 17A, panels a and b) and in SMCs coming from Sympt versus Asympt patients (Figure 17A, panels c and d).

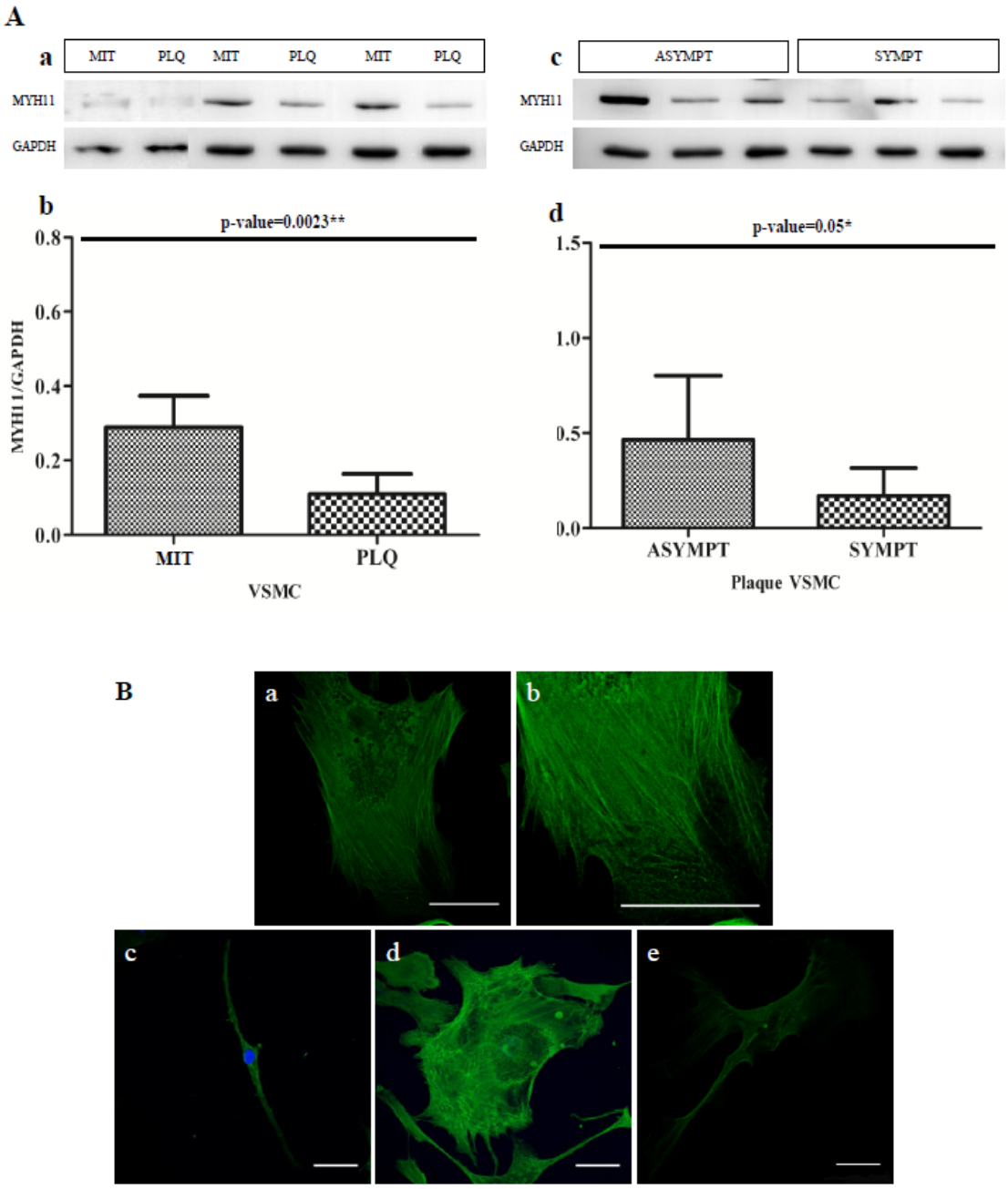

Figure 17. MYH11 protein detection by western blot and immunocytofluorescence. (A) MYH11 protein expression in carotid atherosclerotic SMCs. (**a**,**b**) Western Blot of MYH11 protein in plaque or adjacent MIT area SMCs, and Asympt or Sympt plaque SMCs, respectively; (**c**,**d**) graphic representation of A and B show the average of densitometry values of the bands respect to GAPDH protein expression. (MIT: macroscopically intact tissue area SMCs; PLQ: plaque SMCs; ASYMPT: SMCs from asymptomatic plaques; SYMPT: SMCs from symptomatic plaques) ($p < 0.05$ * and $p < 0.01$ ** were considered statistically significant); **(B)** Immunofluorescence of carotid atherosclerotic SMCs with MYH11 and nuclei staining. (**a**) MIT-SMC myofilaments extend throughout the cell forming a network with weaker MYH11 staining in the cell periphery; (**b**) with 2.00 zoom focusing on the cell periphery where MYH11 staining appears as spots; (**c**,**d**) show MYH11 staining in MIT-SMCs (c image shows elongated and spindle-shaped cell; and d, flattened and polarized cell with lamellipodia); (**e**) PLQ-SMCs present low fluorescence intensity of MYH11 protein and appear forming thin myofilaments. Scale bar 50 µm.

Immunocytofluorescence analysis with anti-MYH11 by confocal microscopy was performed in carotid SMCs with the aim to describe the contractile system. PLQ-SMCs and MIT-SMCs were labeled with anti-MYH11 and DAPI to identify nuclei. Individual myofilaments were not found to be parallel to the long axis of the cell but formed a network of filaments, and they appeared distributed in the cytoplasm in all single planes of the Z-stacks images, from the base (at the cover slip) to the top of the cell. Z-stack images showed homogeneous distribution of myosin filaments creating a thick fiber-mesh in the base of the cell; myosin-containing stress fibers extended as a network towards the periphery of the cell (Figure 17B, panel a), whereas fibers usually end in extending lamellae, and MYH11 appeared as continuous spots (Figure 17B, panel b) [233]. In the upper planes of Z-stacks there was predominant staining of MYH11 in the central region of the cytoplasm with weaker staining in the cell periphery, which could be observed in MIT-SMCs (Figure 18, upper panels), whereas there was lack of this pattern in PLQ-SMCs cells (Figure 18, lower panels). Additionally, in this study, we found that MIT cells showed a higher volume of myofilaments per cell area (Figure 17B, panels c and d) than those SMCs from the center of atheroma plaque (Figure 17B, panel e), which exhibit less fluorescence intensity of myosin staining.

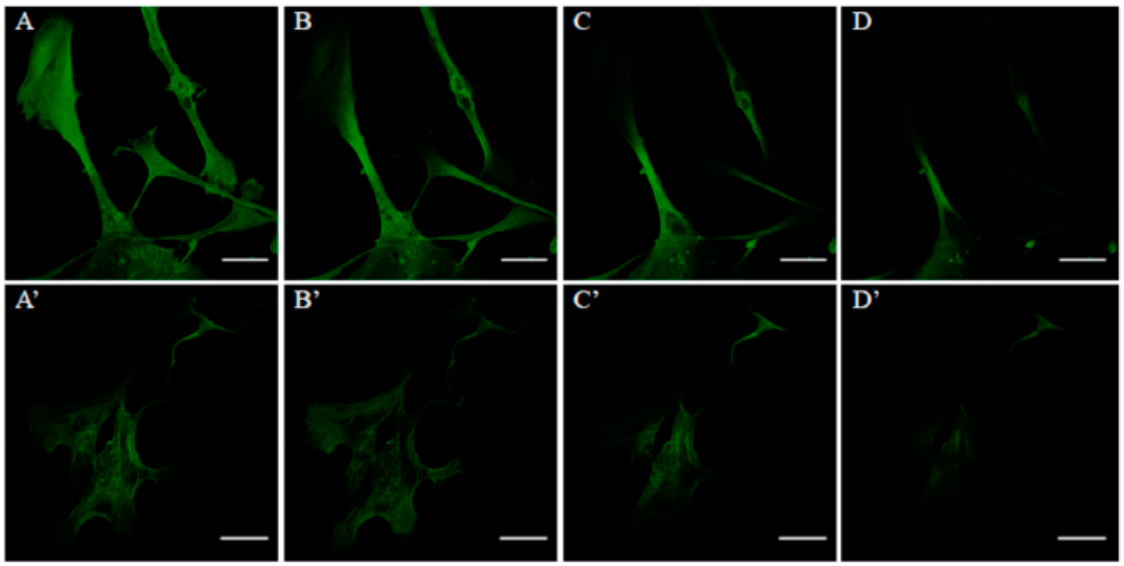

Figure 18. MYH11 staining in SMCs. A, **B**, **C** and **D** SMCs from adjacent site. 0,9 μm z-stacks from the base o the top of the cells. MYH11 staining appear in perinuclear region in the upper planes of the cell foring thick myofilaments. **A'**, **B'**, **C'** and **D'** SMCs from atheroma plaque. 0,9 μm z-stacks from the base to the top of the cells, where there is almost lack of MYH11staining and myofilaments appear as thin fibers. Scale bar 50μm.

4.2. RNA-SEQ STUDY DESIGN

The study was designed with maximum power to detect DEG and DEI, as well as to perform complementary functional enrichment and network analysis. The two main factors to take into

account in RNAseq transcriptomics studies are the number of replicates and the sequencing depth. Thus, RNA sequencing was performed with a depth to obtain around 60 millions reads per sample, which allowed us to reach reliable detection power of differential expression [234]. Sequencing at this depth would allow identifying differential expression with maximum power in 5 replicates, even of those genes with low expression [235]. Also, variability in RNAseq analysis is reduced when studying a specific cell type (i.e. SMC) compared with studying the full atheroma plaque, which is heterogeneous and composed of varying numbers of ECs, SMCs and macrophages. Accordingly, to study the role of SMCs in the development of unstable carotid atherosclerosis, we selected 14 plaque-derived SMCs from 7 Sympt and 7 Asympt patients.

This RNA sequencing analysis was done based in the Illumina sequencing technology, which follows these steps (Figure 19):

1. Cluster Generation: Sequencing templates are immobilized on a proprietary flow cell surface (Figure 1). RNA template molecules amplification (Figures 2–7). On the order of ten million single-molecule clusters per square centimeter are achieved.

2. Sequencing by synthesis (SBS): This technology uses four fluorescently-labeled nucleotides to sequence the millions of clusters (Figures 8-12). Base calls are made directly from signal intensity measurements during each cycle.

3. Data collection, processing, and analysis: Illumina data collection software enables to align sequences to a reference in resequencing applications (Figure 13).

Figure 1: Illumina Flow Cell

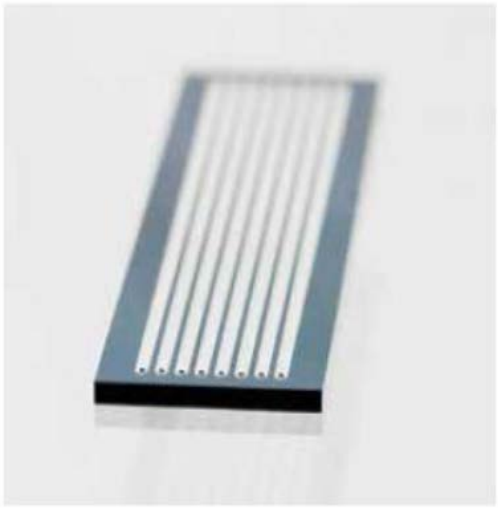

Several samples can be loaded onto the eight-lane flow cell for simultaneous analysis on an Illumina Sequencing System

Figure 2: Prepare Genomic DNA Sample

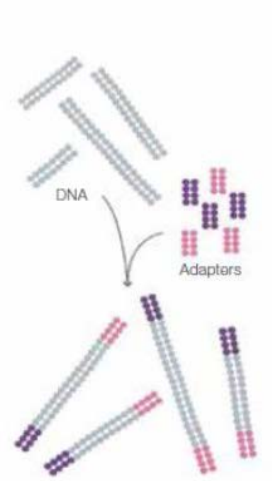

Randomly fragment genomic DNA and ligate adapters to both ends of the fragments.

Figure 3: Attach DNA to Surface

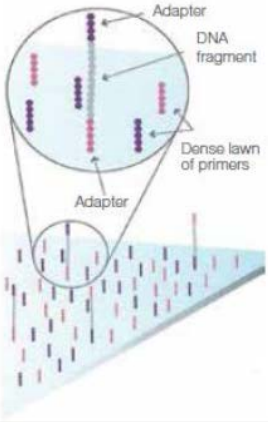

Bind single-stranded fragments randomly to the inside surface of the flow cell channels.

Figure 4: Bridge Amplification

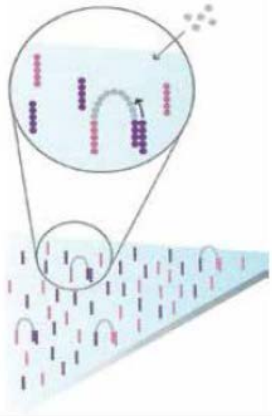

Add unlabeled nucleotides and enzyme to initiate solid-phase bridge amplification.

Figure 5: Fragments Become Double Stranded

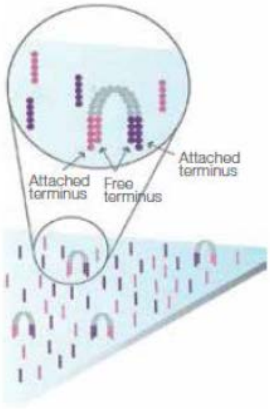

The enzyme incorporates nucleotides to build double-stranded bridges on the solid-phase substrate.

Figure 6: Denature the Double-Standed Molecules

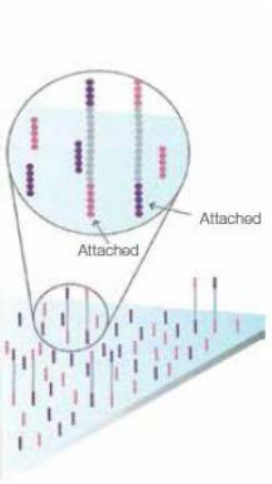

Denaturation leaves single-stranded templates anchored to the substrate.

Figure 7: Complete Amplification

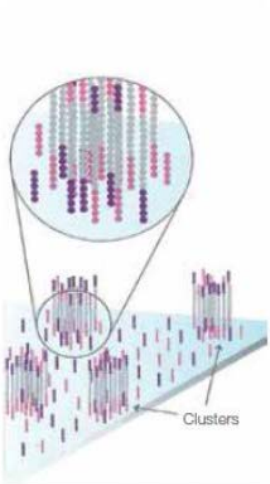

Several million dense clusters of double-stranded DNA are generated in each channel of the flow cell.

Figure 8: Determine First Base

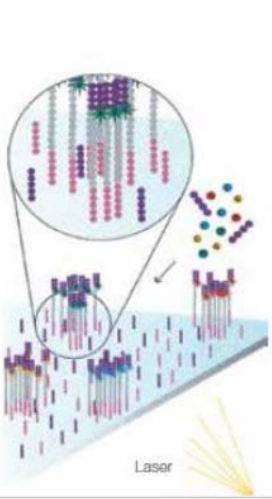

The first sequencing cycle begins by adding four labeled reversible terminators, primers, and DNA polymerase.

Figure 9: Image First Base

After laser excitation, the emitted fluorescence from each cluster is captured and the first base is identified.

Figure 10: Determine Second Base

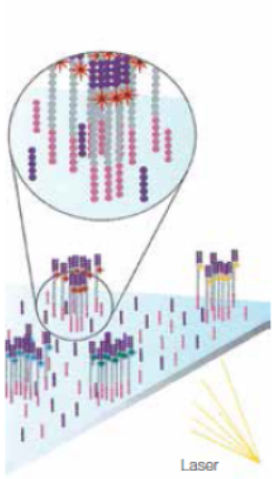

The next cycle repeats the incorporation of four labeled reversible terminators, primers, and DNA polymerase.

Figure 11: Image Second Chemistry Cycle

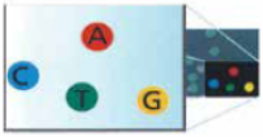

After laser excitation, the image is captured as before, and the identity of the second base is recorded.

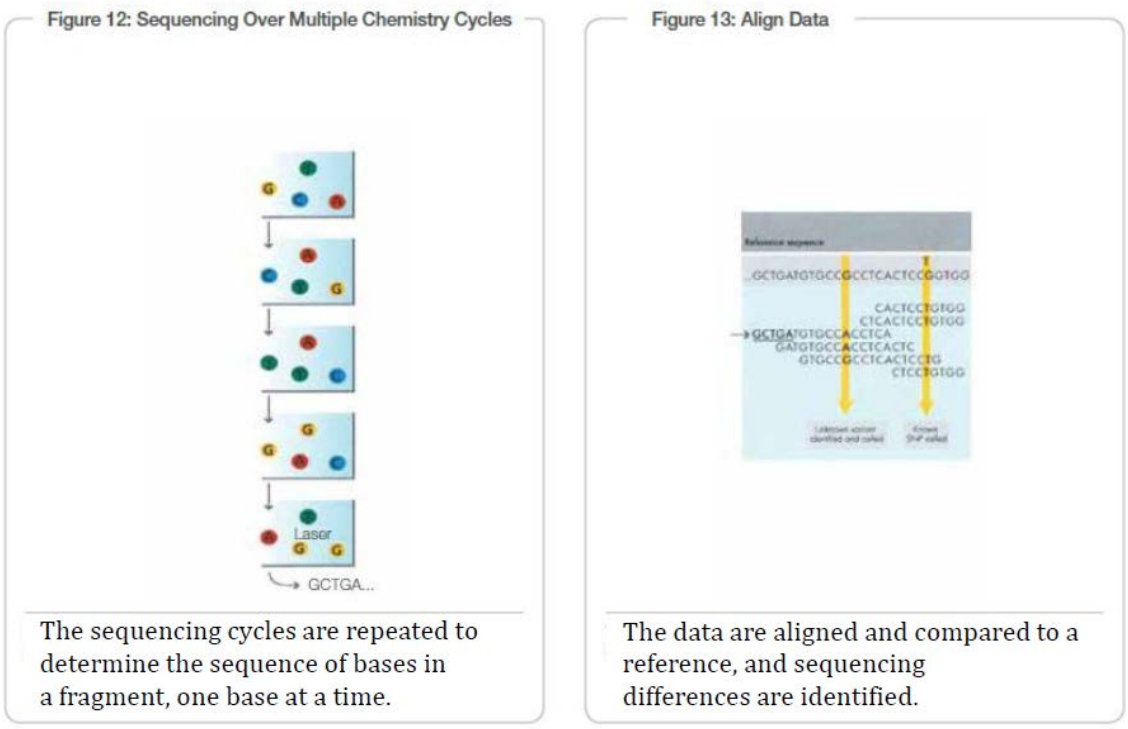

Figure 19. Illumina Sequencing Technology

4.2.1. Primary analysis

Quality Control of produced sequences:

The FASTQ file is the standard method recognized by the bioinformatic tools and any bioinformatic analysis should begin with it. A FASTQ file is a plain text file that contains the biological sequence and the qualities associated with each of the nucleotides of the sequence. Then, FastQC software is responsible to analyze the quality of raw data of the generated sequences.

The quality control of FastQC includes de following tests:

- Per base sequence quality:

The quality per base is a statistic of the quality estimated in that base/position for all the sequences contained in the file FASTQ. Nucleotide sequences are inferring during sequencing reactions by fluorescently labeled terminators. The fluorescence is captured by a camera that will process images into signals that are used to infer the order of nucleotides. Accuracy is typically measured by a Q score (Phred quality score), a common metric to assess the accuracy of a sequencing run. Q scores are defined as logarithmically related to base calling error probability:

$$Q = - 10 \log P / \log 10$$

Then:

Q Score 10 - Base calling accuracy 1 in 10 - Probability of incorrect base 90%

Q Score 20 - Base calling accuracy 1 in 100 - Probability of incorrect base 99%

Q Score 30 - Base calling accuracy 1 in 1,000 - Probability of incorrect base 99.9%

Q Score 40 - Base calling accuracy 1 in 10,000 - Probability of incorrect base 99.99%

Q Score 50 - Base calling accuracy 1 in 100,000 - Probability of incorrect base 99.999%

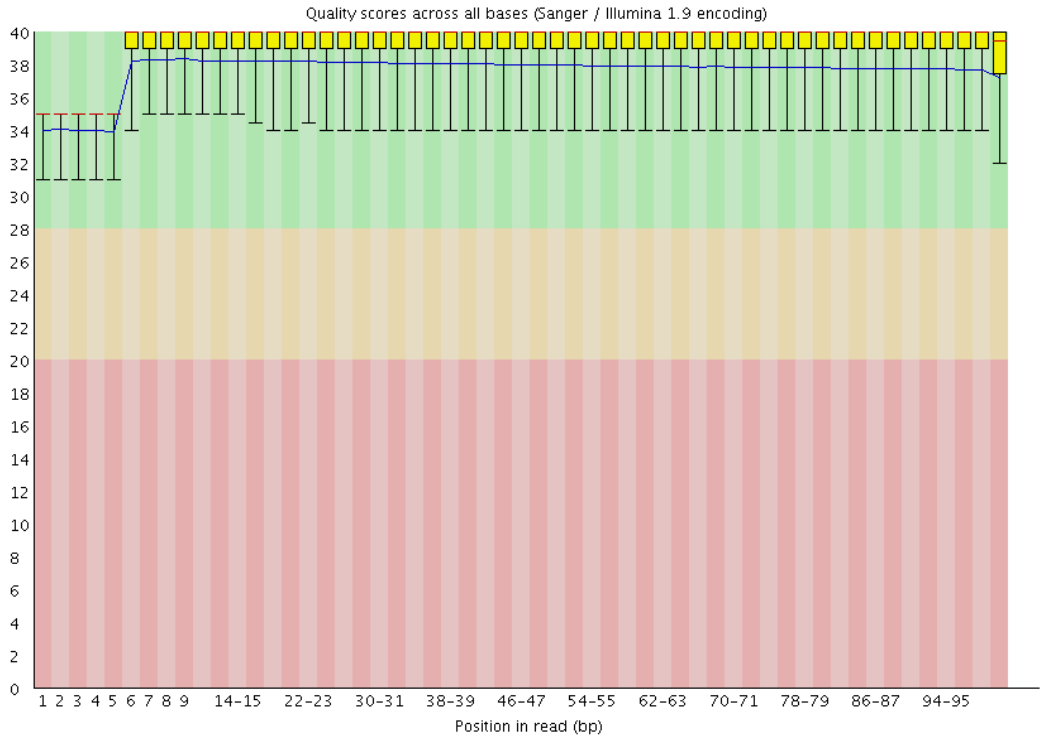

Figure 20. Overview of the range of quality values across all bases at each position in the FastQ file. The central red line is the median value. The yellow box represents the inter-quartile range (25-75%). The upper and lower whiskers represent the 10% and 90% points. The blue line represents the mean quality. The y-axis on the graph shows the quality scores. The background of the graph divides the y axis into very good quality calls (green), calls of reasonable quality (orange), and calls of poor quality (red).

If a sequencing run is assigned a Q score of 40 (Figure 20), this is equal to the probability of an incorrect base call of 1 in 10,000 times, or 99.99% base calling accuracy. The higher is the score the better would be the base call. A lower Q score of 10 means, there is the probability of an incorrect call in 1 of 10 bases. Lower Q scores can lead to increases in false positive variant calls and reduces the overall confidence that an investigator has in their sequencing data.

The quality per base on most platforms will decrease as the run progresses, so it is common to see quality falling at the end of a read in the 90 inter-quartile (Figure 20).

- Per tile sequence quality

The graph allows you to look at the quality scores from each tile across all of your bases to see if there was a loss in quality associated with only one part of the flow cell. Flow cell is a surface to which more than 100 million strands of RNA per cm^2 are adhered.

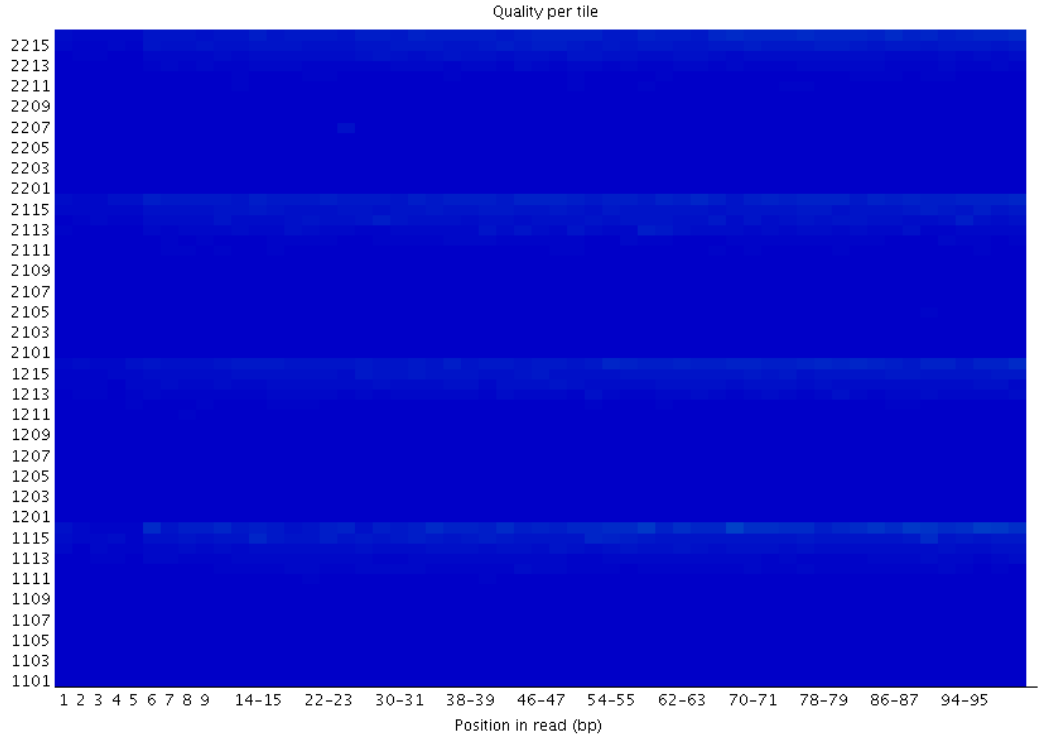

Figure 21. Example of FastQC per title quality of one sample.

The colours of this type of graph are on a cold to hot scale. Cold colours are positions where the quality was at or above the average for that base in the run, and hotter colours indicate that a tile had worse qualities than other tiles for that base. A good plot should be blue all over (Figure 21). Therefore, in the example above, tiles show consistently high quality.

- Per sequence quality score

This quality control shows distribution of sequence quality. Allow seeing if any subset of sequences has low quality. As it can see in Figure 22 most of the sequences have a Q score of ≥ 37. If the sequencing has a good quality, usually just a few sequences have a low Q score.

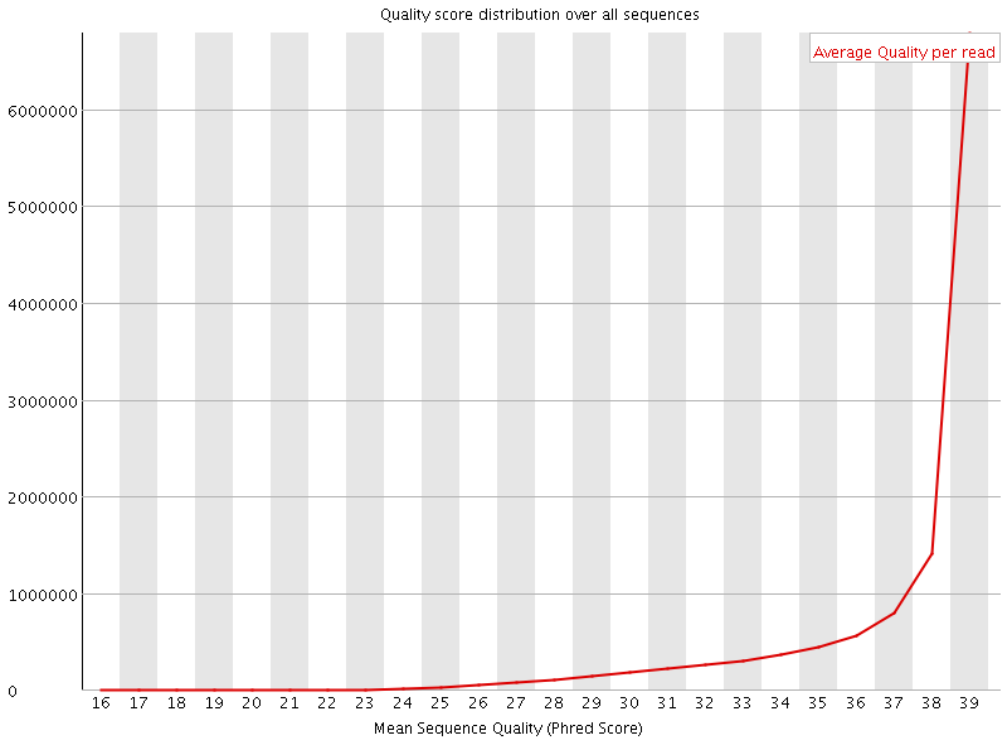

Figure 22. Example of per sequence quality control of one sample. X axis shows Q score while Y axis shows the number of reads.

- Per base sequence content

This quality control represents the proportion of the four bases in each position of different reads. Generally, it is expected that the four bases are equally represented and are seen together in the same line on the graph. It is assumed that up to 10% of difference between bases content can be found, while if the difference between A and T or G and C is above 10% will be necessary to filter the reads with the aim to remove these differences. A bias which is consistent across all bases either indicates that the original library was sequence biased, or that there was a systematic problem during the sequencing of the library. Strong biases which change in different bases usually indicates an overrepresented sequence which is contaminating the library.

Figure 23 shows a homogeneous base content from position 1 4-15 over the reading, remaining below 10%. However, at the beginning of the reads the differences reach 20%. The reason is the use of random hexameric primers that induces biases in the composition of the nucleotide at the beginning of the readings.

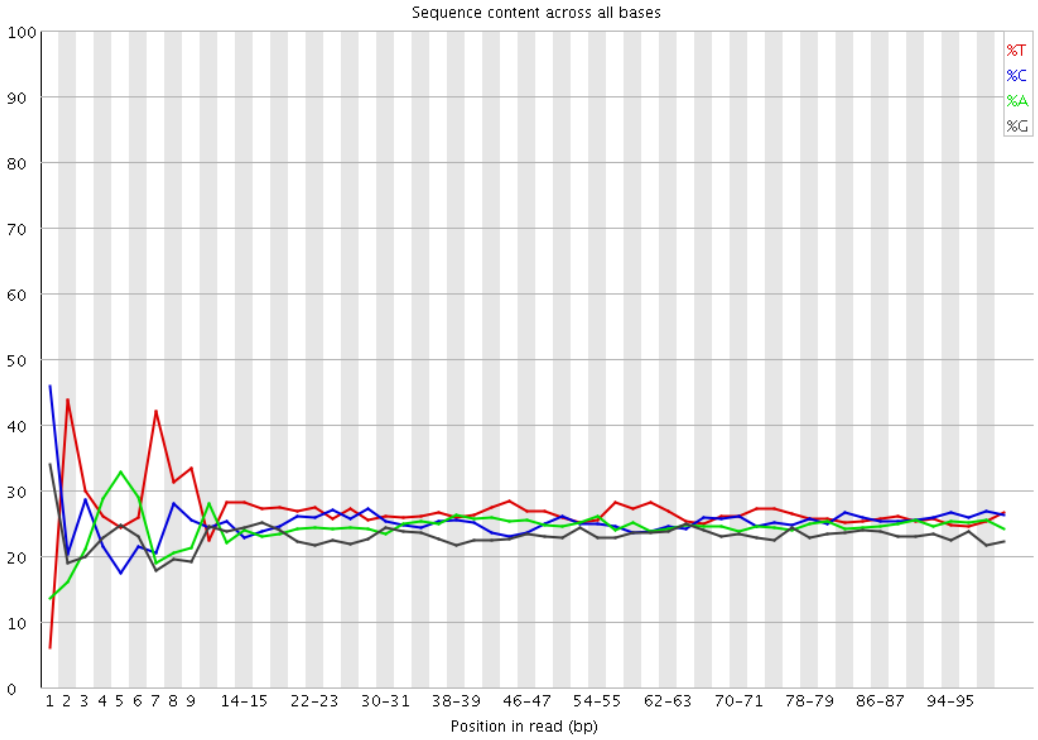

Figure 23. Per base sequence content of one sample.

- Per sequence GC content

This module measures the GC content across the whole length of each sequence in a file and compares it to a modeled normal distribution of GC content.

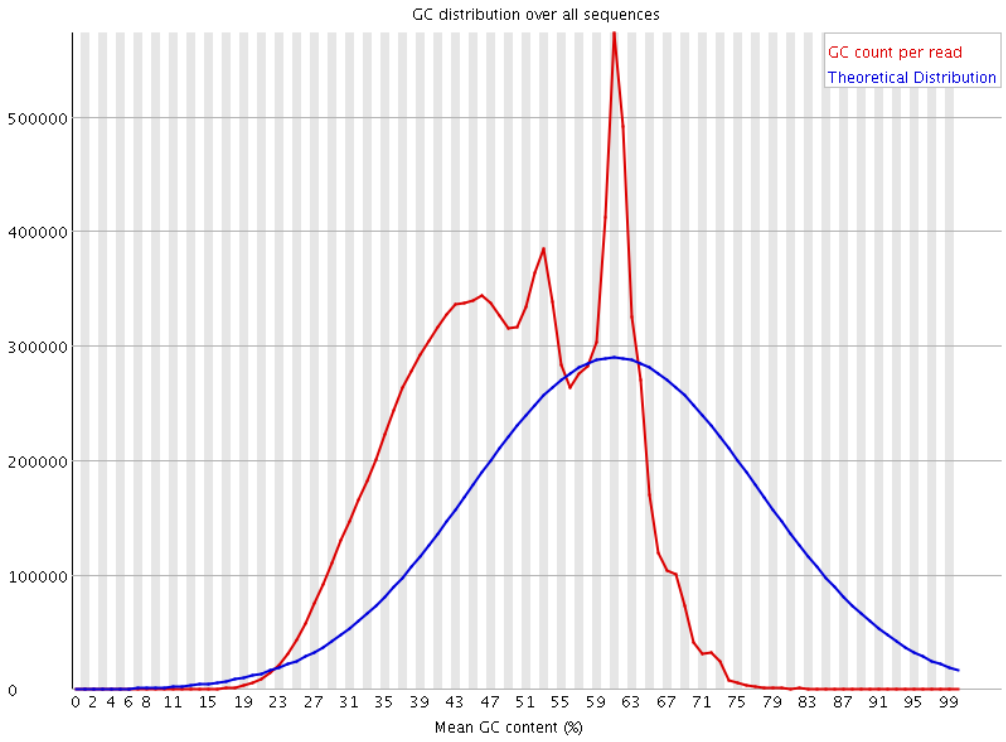

Figure 24. Per sequence GC content quality control. Normal distribution of GC content in blue. Our sample GC content in red.

In a normal random library it would expect to see a roughly normal distribution of GC content where the central peak corresponds to the overall GC content of the underlying genome. Since we do not know the GC content of the genome, the modal GC content is calculated from the observed data and used to build a reference distribution. Figure 24 shows GC content of one sample that do not match with theoretical one, with a little peak at 53% GC and another big one at 61% GC.

- Per base N content

It represents the indetermination of bases throughout the readings. During the sequencing, if a base is not identified, it is collected with an N in the reading, which also implies total loss of quality. The assemblers and aligners have to deal with this basic ambiguity problem. Some sequencers replace Ns with a random base, others put a fixed base; however, all this leads to false mapping.

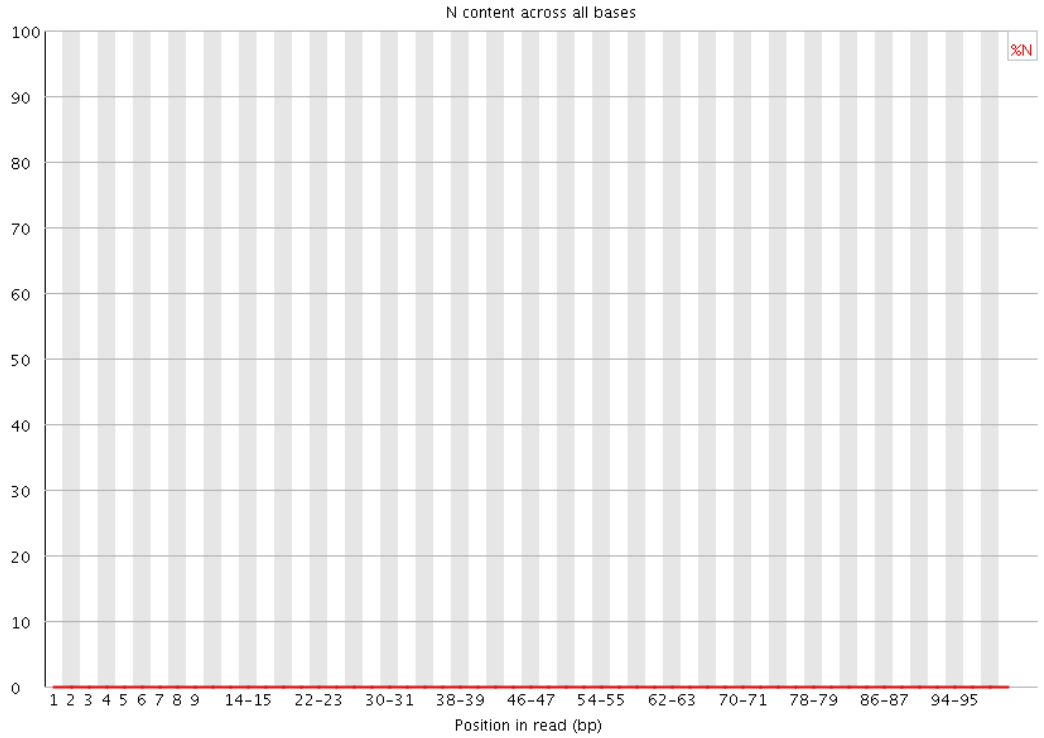

Figure 25. Per base N content FastQC quality control of one sample. Y axis shows read percentages that have Ns in their sequences. X axis shows the position of Ns into the sequences.

If N content exceed the 5%, the sequences have to be manage with caution while if it is over 20% an error will raise. In the case of Figure 25 no N content is demonstrated, which suggest a good quality sequencing for this sample.

- Sequence length distribution

It represents the distribution of sequences based on their length. This high throughput sequencer generates sequence fragments of uniform length. This module generates a graph showing the distribution of fragment sizes in the file which was analyzed. In this case, due to generated fragments are of uniform length, this will produce a simple graph showing a peak only at one size.

In our experiments, the samples have a distribution whose length for the great majority of the sequences is 101 nucleotides as can be seen in the following Figure 26.

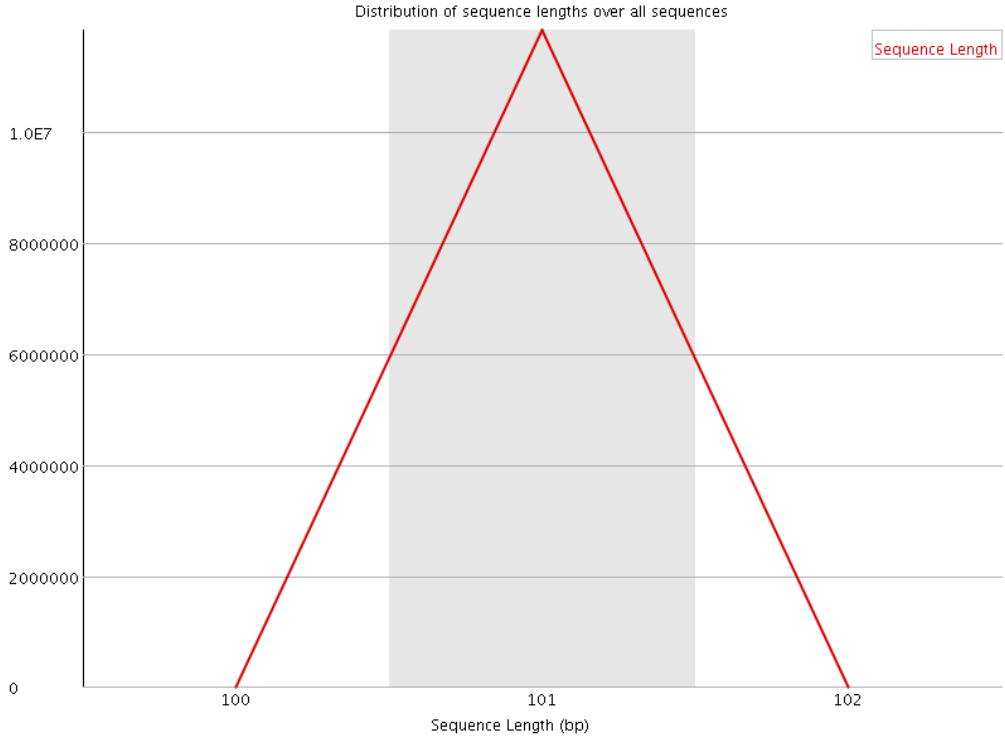

Figure 26. Example of sequence length distribution graphic.

- Sequence duplication level

This module counts the degree of duplication for every sequence in the set and creates a plot showing the relative number of sequences with different degrees of duplication.

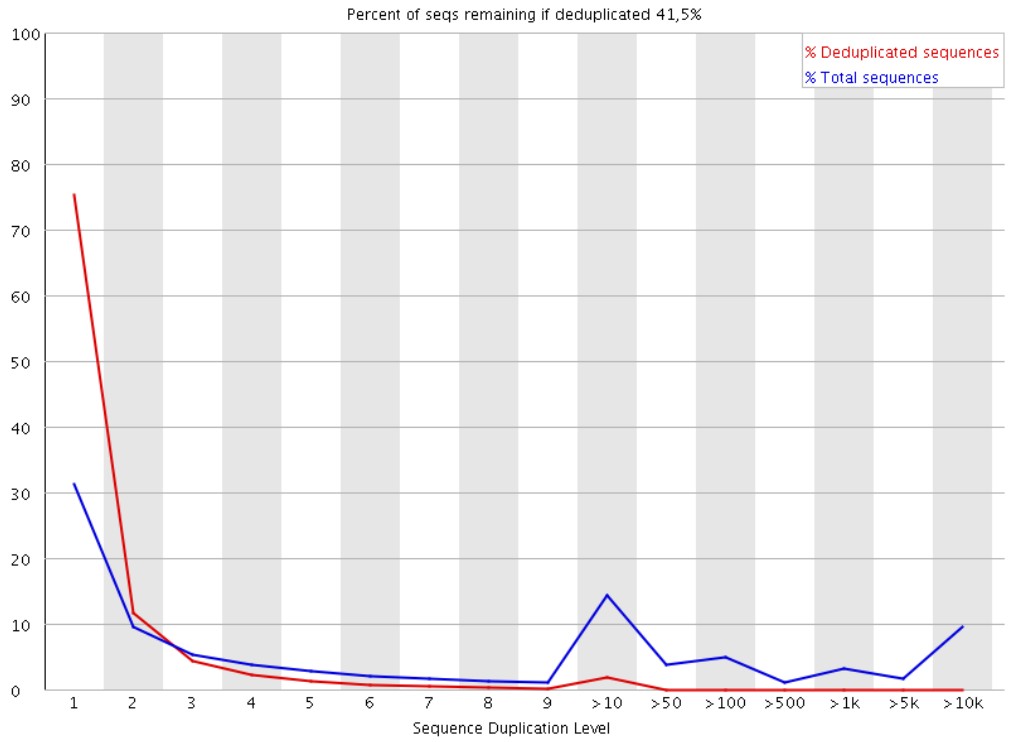

Figure 27. Plot of sequence duplication level. This plot shows the proportion of reads in the library which arise from sequences which occur different numbers of times. The headline figure at the tops tells us that around 56.16% of reads would be lost if the library were to be deduplicated. Blue line indicates percentage of duplicates of total sequences generated in the library. The red line shows the percentage of duplicates would be left after deduplication.

The big problem with identifying and removing technical duplication is that it is not possible to always assume that two reads falling at the same point are the result of technical duplication. When the overall read density in a region gets too high then it will start to see co-incidental duplication from different biological molecules. For regions with very high read density therefore a simplistic measurement of duplication will confuse high biological read depth with technical duplication.

Although due to sequencing, errors, PCR amplification etc. we expected to obtain a set of unique fragments, we found a high percentage of duplicated sequences from >10 to 10K (Figure 27). This can be due to in RNA-seq analysis the high expression of the transcripts appears as sequence duplication. In an RNA-seq sample the expected duplication level will change depending on whether a read comes from an exon, intron or intergenic region, and based on the expression level of the gene it is in. Some regions will be enormously dense with reads, whilst others will be almost empty. Therefore, it is not recommended to remove duplicates (deduplication) if we are interested in doing a differential expression analysis since reads number has to be proportional to expression levels.

- Overrepresented sequences

A normal high-throughput library will contain a diverse set of sequences. Finding that a single sequence is very overrepresented in the set either means that it is highly biologically significant, or indicates that the library is contaminated, or not as diverse as it was expected.

For each overrepresented sequence the program will look for matches in a database of common contaminants and will report the best hit it finds. Hits must be at least 20bp in length and have no more than 1 mismatch. Finding a hit does not necessarily mean that this is the source of the contamination, but may point you in the right direction. It is also worth pointing out that many adapter sequences are very similar to each other so you may get a hit reported which is not technically correct, but which has very similar sequence to the actual match.

This module lists all of the sequence which makes up more than 0.1% of the total reads (Table 7). Only the first 50bp are considered. For RNA-Seq data it is possible that there may be some transcripts that are so abundant that they register as overrepresented sequence.

SEQUENCE	COUNT	PERCENTAGE	POSSIBLE SOURCE
CCTTAGGCAACCTGGTGGTCCCCCGCTCCCGGGAGGTCACCATATTGATG	160953	1.2110797852316633	No Hit
CTTAGGCAACCTGGTGGTCCCCCGCTCCCGGGAGGTCACCATATTGATGC	97509	0.7336997681196018	No Hit
CAGGCTGGAGTGCAGTGGCTATTCACAGGCGCGATCCCACTACTGATCAG	80704	0.6072517007283875	No Hit
GGCTGGAGTGCAGTGGCTATTCACAGGCGCGATCCCACTACTGATCAGCA	68878	0.5182677766005387	No Hit
CTCAGACCGCGTTCTCTCCCTCTCACTCCCCAATACGGAGAGAAGAACGA	64058	0.4820000179081464	No Hit
CTGGAGTCTTGGAAGCTTGACTACCCTACGTTCTCCTACAAATGGACCTT	49657	0.37364068327554445	No Hit
CTGGAGTGCAGTGGCTATTCACAGGCGCGATCCCACTACTGATCAGCACG	44662	0.3360561491119553	No Hit
GTTTCCGACCTGGGCCGGTTCACCCCTCCTTAGGCAACCTGGTGGTCCCC	44283	0.3332043896629062	No Hit
CCAGGCTGGAGTGCAGTGGCTATTCACAGGCGCGATCCCACTACTGATCA	43107	0.32435565849646364	No Hit
CTCAGGCTGGAGTGCAGTGGCTATTCACAGGCGCGATCCCACTACTGATC	39411	0.29654536054478686	No Hit
AGGCTGGAGTGCAGTGGCTATTCACAGGCGCGATCCCACTACTGATCAGC	38389	0.2888553917929975	No Hit
CTCCGTTTCCGACCTGGGCCGGTTCACCCCTCCTTAGGCAACCTGGTGGT	33420	0.2514664928422719	No Hit
GCTCAGGCTGGAGTGCAGTGGCTATTCACAGGCGCGATCCCACTACTGAT	32330	0.24326486276453171	No Hit
GGCAACCTGGTGGTCCCCCGCTCCCGGGAGGTCACCATATTGATGCCGAA	28181	0.21204599745027122	No Hit
CACAAATTATGCAGTCGAGTTTCCCACATTTGGGGAAATCGCAGGGGTCA	27501	0.2069293841907636	No Hit
CCCCACTACCACAAATTATGCAGTCGAGTTTCCCACATTTGGGGAAATCG	25441	0.1914290557869611	No Hit
ATTCACAGGCGCGATCCCACTACTGATCAGCACGGGAGTTTTGACCTGCT	25133	0.18911153095765468	No Hit
AGGCAACCTGGTGGTCCCCCGCTCCCGGGAGGTCACCATATTGATGCCGA	23267	0.17507094221906463	No Hit
GCTATTCACAGGCGCGATCCCACTACTGATCAGCACGGGAGTTTTGACCT	23059	0.1735058605161564	No Hit
CCCACTACCACAAATTATGCAGTCGAGTTTCCCACATTTGGGGAAATCGC	22093	0.16623725991515	No Hit
CCCCTCCTTAGGCAACCTGGTGGTCCCCCGCTCCCGGGAGGTCACCATAT	22068	0.16604914913355046	No Hit
GTCTGTTCCAAGCTCCGGCAAAGGAGGCATCCGCCGGGCCCCTCCCCGAA	20066	0.1509852377430589	No Hit
CCGTTTCCGACCTGGGCCGGTTCACCCCTCCTTAGGCAACCTGGTGGTCC	19859	0.14942768047141466	No Hit
GCTCCGTTTCCGACCTGGGCCGGTTCACCCCTCCTTAGGCAACCTGGTGG	18866	0.1419559202262807	No Hit
CCCTCCTTAGGCAACCTGGTGGTCCCCCGCTCCCGGGAGGTCACCATATT	18744	0.14103793961207492	No Hit

GCTGGAGTGCAGTGGCTATTCACAGGCGCGATCCCACTACTGATCAGCAC	18500	0.13920197838366338	No Hit
CCTCCTTAGGCAACCTGGTGGTCCCCCGCTCCCGGGAGGTCACCATATTG	18418	0.13858497502001688	No Hit
GTGTGGTTGGTGCGCGGACACGCACTGCCTGCGTAACTAGAGGGAGCTGA	17582	0.13229455048332808	No Hit
GTTGCTCAGGCTGGAGTGCAGTGGCTATTCACAGGCGCGATCCCACTACT	16695	0.12562037995217623	No Hit
CCACAAATTATGCAGTCGAGTTTCCCACATTTGGGGAAATCGCAGGGGTC	16445	0.12373927213618077	No Hit
CGCTATGTTGCCCAGGCTGGAGTGCAGTGGCTATTCACAGGCGCGATCCC	15044	0.11319754393534227	No Hit
GTCTGGAGTCTTGGAAGCTTGACTACCCTACGTTCTCCTACAAATGGACC	14212	0.1069372171237094	No Hit
CGTTTCCGACCTGGGCCGGTTCACCCCTCCTTAGGCAACCTGGTGGTCCC	14086	0.10598913878444768	No Hit
CTCCTTAGGCAACCTGGTGGTCCCCCGCTCCCGGGAGGTCACCATATTGA	13891	0.10452187468797125	No Hit
GGCTATTCACAGGCGCGATCCCACTACTGATCAGCACGGGAGTTTTGACC	13795	0.10379952928662899	No Hit
CTATTCACAGGCGCGATCCCACTACTGATCAGCACGGGAGTTTTGACCTG	13682	0.10294926855379904	No Hit
CGCTATGTTGCTCAGGCTGGAGTGCAGTGGCTATTCACAGGCGCGATCCC	13457	0.10125627151940314	No Hit

Table 7. Overrepresented sequences of one sample of RNA from SMCs.

- Adapter content

Sequencers such as Illumina use adapters for RNA organization in the flow-cell. These adapters are sequences of 7-9 nucleotides that must be filtered before the alignment phase. In this quality control only adapters specific to the library are searched.

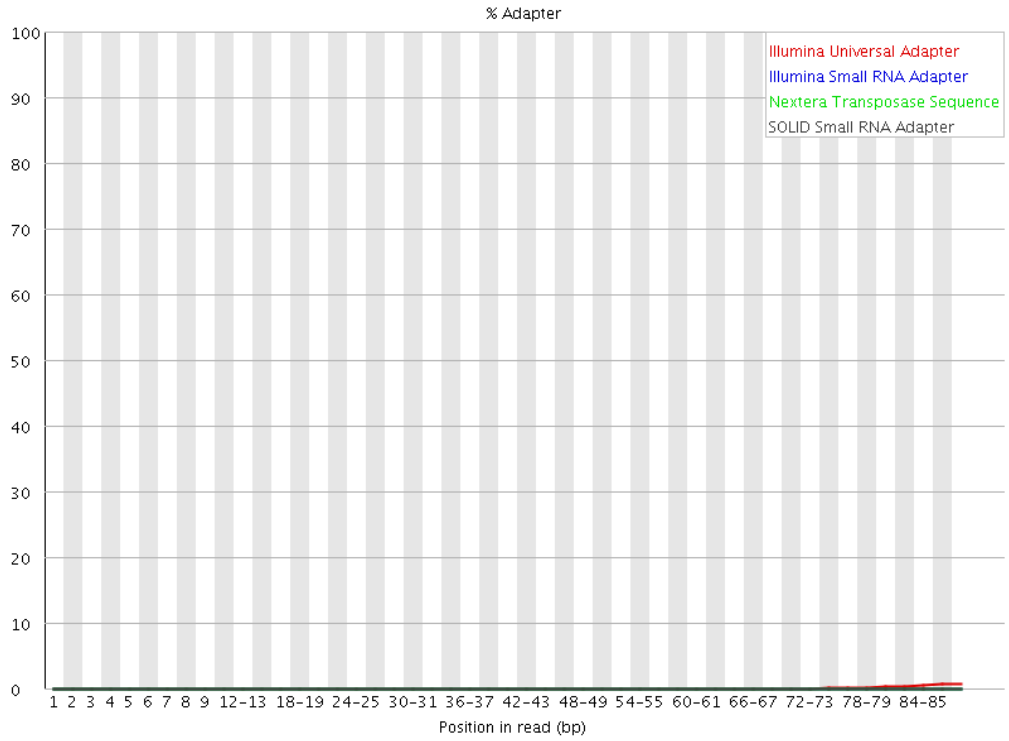

Figure 28. Graphic of adapter content of generated reads.

As it can observe in above graphic (Figure 28), no adapters have been found in our samples.

- Kmer content

Kmer content analysis is complementary to the overrepresented sequences, but in this case it tries to find duplicated sequences in short and poor quality reads. FastQC cut sequences in 7-kmer fragments (7nt) and it proves their representation in all the sequences. Then, it shows the 6 most abundant kmer and it finds their representation along the reads. All this is showed in the following graphic:

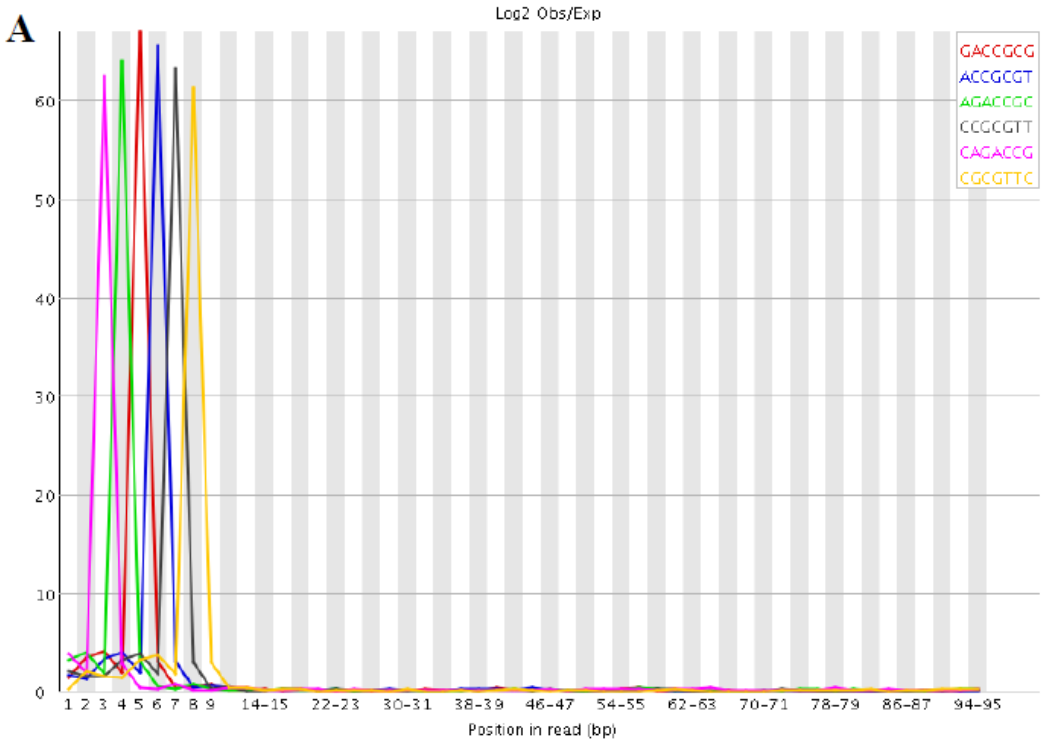

B

Sequence	Count	PValue	Obs/Exp Max	Max Obs/Exp Position
GACCGCG	6020	0.0	66.93695	5
ACCGCGT	6140	0.0	65.52394	6
AGACCGC	6305	0.0	63.98698	4
CCGCGTT	6365	0.0	63.20396	7
CAGACCG	6475	0.0	62.525326	3
CGCGTTC	6570	0.0	61.30206	8
GCGTTCT	7755	0.0	51.99607	9
CGCTATG	8305	0.0	35.680817	1
TCAGACC	12860	0.0	32.40629	2
CTCAGAC	13955	0.0	31.68124	1
GAGTCTT	15335	0.0	31.613401	4
GGAGTCT	15190	0.0	31.538269	3
TACGGAG	6765	0.0	30.996656	34-35
ACCTTCG	5800	0.0	30.625595	94-95
ATACGGA	6830	0.0	30.284046	32-33
GTCGGTT	1975	0.0	30.15275	1
TGGAGTC	16125	0.0	30.03407	2
AATACGG	6210	0.0	29.712955	32-33
CAATACG	6180	0.0	29.318977	30-31
GAACGAT	7080	0.0	29.147858	44-45

Figure 29. Kmer content. (A) Graphic representation of kmer content throught the reads. **(B)** Representative kmers found in the reads.

4.2.2. Secondary analysis

Mapping, identification and quantification of the reads:

New reads were mapped to the last version of a reference genome, i.e. *Homo sapiens*, provided by Ensembl's data base, hg19 (http://www.ensembl.org). The process was carried out by an algorithm from Tophat2 v2.1.0 that maps all the reads in a quickly way and aligns RNA-seq reads to large genomes. This program is highly recommended and widely used.

In a complete transcriptome sequencing process, the number of mapped reads ranges from 75 to 85% of the total reads generated. The results of the mapping process can be viewed in Table 8.

Sample name	Total reads	%HQ reads	%Properly pair	%Splice reads
257	61449044	86.11	72.15	26.38
258	76876864	86.51	71.27	25.33
260	67990002	85.99	70.8	25.14
261	67892558	86.08	70.74	26.91
263	71976326	86.78	72.31	26.78
265	74497186	82.21	72.82	23.61
266	72479266	87.66	71.85	27.01
267	70654274	84.75	72.09	24.79
271	73679062	87.23	71.45	27.43
278	70845658	86.19	71.21	25.85
285	72278906	86.59	72.24	25.42
286	72592062	86.26	70.91	27.36
287	80682878	85.84	73.04	26.56
290	72040720	86.47	70.94	26.49

Table 8. Number of mapping reads (HQ reads), assembled reads per sample (properly pair) and splice reads.

Normal- high values can be observed in the process of mapping the reads. Another interesting factor is the percentage of reads that give information about sites of "Splice Site", this type of information refers to the ability of the system to detect the nature of isoforms studied and splicing events.

Afterwards, poor quality reads of mapping were removed using Picard Tool (http://picard.sourceforge.net). This step is necessary to avoid inferences in the correct alignment of the reads to the reference genome. Therefore, only high quality reads were selected to carry out assembly and gene identification by Bayesian inference using an algorithm provided by Cufflinks v2.11.

Gene quantification was done based on the method of htseq_count 0.6.1p1, while isoform expression and quantification was done by the method of Cufflinks.

One important parameter that can condition the sequencing and mapping process is the GC content of the mappable reads. For this reason, GC content analysis as a quality control of the mapping process is essential. In this step, we assessed the GC distribution (i.e. the proportion of guanine and cytosine bp along the reads), which should have a desired distribution between 40–60%. Second, distribution of duplicates (quality of sequencing indicator) was evaluated to confirm that our sequencing contained small proportion of duplicates.

Figure 30 (left) shows expected distribution for each sample. If there is no statistical bias a normal distribution should be observed, centered on values of 45-55%. All samples presented

normal values in the distribution of GC content and the silhouette has a normal approximation (Gaussian distribution) (Figure 30, left).

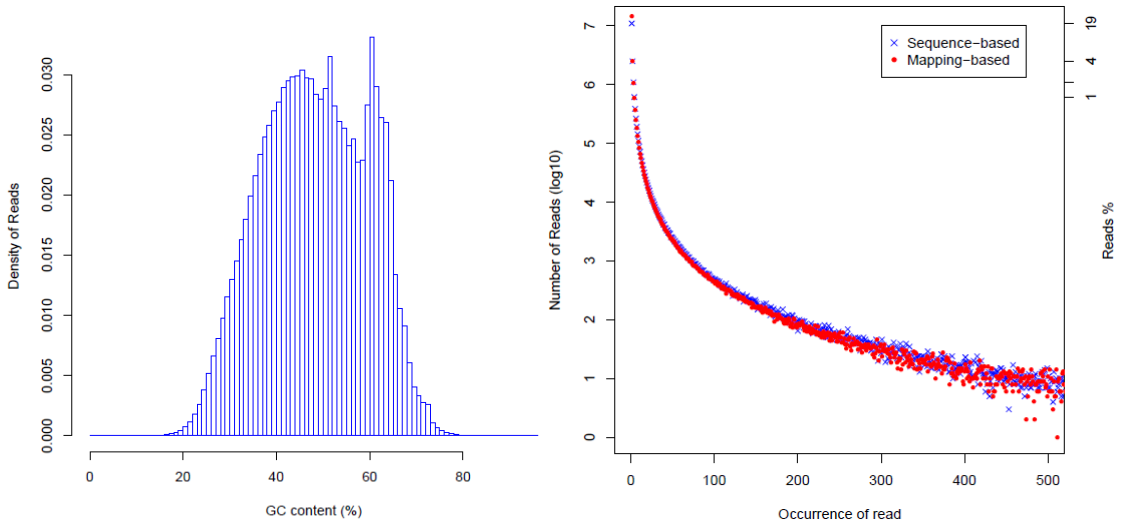

Figura 30. GC percentage distribution in mappable reads of one sample (left). Distribution of duplicates in a RNA-seq process of one sample (right).

Duplication study in processes such as RNA-seq is an indicator of the quality of the sequencing process and is a clear indicator of degradation of biological starting material or important deviations in the sequencing. Figure 30 (right) shows expected distribution in a normal RNA-seq process. It can be observed that a small number of reads has a high number of duplicates, while the great majority has a low or no number of duplicates, both in original and mapping reads. All the samples presented optimal distribution values of the duplicates.

4.2.3. Tertiary analysis

Gene expression analysis:

There are numerous studies [236,237] that indicate the need to normalize the quantification data for the elimination of different statistical deviations that can distort the entire subsequent analysis. Due to the nature of RNA-seq sequencing, the deviations of greater weight are the length of the gene, the library size per sample and GC content among others. Normalization was performed using DESeq2 method to avoid such deviations [237]. Then, normalization allows eliminating or minimizing these effects of distortions. Figure 31 shows the distributions of isoform and gene quantification before and after normalization. It can observe the average values and deviation correction after normalization.

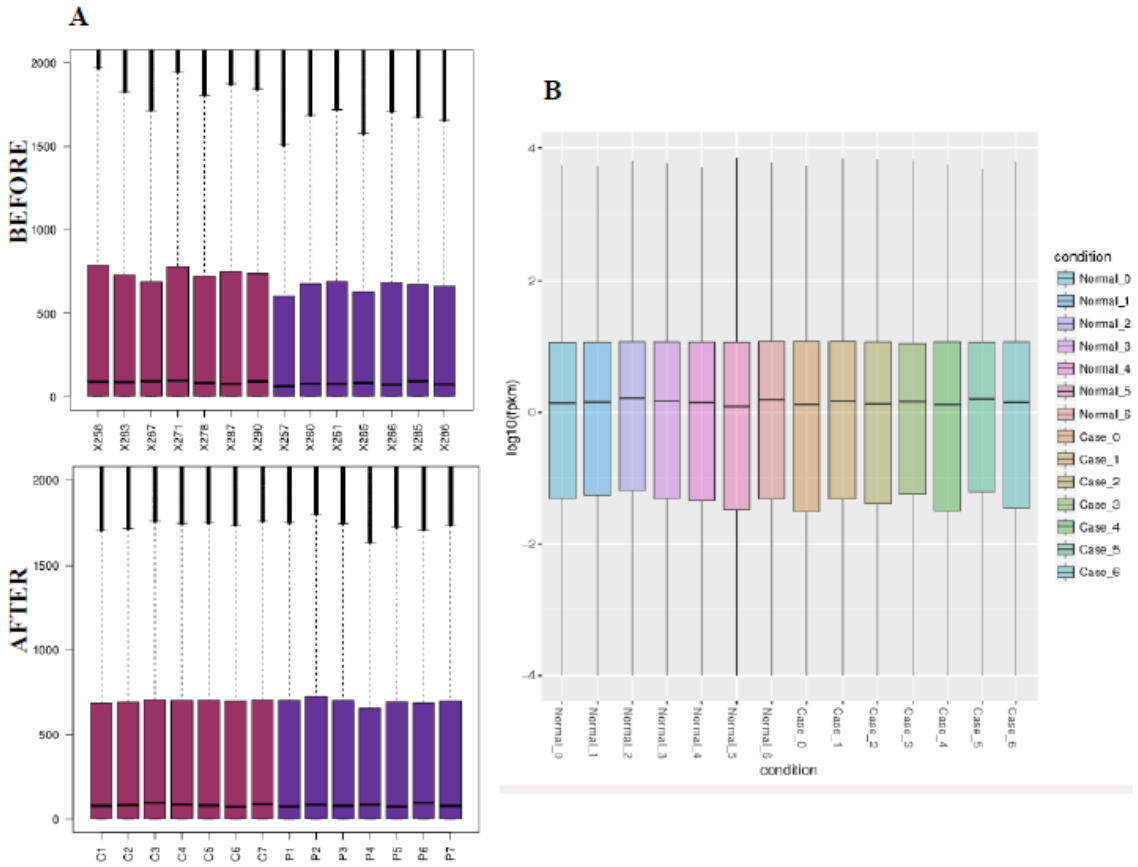

Figure 31. **(A)** Distribution of gene quantification for each sample before (above) and after (below) normalization. X axis shows samples and Y axis number of quantification. Horizontal line into the boxes is the average and vertical continuous black line at the head of the graphic is deviation. C: control (Asympt-SMCs) and P: patient (Sympt-SMCs) **(B)** Distribution of isoform quantification for each sample after normalization. Case: Sympt-SMCs, Normal: Asympt-SMCs.

Differentially expressed gene/isoform between two conditions requires a concordance between samples of the same condition and for that, a study is necessary for the acceptance of the different samples as biological replicates. Then, correlation and elucidation distance between samples study was carried out considering all the transcriptome normalized by the size of the library. This process was done using R statistical program [238] and can be observed in Figure 32 in a Principal Component Analysis (PCA) graphs. PCA was performed on gene expression profiles using the method published before [239]. PCA identifies samples that can be considered as biological replicates and as possible outliers.

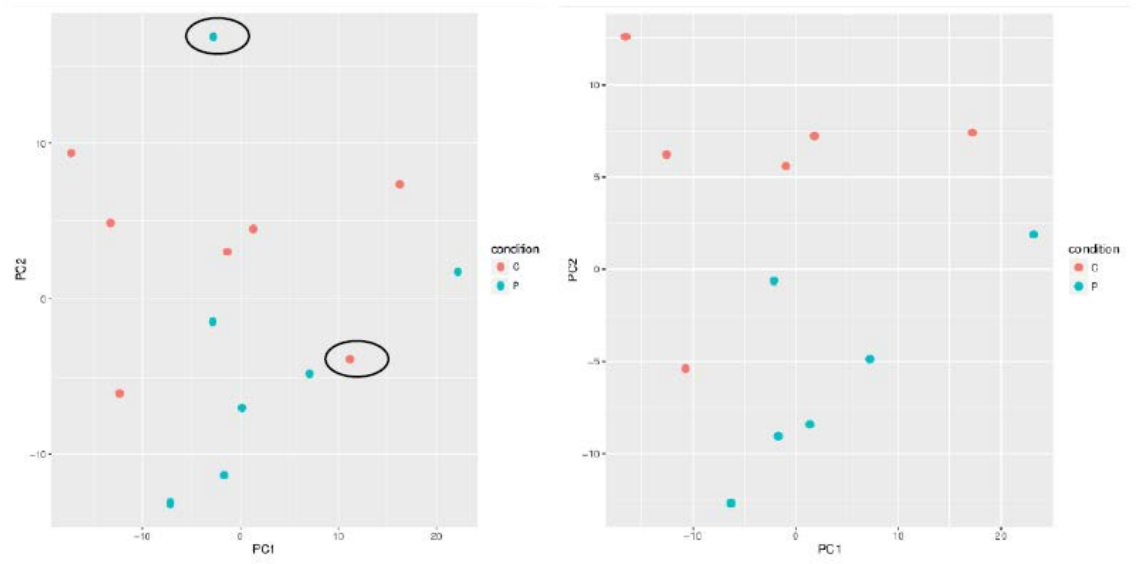

Figure 32. PCA plot. Before (left) and after (right) outlier's detection and removing. Outliers are enclosed by black circles. P: patient (Sympt-SMCs) and C: control (Asympt-SMCs).

Figure 32 shows the detection of 2 outliers between our samples, one of each condition (Sympt and Asympt). Since PCA is based in variance values of analyzed data set and these two samples were far of their data set/condition, they were removed because is understand are not biological replicates and can distort subsequent differential expression results.

Dispersion adjustment illustrates how much the variance deviates from the mean and this was used to shrink the final estimates from the gene-wise estimates towards the fitted estimates, which improves gene expression analysis. Figure 33B shows the dispersion adjustment of gene expression data, performed without the outliers.

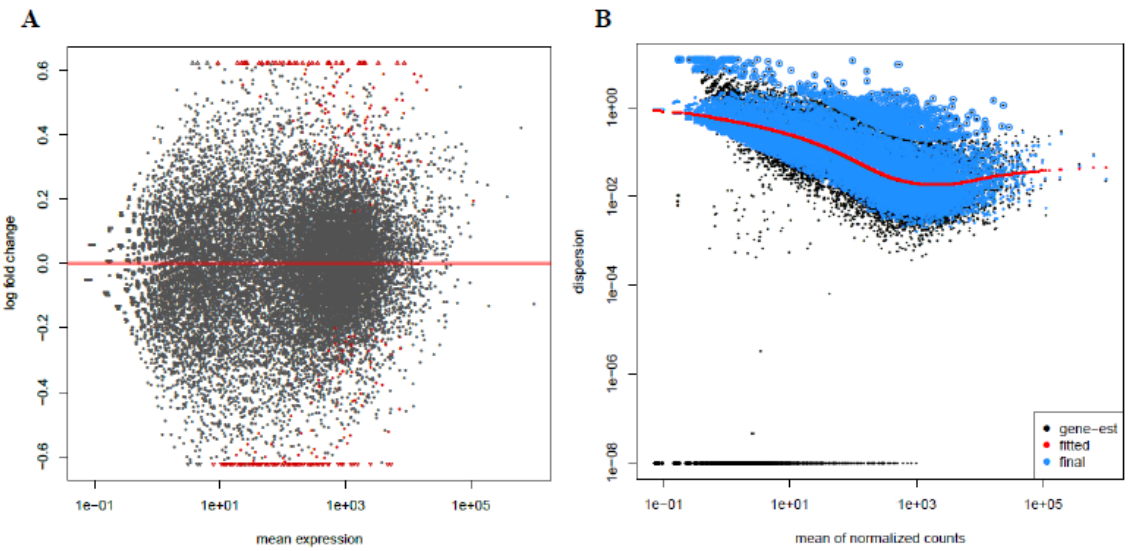

Figure 33. (A) MA plot of Asympt vs. Sympt SMCs. Log2 fold change is on the y-axis and the average of the counts normalized by size factor is shown on the x-axis. Each gene is represented with a dot. Genes

with an adjusted *p*-value below a threshold (0.1) are shown in red. Points which fell out of the window are plotted as open triangles pointing either up or down. **(B)** Dispersion adjustment based on the average of transcript expression. Empirical (black dots), fitted values representing the relationship between the dispersion and the normalized counts (red line), final estimates (blue) and dispersion outlier's values with high gene-wise dispersion, which were not adjusted (blue circle).

Study of differential expression of genes/isoforms between groups of samples was carried out with different statistical packages designed in Python and R. For the study of differential expression, the algorithm proposed by *DESeq2* was used [240]. The package *DESeq2* provides methods to test for differential expression using a Bayesian procedure to moderate (or "shrink") log2 FC from genes with very low counts and highly variable counts. MA plot displays obtained gene expression levels by *DESeq2* (Figure 33A) [222]. The *DESeq2* package uses an MA plot for visual representation of genomic data. The plot visualizes the differences between measurements taken in two group of samples (Sympt and Asympt SMCs), by transforming the data onto M (log ratio) and A (mean average) scales, then plotting these values.

A differentially expressed gene and isoform was considered to be one that has a Fold Change value of less than -1.5 or more than 1.5 and a p-value adjusted by FDR of 0.05 [7].

4.3. TRANSCRIPTOME SEQUENCING ANALYSIS

4.3.1. DEG and DEI analysis

In the differential expression analysis [222,240] we were able to identify 93 genes within the DEG analysis. A complete list of the 93 genes showing FC values ≥1.5 (over-expressed in Sympt vs. Asympt) and FC ≤ -1.5 (under-expressed in Sympt vs. Asympt) with *p*-value ≤0.05 (67 with *p*-value (P_{adj}) corrected by FDR ≤ 0.05) [223] can be found in Table 9.

Gene ID	Symbol	FC	P_{adj}
ENSG00000165507	C10orf10	1,94	0,0006
ENSG00000152049	KCNE4	1,87	0,003
ENSG00000117069	ST6GALNAC5	1,83	0,009
ENSG00000135424	ITGA7	1,81	0,005
ENSG00000128285	MCHR1	1,76	0,02
ENSG00000174564	IL20RB	1,75	0,02
ENSG00000163815	CLEC3B	1,75	0,02
ENSG00000075643	MOCOS	1,75	0,001
ENSG00000074410	CA12	1,72	0,0006
ENSG00000174807	CD248	1,71	0,03
ENSG00000133454	MYO18B	1,70	0,04

ENSG00000179542	SLITRK4	1,65	0,06*
ENSG00000161570	CCL5	1,65	0,06*
ENSG00000148948	LRRC4C	1,65	0,06*
ENSG00000117289	TXNIP	1,64	0,04
ENSG00000123689	G0S2	1,63	0,05
ENSG00000162706	CADM3	1,63	0,07*
ENSG00000120088	CRHR1	1,62	0,07*
ENSG00000184557	SOCS3	1,61	0,03
ENSG00000176438	SYNE3	1,60	0,05
ENSG00000161958	FGF11	1,60	0,04
ENSG00000234745	HLA-B	1,59	0,06*
ENSG00000164236	ANKRD33B	1,59	0,09*
ENSG00000170624	SGCD	1,57	0,08*
ENSG00000259649	RP11-351M8.1	1,57	0,09*
ENSG00000172201	ID4	1,55	0,09*
ENSG00000119938	PPP1R3C	1,54	0,09*
ENSG00000114268	PFKFB4	1,54	0,04
ENSG00000110076	NRXN2	1,53	0,05
ENSG00000136378	ADAMTS7	1,52	0,02
ENSG00000152256	PDK1	1,52	0,03
ENSG00000112837	TBX18	1,51	0,09*
ENSG00000162733	DDR2	1,50	0,02
ENSG00000179348	GATA2	-1,51	0,09*
ENSG00000120693	SMAD9	-1,52	0,05
ENSG00000164736	SOX17	-1,52	0,09*
ENSG00000035664	DAPK2	-1,53	0,09*
ENSG00000144730	IL17RD	-1,54	0,01
ENSG00000133216	EPHB2	-1,55	0,03
ENSG00000166960	CCDC178	-1,55	0,09*
ENSG00000120279	MYCT1	-1,57	0,05
ENSG00000121039	RDH10	-1,57	0,06*
ENSG00000183578	TNFAIP8L3	-1,58	0,09*
ENSG00000145681	HAPLN1	-1,58	0,09*
ENSG00000158125	XDH	-1,59	0,09*
ENSG00000139174	PRICKLE1	-1,59	0,08*
ENSG00000182368	FAM27A	-1,59	0,09*
ENSG00000118137	APOA1	-1,60	0,07*
ENSG00000169684	CHRNA5	-1,60	0,09*
ENSG00000167644	C19orf33	-1,61	0,06*
ENSG00000116106	EPHA4	-1,61	0,05

ENSG00000125968	ID1	-1,61	0,04
ENSG00000123572	NRK	-1,61	0,09*
ENSG00000121361	KCNJ8	-1,63	0,07*
ENSG00000091129	NRCAM	-1,63	0,07*
ENSG00000175746	C15orf54	-1,64	0,05
ENSG00000172602	RND1	-1,64	0,04
ENSG00000095752	IL11	-1,64	0,07*
ENSG00000175866	BAIAP2	-1,65	0,01
ENSG00000127329	PTPRB	-1,65	0,06*
ENSG00000144366	GULP1	-1,66	0,005
ENSG00000143140	GJA5	-1,66	0,04
ENSG00000176399	DMRTA1	-1,68	0,05
ENSG00000168497	SDPR	-1,68	0,02
ENSG00000010319	SEMA3G	-1,69	0,02
ENSG00000254656	RTL1	-1,69	0,03
ENSG00000178445	GLDC	-1,69	0,02
ENSG00000162496	DHRS3	-1,70	0,04
ENSG00000102554	KLF5	-1,70	0,003
ENSG00000172159	FRMD3	-1,70	0,04
ENSG00000164283	ESM1	-1,71	0,03
ENSG00000235109	ZSCAN31	-1,72	0,01
ENSG00000132321	IQCA1	-1,72	0,02
ENSG00000008394	MGST1	-1,72	0,002
ENSG00000164530	PI16	-1,73	0,01
ENSG00000150722	PPP1R1C	-1,73	0,03
ENSG00000116741	RGS2	-1,74	0,02
ENSG00000180660	MAB21L1	-1,76	0,02
ENSG00000155011	DKK2	-1,77	0,01
ENSG00000126950	TMEM35	-1,81	0,02
ENSG00000179104	TMTC2	-1,81	0,004
ENSG00000118777	ABCG2	-1,85	0,01
ENSG00000125848	FLRT3	-1,87	0,007
ENSG00000108375	RNF43	-1,90	0,003
ENSG00000125845	BMP2	-1,90	0,005
ENSG00000138759	FRAS1	-1,90	0,005
ENSG00000108556	CHRNE	-1,91	0,005
ENSG00000163273	NPPC	-1,93	0,003
ENSG00000162595	DIRAS3	-1,93	0,003
ENSG00000109511	ANXA10	-1,93	0,003
ENSG00000154645	CHODL	-2,16	0,0003

ENSG00000138772	ANXA3	-2,23	0,0001
ENSG00000087494	PTHLH	-2,50	1,04E-07

Table 9. Differential gene expression between S and A. Fold Change (FC) valued is obtained by DeSeq2 method and *p* adjusted value (P_{adj}) was calculated using the FDR method. Significant P_{adj} value was considered ≤0.05. *Genes showing a trend towards significance but without reaching it ($P_{adj} \leq 0.09$).

Accurate isoform quantification remains a challenge due to high degree of overlapping between transcripts [241]. The variability in precision of isoform expression estimation across samples would be biased using traditional differential expression packages. For that reason, here we use the Bayesian approach Cufflink, which estimates transcript abundance based on how many reads support each transcript. DEI analysis identified 143 isoforms differently expressed between Sympt and Asympt SMCs. Table 10 illustrates the isoforms with a FC value below −1.5 or higher than 1.5 and with $P_{adj} \leq 0.05$.

Isoform id	Gene id	Symbol	FC	*P* value	P_{adj}
ENST00000358321	ENSG00000099994	SUSD2	11,61	5,00E-05	0,01
ENST00000260227	ENSG00000137673	MMP7	9,25	5,00E-05	0,01
ENST00000506608	ENSG00000185149	NPY2R	8,39	0,0002	0,04
ENST00000264613	ENSG00000047457	CP	7,90	0,0002	0,04
ENST00000374975	ENSG00000198502	HLA-DRB5	5,72	5,00E-05	0,01
ENST00000477717	ENSG00000117069	ST6GALNAC5	4,84	5,00E-05	0,01
ENST00000075322	ENSG00000136960	ENPP2	4,59	5,00E-05	0,01
ENST00000296130	ENSG00000163815	CLEC3B	4,37	5,00E-05	0,01
ENST00000394887	ENSG00000196616	ADH1B	4,07	5,00E-05	0,01
ENST00000259486	ENSG00000136960	ENPP2	3,88	5,00E-05	0,01
ENST00000013222	ENSG00000241644	INMT	3,84	5,00E-05	0,01
ENST00000393078	ENSG00000196136	SERPINA3	3,57	5,00E-05	0,01
ENST00000368125	ENSG00000162706	CADM3	3,53	0,00015	0,03
ENST00000296506	ENSG00000164106	SCRG1	3,43	5,00E-05	0,01
ENST00000256861	ENSG00000123243	ITIH5	3,42	0,00015	0,03
ENST00000294728	ENSG00000162692	VCAM1	3,38	5,00E-05	0,01
ENST00000274938	ENSG00000146197	SCUBE3	3,30	5,00E-05	0,01
ENST00000167586	ENSG00000186847	KRT14	3,06	5,00E-05	0,01
ENST00000374737	ENSG00000155659	VSIG4	3	0,00015	0,03
ENST00000372330	ENSG00000100985	MMP9	2,82	5,00E-05	0,01
ENST00000447544	ENSG00000135218	CD36	2,65	5,00E-05	0,01
ENST00000298295	ENSG00000165507	C10orf10	2,50	5,00E-05	0,01
ENST00000604125	ENSG00000152049	KCNE4	2,48	5,00E-05	0,01
ENST00000542220	ENSG00000159403	C1R	2,42	5,00E-05	0,01

ENST00000553804	ENSG00000135424	ITGA7	2,38	5,00E-05	0,01
ENST00000367662	ENSG00000116183	PAPPA2	2,34	0,00015	0,03
ENST00000006053	ENSG00000006210	CX3CL1	2,29	5,00E-05	0,01
ENST00000361673	ENSG00000198796	ALPK2	2,20	5,00E-05	0,01
ENST00000437043	ENSG00000164308	ERAP2	2,18	0,0001	0,02
ENST00000339732	ENSG00000131386	GALNT15	2,15	0,0002	0,04
ENST00000284322	ENSG00000154175	ABI3BP	2,12	5,00E-05	0,01
ENST00000261799	ENSG00000113721	PDGFRB	2,10	5,00E-05	0,01
ENST00000369317	ENSG00000117289	TXNIP	2,07	5,00E-05	0,01
ENST00000435422	ENSG00000170624	SGCD	2,06	5,00E-05	0,01
ENST00000345517	ENSG00000163017	ACTG2	2	0,00015	0,03
ENST00000257435	ENSG00000134986	NREP	1,99	5,00E-05	0,01
ENST00000429713	ENSG00000172403	SYNPO2	1,99	5,00E-05	0,01
ENST00000412585	ENSG00000234745	HLA-B	1,98	5,00E-05	0,01
ENST00000307365	ENSG00000168209	DDIT4	1,96	5,00E-05	0,01
ENST00000261326	ENSG00000075643	MOCOS	1,95	5,00E-05	0,01
ENST00000178638	ENSG00000074410	CA12	1,94	5,00E-05	0,01
ENST00000254722	ENSG00000132386	SERPINF1	1,93	5,00E-05	0,01
ENST00000335174	ENSG00000186352	ANKRD37	1,90	0,0002	0,04
ENST00000378700	ENSG00000172201	ID4	1,89	5,00E-05	0,01
ENST00000294507	ENSG00000162511	LAPTM5	1,89	5,00E-05	0,01
ENST00000540010	ENSG00000056558	TRAF1	1,89	5,00E-05	0,01
ENST00000330871	ENSG00000184557	SOCS3	1,88	5,00E-05	0,01
ENST00000344366	ENSG00000074410	CA12	1,87	5,00E-05	0,01
ENST00000238994	ENSG00000119938	PPP1R3C	1,86	5,00E-05	0,01
ENST00000217233	ENSG00000101255	TRIB3	1,84	5,00E-05	0,01
ENST00000327299	ENSG00000162433	AK4	1,83	0,0002	0,04
ENST00000328916	ENSG00000182326	C1S	1,79	0,0001	0,02
ENST00000323076	ENSG00000136167	LCP1	1,76	5,00E-05	0,01
ENST00000157600	ENSG00000071282	LMCD1	1,75	0,0001	0,02
ENST00000297848	ENSG00000187955	COL14A1	1,73	5,00E-05	0,01
ENST00000369663	ENSG00000112837	TBX18	1,73	5,00E-05	0,01
ENST00000367288	ENSG00000163431	LMOD1	1,72	5,00E-05	0,01
ENST00000338981	ENSG00000114374	USP9Y	1,70	5,00E-05	0,01
ENST00000566620	ENSG00000140945	CDH13	1,68	5,00E-05	0,01
ENST00000394308	ENSG00000070669	ASNS	1,65	0,0001	0,02
ENST00000402744	ENSG00000109472	CPE	1,65	5,00E-05	0,01
ENST00000367922	ENSG00000162733	DDR2	1,64	5,00E-05	0,01
ENST00000220244	ENSG00000103888	KIAA1199	1,62	0,0002	0,04
ENST00000380250	ENSG00000073910	FRY	1,58	0,00015	0,03

ENST00000409652	ENSG00000221963	APOL6	1,56	0,00015	0,03
ENST00000396680	ENSG00000128272	ATF4	1,55	0,00015	0,03
ENST00000372764	ENSG00000122861	PLAU	1,55	0,0001	0,02
ENST00000375377	ENSG00000165757	KIAA1462	1,54	0,00015	0,03
ENST00000263734	ENSG00000116016	EPAS1	1,53	5,00E-05	0,01
ENST00000295992	ENSG00000163710	PCOLCE2	1,53	5,00E-05	0,01
ENST00000376588	ENSG00000135069	PSAT1	1,53	0,0002	0,04
ENST00000274276	ENSG00000145623	OSMR	1,50	0,0002	0,04
ENST00000358432	ENSG00000142627	EPHA2	-1,50	5,00E-05	0,01
ENST00000260630	ENSG00000138061	CYP1B1	-1,53	0,00015	0,03
ENST00000229416	ENSG00000001084	GCLC	-1,56	0,0002	0,04
ENST00000367466	ENSG00000116711	PLA2G4A	-1,56	0,0001	0,02
ENST00000005257	ENSG00000006451	RALA	-1,56	0,0001	0,02
ENST00000245185	ENSG00000125148	MT2A	-1,57	0,0001	0,02
ENST00000361441	ENSG00000244509	APOBEC3C	-1,58	0,0001	0,02
ENST00000381434	ENSG00000137033	IL33	-1,62	0,0001	0,02
ENST00000272542	ENSG00000144136	SLC20A1	-1,63	5,00E-05	0,01
ENST00000371697	ENSG00000148677	ANKRD1	-1,64	0,00015	0,03
ENST00000248598	ENSG00000127951	FGL2	-1,67	5,00E-05	0,01
ENST00000315711	ENSG00000091972	CD200	-1,68	0,0002	0,04
ENST00000222543	ENSG00000105825	TFPI2	-1,69	5,00E-05	0,01
ENST00000237305	ENSG00000118515	SGK1	-1,72	5,00E-05	0,01
ENST00000367468	ENSG00000073756	PTGS2	-1,77	5,00E-05	0,01
ENST00000258888	ENSG00000136383	ALPK3	-1,78	5,00E-05	0,01
ENST00000426693	ENSG00000164619	BMPER	-1,81	0,0002	0,04
ENST00000379375	ENSG00000078401	EDN1	-1,86	5,00E-05	0,01
ENST00000276925	ENSG00000147883	CDKN2B	-1,91	5,00E-05	0,01
ENST00000377861	ENSG00000184226	PCDH9	-1,91	5,00E-05	0,01
ENST00000265080	ENSG00000113319	RASGRF2	-1,91	5,00E-05	0,01
ENST00000377103	ENSG00000178726	THBD	-1,93	5,00E-05	0,01
ENST00000376112	ENSG00000125968	ID1	-1,99	5,00E-05	0,01
ENST00000252593	ENSG00000130303	BST2	-2,03	5,00E-05	0,01
ENST00000396210	ENSG00000008394	MGST1	-2,04	5,00E-05	0,01
ENST00000330688	ENSG00000077092	RARB	-2,04	5,00E-05	0,01
ENST00000310613	ENSG00000173597	SULT1B1	-2,09	0,0001	0,02
ENST00000327536	ENSG00000183578	TNFAIP8L3	-2,09	5,00E-05	0,01
ENST00000274341	ENSG00000145681	HAPLN1	-2,10	5,00E-05	0,01
ENST00000304141	ENSG00000168497	SDPR	-2,10	5,00E-05	0,01
ENST00000262259	ENSG00000105497	ZNF175	-2,15	5,00E-05	0,01
ENST00000306773	ENSG00000171246	NPTX1	-2,21	5,00E-05	0,01

ENST00000222482	ENSG00000128510	CPA4	-2,27	5,00E-05	0,01
ENST00000377474	ENSG00000178695	KCTD12	-2,35	5,00E-05	0,01
ENST00000321196	ENSG00000179104	TMTC2	-2,35	5,00E-05	0,01
ENST00000315274	ENSG00000196611	MMP1	-2,40	0,00015	0,03
ENST00000444842	ENSG00000082482	KCNK2	-2,43	5,00E-05	0,01
ENST00000286614	ENSG00000156103	MMP16	-2,43	5,00E-05	0,01
ENST00000376468	ENSG00000120937	NPPB	-2,43	5,00E-05	0,01
ENST00000235382	ENSG00000116741	RGS2	-2,45	5,00E-05	0,01
ENST00000546561	ENSG00000127324	TSPAN8	-2,54	5,00E-05	0,01
ENST00000541194	ENSG00000128567	PODXL	-2,59	5,00E-05	0,01
ENST00000247829	ENSG00000127324	TSPAN8	-2,59	5,00E-05	0,01
ENST00000232892	ENSG00000114771	AADAC	-2,69	5,00E-05	0,01
ENST00000297785	ENSG00000165092	ALDH1A1	-2,72	5,00E-05	0,01
ENST00000591504	ENSG00000166510	CCDC68	-2,74	5,00E-05	0,01
ENST00000307407	ENSG00000169429	IL8	-2,82	5,00E-05	0,01
ENST00000284136	ENSG00000153993	SEMA3D	-2,85	5,00E-05	0,01
ENST00000537928	ENSG00000128567	PODXL	-2,86	0,0002	0,04
ENST00000376223	ENSG00000162496	DHRS3	-2,87	5,00E-05	0,01
ENST00000304195	ENSG00000172159	FRMD3	-3	0,00015	0,03
ENST00000359299	ENSG00000109511	ANXA10	-3,13	5,00E-05	0,01
ENST00000355754	ENSG00000162654	GBP4	-3,13	5,00E-05	0,01
ENST00000372930	ENSG00000126950	TMEM35	-3,22	5,00E-05	0,01
ENST00000296575	ENSG00000164161	HHIP	-3,48	5,00E-05	0,01
ENST00000326245	ENSG00000179914	ITLN1	-3,49	0,0001	0,02
ENST00000299502	ENSG00000197632	SERPINB2	-3,50	5,00E-05	0,01
ENST00000261292	ENSG00000101670	LIPG	-3,65	5,00E-05	0,01
ENST00000237612	ENSG00000118777	ABCG2	-3,81	5,00E-05	0,01
ENST00000397463	ENSG00000150551	LYPD1	-3,98	5,00E-05	0,01
ENST00000381405	ENSG00000164283	ESM1	-4,14	5,00E-05	0,01
ENST00000295461	ENSG00000163293	NIPAL1	-4,22	5,00E-05	0,01
ENST00000261405	ENSG00000110799	VWF	-4,25	5,00E-05	0,01
ENST00000378827	ENSG00000125845	BMP2	-4,27	5,00E-05	0,01
ENST00000263174	ENSG00000099260	PALMD	-4,36	5,00E-05	0,01
ENST00000395201	ENSG00000162595	DIRAS3	-4,39	5,00E-05	0,01
ENST00000271348	ENSG00000143140	GJA5	-4,86	5,00E-05	0,01
ENST00000409852	ENSG00000163273	NPPC	-4,93	5,00E-05	0,01
ENST00000282849	ENSG00000140873	ADAMTS18	-6,48	5,00E-05	0,01
ENST00000297316	ENSG00000164736	SOX17	-6,48	5,00E-05	0,01
ENST00000373674	ENSG00000164530	PI16	-8,28	5,00E-05	0,01

Table 10. Analysis of differential isoform expression between S and A using Cufflinks method. FC values are obtained by DeSeq2 method and *p* adjusted value (P_{adj}) was calculated applying the FDR. Significant P_{adj} value was considered ≤0.05.

Identified gene expression differences were also evaluated for gender differences since we had in our cohort only 2 women in Asympt and none in Sympt, and no effect of gender was found within the genes listed in Tables 9 and 10.

4.3.2. Functional enrichment and network analysis

Next, we performed functional and gene network analysis. Enrichment analysis allowing identification of combinations of significant annotations associated with the generated DEG and DEI lists was performed to identify functional relationships between the Sympt and Asympt samples. Bioconductor-based enrichment analysis using as databases GO, KEGG, reactome, DO (disease ontology), OMIM (Online Mendelian Inheritance in Man), and Cincinnati Children's Hospital Medical centre [242–245], generated a list of annotation groups which are significantly different between Sympt and Asympt. Among genes included in Tables 8 and 9, genes are associated with: *cell growth and senescence*, *bone metabolism*, *retinol metabolism*, *vascular disease*, *autophagy*, *immune system*, *muscle development*/ *contraction*. Table 11 illustrates all annotations that included between 2 and 27 genes per group and that showed a *q*-value ≤ 0.05 generated from the DEG list, and Table 12 illustrates the most significant annotations generated from DEI list.

While Bioconductor-based analysis allowed us to identify common functional categories for a cluster of genes, we next compared these categories between the gene clusters by implementation of the algorithm proposed by the tool ClusterProfiler [224]. This tool, which is used for gene cluster comparison (i.e. downregulated and upregulated genes in Sympt versus Asympt), allowed us to visualize biological categories compared between gene clusters. The identified functional profiles based on KEGG, GO, Reactome and DO are illustrated in Figure 34A-B and Figure 35A-B. KEGG-based comparison (Figure 34A) is used to map RNAseq data for biological interpretation of higher-level systemic functions and identified TGF-β signalling pathway, axon guidance and cell adhesion molecules (CAMs) as those categories with higher GeneRatio number and lower P_{adj} value. Retinol dehydrogenase activity was identified in GO-based comparison, which defines functional gene classes and their relationships, as the category with the lowest P_{adj} (Figure 34B).

Category	ID	Name	*q*-value	Hit Count	Hit in Query List
GO: Biological Process	GO:0072359	Circulatory system development	7,91E-06	21	EPHB2,TBX18,BMP2,PTPRB,NRCAM,DHRS3,PRICKLE1,PI16,SGCD,KLF5,ANXA3,KCNJ8,SOCS3,GATA2,SOX17,ID1,XDH,ESM1,FLRT3,MYO18B,ITGA7
GO: Biological Process	GO:0072358	Cardiovascular system development	7,91E-06	21	EPHB2,TBX18,BMP2,PTPRB,NRCAM,DHRS3,PRICKLE1,PI16,SGCD,KLF5,ANXA3,KCNJ8,SOCS3,GATA2,SOX17,ID1,XDH,ESM1,FLRT3,MYO18B,ITGA7
GO: Biological Process	GO:0009888	Tissue development	6,90E-05	27	TBX18,BMP2,NPPC,FRAS1,ADAMTS7,PRICKLE1,PI16,SGCD,KLF5,NRK,DDR2,SOCS3,RDH10,GATA2,SOX17,ID1,ID4,XDH,CLEC3B,FLRT3,SEMA3G,MYO18B,ITGA7,PTHLH,CRHR1,EPHA4,SMAD9
GO: Biological Process	GO:0045595	Regulation of cell differentiation	1,40E-04	24	EPHB2,BMP2,NPPC,CHODL,NRCAM,HLA-B,ADAMTS7,PRICKLE1,PI16,KLF5,DDR2,SOCS3,GATA2,SOX17,ID1,ID4,XDH,APOA1,SEMA3G,LRRC4C,BAIAP2,PTHLH,EPHA4,SMAD9
GO: Biological Process	GO:2000026	Regulation of multicellular organismal development	1,40E-04	25	EPHB2,TBX18,BMP2,CHODL,NRCAM,HLAB,ADAMTS7,PRICKLE1,PI16,ANXA3,NRK,DDR2,SLITRK4,GATA2,SOX17,ID1,ID4,XDH,APOA1,FLRT3,SEMA3G,LRRC4C,BAIAP2,PTHLH,EPHA4
GO: Biological Process	GO:0001655	Urogenital system development	2,28E-04	11	EPHB2,TBX18,BMP2,FRAS1,KCNJ8,RDH10,GATA2,SOX17,ID4,EPHA4,SMAD9

GO: Biological Process	GO:0001568	Blood vessel development	4,59E-04	14	EPHB2,PTPRB,NRCAM,PRICKLE1,KLF5,ANXA3,SOCS3,GATA2,SOX17,ID1,XDH,ESM1,MYO18B,ITGA7
GO: Biological Process	GO:0001944	Vasculature development	6,29E-04	14	EPHB2,PTPRB,NRCAM,PRICKLE1,KLF5,ANXA3,SOCS3,GATA2,SOX17,ID1,XDH,ESM1,MYO18B,ITGA7
GO: Biological Process	GO:0045596	Negative regulation of cell differentiation	6,45E-04	14	EPHB2,BMP2,NPPC,ADAMTS7,PRICKLE1,PI16,GATA2,SOX17,ID1,ID4,XDH,SEMA3G,PTHLH,EPHA4
GO: Biological Process	GO:0051241	Negative regulation of multicellular organismal process	6,45E-04	18	EPHB2,TBX18,BMP2,NPPC,ADAMTS7,PRICKLE1,PI16,GATA2,SOX17,ID1,ID4,IL20RB,XDH,APOA1,SEMA3G,RGS2,PTHLH,EPHA4
GO: Biological Process	GO:2000726	Negative regulation of cardiac muscle cell differentiation	1,18E-03	3	BMP2,PRICKLE1,PI16
GO: Biological Process	GO:0048514	Blood vessel morphogenesis	1,44E-03	12	EPHB2,PTPRB,NRCAM,KLF5,ANXA3,GATA2,SOX17,ID1,XDH,ESM1,MYO18B,ITGA7
Drug	D010100	Oxygen	1,76E-03	23	CA12,PPP1R3C,IL11,KCNE4,RND1,PTPRB,MCHR1,MGST1,DHRS3,PDK1,NRK,G0S2,SOCS3,XDH,TMTC2,APOA1,FGF11,CLEC3B,ABCG2,FLRT3,PFKFB4,FRMD3,HAPLN1
Drug	D002737	Chloroprene	1,82E-03	20	PPP1R3C,RND1,NRCAM,KLF5,MYCT1,G0S2,DDR2,GATA2,SOX17,ID4,XDH,ESM1,TMTC2,ABCG2,FLRT3,BAIAP2,RGS2,RNF43,PTHLH,EPHA4

GO: Biological Process	GO:0051093	Negative regulation of developmental process	2,23E-03	15	EPHB2,TBX18,BMP2,NPPC,ADAMTS7,PRICKLE1,PI16,GATA2,SOX17,ID1,ID4,XDH,SEMA3G,PTHLH,EPHA4
GO: Biological Process	GO:0022603	Regulation of anatomical structure morphogenesis	2,23E-03	16	EPHB2,TBX18,BMP2,SYNE3,NRCAM,ANXA3,GATA2,SOX17,ID1,XDH,APOA1,SEMA3G,LRRC4C,BAIAP2,ITGA7,EPHA4
GO: Biological Process	GO:0007507	Heart development	2,23E-03	12	TBX18,BMP2,DHRS3,PRICKLE1,PI16,SGCD,KCNJ8,GATA2,SOX17,ID1,FLRT3,MYO18B
Drug	C024746	Tobacco tar	2,69E-03	8	FRAS1,NRCAM,PRICKLE1,GLDC,ANXA10,ESM1,DMRTA1,RGS2
GO: Biological Process	GO:0051094	Positive regulation of developmental process	2,72E-03	18	EPHB2,TBX18,BMP2,NPPC,NRCAM,KLF5,ANXA3,DDR2,SLITRK4,SOCS3,GATA2,SOX17,ID4,APOA1,FLRT3,BAIAP2,EPHA4,SMAD9
GO: Biological Process	GO:0048585	Negative regulation of response to stimulus	4,05E-03	19	TBX18,BMP2,DHRS3,HLA-B,PRICKLE1,SOCS3,GATA2,SOX17,IL20RB,XDH,APOA1,FLRT3,SEMA3G,LRRC4C,RGS2,RNF43,CRHR1,DKK2,EPHA4
GO: Biological Process	GO:0002009	Morphogenesis of an epithelium	4,32E-03	11	TBX18,BMP2,FRAS1,PRICKLE1,SOCS3,RDH10,SOX17,ID4,FLRT3,PTHLH,EPHA4
GO: Biological Process	GO:0010769	Regulation of cell morphogenesis involved in differentiation	6,16E-03	9	EPHB2,BMP2,NRCAM,ID1,APOA1,SEMA3G,LRRC4C,BAIAP2,EPHA4
Drug	CID005282222	Xanthoxin	6,22E-03	3	DHRS3,SDPR,MOCOS

Drug	C089730	Rosiglitazone	6,22E-03	20	PPP1R3C,BMP2,RND1,MGST1,DHRS3,PDK1,KLF5,ANXA3,KCNJ8,G0S2,C10orf10,SLITRK4,SOCS3,ANXA10,RDH10,ID1,ID4,XDH,CLEC3B,RGS2
GO: Biological Process	GO:0022604	Regulation of cell morphogenesis	7,76E-03	11	EPHB2,BMP2,SYNE3,NRCAM,ID1,APOA1,SEMA3G,LRRC4C,BAIAP2,ITGA7,EPHA4
Gene Family	ANXA	Annexins	8,94E-03	2	ANXA3,ANXA10
Gene Family	IL	Interleukins and interleukin receptors	8,94E-03	3	IL11,IL20RB,IL17RD
GO: Biological Process	GO:0072001	Renal system development	9,14E-03	8	TBX18,BMP2,FRAS1,KCNJ8,RDH10,SOX17,EPHA4,SMAD9
Drug	CID000093003	6-chloropurine riboside	1,08E-02	3	ID1,XDH,MOCOS
Drug	CID006437077	Ac1o5myk	1,08E-02	5	PPP1R3C,TNFAIP8L3,MGST1,NRK,PPP1R1C
Drug	CID000002524	1-alpha-25-dihydroxycholecalciferol	1,08E-02	14	CA12,IL11,BMP2,TNFAIP8L3,MGST1,SOCS3,GATA2,ID1,PPP1R1C,TMTC2,BAIAP2,ITGA7,RNF43,PTHLH
GO: Biological Process	GO:0045597	Positive regulation of cell differentiation	1,10E-02	14	EPHB2,BMP2,NPPC,NRCAM,KLF5,DDR2,SOCS3,GATA2,SOX17,ID4,APOA1,BAIAP2,EPHA4,SMAD9
GO: Molecular Function	GO:0052650	NADP-retinol dehydrogenase activity	1,15E-02	2	DHRS3,RDH10
GO: Molecular Function	GO:0004745	Retinol dehydrogenase activity	1,15E-02	3	BMP2,DHRS3,RDH10
GO: Molecular Function	GO:0042802	Identical protein binding	1,15E-02	17	EPHB2,CADM3,TBX18,BMP2,NPPC,MGST1,PDK1,GLDC,DAPK2,ID1,XDH,APOA1,DMRTA1,ABCG2,FLRT3,BAIAP2,EPHA4

GO: Molecular Function	GO:0005102	Receptor binding	1,15E-02	19	EPHB2,IL11,CADM3,BMP2,NPPC,RND1,MCHR1,HLA-B,NRXN2,KCNJ8,ESM1,APOA1,FGF11,FLRT3,SEMA3G,ITGA7,RNF43,PTHLH,EPHA4
GO: Biological Process	GO:0007413	Axonal fasciculation	1,21E-02	3	EPHB2,NRCAM,EPHA4
GO: Biological Process	GO:0060284	Regulation of cell development	1,21E-02	14	EPHB2,BMP2,NPPC,CHODL,NRCAM,PI16,GATA2,ID1,ID4,APOA1,SEMA3G,LRRC4C,BAIAP2,EPHA4
GO: Biological Process	GO:0060429	Epithelium development	1,21E-02	16	TBX18,BMP2,FRAS1,PRICKLE1,KLF5,SOCS3,RDH10,SOX17,ID1,ID4,XDH,FLRT3,PTHLH,CRHR1,EPHA4,SMAD9
GO: Biological Process	GO:0055026	Negative regulation of cardiac muscle tissue development	1,31E-02	3	BMP2,PRICKLE1,PI16
GO: Biological Process	GO:0051960	Regulation of nervous system development	1,32E-02	13	EPHB2,BMP2,CHODL,NRCAM,SLITRK4,GATA2,ID1,ID4,FLRT3,SEMA3G,LRRC4C,BAIAP2,EPHA4
GO: Biological Process	GO:0045664	Regulation of neuron differentiation	1,36E-02	11	EPHB2,BMP2,CHODL,NRCAM,GATA2,ID1,ID4,SEMA3G,LRRC4C,BAIAP2,EPHA4
GO: Molecular Function	GO:0030151	Molybdenum ion binding	1,49E-02	2	XDH,MOCOS
GO: Molecular Function	GO:0045499	Chemorepellent activity	1,49E-02	3	APOA1,FLRT3,SEMA3G
GO: Molecular Function	GO:0046983	Protein dimerization activity	1,49E-02	16	CADM3,TBX18,BMP2,NPPC,MGST1,PDK1,GLDC,SOX17,ID1,ID4,XDH,DMRTA1,ABCG2,FLRT3,ITGA7,CHRNA5

GO: Biological Process	GO:0048598	Embryonic morphogenesis	1,51E-02	11	EPHB2,TBX18,FRAS1,PRICKLE1,SOCS3,RDH10,GATA2,SOX17,APOA1,FLRT3,ITGA7
GO: Biological Process	GO:0009790	Embryo development	1,51E-02	15	EPHB2,TBX18,BMP2,FRAS1,PRICKLE1,NRK,SOCS3,RDH10,GATA2,SOX17,APOA1,ABCG2,FLRT3,MYO18B,ITGA7
GO: Biological Process	GO:0023057	Negative regulation of signaling	1,51E-02	16	IL11,TBX18,BMP2,DHRS3,PRICKLE1,SOCS3,GATA2,SOX17,XDH,APOA1,FLRT3,LRRC4C,RGS2,RNF43,CRHR1,DKK2
GO: Molecular Function	GO:0042803	Protein homodimerization activity	1,53E-02	12	CADM3,TBX18,BMP2,NPPC,MGST1,PDK1,GLDC,ID1,XDH,DMRTA1,ABCG2,FLRT3
GO: Cellular Component	GO:0005887	Integral component of plasma membrane	1,56E-02	19	EPHB2,CADM3,BMP2,KCNE4,PTPRB,MCHR1,NRCAM,HLA-B,SGCD,KCNJ8,DDR2,FLRT3,ITGA7,IL17RD,RNF43,CRHR1,CHRNA5,CHRNE,EPHA4
GO: Cellular Component	GO:0031226	Intrinsic component of plasma membrane	1,56E-02	19	EPHB2,CADM3,BMP2,KCNE4,PTPRB,MCHR1,NRCAM,HLA-B,SGCD,KCNJ8,DDR2,FLRT3,ITGA7,IL17RD,RNF43,CRHR1,CHRNA5,CHRNE,EPHA4
GO: Biological Process	GO:0003308	Negative regulation of Wnt signaling pathway involved in heart development	1,60E-02	2	BMP2,SOX17
GO: Biological Process	GO:0010648	Negative regulation of cell communication	1,60E-02	16	IL11,TBX18,BMP2,DHRS3,PRICKLE1,SOCS3,GATA2,SOX17,XDH,APOA1,FLRT3,LRRC4C,RGS2,RNF43,CRHR1,DKK2

GO: Biological Process	GO:2000725	Regulation of cardiac muscle cell differentiation	1,61E-02	3	BMP2,PRICKLE1,PI16
GO: Biological Process	GO:0045669	Positive regulation of osteoblast differentiation	1,61E-02	4	BMP2,NPPC,DDR2,ID4
GO: Biological Process	GO:0045667	Regulation of osteoblast differentiation	1,61E-02	5	BMP2,NPPC,DDR2,ID1,ID4
GO: Biological Process	GO:0001525	Angiogenesis	1,61E-02	9	EPHB2,PTPRB,NRCAM,KLF5,ANXA3,GATA2,SOX17,ID1,ESM1
GO: Biological Process	GO:0051174	Regulation of phosphorus metabolic process	1,61E-02	20	IL11,BMP2,NPPC,TNFAIP8L3,PDK1,NRK,DDR2,SOCS3,ID1,PPP1R1C,XDH,APOA1,FLRT3,LRRC4C,IL17RD,RGS2,PTHLH,CRHR1,DIRAS3,EPHA4
GO: Biological Process	GO:0045995	Regulation of embryonic development	1,67E-02	5	TBX18,NRK,GATA2,SOX17,APOA1
GO: Biological Process	GO:0035295	Tube development	1,68E-02	11	TBX18,BMP2,PRICKLE1,KLF5,RDH10,GATA2,SOX17,ID1,PTHLH,EPHA4,SMAD9
GO: Biological Process	GO:0030178	Negative regulation of Wnt signaling pathway	1,68E-02	6	TBX18,BMP2,PRICKLE1,SOX17,RNF43,DKK2
GO: Biological Process	GO:0048729	Tissue morphogenesis	1,73E-02	11	TBX18,BMP2,FRAS1,PRICKLE1,SOCS3,RDH10,SOX17,ID4,FLRT3,PTHLH,EPHA4
GO: Biological Process	GO:0051154	Negative regulation of striated muscle cell differentiation	1,79E-02	3	BMP2,PRICKLE1,PI16
GO: Biological Process	GO:0030278	Regulation of	1,79E-02	6	BMP2,NPPC,DHRS3,DDR2,ID1,ID4

		ossification			
Drug	D012822	Silicon dioxide	1,93E-02	21	IL11,BMP2,NPPC,FRAS1,PTPRB,PI16,KCNJ8,G0S2,SLITRK4,SOCS3,XDH,ESM1,DMRTA1,CLEC3B,ABCG2,FLRT3,SEMA3G,LRRC4C,RGS2,DIRAS3,HAPLN1
GO: Biological Process	GO:0048710	Regulation of astrocyte differentiation	1,94E-02	3	BMP2,ID4,EPHA4

Table 11. Molecular enrichment associations analysis on DEG performed with Bioconductor tool. Significant annotations with *q*-value ≤ 0.01 are shown.

Category	**ID**	**Name**	**q-value**	**Hit Count**	**Hit in Query List**
Drug	D003907	Dexamethasone	8,61E-18	51	GALNT15,CA12,KCTD12,CYP1B1,AADAC,DDIT4,NPPB,PSAT1,NPPC,KRT14,DHRS3,PDGFRB,PI16,LMCD1,SGK1,ENPP2,SERPINF1,ACTG2,CP,CPE,RGS2,PTGS2,EDN1,TXNIP,BMP2,GJA5,MT2A,TRIB3,MGST1,GCLC,SLC20A1,CD36,ANKRD1,ASNS,KCNK2,PLA2G4A,PLAU,CLEC3B,ATF4,ABCG2,ALDH1A1,MMP1,BMPER,MMP9,MMP16,CX3CL1,IL33,VCAM1,SDPR,ALPK2,CDH13
Drug	D010100	Oxygen	6,51E-17	49	CA12,CYP1B1,DDIT4,NPPB,PSAT1,SYNPO2,NPTX1,DHRS3,PDGFRB,LMCD1,PODXL,SGK1,ANKRD37,ENPP2,SOCS3,ACTG2,CP,TMTC2,CPE,NREP,PTGS2,EDN1,ITIH5,HAPLN1,PPP1R3C,TXNIP,MT2A,KCNE4,MGST1,GCLC,LIPG,CD36,ANKRD1,ASNS,SERPINB2,COL14A1,AK4,PLAU,CLEC3B,ATF4,ABCG2,MMP1,MMP7,MMP9,CX3CL1,EPAS1,VCAM1,CDH13,FRMD3

GO: Biological Process	GO:0072359	Circulatory system development	1,14E-11	35	CYP1B1,NPPB,NPY2R,RARB,DHRS3,PDGFRB,PI16,SGCD,ENPP2,SERPINF1,SOCS3,SOX17,ID1,ESM1,CPE,ITGA7,PTGS2,EDN1,TBX18,BMP2,GJA5,HHIP,EPHA2,CD36,ANKRD1,KCNK2,ALPK3,COL14A1,PLAU,BMPER,MMP9,CX3CL1,EPAS1,VCAM1,CDH13
GO: Biological Process	GO:0072358	Cardiovascular system development	1,14E-11	35	CYP1B1,NPPB,NPY2R,RARB,DHRS3,PDGFRB,PI16,SGCD,ENPP2,SERPINF1,SOCS3,SOX17,ID1,ESM1,CPE,ITGA7,PTGS2,EDN1,TBX18,BMP2,GJA5,HHIP,EPHA2,CD36,ANKRD1,KCNK2,ALPK3,COL14A1,PLAU,BMPER,MMP9,CX3CL1,EPAS1,VCAM1,CDH13
GO: Cellular Component	GO:0005615	Extracellular space	1,16E-09	37	CPA4,SERPINA3,NPPB,NPPC,ABI3BP,PI16,LMCD1,PODXL,ENPP2,HLA-DRB5,SERPINF1,ACTG2,CP,SCRG1,CPE,LCP1,EDN1,FGL2,BMP2,SEMA3D,THBD,LIPG,CD36,SERPINB2,C1R,C1S,COL14A1,PLAU,CLEC3B,MMP1,BMPER,MMP7,MMP9,CX3CL1,IL33,VCAM1,CDH13
GO: Biological Process	GO:0001525	Angiogenesis	1,04E-07	20	CYP1B1,NPPB,PDGFRB,ENPP2,SERPINF1,SOX17,ID1,ESM1,PTGS2,EDN1,GJA5,HHIP,EPHA2,CD36,PLAU,BMPER,MMP9,CX3CL1,EPAS1,CDH13
Pathway	812256	TNF signaling pathway	1,74E-03	8	TRAF1,SOCS3,PTGS2,EDN1,ATF4,MMP9,CX3CL1,VCAM1

Pathway	576262	Extracellular matrix organization	1,74E-03	12	DDR2,ITGA7,HAPLN1,BMP2,ADAMTS18,COL14A1,PCOLCE2,MMP1,MMP7,MMP9,MMP16,VCAM1
GO: Cellular Component	GO:0098590	Plasma membrane region	2,53E-03	20	KCTD12,DHRS3,PDGFRB,PODXL,ITLN1,DDR2,CPE,LCP1,PTGS2,HHIP,KCNE4,BST2,EPHA2,CD36,KCNK2,ATF4,ABCG2,OSMR,SDPR,CDH13

Table 12. Bioconductor molecular enrichment association analysis on DEI. Selected annotations illustrated are those showing significant *q*-value ≤ 0,003 from each category.

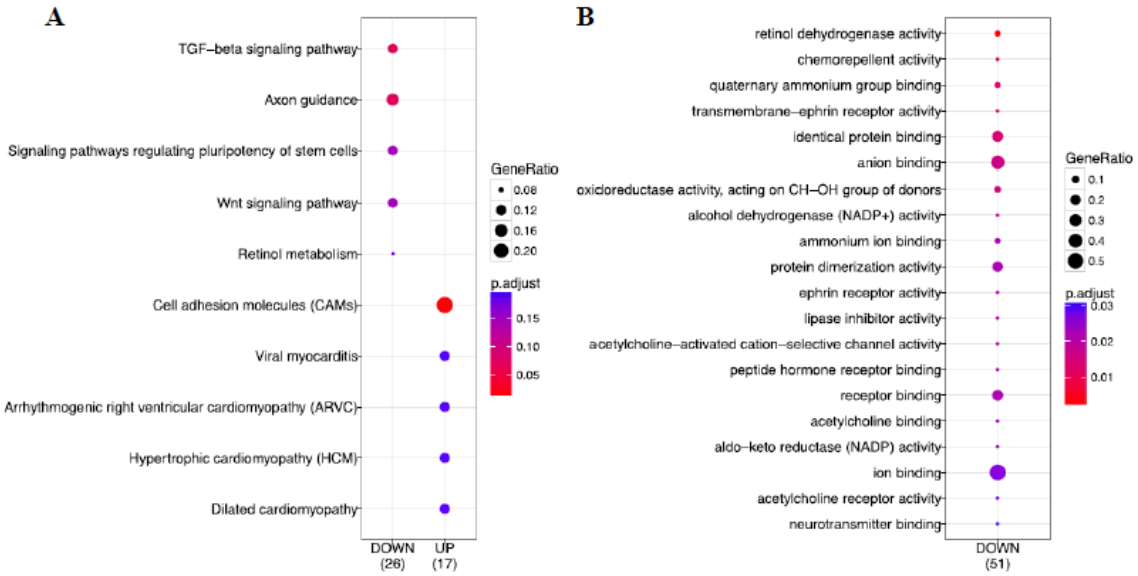

Figure 34. Comparative study between under-expressed and over-expressed genes using ClusterProfiler method. (A) Comparative analysis based on KEGG. **(B)** Comparative analysis based on Gene Ontology. GeneRatio corresponds to the number of genes from a specific category. Enrichment term is represented by coloured dots (red indicates high enrichment and blue indicates low enrichment).

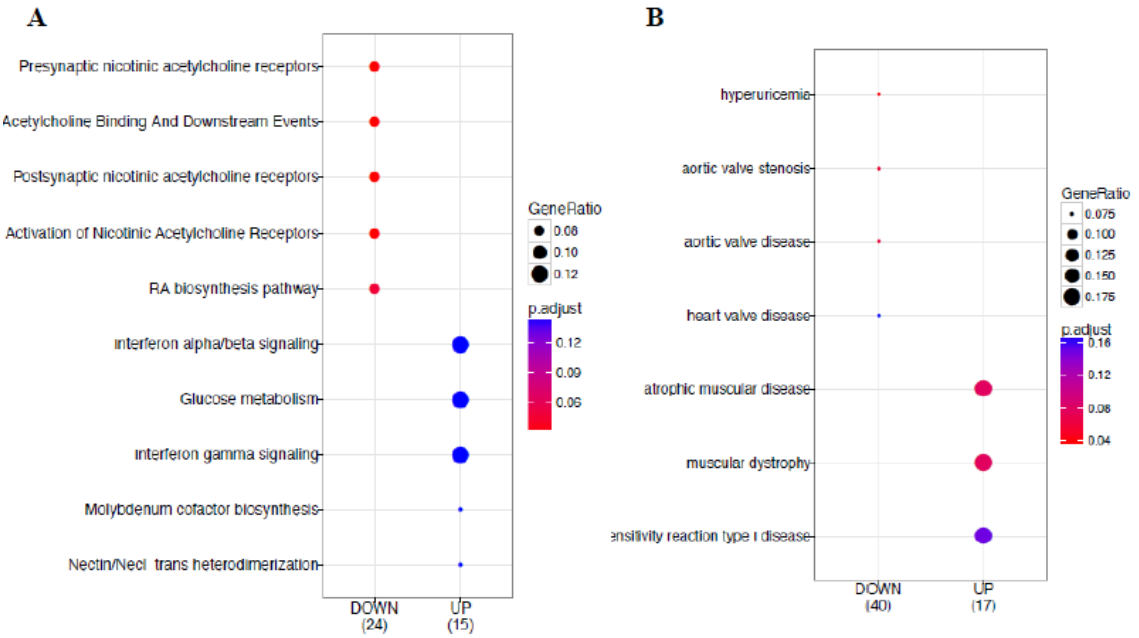

Figure 35. Comparative study between under-expressed and overexpressed genes using ClusterProfiler method. (A) Comparative analysis based on Reactome. **(B)** Comparative analysis based on Disease Ontology. GeneRatio is the number of genes from a specific category. Enrichment term is represented by coloured dots (red indicates high enrichment and blue indicates low enrichment).

In addition, functional interaction network analysis using several sources of information such as protein interaction, genomics, pathways, etc. was performed using the program called GeneMANIA (Gene Multiple Association Network Integration Algorithm) [246]. Figure 36 shows the functional network of genes obtained by GeneMANIA including clusters related with

transforming growth factor beta (TFG-β) signalling, axon guidance, cell adhesion molecules and activin receptor-like kinase (ALK) 1 signalling. Subsequently, a further network analysis to identify a core network from the functional network generated with GeneMANIA was done with the method MCODE (Molecular Complex Detection) [247]. MCODE performs a network clustering step, which reduces the unconnected nodes in network clusters. Thus, the final cluster identified by MCODE was that with higher specificity and showed that the TGF-β, BMP and ALK1 signalling pathways arose as a functional process, which distinguish SMCs isolated from Sympt or Asympt carotid plaques. Also notable is the identification in this network clustering analysis of 3 downregulated genes/isoforms: bone morphogenetic protein 2 (*BMP2*; DEG: FC −1,9; P_{adj} 0,004/DEI: FC-4,27; P_{adj} 0,01), smad family member 9 (*SMAD9*; DEG: FC −1,51; P_{adj} 0,05) and inhibitor of DNA binding 1 (*ID1*; DEG: FC −1,61; P_{adj} 0,03/DEI: FC-1,99; P_{adj} 0,01). It was also found inhibitor of DNA binding 4 (*ID4*; DEG: FC 1,55; P_{adj} 0,09/DEI: FC 1,89; P_{adj} 0,01) as upregulated gene/isoform in SMCs associated with plaque destabilization (Figure 37).

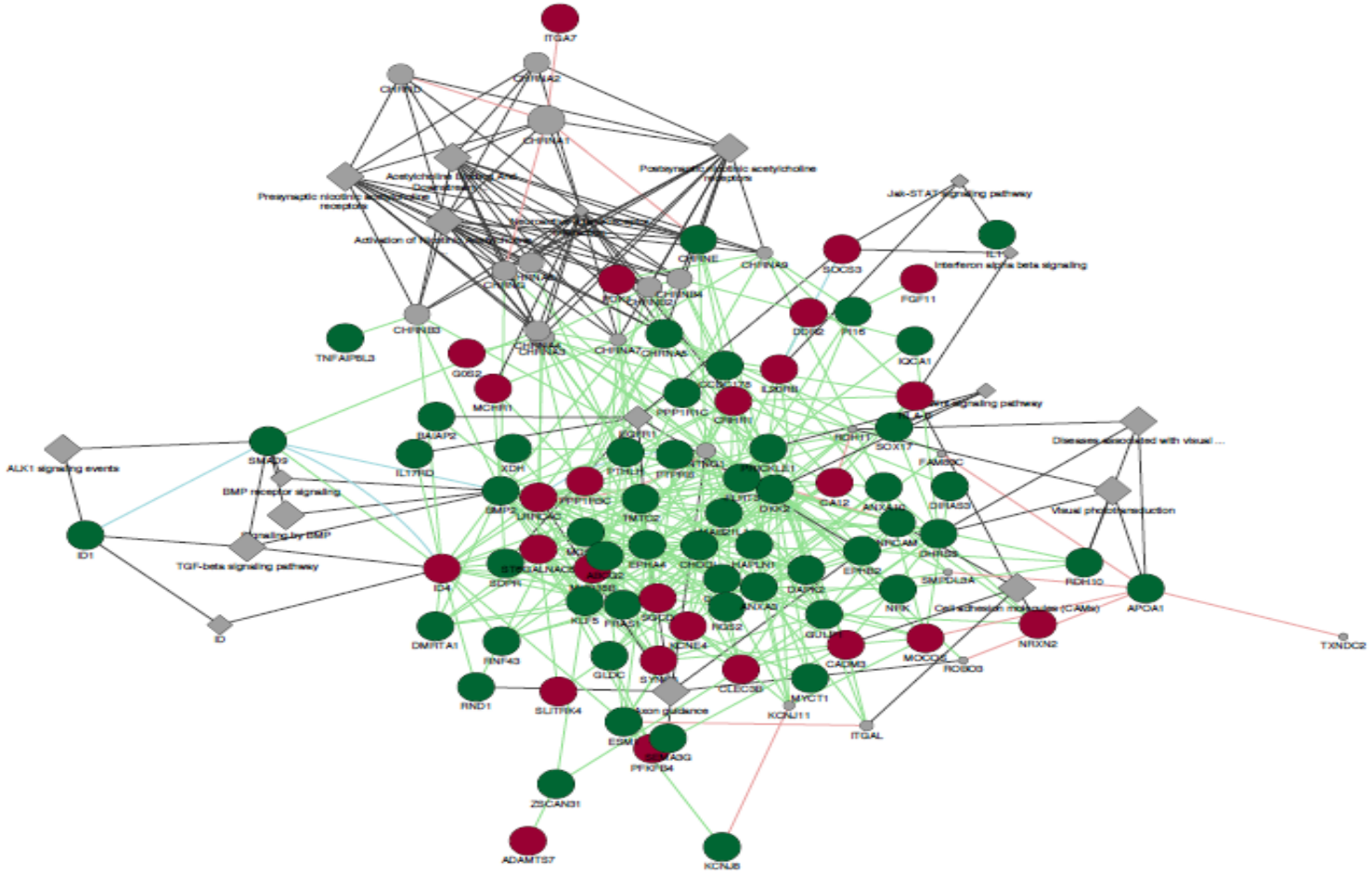

Figure 36. GeneMANIA network diagram. Red and green circles are query genes identified as upregulated and downregulated between Sympt and Asympt respectively by RNAseq. Grey circles are extra genes connected by prediction. Rhomboids represent protein domains. Green lines represent genetic interactions. Blue lines represents pathway database.

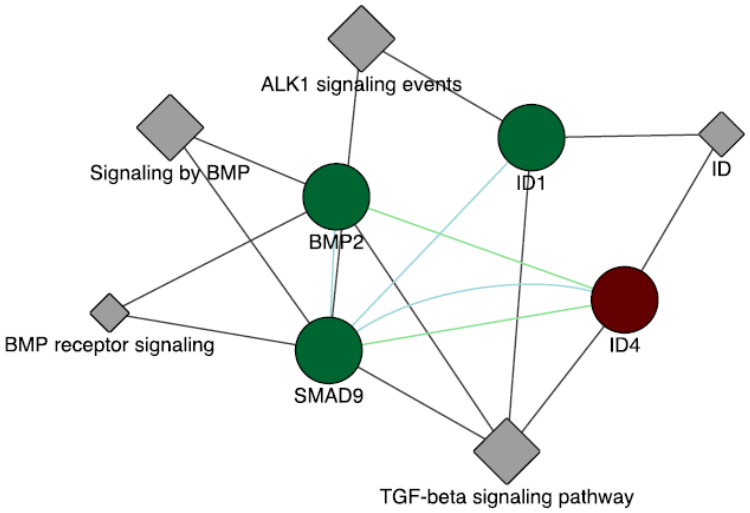

Figure 37. MCODE network clustering analysis. Illustration of the identified cluster by the network clustering algorithm MCODE showing the interaction between ID4, ID1, BMP2, SMAD9, TGF-beta signaling, BMP signalling and ALK1 signaling. The circles are genes and the rhomboids are protein domains. Green lines represent genetic interactions. Green circles indicate downregulated genes in Sympt vs. Asympt and the purple circle indicates upregulated gene in Sympt vs. Asympt. Blue lines represent pathways. Grey lines indicate gene-pathway associations.

4.3.3. Effect of cell culture and passaging on gene expression

Based on the found DEGs, we have analyzed these gene expressions during passage 0 and 1 with the aim to verify that these DEGs are not an effect of SMC culture.

Analysis of gene expression of SMC specific marker *MYH11* in SMCs isolated after 3 hours of digestion or 16 hours showed no differences (Figure 38A). Furthermore, Figure 38B, C and D show no significant differences in gene expression of *MYH11*, *BMP2*, *ID1* and *ID4* genes in SMCs isolated from passage 0 and 1.

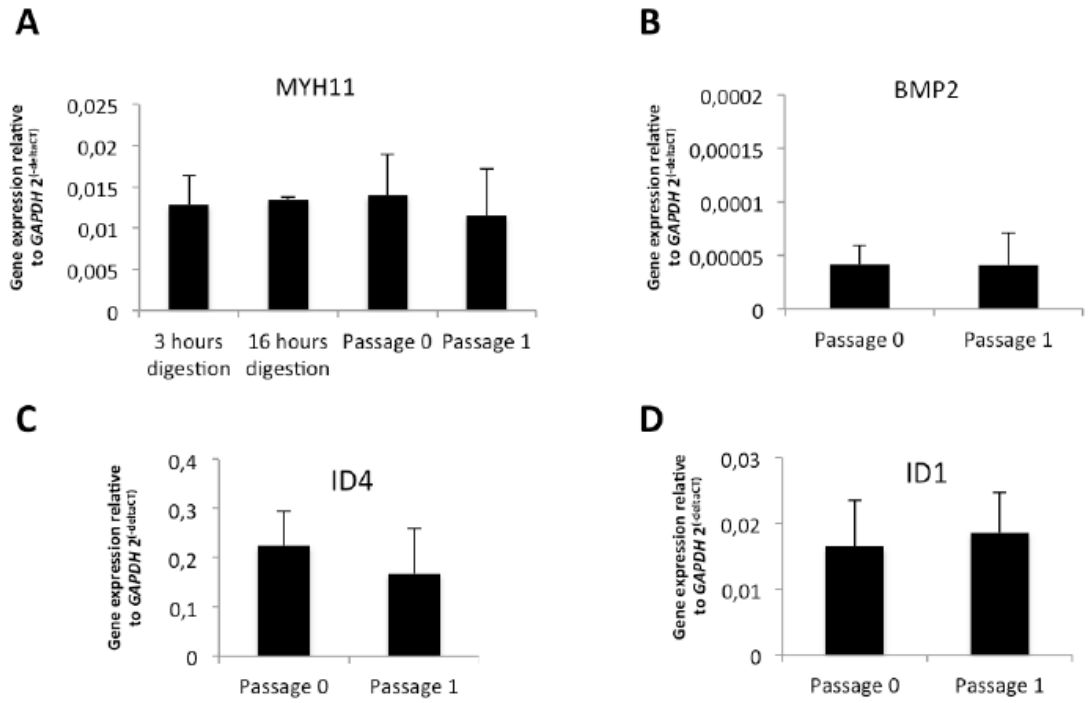

Figure 38. (A) Differential gene expression analysis of *MYH11* in SMCs isolated after 3 and 16 hours of collagenase digestion and in SMCs from passage 0 and 1. **(B)** Differential gene expression of *BMP2* in passage 0 vs passage 1. **(C)** Differential gene expression of *ID4* in passage 0 vs passage 1. **(D)** Differential gene expression of *ID1* in SMCs from passage 0 and passage 1. *GAPDH* was used as housekeeping gene for normalization. Figure shows a representative analysis of gene expression levels in two different SMCs samples in each condition with 4 performed replicates to illustrate quality control (MYH11).

4.3.4. Confirmation of RNAseq identified biomarkers by digital PCR

Forty-one of the identified DEG RNAseq genes were selected for replication in 13 of the RNAseq-analysed samples (1 sample was not available) and for further validation in an additional cohort of 11 independent samples (4Sympt and 7Asympt) by digital qPCR (dPCR). The replication by dPCR showed very similar results to those found by RNAseq (Table 12) with similar fold change directions (− or +) for 38 of these genes. Studies comparing RNAseq and qPCR data have indeed demonstrated very good correlation (Table 13) [248]. We could not detect 3 of the selected genes. In one case (*CHODL*, chondrolectin) this may have been due to very low expression levels seen in the RNAseq data, which were undetectable by digital dPCR. In the other two cases (*SOCS3*, suppressor of cytokine signaling 3 and *TNFAIP8L3*, TNF-α-induced protein 8-like 3), where the expected expression levels should not have been low, technical issues relating to dPCR amplification and primer specificity may have been at stake. Combined analysis of the replication and validation datasets revealed significant fold changes coinciding with those of the original RNAseq with the exception of one gene (*KCNE4*, potassium voltage-gated channel subfamily E regulatory subunit 4; FC = 1.01). Thus, validation

of 37 out of 38 genes attests to the accuracy of the RNAseq data. In the gene expression analysis done with only the 11 additional samples, the majority of genes apart of two (*HAPLN1*, hyaluronan and proteoglycan link protein 1; and *TBX18*, T-box 18) showed similar fold change tendency. From those, 16 genes showed significant fold change differences, 7 genes showed tendency toward significance and 15 genes did not show any significant differences.

Gene symbol	RNAseq (n=14)		dPCR replication (n=13)		dPCR validation (n=11)		qPCR replication + validation	
	FC	P_{adj}	FC	*p*-value	FC	*p*-value	FC	*p*-value
PTHLH	-2,50	<0,0001	-1,32	0,001	-1,12	> 0,1	-1,23	0,006
ANXA3	-2,23	<0,0001	1,08	0,02	-1,13	0,02	1,08	0,009
NPPC	-1,93	0,0038	-3,75	<0,0001	-10,16	0,0004	-4,54	<0,0001
ANXA10	-1,93	0,0035	-2,61	<0,0001	-1,63	0,09	-2,06	0,0003
DIRAS3	-1,93	0,0039	-2,80	0,0003	-1,29	0,08	-2,31	<0.0001
BMP2	-1,90	0,0049	-2,42	0,005	-3,87	0,08	-3,70	0,0018
ABCG2	-1,85	0,0104	-1,81	0,0008	-3,44	<0,0001	-2,09	<0,0001
TMTC2	-1,81	0,0159	-2,04	<0,0001	-1,73	0.03	-2,08	<0,0001
TMEM35	-1,81	0,0159	-2,37	0,03	-1,59	0,05	-2,13	0,0003
RGS2	-1,74	0,0188	-2,42	<0,0001	-1,71	0,08	-2,07	0,0006
ZSCAN31	-1,72	0,0107	-1,90	<0,0001	-1,82	0,03	-1,92	0,0001
MGST1	-1,72	0,0010	-1,33	0,007	-1,29	0,09	-1,32	<0,007
ESM1	-1,71	0,0329	-2,03	0,02	-1,99	0,05	-1,90	0,0017
KLN5	-1,70	0,0031	-1,49	0,0003	-1,39	0,04	-1,51	<0,0001
DHRS3	-1,70	0,0437	-2,96	<0,0001	-2,57	0,02	-3,14	<0,0001
FRMD3	-1,70	0,0419	-1,67	0,005	-1,85	0,02	-1,75	0,0005
ID1	-1,61	0,0368	-1,69	0,05	-5,01	0,009	-4,11	0,0008
EPHA4	-1,61	0,0470	-1,69	0,0002	-1,39	>0,1	-1,59	0,0003
HAPLN1	-1,58	0,0997	-2,16	0,0003	1,58	0,0038	-1,14	0,08
RDH10	-1,57	0,0585	-1,60	0,0002	-1,17	>0,1	-1,50	0,0019
EPHB2	-1,55	0,0278	-1,91	<0,0001	1,25	>0,1	-1,30	0,017
IL17RD	-1,54	0,0126	-1,28	0,01	-1,04	>0,1	-1,22	0,015
SMAD9	-1,52	0,0548	-1,68	0,003	-1,20	>0,1	-1,45	0,01
GULP1	-1,41	0,0471	-1,69	0,0003	-1,30	>0,1	-1,48	0,0032
DDR2	1,50	0,0219	1,48	0,001	1,01	>0,1	1,32	0,017
TBX18	1,51	0,0900	1,59	0,0003	-1,39	0,03	1,19	0,05
ADAMTS7	1,52	0,0224	1,96	<0,0001	1,04	>0,1	1,32	0,0017
PDK1	1,52	0,0339	1,71	<0,0001	1,17	>0,1	1,40	0,0002
PFKFB4	1,54	0,0389	1,33	0,003	1,27	>0,1	1,13	0,02

ID4	1,55	0,0900	1,73	0,001	1,01	>0,1	1,47	0,0037
SYNE3	1,60	0,0460	2,00	0,0019	1,01	>0,1	1,79	0,0067
CA12	1,72	0,0006	1,53	0,001	1,27	0,03	1,47	0,0002
MOCOS	1,75	0,0011	1,56	0,008	1,92	0,003	1,79	<0,0001
ITGA7	1,81	0,0051	3,05	<0,0001	1,58	0,09	2,06	<0,0001
ST6GALNAC5	1,83	0,0096	5,74	<0,0001	2,31	0,04	4,44	<0,0001
KCNE4	1,87	0,0031	1,33	0,02	1,01	>0,1	1,19	>0,1
MYO18B	1,70	0,0419	2,71	0,0002	1,06	>0,1	1,95	0,0021
C10orf10	1,94	0,0006	2,64	<0,0001	1,02	0,06	1,62	0,011

Table 13. Replication of 38 genes in RNAseq samples and validation in independent cohort.

4.3.5. Inflammatory pathways in carotid atheroma SMCs

Based on gene expression profiles disclosed by RNAseq SMCs actively participate in enhancing the characteristic inflammation of this disease and in this context, may also be causally involved in the rupture of the plaque (Table 9). Extensive purity controls were performed to confirm that SMC cultures were devoid of macrophages, lymphocytes and DCs based on the absence of *CXCL9*, *CXCL10* and *CD5L* expression (Figure 13). This was supported post factum by absence or very low counts of *CD3*, *CD19*, *CD57* and *CD209* reads, characteristic of professional immune cells present in the plaque, in the SMC RNAseq profiles. ECs were also found not to contaminate SMC cultures given the absence of their marker PECAM-1 in the SMC cultures (Figure 12).

RNAseq-Identified Highly Expressed Cytokines, Chemokines and TNF Superfamily Members in SMCs from Carotid Atherosclerosis Plaques

Both SMCs from Asympt and Sympt patients expressed overlapping sets of cytokines that may promote further inflammation into the atherosclerotic carotid plaque. Among identified genes with differences in expression levels between Sympt and Asympt SMCs of carotid atherosclerotic plaque, can be found genes associated with immune system (Table 9). Enrichment analysis demonstrated that immune response function arose as an enriched category (p-value<0.01).

We have focused in interleukin-mediated signaling (ILs, IL receptors, SOCS, JAK/STAT), chemotaxis molecules, leukocyte immunoglobulin-like receptors (LILRs) and TNF, IFN and NF-κB family members. The most active pathways relative to immune system appeared to be related to positive regulation of lymphocyte activation, especially T lymphocytes, cytokine production, cell proliferation, leukocyte and monocyte chemotaxis, apoptosis, TNF-α and NF-

κβ signaling pathways and calcium ion import. The engagement of these pathways is correlated with the expression of molecules such as ILs, IL receptors, CCLs, TNF family members and signal transduction factors (Figure 38) that are expressed at high levels in carotid plaque SMCs (>1000 reads) and may function to maintain the inflammatory state within the atherosclerotic plaque.

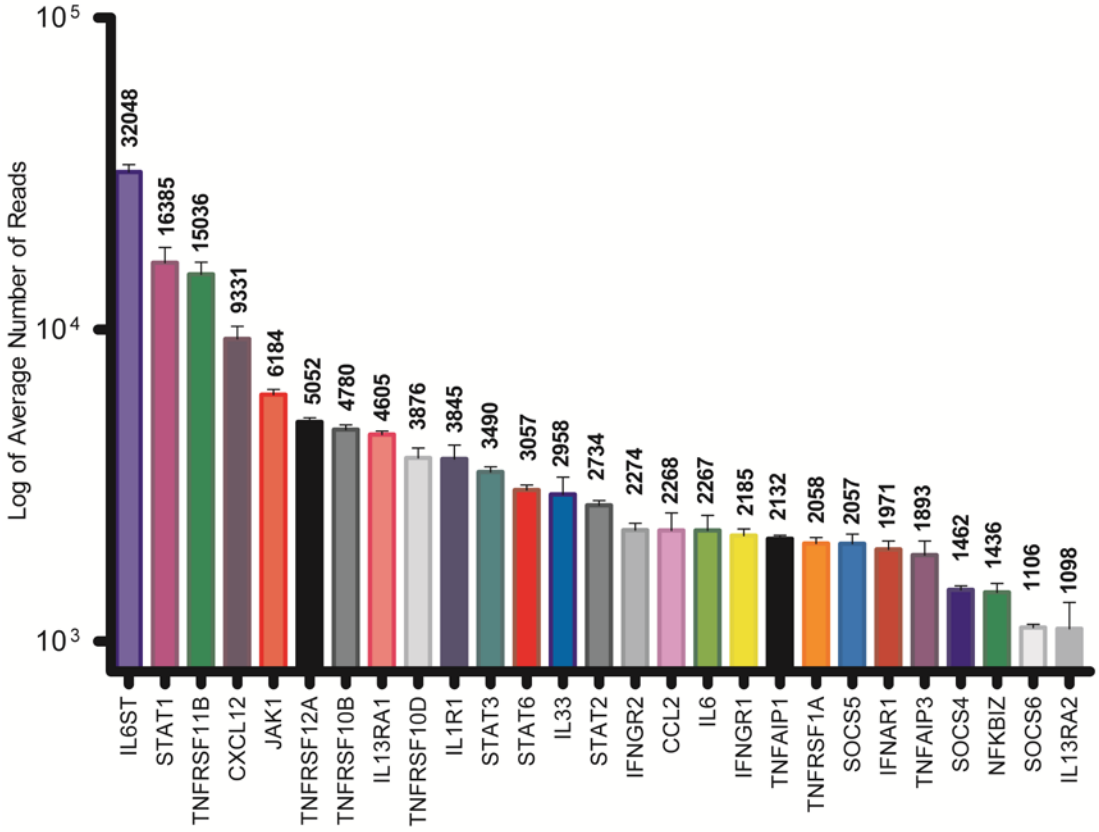

Figure 38. The most highly expressed cytokines & inflammation-related genes of human SMCs isolated from atherosclerotic plaques. Expressed in logarithmic scale based on the average number of reads obtained by RNAseq analysis (from 12 individual samples ± SEM). In the top of each bar in vertical appears the average Reads Nº for each gene.

Interleukin-6 signal transducer (IL-6ST, also called gp130) is the common subunit of the IL-6 receptor complex and appears to be the most expressed cytokine gene (Figure 38). The IL6-ST signaling pathway involves Janus kinase (JAK) 1, signal transducer and activator of transcription (STAT) 1 and 3 as well as its ligand IL-6, all of which feature among the highly expressed inflammatory SMC genes (Figure 38), while further ligands are less abundantly expressed e.g. IL-11 (Table 14), or not (OSM,oncostatin M; IL-27; IL-35) [249]. IL-6 receptor (IL-6R), which is a part of IL-6 receptor complex binding to IL-6, appeared also to be expressed by SMCs from human carotid atherosclerotic plaques, albeit at lower levels than *IL6ST* (Reads Nº ± SEM: 176 ± 18) (data not shown). IL6-ST/STAT3 signaling attenuation is driven by IL6-

ST itself recruiting SOCS3 (discussed below) which promotes receptor signaling complex degradation [250].

In addition to IL-6 [251], *TNFRSF12A* (Figure 38), TNF receptor superfamily member 12A, is the receptor of TNF-like weak inducer of apoptosis (TWEAK) which upon binding is also able to induce CCL2 expression [252], which can be found with 2268 number of reads (logarithmic scale).

Osteoprotegerin (OPG) is the protein encoded by the TNF receptor superfamily member 11b gene (*TNFRSF11B*) and, like *IL6ST*, is highly expressed by carotid plaque SMCs (Figure 38). It is a soluble member of the tumor necrosis factor receptor superfamily that regulates osteoclastogenesis and has been related to bone and mineral formation [253].

OPG can bind to TNF-related apoptosis-inducing ligand (TRAIL or *TNFSF10* gene) which is a potent activator of apoptosis [254]. It seems that OPG and TRAIL may function to inhibit each other, thus, OPG blocks TRAIL-induced apoptosis and this latter one inhibits the OPG-induced inhibition of osteoclastogenesis [254]. Although *TNFSF10* seems not to be expressed by carotid plaque SMCs at appreciable levels, another two receptors for TRAIL named *TNFRSF10B* (DR5: death receptor 5) and *TNFRSF10D* (DCR2: decoy receptor 2) are found to be among the most abundantly expressed inflammation-related genes by SMCs. The first one is able to induce apoptosis upon binding to TRAIL, the second, on the contrary, is a decoy receptor that blocks TRAIL before its binding to the membrane receptor thus protecting against TRAIL-mediated induction of apoptosis [255].

CXCL12 or stromal cell-derived factor 1 (SDF-1) is a member of the CXC chemokine family. This chemokine consists of various isoforms which are functionally indistinguishable and have been found to be involved in platelets aggregation in the initial steps of atherosclerosis development. Now, we can involve SMCs in platelets chemoattraction by *CXCL12* expression (Figure 38) [256].

IL1R1 (Figure 38) and IL1RAP (Reads Nº ± SEM: 825 ± 60) are cytokine receptors whose ligands IL-1α (Reads Nº ± SEM: 20 ± 7) and IL-1β (Reads Nº ± SEM: 88 ±29) seem not or poorly expressed in SMCs. Another member of the IL-1 family, signaling through *IL1RAP* and *IL1RL1*, *IL-33*, is abundantly expressed (Figure 38).

Carotid atherosclerosis SMCs show virtual absence of TNF-α production (Reads Nº ± SEM: 8 ± 4), but *TNFRSF1A*, its receptor, appears to be highly expressed (Figure 38). Furthermore, two TNF-α-induced proteins (TNFAIP1 and 3) count as well among the highly expressed immune genes (Figure 38). These may participate in proteasome-mediated ubiquitin-dependent protein catabolic processes [257] or constitute an ubiquitin-editing enzyme containing both ubiquitin

ligase and deubiquitinase activities [258], respectively. TNFAIP3 can function as a blocking factor for IFN-β and IFN-γ signaling in SMCs through their corresponding receptors IFN alpha and beta subunit 1, 2 receptor complex (IFNAR1 and IFNRA2) and interferon gamma receptor 1, 2 complex (IFNGR1 and IFNGR2), respectively (Figure 38). Both signaling pathways are active in atherosclerotic plaque SMCs and work through STAT1, which can be induced by IFN-β.

4.3.6. Cytokine and chemokine expression based on patient symptomatology

A subset of 20 genes of cytokines, chemokines, cytokine receptors and associated factors showed significant differences in expression levels between Asympt and Sympt patients. The most significant were *IL17RD*, *IL20RB* and *SOCS3*, which retained significance at the 0.05 level after *p*-value adjustment, followed by C-C motif chemokine ligand 5 (*CCL5*), *IL11* and *TNFAIP8L3* ($p<0.005$, $P_{adj}< 0.1$), and a further series of factors with non-significant trends (Table 14).

GENE ID	GENE NAME	FC	*p*-value	P_{Adj}	ASYMPTOMATIC		SYMPTOMATIC	
					NUM. READS	SEM	NUM. READS	SEM
ENSG00000174564	IL20RB	1,75	0,0001	0,0248**	36	3	103	28
ENSG00000161570	CCL5	1,65	0,0004	0,0585*	25	2	88	38
ENSG00000184557	SOCS3	1,61	0,0001	0,0316**	619	95	1163	119
ENSG00000115604	IL18R1	1,32	0,0519	0,4660	52	5	84	22
ENSG00000157368	IL34	1,29	0,0757	0,5318	335	110	601	109
ENSG00000006210	CX3CL1	1,28	0,0592	0,4878	141	23	327	143
ENSG00000115594	IL1R1	1,28	0,0406	0,4286	3224	236	4466	743
ENSG00000145779	TNFAIP8	1,27	0,0432	0,4377	382	33	521	84
ENSG00000163735	CXCL5	1,27	0,0658	0,5091	41	10	97	45
ENSG00000196083	IL1RAP	1,24	0,0274	0,3756	722	66	929	89
ENSG00000171150	SOCS5	1,24	0,0388	0,4224	1800	105	2315	251
ENSG00000027697	IFNGR1	1,19	0,0325	0,3979	1981	140	2389	127
ENSG00000162434	JAK1	1,18	0,0058	0,2009	5645	219	6722	311
ENSG00000159128	IFNGR2	1,16	0,0834	0,5513	2092	164	2455	139
ENSG00000169429	CXCL8	-1,31	0,0374	0,4192	999	323	372	101
ENSG00000115008	IL1A	-1,36	0,0053	0,1917	36	15	5	3
ENSG00000215788	TNFRSF25	-1,37	0,0264	0,3682	31	4	18	5
ENSG00000144730	IL17RD	-1,54	0,0000	0,0125**	138	5	83	9
ENSG00000183578	TNFAIP8L3	-1,58	0,0011	0,0998*	368	58	177	32
ENSG00000095752	IL11	-1,64	0,0005	0,0692*	117	20	46	11

Table 14. Differentially expressed immune-relevant genes in SMCs of carotid atherosclerotic plaques extracted from Asympt and Sympt patients. The gene expression levels in SMCs from Sympt

patients relative to Asympt are expressed by fold change. Only genes with p-value<0.1 have been selected. * means p-adjusted value<0.1 while ** is a p-adjusted value<0.05. Num. reads: Average number of transcript reads for each gene in Asympt versus Sympt patients (6 each). SEM: standard error of the mean.

IL-17 receptor D (*IL-17RD*), an orphan receptor with no reported physiological role in IL-17 signaling [259], arose as the gene with the most highly significant difference between A and S (Table 14), and no literature data are available on a putative role in atherosclerosis or vascular disease. The second most significant molecule is IL-20 receptor beta subunit (*IL-20RB*). This one functions heterodimerized with IL-20RA for signaling by IL-19, -20 and -24, and can, in addition, also pair with IL22-RA1 to bind IL-20 and IL-24 [260]. *IL20-RA* and *IL22-RA1* appeared not to be, or at very low levels (Reads Nº ± SEM for IL20-RA: 3 ± 0.7; for IL-22RA1: 4 ± 0.9), expressed in SMCs; however, *IL20RB* was expressed at significantly higher level in SMCs coming from symptomatic atherosclerotic plaques (Table 14).

SOCS3 is a negative regulator of the Janus kinase/signal transducers and activators of transcription (JAK/STAT) signaling pathway that induces the expression of inflammatory genes that regulate key atherosclerotic processes, such as leukocyte recruitment, migration and proliferation of vascular SMCs, apoptosis and foam cell formation [261].

Expression of SOCS3 leads to the inhibition of signaling of a wide range of cytokines, hormones and growth factors by blocking the signal transduction through their receptors [262,263]. SMCs from atherosclerotic plaques express multiple target receptors for SOCS3 such as leukemia inhibitory factor receptor (LIFR), oncostatin M receptor (OSMR), IL-4R, IFNGR-1/2, IFNAR1/2, insulin-like growth factor 1 receptor (IGF1R), leptin receptor (LEPR), growth hormone receptor (GHR), erythropoietin receptor (EPOR) and IL-12 receptor β 2 (IL-12Rβ2). All of these are associated to some of the STAT1, 2, 3, 4 and 6 through which they mediate signaling.

IL-11 belongs to the IL-6 cytokine family and is one of the cytokines that signals through the common signal transducing subunit IL-6ST [264]. *IL11* appeared more abundantly expressed in SMCs from Asympt patient carotid atherosclerotic plaques (Table 14).

Our RNAseq study provide additional support showing that chemokines such as *CCL5* are expressed in SMCs coming from atherosclerotic plaques, which, moreover, appears to be over-expressed in Sympt patients compared to Asympt (Table 14). Expression of the chemokine *CCL5* can be induced by TNF-α, rather than IL-6, through TNFR1 (*TNFRSF1A*) and posterior JAK2 activation and STAT3 phosphorylation, culminating in *CCL5* transcription in mice vascular SMCs [265]. This CCL5 exerts its function through the receptors C-C motif chemokine

receptor (CCR) 1, 3 and 5, of which only *CCR1* appeared to be highly expressed by SMCs (Reads Nº ± SEM: CCR1: 246 ± 64; CCR3: 0 ± 0; CCR5: 25 ± 9) [265,266].

The TIPE (tumor necrosis factor-α-induced protein 8-like, or TNFAIP8L) family comprises regulators of immunity and tumorigenesis and is composed of TNFAIP8 (TIPE0), TNFAIP8L1 (TIPE1), TNFAIP8L2 (TIPE2) and TNFAIP8L3 (TIPE3). This family is involved in signaling pathways of chemotaxis, inflammation, tumorigenicity and wound healing [267]. *TNFAIP8L3* showed higher expression in SMCs from Asympt plaques. It is the most recently discovered TIPE family member and still awaits functional characterization.

5. DISCUSSION

5.1. ATHEROMA PLAQUE SMC CHARACTERIZATION

SMCs keep their plasticity and can undergo cellular modulation from contractile to synthetic-state or reverse the phenotype toward the contractile stage in response to changes in local environmental cues [173]. Upon injury in atherosclerosis, when remodeling is required, SMCs are able to switch between distinct phenotypes with a trend towards increased rates of proliferation and migration accompanied by enhanced extracellular matrix component production. Also, calcification or release of inflammatory signals is coordinated with a decrease in SMC contractile markers [175]. This study has documented the expression patterns of relevant genes associated with phenotypic modulation in SMCs by comparing carotid atherosclerotic lesions with macroscopically intact regions located within the surgically excised carotid artery areas. In addition, the SMCs' expression pattern was compared between those from symptomatic versus asymptomatic to evaluate if any changes were associated with symptomatology or plaque rupture.

The contractile function of SMCs is achieved by expression of a unique repertoire of proteins such as ACTA2, MYH11, CALD1, and SM22α/TAGLN [196]. Myocardin binds to the globally expressed transcription factor SRF, and this complex regulates the expression of these SMC-specific markers. SMC contractile specific genes contain a functional CArG box in their promoter region, to which the myocardin–SRF complex binds in order to promote SMC gene expression. SMCs express *MKL2*, which is a transcriptional co-factor for SMC-specific genes [268].The expression of transcription factor *MKL2*, and moreover *SRF*, were decreased in PLQ-SMCs compared to MIT-SMCs. This result suggests that cells present in damaged areas have gone through a phenotypic modulation possibly regulated by the SRF transcriptional pathway [199]. Furthermore, KLF4 is a member of a large family of zinc finger-containing DNA-binding transcription factors and is known to regulate the expression of SMC markers [269] since it is a repressor of SRF/myocardin [270]. Krüppel-like factors have been identified as

atheroprotective factors [271] and KFL4, specifically, has been identified as a critical marker that regulates SMC phenotypic transition inhibiting expression of contractile genes. Contrary to this, it has also been suggested to play a proatherogenic role due to its involvement in inhibiting the cell proliferation cycle. *KFL4* expression is very low under basal conditions; however, injury promotes its expression in vascular tissues [272]. This evidence supports our observation that *KLF4* is upregulated in PLQ-SMCs, suggesting that de-differentiated SMCs are mainly restricted to the area of the lesion, while MIT-SMCs seem to remain predominantly contractile.

In this study, we found that carotid PLQ-SMCs showed a decreased expression of specific contractile phenotype markers MYH11 (protein and mRNA level) and CALD1 (mRNA level) compared to MIT-SMCs. MYH11 has been identified as a marker for specific SMC lineage [175,273] and is a late marker during development, expressed only in fully differentiated cells and showing a high degree of specificity for contractile phenotype SMCs [274]. In addition, data obtained from HIASMCs from a healthy donor treated with 7KC, one of the major components of oxidized lipoproteins in atheroma plaques, indicates that healthy SMCs under these conditions proceed towards a de-differentiation process. Furthermore, decreased levels of SMC contractile markers have been reported before in atherosclerosis [175]. Thus, our results suggest that PLQ-SMCs might have a decreased contractile capacity.

We demonstrated that carotid SMCs from PLQ and MIT were positive for MYH11 protein staining by immunofluorescence microscopy and that PLQ-SMCs showed a lower volume of myofilaments per cell area with lower fluorescence intensity of the protein, in line with the results of a previous work in which significantly reduced MYH11 protein staining was observed in switched SMCs coming from atherosclerotic carotids [275]. In addition, Song and coworkers [276] suggested that myofilament disassembly, especially in the upper cortex, could reflect SMC phenotypic modulation, contractile components degradation, and reorganization of contractile and cytoskeletal proteins within the cell [182]. Similarly, our analysis performed by z-stack to observe the whole thickness of cells showed that staining of MYH11 was predominant in the central region of the cytoplasm in the upper planes of the MIT-SMCs, unlike PLQ-SMCs that displayed less prominent myosin staining in the perinuclear area, in which myofilaments appeared to be disassembled, such Saltis et al. [277] reported before. Therefore, immunofluorescence microscopy shows that MYH11 in MIT-SMCs forms strong myofilament bundles, whereas they appear as thin and disassembled fibers in PLQ-SMCs, which is characteristic of phenotype modulation in SMCs.

We have also found increased levels of *CD68*, *LGALS3*, and *SPP1*, together with the reduced expression of contractile proteins in PLQ-SMCs compared to SMCs from MIT area, suggesting that PLQ-SMCs may have undergone a phenotypic alteration towards a macrophage-like cell to

adapt to such changes. This is consistent with results reported before [205,278], demonstrating that SMCs have the potential to become macrophage-like cells with a capacity to migrate and to display phagocytic behavior to digest excessive material present at the lesion site. In line with this notion, we have also analyzed the expression of the autophagy marker MAP1LC3B, which is known to be important in the de-differentiation of SMCs through removing contractile proteins by autophagy [279] and in carotid plaque stability [280]. Interestingly, PLQ-SMCs showed higher expression of *MAP1LC3B* than MIT-SMCs. HIASMCs treated with 7KC also exhibited increased autophagy marker *MAP1LC3B* expression alongside augmentation of *CD68* and *LGALS3*. Thus, similarly to what was reported for mouse SMCs and human coronary SMCs [281], in our study, HIASMCs loaded with cholesterol may initiate conversion towards foam-type cells as indicated by their loss of SMC features and their acquisition of macrophage-type characteristics. SMC-derived macrophage cells not only make a significant contribution to plaque volume and necrotic core formation but also suppress plaque stability and promote plaque instability [282].

In addition, with the aim to explore any potential correlation between SMC phenotypes and patient symptomatology, we have analyzed these contractile markers in SMCs from symptomatic and asymptomatic plaques. Interestingly, plaques showed a similar expression pattern of PLQ vs. MIT for MYH11 expression, i.e., reduced expression at mRNA and protein level in SMCs coming from symptomatic plaques compared to asymptomatic plaques. This suggests that SMCs from symptomatic plaques may have suffered a phenotypic modulation, while SMCs from asymptomatic plaques retain the contractile capacity associated with MYH11 expression [175].

5.2. SMC TRANSCRIPTOMIC ANALYSIS

RNAseq technologies have been used as promising means for biomarker identification in several diseases lately [283,284]. Since its discovery around 10 years ago, RNAseq has become an innovative tool for transcriptomics [285]. Stroke is a heterogeneous disease and the use of combination of biomarkers included in panels may enhance sensitivity and specificity of the applicability of biomarkers [286]. In this study, RNAseq based transcriptomic data was generated from RNA extracted from SMCs isolated from carotid atheroma plaques from 7 Asympt and 7 Sympt patients with the aim of identifying candidate genes and pathways that could discriminate the two groups studied, Sympt and Asympt. We identified genes/transcripts candidates for panel/s, which have a potential to classify these two studied groups (Asympt and Sympt) (Tables 9 and 10).

TGF-β signaling was identified in this study as a crucial pathway in symptomatology of carotid atherosclerosis at the vascular smooth muscle cell level. TGF-β signaling emerged initially in the functional enrichment analysis performed (Figure 34A) and the subsequent MCODE network clustering also identified TFG-β signaling but together with BMP and ALK1 signaling with highly interacting nodes (Figure 37). TGF-β superfamily members are involved in several processes including cell proliferation, migration, extracellular matrix production, bone morphogenesis, etc. and can be classified into two groups: TGF-β/activin/nodal and BMP/growth differentiation factors (GDFs) [287]. BMP proteins have multiple functions that are associated with growth, differentiation and cell death during embryonic development [288]. Some BMPs proteins have osteogenic activity capacity, in fact, BMPs are the active proteins responsible for ectopic bone formation [289]; in particular BMP2, which belongs to the BMPs that play a role in ossification [290]. It has been reported that BMP2 inhibits SMCs cell growth and migration, promoting a contractile phenotype [291], which is observed in normal vessels. High levels of BMP2 in blood have been recently associated with plaque progression and calcification in coronary atherosclerosis [292]. We found significantly lower levels of expression of *BMP2* in our symptomatic SMCs compared with asymptomatic, which is indicative for a beneficial role of BMP2 in atheroma plaque stability both by contributing to the stabilization through bone morphogenesis and by promoting a protective phenotype, which may be called an osteogenic phenotype. BMP2 plays a role in ALK1 signaling, in which ALK1 is a type I receptor of TGF-β that is regulated by BMP2 expression in vascular cells enhancing expression of SMC lineage markers [293].

TGF- β pathway can directly transduce extracellular cues from the cell-surface transmembrane receptors to the nucleus through intracellular mediators, known as Smads (R-Smad, Co-Smad, I-Smads). Smads accumulate in the nucleus and elicit transcriptional responses to alter gene expression [294]. The subfamily of Smads called R-Smads includes several proteins of which some are involved in the BMP signaling branch (i.e. Smad1, Smad5 and Smad9) [295]. Particularly, increased transcription of *SMAD9* has been found in response to stimulation with BMP [288]. Thus, BMP-activated *SMAD9* gene [294] has found to be expressed at lower levels in Sympt than in Asympt SMCs, as *BMP2* (Tables 9 and 10).

BMP proteins are also related to Id genes (Inhibitors of differentiation: *ID1*, *ID2*, *ID3* and *ID4*), since they are major downstream transcriptional targets of BMP signaling [296]. In particular, *ID1*, *ID2* and *ID3* genes have been identified as early response genes in BMP signaling that are required for Smad protein binding to DNA [288]. BMPs induce Id gene expression in vascular smooth muscle cells. Besides BMPs, growth and differentiation factor 5 (GDF5) and TGF-β also regulate the expression of Id proteins [297]. In mammals, four Id proteins partially overlap in their profiles of expression and display some functional redundancy in vivo [298]. These

proteins have been associated with regulation of several cellular processes such as cell growth, senescence, angiogenesis and apoptosis. Interestingly, BMP2 induced the expression of *ID1* in the mouse myoblast cell line C2C12 [289] and upregulation of the *ID1* gene is known to delay senescence in endothelial cells [299,300]. Similarly to endothelial cells, our results suggest that *ID1* expression in SMCs may be exhibiting a role as anti-senescence factor due to high expression in Asympt SMCs. Senescence of vascular SMCs involve inhibition of cell cycle, then, SMCs in the fibrous cap may contribute significantly to inefficient plaque repair and also overexpress genes that directly promote plaque instability including adhesion molecules, regulators of haemostasis and MMPs, which may be associated with plaque stability [301]. While *ID1, 2* and *3* are expressed in multiple tissues, *ID4* has been reported to be expressed in neuronal tissues and intestinal embryonic epithelium [297,302]. Although *ID4* is expressed at a much lower level in the vascular wall than the other three Id proteins [302], we found that *ID4* expression levels in all our SMCs samples were not lower but even higher than the other Id genes. Also upon comparison of *ID4* levels between Sympt and Asympt, we found that *ID4* expression was higher in symptomatic SMC samples. This is also consistent with the observation that over-expression of *ID4* in astrocyte-derive cell line induces apoptotic cell death [303], suggestive for senescence-like phenotype. Thus, based in this hypothesis we can also suggest that Sympt cells may also be in a senescence phenotype.

Other genes identified in our differential expression analysis include those related to bone mineralization matter, such as carbonic anhydrase 12 (*CA12*), parathyroid hormone-like hormone (*PTHLH*) and natriuretic peptide C (*NPPC*). CA12 showed higher expression in SMCs from Sympt vs. Asympt (FC 1,72; P_{adj} = 0,0006) in our study and although during initial phase of atherosclerosis bone resorption could be beneficial [304], in later stages, such as in advanced plaques from symptomatic patients, bone resorption may affect the plaque destabilization process. Conversely, *PTHLH* was found to be downregulated in SMCs from Sympt vs. Asympt (FC −2,5; P_{adj} = 0,0000). PTHLH has been shown to increase bone formation and decrease bone resorption [305]. Similarly, *NPPC* (FC −1,93; P_{adj} = 0,0038) was found to be downregulated in Sympt vs. Asympt and is as well considered a positive regulator of bone formation [306]. Thus, this finding may reinforce our hypothesis that SMCs from Asympt benefit from bone mineralization processes.

In summary, taken together our gene expression profiling data and combined analysis, SMCs isolated from asymptomatic patients may exhibit a calcified/osteogenic-like phenotype, while SMCs from symptomatic patients exhibit a senescence-like phenotype.

5.3. CYTOKINE PATHWAYS UNEARTHED BY RNASEQ IN CAROTID ATHEROMA SMOOTH MUSCLE CELLS

Although the main producers of cytokines are helper T cells (Th) and macrophages [307], activated SMCs were already known to produce many cytokines in atherosclerotic plaques [308]. This study adds now new candidates not identified before in this context, and provides the genome-wide quantitative expression profiles of cytokine and associated transcripts in SMCs coming from atherosclerotic carotid plaques. Both SMCs from Asympt and Sympt patients expressed overlapping sets of cytokines that may promote further inflammation into the atherosclerotic carotid plaque.

Based on identified cytokines (Figure 38), the most active pathways identified in SMCs of atherosclerotic plaques involves the IL-6ST. IL-6 is considered one of the most highly expressed mediators of inflammation and orchestrates chemokine-directed leukocyte trafficking and transition from innate to adaptive immunity through regulation of leukocyte activation, differentiation and proliferation [309]. It exerts its function through binding to the IL-6ST and IL-6R complex, and while IL-6ST displays a more ubiquitous expression, that of IL-6 receptor (IL-6R) is highly restricted to hepatocytes, leukocyte subsets and megakaryocytes [310].

IL6R appeared to be expressed by SMCs from human carotid atherosclerotic plaques, albeit at lower levels than *IL6ST* (Reads Nº ± SEM: 176 ± 18), which may suggest that SMCs are participating in plaque inflammation at least via IL6-IL6R-IL-6ST. Normal human vascular SMCs express scant amounts of *IL6ST*-encoded gp130, however, its high expression by SMCs of atherosclerotic plaque may be consequential to activation by “trans-signalling” IL-6/sIL-6R (soluble IL-6R) complexes leading to upregulation of *IL6ST* mRNA and IL-6 secretion. These triggering IL-6/sIL-6R complexes are likely to be produced by infiltrating T lymphocytes and monocytes. Consequential to these multiple effects of IL-6, a positive regulation of IL-6 production will be developed by creating an autocrine loop through which SMCs will acquire a proinflammatory state [251].

Furthermore, among the most expressed inflammatory genes we found many molecules associated with IL-6 signaling pathway. For instance, IL-6 signaling through IL6-R/IL-6ST induces a massive and rather selective expression of *CCL2* in SMCs [251] through STAT3 and protein coding IκBζ of NFKB inhibitor zeta (*NFKBIZ*) gene (Figure 38) [311]. This may result in monocyte and T lymphocyte chemotaxis from the circulation to the site of inflammation and induces migration of SMCs to the lesion [312]. In addition to IL-6, *TNFRSF12A* (Figure 38) encodes to the TNF receptor superfamily member 12A that is the receptor of TWEAK which upon binding is also able to induce *CCL2* expression increasing inflammatory state of the lesion [252].

Besides, CCL2, CXCL12 is also produced by SMC of carotid atherosclerotic plaques (Figure 38). CXCL12 increases the content of SMC's collagen and hence, the fibrous cap thickness and it, as well, decreases the number of macrophages in advanced lesions of the carotid artery [313]. Although it seems to be an antiatherogenic factor it has also the ability to promote rupture-prone plaques inducing angiogenesis [314] and platelet aggregation in order to form a thrombus [315] after the rupture of atherosclerotic plaque [316].

Among the multiple roles of IL-6 in atherosclerotic plaques may also count its participation in the increase of OPG protein and the subsequent induction of osteoclast-like cells when it is used in combination with the inflammatory cytokine TNF-α [317]. Its expression within atherosclerotic plaques has previously been demonstrated and positively associated with the presence and severity of carotid atherosclerosis [253], carotid stenosis [159], vulnerable carotid plaques [318] and to predict atherosclerotic plaque growth [319]. Although the presence of this factor highlights the potential of arterial wall cells to promote calcification and osteogenesis under specific conditions, the cellular origin of it remains uncertain [253]. However, our data confirm that *TNFRSF11B* – OPG encoding gene – is one of the most highly expressed inflammatory genes in SMCs coming from carotid atherosclerotic plaques.

The fact that carotid atheroma SMCs express high levels of JAK1, STAT1, 2, 3 and 6, as well as of the poorly characterized members of SOCS family SOCS4 and 6 (associated with the regulation of growth factor receptor signaling [320]), and 5 (IL19, IL4R, IL20RB signaling pathways [320,321]) indicates their multi-faceted capacity to regulate cytokine responses (Figure 38). SOCS4 and 6, like all SOCS proteins, may be involved in the mechanism of accelerating proteasome-mediated destruction of the activated cytokine-receptor complex attenuating the signal from the activated cytokine receptor itself and additionally, decreasing cell sensitivity to cytokines [322]. However, the activating molecules of these SOCS proteins are as yet unknown [323].

IL-6ST has been highlighted above as the most active inflammatory pathway found in SMCs from human carotid atherosclerotic plaques (Figure 38) and is one of the receptors regulated by SOCS3. After IL-6 binding to IL-6ST, JAK/STAT pathway is activated. IL6-ST/STAT3 signaling attenuation is driven by IL6-ST itself recruiting SOCS3 which promotes receptor signaling complex degradation [250]. This signaling pathway needs interaction between JAK and SOCS3 to yield inhibition of STAT1 and 3 signaling [324]. A second phosphorylation and hence, activation of STAT3 upon inhibition by SOCS3, has been described. This re-phosphorylation does not require IL-6ST, and instead uses the association of IL-6R and epidermal growth factor receptor (EGFR) to accomplish the activation of STAT3 [263].

Both receptor, *IL6R* and *EGFR* (Reads Nº ± SEM: 1614 ± 90) are expressed by SMCs of atherosclerotic plaques, which leads us to think that SMCs can respond to IL-6 through STAT3 despite the SOCS3-induced attenuation of its signaling. Moreover, the finding of *SOCS3* being upregulated in SMCs from symptomatic patients is suggestive for a status of excessive inflammation in these plaques and the engagement of SMCs to deal with it. However, SOCS3 is involved in several signaling pathways in which it can exert contradictory roles – certainly so in T cell regulation, because of the multiple effects of STAT3 on the production of antiinflammatory (e.g. IL-10) and proinflammatory (e.g. IL-6) cytokines [325].

Th cells are abundantly present in carotid plaques, which can be found Th17 cells expressing IL-17A and IL-17F cytokines, as well as IL-21 and -22 which have been found in human atherosclerotic plaques [326]. However, the role of Th17 cells is still controversial since they have been associated with proatherogenic as well as antiatherogenic effects [327]. SMCs within carotid atherosclerotic plaques appear to be sensitive to the IL-17 family cytokines since *IL17RD*, an orphan receptor with no reported physiological role in IL-17 signaling [259], arose as the gene with the most highly significant difference between Asympt and Sympt (Table 14). No literature data are available on a putative role in atherosclerosis or vascular disease. Nevertheless, a recent study shows that IL-17RD deficiency is associated with enhanced proinflammatory signaling because of the negative regulation of IL-17A-induced activation of NF-κβ by IL-17RD and hence, with increased expression of IL-6 [259]. Additionally, a study by Fusch and colleagues indicated that this inactivation of NF-κB could also inhibit IL-1 expression and TNF signaling [328]. A more recent study shows the ability of IL-17RD to inhibit Toll-like receptor (TLR) signaling [329]. Thus, it seems that IL-17RD may play a role in controlling exaggerated inflammatory responses [329] and therefore, the finding of higher expression in SMCs from Asympt patients may suggest a key role in establishing an antiinflammatory status in these plaques.

Although the direct roles of SOCS3 and IL-17 production in the modulation of vascular inflammation and atherosclerotic lesion development remain unknown, T cells deficient in SOCS3 have been found to promote polarization of Th17 cells accompanied with reduction of infiltrating T cells in murine atherosclerotic plaques [261]. Accordingly, the upregulation of *IL17RD* taken together with downregulation of *SOCS3* in asymptomatic SMCs, suggests that SMCs in asymptomatic plaques exert a stronger regulatory role toward the stabilization of the plaque.

Besides IL-17RD, another receptor related to cytokines expressed by T cells is IL-20RB. IL-20 signals through IL-20RA/IL-20RB (Type I receptor) and IL-22RA1/IL-20RB (Type II receptor) complexes. The other members of IL-20 subfamily of cytokines, i.e. IL- 19 and IL-24, signal

through these receptors complexes too. IL-24 uses the same receptors as IL-20, unlike IL-19 that only can signal through type II receptor. Both type I and II have been observed only on cells of epithelial origin while IL-20 subfamily cytokines are produced by T cells, macrophages and DCs, suggesting a role for cross-talk between them [330].

IL20RB was expressed at significantly higher level in SMCs coming from symptomatic atherosclerotic plaques (Table 14). However, the subunits of complete IL-20 receptor, i.e. *IL20RA* and *IL22RA1*, appeared not to be, or at very low levels (Reads Nº ± SEM for IL20-RA: 3 ± 0.7; for IL-22RA1: 4 ± 0.9), expressed in SMCs. Although it is not clear whether IL-20RB can bind interleukins and activate a signaling cascade by its own, IL-20RB but not IL-20RA or IL-22RA1, have been detected in most immune cells [331,332]. Wahl and colleagues showed that IL-19, IL-20, and IL-24 can act on T cells, and that IL-20RB signaling directly influenced both in vitro and in an in vivo mouse model responses including downregulating CD8 activation and inducing Th1-like immune responses of CD4 T cells [333]. Therefore, they suggested that these cytokines acting through IL-20RB have immune regulatory function and might be instrumental in the control of excessive immune reactions [333]. Supporting these ideas, it has been hypothesized that another receptor chain must pair with IL-20RB to induce IL-20 sub-family cytokines (IL-19, 20, 24) signaling on immune cells [331].

IL-24 is associated with attenuation of vascular calcification, as Lee et al. [334] have demonstrated in rat vascular SMCs, whereas IL-19 inhibits oxLDL uptake by and foam cell formation of human vascular SMCs [335], as well as, intimal hyperplasia through SOCS5 activation [321] and hence, reduces inflammatory induction of genes such as *IL1β* and *CXCL8* [336].

Although any functionality of IL-20RB by itself in SMCs has not been described yet, the mentioned reports [321,334–336] illustrate the capacity of SMCs to respond to the IL-20 cytokine family. Therefore, the higher *IL20RB* expression by SMCs from symptomatic patients may have a role in attenuating proinflammatory signaling, as well as in regulating calcification of the plaque in response to IL-19 and IL-24.

The ability of human vascular SMCs to produce IL-11 was described years ago; however, the role of IL-11 in vascular wall SMCs within atherosclerotic plaques is not exactly clear [264]. IL-11 may be envisaged to exert several positive effects on the atherosclerotic vascular wall; protection of ECM, prevention of apoptosis and proinflammatory cytokine production and intimal hyperplasia because of its anti-proliferative ability, and importantly, BMP production toward a stable calcified plaque [337–339]. *TNFAIP8L3*, in contrast, showed higher expression in SMCs from Asympt plaques. Although its role in atherosclerosis has not been studied yet, a limited number of articles focused on cancer and cell tumorigenesis awarded anti-apoptotic,

pro-proliferative and pro-migratory roles to TNFAIP8L3 [267,340]. Therefore, pending further investigation, TNFAIP8L3 may be of relevance as biomarker of progression of asymptomatic atherosclerotic plaque towards a symptomatic and rupture-prone phenotype, based on its association with degree of invasion and malignancy in cancer [340].

The chemokine/chemokine receptor network is of great importance in the regulation of cell recruitment during atherosclerosis, and thus numerous reports document the importance of their involvement [341,342]. Many chemokines such as CCL2 or CCL5 are upregulated in vascular wall cells (Figura 38 and Table 9) and cooperate in leukocyte recruitment to the injured artery in vascular remodeling [343]. Early events surrounding the initiation of the vascular inflammatory response program to vascular injury are hallmarked by *CCL5* upregulation produced by SMCs, as observed in mice [265]. Among the multitudinous effects of CCL5, which generally are proinflammatory, T lymphocyte and monocyte chemoattraction are the most characteristic ones [344], although it is also involved in angiogenesis, which has been related to plaque instability and rupture [36]. Expression of the chemokine CCL5 is colocalized at the site of inflammation within atheroma plaques [266] and can be induced by TNF-α, rather than IL-6, through TNFRSF1A and posterior JAK2 activation and STAT3 phosphorylation, culminating in CCL5 transcription in mice vascular SMCs [265]. Moreover, CCL5 was found to be increased in patients with unstable angina in the study reported by Kraaijeveld [345] and afterward, Koenen & Weber [346] suggested that this chemokine could serve as predictor of cardiovascular risk.

As aforementioned, BMP2 is involved in bone formation and is found to be highly expressed in SMCs from asymptomatic patients, suggesting a calcified phenotype for these cells and stable phenotype for these plaques. The resorption of bone is a timed phase of bone destruction and implies maturation of multinucleated osteoclasts and initiation of matrix degradation in which CCL2 and CCL5 are involved (Figure 38 and Table 9) [347,348]. The effect of acidosis on bone has been studied by Mendoza et al. [349], who allude to increased production of IL-6 and CCL5 by SMCs after acidosis stimulation *in vitro*, resulting in bone dissolution. Thus, CCL5 may serve as an indicator of bone dissolution in atherosclerotic plaques. Therefore, in accordance with results from transcriptomic analysis, SMCs from symptomatic plaques displayed more *CCL5* expression than those from asymptomatic ones that presented a calcified phenotype [231].

As TGF-β signalling pathway regulates a wide range of cellular processes through diverse effects, such as modulation of angiogenesis by affecting cell proliferation, migration and differentiation, it has been considered a target for cardiovascular diseases (62). Several cardiovascular disorders have been linked to TGF-β signalling pathways: (i) in hemorrhagic telangiectasia type I (HHT-1), Loeys-Dietz síndrome, pulmonary arterial hypertension (PAH).

6. CONCLUSION

The exact mechanism involved in plaque destabilization is not known but includes among other events SMC differentiation. Our study results contribute to a better understanding of how VSMC phenotype affects atheroma plaque development process, which may be valuable for future therapeutic approaches in carotid atherosclerosis disease. Furthermore, RNAseq transcriptomics has revealed significant differences in gene expression profiles between SMCs from Asympt and Sympt carotid plaques and this has provided clues as to the role SMCs may play in carotid atheroma plaque destabilization. Osteogenic-like phenotype SMCs may positively affect carotid atheroma plaque through participation in plaque stabilization via bone formation processes. On the other hand, plaques containing senescence-like phenotype SMCs may be more prone to rupture. Our results substantiate an important role of SMCs in carotid atheroma plaque disruption. In addition, an improved understanding of the multifaceted roles of SMCs in inflammatory processes happening during atherosclerosis would provide the scientific community with clues for additional targets for therapeutic intervention. The goal of such therapies would be in first place, to stabilize existing plaques so as to minimize the risk to develop stroke and to prevent plaque rupture in patients who may present a higher risk to develop the disease.

7. REFERENCES

[1] American heart association, Atherosclerosis: what role does cholesterol play?, Am. Hear. Assoc. (2018). http://www.heart.org/HEARTORG/Conditions/Cholesterol/WhyCholesterolMatters/Atherosclerosis_UCM_305564_Article.jsp#.Wt2E6H-YPIU.

[2] I. Tabas, G. García-Cardeña, G.K. Owens, Recent insights into the cellular biology of atherosclerosis, J. Cell Biol. 209 (2015) 13–22. doi:10.1083/jcb.201412052.

[3] A.J. Lusis, Atherosclerosis, Nature. 407 (2000) 233–241. doi:10.1038/35025203.

[4] C. Hahn, M.A. Schwartz, Mechanotransduction in vascular physiology and atherogenesis, Nat Rev Mol Cell Biol. 10 (2009) 53–62. doi:10.1038/nrm2596.

[5] Organización Mundial de la Salud, Prevención de las enfermedades cardiovasculares. Guía de bolsillo para la estimación y el manejo del riesgo cardiovascular, Organ. Mund. La Salud. 1 (2008) 1–38.

[6] C. Lahoz, J.M. Mostaza, La aterosclerosis como enfermedad sistémica, Rev. Española Cardiol. 60 (2007) 184–195. doi:10.1157/13099465.

[7] World health organization, Cardiovascular diseases, World Hear. Organ. (2017). http://www.who.int/mediacentre/factsheets/fs317/en/.

[8] American heart association, Impact of stroke (stroke statistics), Am. Hear. Assoc. (2017).

http://www.strokeassociation.org/STROKEORG/AboutStroke/Impact-of-Stroke-Stroke-statistics_UCM_310728_Article.jsp#.Wt2Xx3-YPIV.

[9] J. Pelisek, H.-H. Eckstein, A. Zernecke, Pathophysiological Mechanisms of Carotid Plaque Vulnerability: Impact on Ischemic Stroke, Arch. Immunol. Ther. Exp. (Warsz). 60 (2012) 431–442. doi:10.1007/s00005-012-0192-z.

[10] E.J. Benjamin, M.J. Blaha, S.E. Chiuve, M. Cushman, S.R. Das, R. Deo, S.D. de Ferranti, J. Floyd, M. Fornage, C. Gillespie, C.R. Isasi, M.C. Jiménez, L.C. Jordan, S.E. Judd, D. Lackland, J.H. Lichtman, L. Lisabeth, S. Liu, C.T. Longenecker, R.H. Mackey, K. Matsushita, D. Mozaffarian, M.E. Mussolino, K. Nasir, R.W. Neumar, L. Palaniappan, D.K. Pandey, R.R. Thiagarajan, M.J. Reeves, M. Ritchey, C.J. Rodriguez, G.A. Roth, W.D. Rosamond, C. Sasson, A. Towfighi, C.W. Tsao, M.B. Turner, S.S. Virani, J.H. Voeks, J.Z. Willey, J.T. Wilkins, J.H.Y. Wu, H.M. Alger, S.S. Wong, P. Muntner, Heart disease and stroke statistics—2017 update: a report from the american heart association, Circulation. 135 (2017) e146–e603. doi:10.1161/CIR.0000000000000485.

[11] A.R. Naylor, Time is brain!, Surgeon. 5 (2007) 23–30. http://www.ncbi.nlm.nih.gov/pubmed/17313125.

[12] J. Golledge, R.M. Greenhalgh, A.H. Davies, The symptomatic carotid plaque, Stroke. 31 (2000) 774–781.

[13] A. Ois, E. Cuadrado-Godia, A. Rodriguez-Campello, J. Jimenez-Conde, J. Roquer, High Risk of Early Neurological Recurrence in Symptomatic Carotid Stenosis, Stroke. 40 (2009) 2727–2731. doi:10.1161/STROKEAHA.109.548032.

[14] C.K. Zarins, D.P. Giddens, B.K. Bharadvaj, V.S. Sottiurai, R.F. Mabon, S. Gladov, S. Glagov, Carotid bifurcation atherosclerosis: Quantative correlation of plaque localization with flow velocity profiles and wall shear stress, Circ. Res. 53 (1983) 502–514. doi:10.1161/01.RES.53.4.502.

[15] C.R. White, J.A. Frangos, The shear stress of it all: the cell membrane and mechanochemical transduction, Philos. Trans. R. Soc. B Biol. Sci. 362 (2007) 1459–1467. doi:10.1098/rstb.2007.2128.

[16] P.F. Davies, Flow-mediated endothelial mechanotransduction, Physiol. Rev. 75 (1995) 519–560.

[17] O. Traub, B.C. Berk, Laminar shear stress: mechanisms by which endothelial cells transduce an atheroprotective force, Arterioscler. Thromb. Vasc. Biol. 18 (1998) 677–685.

[18] S. Glagov, C. Zarins, D.P. Giddens, D.N. Ku, Hemodynamics and atherosclerosis. Insights and perspectives gained from studies of human arteries, Arch. Pathol. Lab. Med. 112 (1988) 1018–1031. http://www.ncbi.nlm.nih.gov/pubmed/3052352.

[19] A.M. Malek, S.L. Alper, S. Izumo, Hemodynamic shear stress and its role in atherosclerosis., JAMA. 282 (1999) 2035–2042. http://www.ncbi.nlm.nih.gov/pubmed/10591386.

[20] A.R. Brooks, P.I. Lelkes, G.M. Rubanyi, Gene Expression Profiling of Vascular Endothelial Cells Exposed to Fluid Mechanical Forces: Relevance for Focal Susceptibility to Atherosclerosis, Endothelium. 11 (2004) 45–57. doi:10.1080/10623320490432470.

[21] Y.-S.J. Li, J.H. Haga, S. Chien, Molecular basis of the effects of shear stress on vascular endothelial cells, J. Biomech. 38 (2005) 1949–1971. doi:10.1016/j.jbiomech.2004.09.030.

[22] L.M. Blanco-Colio, J.L. Martín-Ventura, F. Vivanco, J.B. Michel, O. Meilhac, J. Egido, Biology of atherosclerotic plaques: What we are learning from proteomic analysis, Cardiovasc. Res. 72 (2006) 18–29. doi:10.1016/j.cardiores.2006.05.017.

[23] J. Dunn, H. Qiu, S. Kim, D. Jjingo, R. Hoffman, C.W. Kim, I. Jang, D.J. Son, D. Kim, C. Pan, Y. Fan, I.K. Jordan, H. Jo, Flow-dependent epigenetic DNA methylation regulates endothelial gene expression and atherosclerosis, J. Clin. Invest. 124 (2014) 3187–3199. doi:10.1172/JCI74792.

[24] P.A. Murphy, R.O. Hynes, Alternative Splicing of Endothelial Fibronectin Is Induced by Disturbed Hemodynamics and Protects Against Hemorrhage of the Vessel Wall, Arterioscler. Thromb. Vasc. Biol. 34 (2014) 2042–2050. doi:10.1161/ATVBAHA.114.303879.

[25] E. Adiguzel, P.J. Ahmad, C. Franco, M.P. Bendeck, Collagens in the progression and complications of atherosclerosis, Vasc. Med. 14 (2009) 73–89. doi:10.1177/1358863X08094801.

[26] H.C. Stary, Natural history and histological classification of atherosclerotic lesions : an update, Arterioscler. Thromb. Vasc. Biol. 20 (2000) 1177–1178. doi:10.1161/01.ATV.20.5.1177.

[27] R. Ross, Inflammation or Atherogenesis, N. Engl. J. Med. 340 (1999) 115–126. doi:10.1056/NEJM199901143400207.

[28] D.C. Chappell, S.E. Varner, R.M. Nerem, R.M. Medford, R.W. Alexander, Oscillatory Shear Stress Stimulates Adhesion Molecule Expression in Cultured Human Endothelium, Circ. Res. 82 (1998) 532–539. doi:10.1161/01.RES.82.5.532.

[29] G.C. Fernández, F.M. Tardáguila, C. Trinidad, L. María, V. Pilar, S. Miguel, A. De, Fisiopatología de la placa de ateroma y sus implicaciones en la imagen atherosclerotic plaque and, 45 (2003) 107–114.

[30] J. Martínez-González, V. Llorente-Cortés, L. Badimon, Biología celular y molecular de las lesiones ateroscleróticas, Rev. Española Cardiol. 54 (2001) 218–231. doi:10.1016/S0300-8932(01)76294-X.

[31] W. Insull, The Pathology of Atherosclerosis: Plaque Development and Plaque Responses to Medical Treatment, Am. J. Med. 122 (2009) S3–S14. doi:10.1016/j.amjmed.2008.10.013.

[32] L. Badimón, G. Vilahur, T. Padró, L. Badimón, Lipoproteins, Platelets, and Atherothrombosis, Rev Esp Cardiol. Cardiovasc. Transl. Med. 62 (2009) 1161–78.

[33] T. Inaba, T. Gotoda, H. Shimano, M. Shimada, K. Harada, K. Kozaki, Y. Watanabe, E. Hoh, K. Motoyoshi, Y. Yazaki, Platelet-derived growth factor induces c-fms and scavenger receptor genes in vascular smooth muscle cells, J Biol Chem. 267 (1992) 13107–13112.

[34] P. Vijayagopal, D.L. Glancy, Macrophages stimulate cholesteryl ester accumulation in cocultured smooth muscle cells incubated with lipoprotein-proteoglycan complex, Arterioscler. Thromb. Vasc. Biol. 16 (1996) 1112–1121. http://www.ncbi.nlm.nih.gov/pubmed/8792764.

[35] F.D. Kolodgie, A.P. Burke, G. Nakazawa, R. Virmani, Is pathologic intimal thickening the key to understanding early plaque progression in human atherosclerotic disease?, Arterioscler. Vasc. Biol. 27 (2007) 986–989. doi:10.1161/01.ATV.0000258865.44774.41.

[36] R. Di Stefano, F. Felice, A. Balbarini, Angiogenesis as risk factor for plaque vulnerability, Curr. Pharm. Des. 15 (2009) 1095–106. doi:10.2174/138161209787846892.

[37] B. Ho-Tin-Noé, J.B. Michel, Initiation of angiogenesis in atherosclerosis: smooth muscle cells as mediators of the angiogenic response to atheroma formation, Trends Cardiovasc. Med. 21 (2011) 183–187. doi:10.1016/j.tcm.2012.05.007.

[38] C. Camaré, M. Pucelle, A. Nègre-Salvayre, R. Salvayre, Angiogenesis in the atherosclerotic plaque, Redox Biol. 12 (2017) 18–34. doi:10.1016/j.redox.2017.01.007.

[39] P.K. Shah, Z.S. Galis, Matrix Metalloproteinase Hypothesis of Plaque Rupture: Players Keep Piling Up But Questions Remain, Circulation. 104 (2001) 1878–1880.

[40] J.L. Johnson, Matrix metalloproteinases: influence on smooth muscle cells and atherosclerotic plaque stability, Expert Rev. Cardiovasc. Ther. 5 (2007) 265–282. doi:10.1586/14779072.5.2.265.

[41] A. Müller, S.D. Krämer, R. Meletta, K. Beck, S. V. Selivanova, Z. Rancic, P.A. Kaufmann, B. Vos, J. Meding, T. Stellfeld, T.K. Heinrich, M. Bauser, J. Hütter, L.M. Dinkelborg, R. Schibli, S.M. Ametamey, Gene expression levels of matrix metalloproteinases in human atherosclerotic plaques and evaluation of radiolabeled inhibitors as imaging agents for plaque vulnerability, Nucl. Med. Biol. 41 (2014) 562–569. doi:10.1016/j.nucmedbio.2014.04.085.

[42] J.L. Johnson, N.P. Jenkins, W.-C. Huang, K. Di Gregoli, G.B. Sala-Newby, V.P.W. Scholtes, F.L. Moll, G. Pasterkamp, A.C. Newby, Relationship of MMP-14 and TIMP-3 Expression with Macrophage Activation and Human Atherosclerotic Plaque Vulnerability, Mediators Inflamm. 2014 (2014) 1–17. doi:10.1155/2014/276457.

[43] P.K. Shah, Biomarkers of Plaque Instability, Curr. Cardiol. Rep. 16 (2014) 547. doi:10.1007/s11886-014-0547-7.

[44] L. Badimon, G. Vilahur, Thrombosis formation on atherosclerotic lesions and plaque rupture, J. Intern. Med. 276 (2014) 618–632. doi:10.1111/joim.12296.

[45] S.A. Steitz, M.Y. Speer, G. Curinga, H.-Y. Yang, P. Haynes, R. Aebersold, T. Schinke, G. Karsenty, C.M. Giachelli, Smooth Muscle Cell Phenotypic Transition Associated With Calcification: Upregulation of Cbfa1 and Downregulation of Smooth Muscle Lineage Markers, Circ. Res. 89 (2001) 1147–1154. doi:10.1161/hh2401.101070.

[46] M. Slevin, A.B. Elasbali, M. Miguel Turu, J. Krupinski, L. Badimon, J. Gaffney, Identification of Differential Protein Expression Associated with Development of Unstable Human Carotid

Plaques, Am. J. Pathol. 168 (2006) 1004–1021. doi:10.2353/ajpath.2006.050471.

[47] J.M. Seeger, E. Barratt, G.A. Lawson, N. Klingman, The relationship between carotid plaque composition, plaque morphology, and neurologic symptoms., J. Surg. Res. 58 (1995) 330–336.

[48] M. de Weerd, J.P. Greving, B. Hedblad, M.W. Lorenz, E.B. Mathiesen, D.H. O'Leary, M. Rosvall, M. Sitzer, E. Buskens, M.L. Bots, Prevalence of Asymptomatic Carotid Artery Stenosis in the General Population: An Individual Participant Data Meta-Analysis, Stroke. 41 (2010) 1294–1297. doi:10.1161/STROKEAHA.110.581058.

[49] D. Inzitari, M. Eliasziw, P. Gates, B.L. Sharpe, R.K. Chan, H.E. Meldrum, H.J. Barnett, The causes and risk of stroke in patients with asymptomatic internal-carotid-artery stenosis, N. Engl. J. Med. 342 (2000) 1693–1700.

[50] A.L. Abbott, B.R. Chambers, J.L. Stork, C.R. Levi, C.F. Bladin, G.A. Donnan, Embolic Signals And Prediction of Ipsilateral Stroke or Transient Ischemic Attack in Asymptomatic Carotid Stenosis: A Multicenter Prospective Cohort Study, Stroke. 36 (2005) 1128–1133. doi:10.1161/01.STR.0000166059.30464.0a.

[51] Randomised trial of endarterectomy for recently symptomatic carotid stenosis: final results of the MRC European Carotid Surgery Trial (ECST), Lancet (London, England). 351 (1998) 1379–1387. http://www.ncbi.nlm.nih.gov/pubmed/9593407.

[52] K. Skagen, M. Skjelland, M. Zamani, D. Russell, Unstable carotid artery plaque: new insights and controversies in diagnostics and treatment, Croat. Med. J. 57 (2016) 311–320. doi:10.3325/cmj.2016.57.311.

[53] G.W. van Lammeren, A.G. den Hartog, G. Pasterkamp, A. Vink, J.-P.P.M. de Vries, F.L. Moll, G.J. de Borst, Asymptomatic Carotid Artery Stenosis: Identification of Subgroups with Different Underlying Plaque Characteristics, Eur. J. Vasc. Endovasc. Surg. 43 (2012) 632–636. doi:10.1016/j.ejvs.2012.03.011.

[54] A. van der Wal, A.E. Becker, Atherosclerotic plaque rupture – pathologic basis of plaque stability and instability, Cardiovasc. Res. 41 (1999) 334–344. doi:10.1016/S0008-6363(98)00276-4.

[55] L. Perisic, S. Aldi, Y. Sun, L. Folkersen, A. Razuvaev, J. Roy, M. Lengquist, S. Åkesson, C.E. Wheelock, L. Maegdefessel, A. Gabrielsen, J. Odeberg, G.K. Hansson, G. Paulsson-Berne, U. Hedin, Gene expression signatures, pathways and networks in carotid atherosclerosis, J. Intern. Med. 279 (2016) 293–308. doi:10.1111/joim.12448.

[56] S. Carr, A. Farb, W.H. Pearce, R. Virmani, J.S.T. Yao, Atherosclerotic plaque rupture in symptomatic carotid artery stenosis, J. Vasc. Surg. 23 (1996) 755–766. doi:10.1016/S0741-5214(96)70237-9.

[57] L. Hermus, G.M. van Dam, C.J. Zeebregts, Advanced Carotid Plaque Imaging, Eur. J. Vasc. Endovasc. Surg. 39 (2010) 125–133. doi:10.1016/j.ejvs.2009.11.020.

[58] M.T. Dirksen, A.C. Van Der Wal, F.M. Van Den Berg, C.M. Van Der Loos, A.E. Becker,

Distribution of inflammatory cells in atherosclerotic plaques relates to the direction of flow, Circulation. 98 (1998) 2000–2003. doi:10.1161/01.CIR.98.19.2000.

[59] B. Fagerberg, M. Ryndel, J. Kjelldahl, L.M. Akyürek, L. Rosengren, L. Karlström, G. Bergström, F.J. Olson, Differences in Lesion Severity and Cellular Composition between in vivo Assessed Upstream and Downstream Sides of Human Symptomatic Carotid Atherosclerotic Plaques, J. Vasc. Res. 47 (2010) 221–230. doi:10.1159/000255965.

[60] L. Baroncini, A. Filho, S. Ramos, A. Martins, L. Murta, Histological composition and progression of carotid plaque, Thromb. J. 5 (2007) 4. doi:10.1186/1477-9560-5-4.

[61] A.J. Lepedda, A. Cigliano, G.M. Cherchi, R. Spirito, M. Maggioni, F. Carta, F. Turrini, C. Edelstein, A.M. Scanu, M. Formato, A proteomic approach to differentiate histologically classified stable and unstable plaques from human carotid arteries, Atherosclerosis. 203 (2009) 112–118. doi:10.1016/j.atherosclerosis.2008.07.001.

[62] B. Verhoeven, W.E. Hellings, F.L. Moll, J.P. de Vries, D.P.V. de Kleijn, P. de Bruin, E. Busser, A.H. Schoneveld, G. Pasterkamp, Carotid atherosclerotic plaques in patients with transient ischemic attacks and stroke have unstable characteristics compared with plaques in asymptomatic and amaurosis fugax patients, J. Vasc. Surg. 42 (2005) 1075–1081. doi:10.1016/j.jvs.2005.08.009.

[63] A.E. Park, W.J. McCarthy, W.H. Pearce, J.S. Matsumura, J.S.T. Yao, Carotid plaque morphology correlates with presenting symptomatology, J. Vasc. Surg. 27 (1998) 872–879. doi:10.1016/S0741-5214(98)70267-8.

[64] J.-B. Michel, R. Virmani, E. Arbustini, G. Pasterkamp, Intraplaque haemorrhages as the trigger of plaque vulnerability, Eur. Heart J. 32 (2011) 1977–1985. doi:10.1093/eurheartj/ehr054.

[65] Y.-C. Chen, A.L. Huang, T.S. Kyaw, A. Bobik, K. Peter, Atherosclerotic Plaque Rupture, Arterioscler. Thromb. Vasc. Biol. 36 (2016) e63–e72. doi:10.1161/ATVBAHA.116.307993.

[66] H. Van Damme, M. Vivario, J. Boniver, R. Limet, Histologic characterization of carotid plaques, Cardiovasc. Pathol. 3 (1994) 9–17. doi:10.1016/1054-8807(94)90003-5.

[67] C.D. Liapis, E.D. Avgerinos, N.P. Kadoglou, J.D. Kakisis, What a vascular surgeon should know and do about atherosclerotic risk factors, J. Vasc. Surg. 49 (2009) 1348–1354. doi:10.1016/j.jvs.2008.12.046.

[68] R. Stocker, J.F. Keaney, Role of Oxidative Modifications in Atherosclerosis, Physiol. Rev. 84 (2004) 1381–1478. doi:10.1152/physrev.00047.2003.

[69] F.R. Maxfield, I. Tabas, Role of cholesterol and lipid organization in disease, Nature. 438 (2005) 612–621. doi:10.1038/nature04399.

[70] J.F. Bentzon, F. Otsuka, R. Virmani, E. Falk, Mechanisms of Plaque Formation and Rupture, Circ. Res. 114 (2014) 1852–1866. doi:10.1161/CIRCRESAHA.114.302721.

[71] R.J. Doonan, A. Hafiane, C. Lai, J.P. Veinot, J. Genest, S.S. Daskalopoulou, Cholesterol Efflux

Capacity, Carotid Atherosclerosis, and Cerebrovascular Symptomatology, Arterioscler. Thromb. Vasc. Biol. 34 (2014) 921–926. doi:10.1161/ATVBAHA.113.302590.

[72] P. Sobieszczyk, J. Beckman, Carotid Artery Disease, Circulation. 114 (2006) e244–e247. doi:10.1161/CIRCULATIONAHA.105.542860.

[73] S. LEHOUX, Y. CASTIER, A. TEDGUI, Molecular mechanisms of the vascular responses to haemodynamic forces, J. Intern. Med. 259 (2006) 381–392. doi:10.1111/j.1365-2796.2006.01624.x.

[74] P. Jankowski, G. Bilo, K. Kawecka-Jaszcz, The pulsatile component of blood pressure – Its role in the pathogenesis of atherosclerosis, Blood Press. 16 (2007) 238–245. doi:10.1080/08037050701428166.

[75] S. Lewington, R. Clarke, N. Qizilbash, R. Peto, R. Collins, Age-specific relevance of usual blood pressure to vascular mortality: a meta-analysis of individual data for one million adults in 61 prospective studies.Age-specific relevance of usual blood pressure to vascular mortality: a meta-analysis of individual d, Lancet. 360 (2002) 1903–13. http://www.ncbi.nlm.nih.gov/pubmed/12493255.

[76] J.R. Romero, J. Morris, A. Pikula, Stroke prevention: modifying risk factors, Ther. Adv. Cardiovasc. Dis. 2 (2008) 287–303. doi:10.1177/1753944708093847.

[77] M.K. Gaba, S. Gaba, L.T. Clark, Cardiovascular disease in patients with diabetes: clinical considerations, J. Assoc. Acad. Minor. Phys. 10 (1999) 15–22. http://www.ncbi.nlm.nih.gov/pubmed/10826004.

[78] A. Bruno, S.R. Levine, M.R. Frankel, T.G. Brott, Y. Lin, B.C. Tilley, P.D. Lyden, J.P. Broderick, T.G. Kwiatkowski, S.E. Fineberg, Admission glucose level and clinical outcomes in the NINDS rt-PA Stroke Trial, Neurology. 59 (2002) 669–674. doi:10.1212/WNL.59.5.669.

[79] M.W. Parsons, P.A. Barber, P.M. Desmond, T.A. Baird, D.G. Darby, G. Byrnes, B.M. Tress, S.M. Davis, Acute hyperglycemia adversely affects stroke outcome: A magnetic resonance imaging and spectroscopy study, Ann. Neurol. 52 (2002) 20–28. doi:10.1002/ana.10241.

[80] C.A. Kawamura M, Heinecke JW, Pathophysiological concentrations of glucose promote oxidative modification of low density lipoprotein by a superoxide- dependent pathway., J Clin Invest. 94 (1994) 771–778.

[81] J.W. Stephens, M.P. Khanolkar, S.C. Bain, The biological relevance and measurement of plasma markers of oxidative stress in diabetes and cardiovascular disease, Atherosclerosis. 202 (2009) 321–329. doi:10.1016/j.atherosclerosis.2008.06.006.

[82] R.S. Shah, J.W. Cole, Smoking and stroke: the more you smoke the more you stroke, Expert Rev. Cardiovasc. Ther. 8 (2010) 917–932. doi:10.1586/erc.10.56.

[83] A.D. Gepner, M.E. Piper, H.M. Johnson, M.C. Fiore, T.B. Baker, J.H. Stein, Effects of smoking and smoking cessation on lipids and lipoproteins: Outcomes from a randomized clinical trial, Am.

Heart J. 161 (2011) 145–151. doi:10.1016/j.ahj.2010.09.023.

[84] S.Y. Woo, J.H. Joh, S.-A. Han, H.-C. Park, Prevalence and risk factors for atherosclerotic carotid stenosis and plaque, Medicine (Baltimore). 96 (2017) e5999. doi:10.1097/MD.0000000000005999.

[85] T. Truelsen, S. Begg, C. Mathers, The global burden of cerebrovascular disease, World Heal. Organ. (2006) 1–67.

[86] R.L. Sacco, R. Adams, G. Albers, M.J. Alberts, O. Benavente, K. Furie, L.B. Goldstein, P. Gorelick, J. Halperin, R. Harbaugh, S.C. Johnston, I. Katzan, M. Kelly-Hayes, E.J. Kenton, M. Marks, L.H. Schwamm, T. Tomsick, Guidelines for Prevention of Stroke in Patients With Ischemic Stroke or Transient Ischemic Attack: A Statement for Healthcare Professionals From the American Heart Association/American Stroke Association Council on Stroke: Co-Sponsored by the Council on C, Stroke. 37 (2006) 577–617. doi:10.1161/01.STR.0000199147.30016.74.

[87] S.-H. Suk, R.L. Sacco, B. Boden-Albala, J.F. Cheun, J.G. Pittman, M.S. Elkind, M.C. Paik, Abdominal Obesity and Risk of Ischemic Stroke: The Northern Manhattan Stroke Study, Stroke. 34 (2003) 1586–1592. doi:10.1161/01.STR.0000075294.98582.2F.

[88] S.N. Blair, J.B. Kampert, H.W. Kohl, C.E. Barlow, C.A. Macera, R.S. Paffenbarger, L.W. Gibbons, E. Bouchard C, Shephard RJ, Stephens T, W.P. Stefanick ML, P.M. Kriska AM, Blair SN, A.C. of S. Medicine, B. SN, H.C. Paffenbarger RS Jr, Hyde RT, Wing AL, B.E. Morris JN, Clayton DG, Everitt MG, Semmence AM, G.L. Blair SN, Kohl HW III, Paffenbarger RS Jr, Clark DG, Cooper KH, K.J. Paffenbarger RS Jr, Hyde RT, Wing AL, Lee I, Jung DL, M.C. Blair SN, Kohl HW III, Barlow CE, Paffenbarger RS Jr, Gibbons LW, P.M. Peters RK, Cady LD Jr, Bischoff DP, Bernstein L, P.R.J. Helmrich SP, Ragland DR, Leung RW, W.R. Balke B, et al Pollock ML, Bohannon RL, Cooper KH, W.A. Pollock ML, Foster C, Schmidt D, Hellman C, Linnerud AC, A.C. of S. Medicine, C. DR, T.C. Fagard RH, Influences of Cardiorespiratory Fitness and Other Precursors on Cardiovascular Disease and All-Cause Mortality in Men and Women, JAMA J. Am. Med. Assoc. 276 (1996) 205–210. doi:10.1001/jama.1996.03540030039029.

[89] M.B. Britten, A.M. Zeiher, V. Schächinger, Clinical importance of coronary endothelial vasodilator dysfunction and therapeutic options, J. Intern. Med. 245 (1999) 315–327. doi:10.1046/j.1365-2796.1999.00449.x.

[90] R.L. Sacco, R. Gan, B. Boden-Albala, I.F. Lin, D.E. Kargman, W.A. Hauser, S. Shea, M.C. Paik, Leisure-time physical activity and ischemic stroke risk: the Northern Manhattan Stroke Study., Stroke A J. Cereb. Circ. 29 (1998) 380–387. http://www.ncbi.nlm.nih.gov/pubmed/9472878.

[91] C. Do Lee, A.R. Folsom, S.N. Blair, Physical Activity and Stroke Risk: A Meta-Analysis, Stroke. 34 (2003) 2475–2482. doi:10.1161/01.STR.0000091843.02517.9D.

[92] G. Wendel-Vos, A. Schuit, H. Boshuizen, W. Verschuren, W. Saris, D. Kromhout, Physical activity and stroke. A meta-analysis of observational data, Int. J. Epidemiol. 33 (2004) 787–798.

doi:10.1093/ije/dyh168.

[93] M. Endres, K. Gertz, U. Lindauer, J. Katchanov, J. Schultze, H. Schrok, G. Nickenig, W. Kuschinsky, U. Dirnagl, U. Laufs, Mechanisms of stroke prevention by physical activity, Ann. Neurol. 54 (2003) 582–590.

[94] Y.-H. Ding, C.N. Young, X. Luan, J. Li, J.A. Rafols, J.C. Clark, J.P. McAllister, Y. Ding, Exercise preconditioning ameliorates inflammatory injury in ischemic rats during reperfusion, Acta Neuropathol. 109 (2005) 237–246. doi:10.1007/s00401-004-0943-y.

[95] P. Rothwell, M. Eliasziw, S. Gutnikov, C. Warlow, H. Barnett, Endarterectomy for symptomatic carotid stenosis in relation to clinical subgroups and timing of surgery, Lancet. 363 (2004) 915–924. doi:10.1016/S0140-6736(04)15785-1.

[96] K. Cheng, D. Mikhailidis, G. Hamilton, A. Seifalian, A review of the carotid and femoral intima-media thickness as an indicator of the presence of peripheral vascular disease and cardiovascular risk factors, Cardiovasc. Res. 54 (2002) 528–538. doi:10.1016/S0008-6363(01)00551-X.

[97] O. Joakimsen, K.H. Bonna, E. Stensland-bugge, B.K. Jacobsen, Age and Sex Differences in the Distribution and Ultrasound Morphology of Carotid Atherosclerosis The Tromsø Study, Arterioscler. Thromb. Vasc. Biol. 19 (1999) 3007–3013.

[98] A.L. Abbott, G.A. Donnan, Does the 'High Risk' Patient with Asymptomatic Carotid Stenosis Really Exist?, Eur. J. Vasc. Endovasc. Surg. 35 (2008) 524–533. doi:10.1016/j.ejvs.2008.01.017.

[99] G. Sangiorgi, S. Roversi, G. Biondi Zoccai, M.G. Modena, F. Servadei, A. Ippoliti, A. Mauriello, Sex-related differences in carotid plaque features and inflammation, J. Vasc. Surg. 57 (2013) 338–344. doi:10.1016/j.jvs.2012.07.052.

[100] A.J. Comerota, S.X. Salles-Cunha, Y. Daoud, L. Jones, H.G. Beebe, Gender differences in blood velocities across carotid stenoses, J. Vasc. Surg. 40 (2004) 939–944. doi:10.1016/j.jvs.2004.08.030.

[101] B.D. MacNeill, I.-K. Jang, B.E. Bouma, N. Iftimia, M. Takano, H. Yabushita, M. Shishkov, C.R. Kauffman, S.L. Houser, H.T. Aretz, D. DeJoseph, E.F. Halpern, G.J. Tearney, Focal and multi-focal plaque macrophage distributions in patients with acute and stable presentations of coronary artery disease, J. Am. Coll. Cardiol. 44 (2004) 972–979. doi:10.1016/j.jacc.2004.05.066.

[102] F. Iemolo, Sex Differences in Carotid Plaque and Stenosis, Stroke. 35 (2004) 477–481. doi:10.1161/01.STR.0000110981.96204.64.

[103] E. Marulanda-Londoño, S. Chaturvedi, Carotid stenosis in women: time for a reappraisal, BMJ. 1 (2016) 192–196. doi:10.1136/svn-2016-000043.

[104] O. van Oostrom, E. Velema, A.H. Schoneveld, J.P.P.M. de Vries, P. de Bruin, C.A. Seldenrijk, D.P.V. de Kleijn, E. Busser, F.L. Moll, J.H. Verheijen, R. Virmani, G. Pasterkamp, Age-related changes in plaque composition, Cardiovasc. Pathol. 14 (2005) 126–134. doi:10.1016/j.carpath.2005.03.002.

[105] S. Homma, N. Hirose, H. Ishida, T. Ishii, G. Araki, J.H. Halsey, Carotid Plaque and Intima-Media Thickness Assessed by B-Mode Ultrasonography in Subjects Ranging From Young Adults to Centenarians, Stroke. 32 (2001) 830–835. doi:10.1161/01.STR.32.4.830.

[106] G. Gennaro, C. Ménard, E. Giasson, S.-É. Michaud, M. Palasis, S. Meloche, A. Rivard, Role of p44/p42 MAP Kinase in the Age-Dependent Increase in Vascular Smooth Muscle Cell Proliferation and Neointimal Formation, Arterioscler. Thromb. Vasc. Biol. 23 (2003) 204–210. doi:10.1161/01.ATV.0000053182.58636.BE.

[107] G. Milio, E. Corrado, D. Sorrentino, I. Muratori, S. La Carrubba, G. Mazzola, R. Tantillo, G. Vitale, S. Mansueto, S. Novo, Asymptomatic Carotid Lesions and Aging: Role of Hypertension and Other Traditional and Emerging Risk Factors, Arch. Med. Res. 37 (2006) 342–347. doi:10.1016/j.arcmed.2005.06.012.

[108] E. Ammirati, F. Fogacci, Clinical relevance of biomarkers for the identification of patients with carotid atherosclerotic plaque: Potential role and limitations of cysteine protease legumain, Atherosclerosis. 257 (2017) 248–249. doi:10.1016/j.atherosclerosis.2017.01.003.

[109] T. Benedek, P. Maurovich-Horváth, P. Ferdinandy, B. Merkely, The Use of Biomarkers for the Early Detection of Vulnerable Atherosclerotic Plaques and Vulnerable Patients. A Review, J. Cardiovasc. Emergencies. 2 (2016) 106–113. doi:10.1515/jce-2016-0017.

[110] B. Lindahl, Are there really biomarkers of vulnerable plaque?, Clin. Chem. 58 (2012) 151–153. doi:10.1373/clinchem.2011.165811.

[111] S.Z.H. Rittersma, A.C. van der Wal, K.T. Koch, J.J. Piek, J.P.S. Henriques, K.J. Mulder, J.P.H.M. Ploegmakers, M. Meesterman, R.J. de Winter, Plaque Instability Frequently Occurs Days or Weeks Before Occlusive Coronary Thrombosis: A Pathological Thrombectomy Study in Primary Percutaneous Coronary Intervention, Circulation. 111 (2005) 1160–1165. doi:10.1161/01.CIR.0000157141.00778.AC.

[112] P. Libby, P.M. Ridker, G.K. Hansson, Progress and challenges in translating the biology of atherosclerosis, Nature. 473 (2011) 317–325. doi:10.1038/nature10146.

[113] V.R. Taqueti, M.F. Di Carli, M. Jerosch-Herold, G.K. Sukhova, V.L. Murthy, E.J. Folco, R.Y. Kwong, C.K. Ozaki, M. Belkin, M. Nahrendorf, R. Weissleder, P. Libby, Increased Microvascularization and Vessel Permeability Associate With Active Inflammation in Human Atheromata, Circ. Cardiovasc. Imaging. 7 (2014) 920–929. doi:10.1161/CIRCIMAGING.114.002113.

[114] M.-L.M. Grønholdt, B.G. Nordestgaard, J. Bentzon, B.M. Wiebe, J. Zhou, E. Falk, H. Sillesen, Macrophages are associated with lipid-rich carotid artery plaques, echolucency on B-mode imaging, and elevated plasma lipid levels, J. Vasc. Surg. 35 (2002) 137–145. doi:10.1067/mva.2002.119042.

[115] P. Poredos, A. Spirkoska, L. Lezaic, M.B. Mijovski, M.K. Jezovnik, Patients with an Inflamed Atherosclerotic Plaque have Increased Levels of Circulating Inflammatory Markers, J.

Atheroscler. Thromb. 24 (2017) 39–46. doi:10.5551/jat.34884.

[116] R. Blackburn, P. Giral, E. Bruckert, J.-M. André, S. Gonbert, M. Bernard, M.J. Chapman, G. Turpin, Elevated C-Reactive Protein Constitutes an Independent Predictor of Advanced Carotid Plaques in Dyslipidemic Subjects, Arterioscler. Thromb. Vasc. Biol. 21 (2001) 1962–1968. doi:10.1161/hq1201.099433.

[117] S.K. Singh, M. V. Suresh, B. Voleti, A. Agrawal, The connection between C-reactive protein and atherosclerosis, Ann. Med. 40 (2008) 110–120. doi:10.1080/07853890701749225.

[118] M. Di Napoli, F. Papa, V. Bocola, Prognostic influence of increased C-reactive protein and fibrinogen levels in ischemic stroke, Stroke. 32 (2001) 133–138. doi:10.1161/01.STR.32.1.133.

[119] H. Grufman, I. Gonçalves, A. Edsfeldt, M. Nitulescu, A. Persson, M. Nilsson, J. Nilsson, Plasma levels of high-sensitive C-reactive protein do not correlate with inflammatory activity in carotid atherosclerotic plaques, J. Intern. Med. 275 (2014) 127–133. doi:10.1111/joim.12133.

[120] O. Yousuf, B.D. Mohanty, S.S. Martin, P.H. Joshi, M.J. Blaha, K. Nasir, R.S. Blumenthal, M.J. Budoff, High-Sensitivity C-Reactive Protein and Cardiovascular Disease, J. Am. Coll. Cardiol. 62 (2013) 397–408. doi:10.1016/j.jacc.2013.05.016.

[121] A. Edsfeldt, H. Grufman, G. Asciutto, M. Nitulescu, A. Persson, M. Nilsson, J. Nilsson, I. Gonçalves, Circulating cytokines reflect the expression of pro-inflammatory cytokines in atherosclerotic plaques, Atherosclerosis. 241 (2015) 443–449. doi:10.1016/j.atherosclerosis.2015.05.019.

[122] W. Peeters, W.E. Hellings, D.P.V. de Kleijn, J.P.P.M. de Vries, F.L. Moll, A. Vink, G. Pasterkamp, Carotid Atherosclerotic Plaques Stabilize After Stroke: Insights Into the Natural Process of Atherosclerotic Plaque Stabilization, Arterioscler. Thromb. Vasc. Biol. 29 (2009) 128–133. doi:10.1161/ATVBAHA.108.173658.

[123] Y. Seino, U. Ikeda, M. Ikeda, K. Yamamoto, Y. Misawa, T. Hasegawa, S. Kano, K. Shimada, Interleukin 6 gene transcripts are expressed in human atherosclerotic lesions, Cytokine. 6 (1994) 87–91. doi:1043-4666(94)90013-2 [pii].

[124] O. Reikerås, P. Borgen, Activation of Markers of Inflammation, Coagulation and Fibrinolysis in Musculoskeletal Trauma, PLoS One. 9 (2014) e107881. doi:10.1371/journal.pone.0107881.

[125] B. Schieffer, Impact of Interleukin-6 on Plaque Development and Morphology in Experimental Atherosclerosis, Circulation. 110 (2004) 3493–3500. doi:10.1161/01.CIR.0000148135.08582.97.

[126] X. Shi, W.-L. Xie, W.-W. Kong, D. Chen, P. Qu, Expression of the NLRP3 Inflammasome in Carotid Atherosclerosis, J. Stroke Cerebrovasc. Dis. 24 (2015) 2455–2466. doi:10.1016/j.jstrokecerebrovasdis.2015.03.024.

[127] Z. Mallat, A. Corbaz, A. Scoazec, S. Besnard, G. Lesèche, Y. Chvatchko, A. Tedgui, Expression of Interleukin-18 in human atherosclerotic plaques and relation to plaque instability, Circulation. 104 (2001) 1598–1603.

[128] M.K. Salem, H.Z. Butt, E. Choke, D. Moore, K. West, T.G. Robinson, R.D. Sayers, A.R. Naylor, M.J. Bown, Gene and Protein Expression of Chemokine (C-C-Motif) Ligand 19 is Upregulated in Unstable Carotid Atherosclerotic Plaques, Eur. J. Vasc. Endovasc. Surg. 52 (2016) 427–436. doi:10.1016/j.ejvs.2016.05.018.

[129] C. Erbel, T. Dengler, S. Wangler, F. Lasitschka, F. Bea, N. Wambsganss, M. Hakimi, D. Böckler, H. Katus, C. Gleissner, Expression of IL-17A in human atherosclerotic lesions is associated with increased inflammation and plaque vulnerability, Basic Res. Cardiol. 106 (2011) 125–134. doi:10.1007/s00395-010-0135-y.

[130] A.E. Michelsen, C.N. Rathcke, M. Skjelland, S. Holm, T. Ranheim, K. Krohg-Sørensen, M.F. Klingvall, F. Brosstad, E. Oie, H. Vestergaard, P. Aukrust, B. Halvorsen, Increased YKL-40 expression in patients with carotid atherosclerosis, Atherosclerosis. 211 (2010) 589–595. doi:10.1016/j.atherosclerosis.2010.02.035.

[131] Y.-N. Qian, Y.-T. Luo, H.-X. Duan, L.-Q. Feng, Q. Bi, Y.-J. Wang, X.-Y. Yan, Adhesion Molecule CD146 and its Soluble Form Correlate Well with Carotid Atherosclerosis and Plaque Instability, CNS Neurosci. Ther. 20 (2014) 438–445. doi:10.1111/cns.12234.

[132] A. Edsfeldt, M. Nitulescu, H. Grufman, C. Gronberg, A. Persson, M. Nilsson, M. Persson, H. Bjorkbacka, I. Goncalves, Soluble Urokinase Plasminogen Activator Receptor is Associated With Inflammation in the Vulnerable Human Atherosclerotic Plaque, Stroke. 43 (2012) 3305–3312. doi:10.1161/STROKEAHA.112.664094.

[133] A. Abbas, I. Gregersen, S. Holm, I. Daissormont, V. Bjerkeli, K. Krohg-Sørensen, K.R. Skagen, T.B. Dahl, D. Russell, T. Almås, D. Bundgaard, L.H. Alteheld, A. Rashidi, C.P. Dahl, A.E. Michelsen, E.A. Biessen, P. Aukrust, B. Halvorsen, M. Skjelland, Interleukin 23 levels are increased in carotid atherosclerosis. Possible role for the interleukin 23/interleukin 17 axis, Stroke. 46 (2015) 793–799. doi:10.1161/STROKEAHA.114.006516.

[134] T.B. Dahl, A. Yndestad, M. Skjelland, E. Oie, A. Dahl, A. Michelsen, J.K. Damas, S.H. Tunheim, T. Ueland, C. Smith, B. Bendz, S. Tonstad, L. Gullestad, S.S. Froland, K. Krohg-Sorensen, D. Russell, P. Aukrust, B. Halvorsen, Increased Expression of Visfatin in Macrophages of Human Unstable Carotid and Coronary Atherosclerosis: Possible Role in Inflammation and Plaque Destabilization, Circulation. 115 (2007) 972–980. doi:10.1161/CIRCULATIONAHA.106.665893.

[135] W.-J. Kim, H. Kim, K. Suk, W.-H. Lee, Macrophages express granzyme B in the lesion areas of atherosclerosis and rheumatoid arthritis, Immunol. Lett. 111 (2007) 57–65. doi:10.1016/j.imlet.2007.05.004.

[136] A. Abbas, P. Aukrust, T.B. Dahl, V. Bjerkeli, E.B.L. Sagen, A. Michelsen, D. Russell, K. Krohg-Sorensen, S. Holm, M. Skjelland, B. Halvorsen, High Levels of S100A12 Are Associated With Recent Plaque Symptomatology in Patients With Carotid Atherosclerosis, Stroke. 43 (2012) 1347–1353. doi:10.1161/STROKEAHA.111.642256.

[137] D. Rodríguez, C.J. Morrison, C.M. Overall, Matrix metalloproteinases: What do they not do? New substrates and biological roles identified by murine models and proteomics, Biochim. Biophys. Acta - Mol. Cell Res. 1803 (2010) 39–54. doi:10.1016/j.bbamcr.2009.09.015.

[138] Z.S. Galis, G.K. Sukhova, M.W. Lark, P. Libby, Increased expression of matrix metalloproteinases and matrix degrading activity in vulnerable regions of human atherosclerotic plaques., J. Clin. Invest. 94 (1994) 2493–2503. doi:10.1172/JCI117619.

[139] J.L. Johnson, Metalloproteinases in atherosclerosis, Eur. J. Pharmacol. 816 (2017) 93–106. doi:10.1016/j.ejphar.2017.09.007.

[140] I.M. Loftus, A.R. Naylor, S. Goodall, M. Crowther, L. Jones, P.R.F. Bell, M.M. Thompson, Increased Matrix Metalloproteinase-9 Activity in Unstable Carotid Plaques, Stroke. 31 (2000) 40–47.

[141] K.J. Molloy, M.M. Thompson, J.L. Jones, E.C. Schwalbe, P.R.F. Bell, A.R. Naylor, I.M. Loftus, Unstable Carotid Plaques Exhibit Raised Matrix Metalloproteinase-8 Activity, Circulation. 110 (2004) 337–343. doi:10.1161/01.CIR.0000135588.65188.14.

[142] A. Abbas, P. Aukrust, D. Russell, K. Krohg-Sørensen, T. Almås, D. Bundgaard, V. Bjerkeli, E.L. Sagen, A.E. Michelsen, T.B. Dahl, S. Holm, T. Ueland, M. Skjelland, B. Halvorsen, Matrix Metalloproteinase 7 Is Associated with Symptomatic Lesions and Adverse Events in Patients with Carotid Atherosclerosis, PLoS One. 9 (2014) e84935. doi:10.1371/journal.pone.0084935.

[143] H. Williams, J.L. Johnson, C.L. Jackson, S.J. White, S.J. George, MMP-7 mediates cleavage of N-cadherin and promotes smooth muscle cell apoptosis, Cardiovasc. Res. 87 (2010) 137–146. doi:10.1093/cvr/cvq042.

[144] J.P.G. Sluijter, W.P.C. Pulskens, A.H. Schoneveld, E. Velema, C.F. Strijder, F. Moll, J.-P. de Vries, J. Verheijen, R. Hanemaaijer, D.P.V. de Kleijn, G. Pasterkamp, Matrix Metalloproteinase 2 Is Associated With Stable and Matrix Metalloproteinases 8 and 9 With Vulnerable Carotid Atherosclerotic Lesions: A Study in Human Endarterectomy Specimen Pointing to a Role for Different Extracellular Matrix Metalloproteinase In, Stroke. 37 (2006) 235–239. doi:10.1161/01.STR.0000196986.50059.e0.

[145] N. Eldrup, M.-L.M. Gronholdt, H. Sillesen, B.G. Nordestgaard, Elevated Matrix Metalloproteinase-9 Associated With Stroke or Cardiovascular Death in Patients With Carotid Stenosis, Circulation. 114 (2006) 1847–1854. doi:10.1161/CIRCULATIONAHA.105.593483.

[146] N. Oksala, M. Levula, N. Airla, M. Pelto-Huikko, R.M. Ortiz, O. Järvinen, J. Salenius, B. Ozsait, E. Komurcu-Bayrak, N. Erginel-Unaltuna, A.J. Huovila, L. Kytömäki, J.T. Soini, M. Kähönen, P.J. Karhunen, R. Laaksonen, T. Lehtimäki, ADAM-9, ADAM-15, and ADAM-17 are upregulated in macrophages in advanced human atherosclerotic plaques in aorta and carotid and femoral arteries—Tampere vascular study, Ann. Med. 41 (2009) 279–290. doi:10.1080/07853890802649738.

[147] C. Lipp, F. Lohoefer, C. Reeps, M. Rudelius, M. Baummann, U. Heemann, H.-H. Eckstein, J.

Pelisek, Expression of a Disintegrin and Metalloprotease in Human Abdominal Aortic Aneurysms, J. Vasc. Res. 49 (2012) 198–206. doi:10.1159/000332959.

[148] G. Musumeci, R. Coleman, R. Imbesi, G. Magro, R. Parenti, M.A. Szychlinska, R. Scuderi, C.S. Cinà, S. Castorina, P. Castrogiovanni, ADAM-10 could mediate cleavage of N-cadherin promoting apoptosis in human atherosclerotic lesions leading to vulnerable plaque: A morphological and immunohistochemical study, Acta Histochem. 116 (2014) 1148–1158. doi:10.1016/j.acthis.2014.06.002.

[149] D. Wågsäter, H. Björk, C. Zhu, J. Björkegren, G. Valen, A. Hamsten, P. Eriksson, ADAMTS-4 and -8 are inflammatory regulated enzymes expressed in macrophage-rich areas of human atherosclerotic plaques, Atherosclerosis. 196 (2008) 514–522. doi:10.1016/j.atherosclerosis.2007.05.018.

[150] E. Bengtsson, K. Hultman, P. Dunér, G. Asciutto, P. Almgren, M. Orho-Melander, O. Melander, J. Nilsson, A. Hultgårdh-Nilsson, I. Gonçalves, ADAMTS-7 is associated with a high-risk plaque phenotype in human atherosclerosis, Sci. Rep. 7 (2017) 3753. doi:10.1038/s41598-017-03573-4.

[151] A.-C. Jönsson Rylander, A. Lindgren, J. Deinum, G.M.L. Bergström, G. Böttcher, I. Kalies, K. Wåhlander, Fibrinolysis inhibitors in plaque stability: a morphological association of PAI-1 and TAFI in advanced carotid plaque, J. Thromb. Haemost. 15 (2017) 758–769. doi:10.1111/jth.13641.

[152] S. Ding, M. Zhang, Y. Zhao, W. Chen, G. Yao, C. Zhang, P. Zhang, Y. Zhang, The role of carotid plaque vulnerability and inflammation in the pathogenesis of acute ischemic stroke, Am. J. Med. Sci. 336 (2008) 27–31. doi:10.1097/MAJ.0b013e31815b60a1.

[153] P. Musialek, W. Tracz, L. Tekieli, P. Pieniazek, A. Kablak-Ziembicka, T. Przewlocki, E. Stepien, P. Kapusta, R. Motyl, J. Stepniewski, A. Undas, P. Podolec, Multimarker Approach in Discriminating Patients with Symptomatic and Asymptomatic Atherosclerotic Carotid Artery Stenosis, J. Clin. Neurol. 9 (2013) 165–175. doi:10.3988/jcn.2013.9.3.165.

[154] R.P. Fabunmi, G.K. Sukhova, S. Sugiyama, P. Libby, Expression of tissue inhibitor of metalloproteinases-3 in human atheroma and regulation in lesion-associated cells: a potential protective mechanism in plaque stability., Circ. Res. 83 (1998) 270–278. http://circres.ahajournals.org/cgi/content/abstract/83/3/270.

[155] I. Koskivirta, O. Rahkonen, M. Mäyränpää, S. Pakkanen, M. Husheem, A. Sainio, H. Hakovirta, J. Laine, E. Jokinen, E. Vuorio, P. Kovanen, H. Järveläinen, Tissue inhibitor of metalloproteinases 4 (TIMP4) is involved in inflammatory processes of human cardiovascular pathology, Histochem. Cell Biol. 126 (2006) 335–342. doi:10.1007/s00418-006-0163-8.

[156] P. Heider, N. Pfäffle, J. Pelisek, M. Wildgruber, H. Poppert, M. Rudelius, H.-H. Eckstein, Is Serum Pregnancy-Associated Plasma Protein A Really a Potential Marker of Atherosclerotic Carotid Plaque Stability?, Eur. J. Vasc. Endovasc. Surg. 39 (2010) 668–675. doi:10.1016/j.ejvs.2010.03.012.

[157] G. Sangiorgi, A. Mauriello, E. Bonanno, C. Oxvig, C.A. Conover, M. Christiansen, S. Trimarchi, V. Rampoldi, D.R. Holmes, R.S. Schwartz, L.G. Spagnoli, Pregnancy-Associated Plasma Protein-A Is Markedly Expressed by Monocyte-Macrophage Cells in Vulnerable and Ruptured Carotid Atherosclerotic Plaques, J. Am. Coll. Cardiol. 47 (2006) 2201–2211. doi:10.1016/j.jacc.2005.11.086.

[158] A. Mauriello, G. Sangiorgi, G. Palmieri, R. Virmani, D.R. Holmes, R.S. Schwartz, R. Pistolese, A. Ippoliti, L.G. Spagnoli, Hyperfibrinogenemia is associated with specific histocytological composition and complications of atherosclerotic carotid plaques in patients affected by transient ischemic attacks, Circulation. 101 (2000) 744–50. http://www.ncbi.nlm.nih.gov/pubmed/10683347.

[159] J. Golledge, M. McCann, S. Mangan, A. Lam, M. Karan, Osteoprotegerin and osteopontin are expressed at high concentrations within symptomatic carotid atherosclerosis, Stroke. 35 (2004) 1636–1641. doi:10.1161/01.STR.0000129790.00318.a3.

[160] D.P. V. de Kleijn, F.L. Moll, W.E. Hellings, G. Ozsarlak-Sozer, P. de Bruin, P.A. Doevendans, A. Vink, L.M. Catanzariti, A.H. Schoneveld, A. Algra, M.J. Daemen, E.A. Biessen, W. de Jager, H. Zhang, J.-P. de Vries, E. Falk, S.K. Lim, P.J. van der Spek, S.K. Sze, G. Pasterkamp, Local Atherosclerotic Plaques Are a Source of Prognostic Biomarkers for Adverse Cardiovascular Events, Arterioscler. Thromb. Vasc. Biol. 30 (2010) 612–619. doi:10.1161/ATVBAHA.109.194944.

[161] S. Rocchiccioli, G. Pelosi, S. Rosini, M. Marconi, F. Viglione, L. Citti, M. Ferrari, M. Trivella, A. Cecchettini, Secreted proteins from carotid endarterectomy: an untargeted approach to disclose molecular clues of plaque progression, J. Transl. Med. 11 (2013) 260. doi:10.1186/1479-5876-11-260.

[162] X.-D. Xiong, W.-D. Xiong, S.-S. Xiong, G.-H. Chen, Research Progress on the Risk Factors and Outcomes of Human Carotid Atherosclerotic Plaques, Chin. Med. J. (Engl). 130 (2017) 722. doi:10.4103/0366-6999.201598.

[163] Z. Chen, M. Ichetovkin, M. Kurtz, E. Zycband, D. Kawka, J. Woods, X. He, A.S. Plump, E. Hailman, Cholesterol in human atherosclerotic plaque is a marker for underlying disease state and plaque vulnerability, Lipids Health Dis. 9 (2010) 61. doi:10.1186/1476-511X-9-61.

[164] K. Nishi, H. Itabe, M. Uno, K.T. Kitazato, H. Horiguchi, K. Shinno, N. Shinji, Oxidized LDL in Carotid Plaques and Plasma Associates With Plaque Instability, Arterioscler. Thromb. Vasc. Biol. 22 (2002) 1649–1654. doi:10.1161/01.ATV.0000033829.14012.18.

[165] E. Verhoye, M.R. Langlois, Circulating oxidized low-density lipoprotein: a biomarker of atherosclerosis and cardiovascular risk?, Clin. Chem. Lab. Med. 47 (2009) 128–137. doi:10.1515/CCLM.2009.037.

[166] D. Alkazemi, G. Egeland, J. Vaya, S. Meltzer, S. Kubow, Oxysterol as a Marker of Atherogenic Dyslipidemia in Adolescence, J. Clin. Endocrinol. Metab. 93 (2008) 4282–4289.

doi:10.1210/jc.2008-0586.

[167] V.M. Olkkonen, M. Lehto, Oxysterols and oxysterol binding proteins: role in lipid metabolism and atherosclerosis, Ann. Med. 36 (2004) 562–572. doi:10.1080/07853890410018907.

[168] A. Daugherty, J.L. Dunn, D.L. Rateri, J.W. Heinecke, Myeloperoxidase, a catalyst for lipoprotein oxidation, is expressed in human atherosclerotic lesions., J. Clin. Invest. 94 (1994) 437–444. doi:10.1172/JCI117342.

[169] M. Exner, E. Minar, W. Mlekusch, S. Sabeti, J. Amighi, W. Lalouschek, G. Maurer, C. Bieglmayer, H. Kieweg, O. Wagner, M. Schillinger, Myeloperoxidase Predicts Progression of Carotid Stenosis in States of Low High-Density Lipoprotein Cholesterol, J. Am. Coll. Cardiol. 47 (2006) 2212–2218. doi:10.1016/j.jacc.2006.01.067.

[170] L. Zheng, M. Settle, G. Brubaker, D. Schmitt, S.L. Hazen, J.D. Smith, M. Kinter, Localization of Nitration and Chlorination Sites on Apolipoprotein A-I Catalyzed by Myeloperoxidase in Human Atheroma and Associated Oxidative Impairment in ABCA1-dependent Cholesterol Efflux from Macrophages, J. Biol. Chem. 280 (2005) 38–47. doi:10.1074/jbc.M407019200.

[171] P. Maitrias, V. Metzinger-Le Meuth, Z.A. Massy, E. M'Baya-Moutoula, T. Reix, T. Caus, L. Metzinger, MicroRNA deregulation in symptomatic carotid plaque, J. Vasc. Surg. 62 (2015) 1245–1250.e1. doi:10.1016/j.jvs.2015.06.136.

[172] S. Dolz, D. Górriz, J.I. Tembl, D. Sánchez, G. Fortea, V. Parkhutik, A. Lago, Circulating MicroRNAs as Novel Biomarkers of Stenosis Progression in Asymptomatic Carotid Stenosis, Stroke. 48 (2017) 10–16. doi:10.1161/STROKEAHA.116.013650.

[173] E.M. Rzucidlo, K.A. Martin, R.J. Powell, Regulation of vascular smooth muscle cell differentiation, J. Vasc. Surg. 45 (2007) A25–A32. doi:10.1016/j.jvs.2007.03.001.

[174] J.E. Hungerford, C.D. Little, Developmental biology of the vascular smooth muscle cell: Building a multilayered vessel wall, J. Vasc. Res. 36 (1999) 2–27. doi:10.1159/000025622.

[175] D. Gomez, G.K. Owens, Smooth muscle cell phenotypic switching in atherosclerosis, Cardiovasc. Res. 95 (2012) 156–164. doi:10.1093/cvr/cvs115.

[176] L.A. Martinez-Lemus, X. Wu, E. Wilson, M.A. Hill, G.E. Davis, M.J. Davis, G.A. Meininger, Integrins as Unique Receptors for Vascular Control, J. Vasc. Res. 40 (2003) 211–233. doi:10.1159/000071886.

[177] W.B. Campbell, J.R. Falck, Arachidonic acid metabolites as endothelium-derived hyperpolarizing factors, Hypertension. 49 (2007) 590–596. doi:10.1161/01.HYP.0000255173.50317.fc.

[178] F.J. Haddy, P.M. Vanhoutte, M. Feletou, Role of potassium in regulating blood flow and blood pressure, Am. J. Physiol. Integr. Comp. Physiol. 290 (2006) R546–R552. doi:10.1152/ajpregu.00491.2005.

[179] K.G. Birukov, N. Bardy, S. Lehoux, R. Merval, V.P. Shirinsky, A. Tedgui, Intraluminal pressure is essential for the maintenance of smooth muscle caldesmon and filamin content in aortic organ

culture, Arterioscler. Thromb. Vasc. Biol. 18 (1998) 922–927. doi:10.1161/01.ATV.18.6.922.

[180] G.K. Owens, M.S. Kumar, B.R. Wamhoff, Molecular regulation of vascular smooth muscle cell differentiation in development and disease., Physiol. Rev. 84 (2004) 767–801. doi:10.1152/physrev.00041.2003.

[181] S.S.M. Rensen, P.A.F.M. Doevendans, G.J.J.M. van Eys, Regulation and characteristics of vascular smooth muscle cell phenotypic diversity., Neth. Heart J. 15 (2007) 100–108. http://www.ncbi.nlm.nih.gov/pubmed/17612668.

[182] J. Chamley-Campbell, G.R. Campbell, R. Ross, The smooth muscle cell in culture., Physiol. Rev. 59 (1979) 1–61. http://physrev.physiology.org/content/59/1/1.full.pdf.

[183] M.R. Bennett, S. Sinha, G.K. Owens, Vascular Smooth Muscle Cells in Atherosclerosis, Circ. Res. 118 (2016) 692–702. doi:10.1161/CIRCRESAHA.115.306361.

[184] H. Shen, K. Eguchi, N. Kono, K. Fujiu, S. Matsumoto, M. Shibata, Y. Oishi-Tanaka, I. Komuro, H. Arai, R. Nagai, I. Manabe, Saturated Fatty Acid Palmitate Aggravates Neointima Formation by Promoting Smooth Muscle Phenotypic Modulation, Arterioscler. Thromb. Vasc. Biol. 33 (2013) 2596–2607. doi:10.1161/ATVBAHA.113.302099.

[185] R.A. Deaton, Q. Gan, G.K. Owens, Sp1-dependent activation of KLF4 is required for PDGF-BB-induced phenotypic modulation of smooth muscle, Am. J. Physiol. Circ. Physiol. 296 (2009) H1027–H1037. doi:10.1152/ajpheart.01230.2008.

[186] S. Li, D.-Z. Wang, Z. Wang, J.A. Richardson, E.N. Olson, The serum response factor coactivator myocardin is required for vascular smooth muscle development, Proc. Natl. Acad. Sci. 100 (2003) 9366–9370. doi:10.1073/pnas.1233635100.

[187] J.M. Miano, X. Long, K. Fujiwara, Serum response factor: master regulator of the actin cytoskeleton and contractile apparatus, Am. J. Physiol. Physiol. 292 (2007) C70–C81. doi:10.1152/ajpcell.00386.2006.

[188] S. Shinohara, S. Shinohara, T. Kihara, J. Miyake, Regulation of Differentiated Phenotypes of Vascular Smooth Muscle Cells, in: Curr. Basic Pathol. Approaches to Funct. Muscle Cells Tissues - From Mol. to Humans, InTech, 2012: pp. 331–344. doi:10.5772/48573.

[189] P. Lacolley, V. Regnault, A. Nicoletti, Z. Li, J.B. Michel, The vascular smooth muscle cell in arterial pathology: A cell that can take on multiple roles, Cardiovasc. Res. 95 (2012) 194–204. doi:10.1093/cvr/cvs135.

[190] J. Thyberg, K. Blomgren, J. Roy, P.K. Tran, U. Hedin, Phenotypic modulation of smooth muscle cells after arterial injury is associated with changes in the distribution of laminin and fibronectin, J Histochem Cytochem. 45 (1997) 837–846. doi:10.1177/002215549704500608.

[191] J.L. Johnson, Emerging regulators of vascular smooth muscle cell function in the development and progression of atherosclerosis., Cardiovasc. Res. 103 (2014) 452–60. doi:10.1093/cvr/cvu171.

[192] Y. Vengrenyuk, H. Nishi, X. Long, M. Ouimet, N. Savji, F.O. Martinez, C.P. Cassella, K.J. Moore, S.A. Ramsey, J.M. Miano, E.A. Fisher, Cholesterol loading reprograms the microRNA-143/145-Myocardin axis to convert aortic smooth muscle cells to a dysfunctional macrophage-like phenotype, Arterioscler. Thromb. Vasc. Biol. 35 (2015) 535–546. doi:10.1161/ATVBAHA.114.304029.

[193] T. Yoshida, M. Yamashita, M. Hayashi, Krüppel-like Factor 4 Contributes to High Phosphate-induced Phenotypic Switching of Vascular Smooth Muscle Cells into Osteogenic Cells, J. Biol. Chem. 287 (2012) 25706–25714. doi:10.1074/jbc.M112.361360.

[194] J.A. Leopold, Vascular calcification: Mechanisms of vascular smooth muscle cell calcification, Trends Cardiovasc. Med. 25 (2015) 267–274. doi:10.1016/j.tcm.2014.10.021.

[195] M.R. Alexander, G.K. Owens, Epigenetic Control of Smooth Muscle Cell Differentiation and Phenotypic Switching in Vascular Development and Disease, Annu. Rev. Physiol. 74 (2012) 13–40. doi:10.1146/annurev-physiol-012110-142315.

[196] C. Chaabane, M. Coen, M.-L. Bochaton-Piallat, Smooth muscle cell phenotypic switch: implication for foam cell formation, Curr. Opin. Lipidol. 25 (2014) 374–379. doi:10.1097/MOL.0000000000000113.

[197] D.A. Chistiakov, A.N. Orekhov, Y. V. Bobryshev, Vascular smooth muscle cell in atherosclerosis, Acta Physiol. 214 (2015) 33–50. doi:10.1111/apha.12466.

[198] N.A. Pidkovka, O.A. Cherepanova, T. Yoshida, M.R. Alexander, R.A. Deaton, J.A. Thomas, N. Leitinger, G.K. Owens, Oxidized Phospholipids Induce Phenotypic Switching of Vascular Smooth Muscle Cells In Vivo and In Vitro, Circ. Res. 101 (2007) 792–801. doi:10.1161/CIRCRESAHA.107.152736.

[199] L.S. Shankman, D. Gomez, O.A. Cherepanova, M. Salmon, G.F. Alencar, R.M. Haskins, P. Swiatlowska, A.A.C. Newman, E.S. Greene, A.C. Straub, B. Isakson, G.J. Randolph, G.K. Owens, KLF4-dependent phenotypic modulation of smooth muscle cells has a key role in atherosclerotic plaque pathogenesis, Nat. Med. 21 (2015) 628–637. doi:10.1038/nm.3866.

[200] D.M. Schrijvers, Phagocytosis of Apoptotic Cells by Macrophages Is Impaired in Atherosclerosis, Arterioscler. Thromb. Vasc. Biol. 25 (2005) 1256–1261. doi:10.1161/01.ATV.0000166517.18801.a7.

[201] L.L. Demer, Y. Tintut, Inflammatory, Metabolic, and Genetic Mechanisms of Vascular Calcification, Arterioscler. Thromb. Vasc. Biol. 34 (2014) 715–723. doi:10.1161/ATVBAHA.113.302070.

[202] V.J. Dzau, R.C. Braun-Dullaeus, D.G. Sedding, Vascular proliferation and atherosclerosis: new perspectives and therapeutic strategies, Nat. Med. 8 (2002) 1249–1256. doi:10.1038/nm1102-1249.

[203] J.A. Beamish, P. He, K. Kottke-Marchant, R.E. Marchant, Molecular Regulation of Contractile Smooth Muscle Cell Phenotype: Implications for Vascular Tissue Engineering, Tissue Eng. Part

B Rev. 16 (2010) 467–491. doi:10.1089/ten.TEB.2009.0630.

[204] C.L. Papke, J. Cao, C.S. Kwartler, C. Villamizar, K.L. Byanova, S.-M. Lim, H. Sreenivasappa, G. Fischer, J. Pham, M. Rees, M. Wang, C. Chaponnier, G. Gabbiani, A.Y. Khakoo, J. Chandra, A. Trache, W. Zimmer, D.M. Milewicz, Smooth muscle hyperplasia due to loss of smooth muscle α-actin is driven by activation of focal adhesion kinase, altered p53 localization and increased levels of platelet-derived growth factor receptor-β, Hum. Mol. Genet. 22 (2013) 3123–3137. doi:10.1093/hmg/ddt167.

[205] M.E. Sandison, J. Dempster, J.G. Mccarron, The Transition of Smooth Muscle Cells from a Contractile to a Migratory , Phagocytic Phenotype : Direct Demonstration of Phenotypic Modulation, J. Physiol. epub befor (2016) 6189–6209. doi:10.1113/JP272729.This.

[206] L.H. Dong, J.K. Wen, G. Liu, M.A. McNutt, S.B. Miao, R. Gao, B. Zheng, H. Zhang, M. Han, Blockade of the Ras-Extracellular Signal-Regulated Kinase 1/2 Pathway Is Involved in Smooth Muscle 22 -Mediated Suppression of Vascular Smooth Muscle Cell Proliferation and Neointima Hyperplasia, Arterioscler. Thromb. Vasc. Biol. 30 (2010) 683–691. doi:10.1161/ATVBAHA.109.200501.

[207] M. Han, L.-H. Dong, B. Zheng, J.-H. Shi, J.-K. Wen, Y. Cheng, Smooth muscle 22 alpha maintains the differentiated phenotype of vascular smooth muscle cells by inducing filamentous actin bundling, Life Sci. 84 (2009) 394–401. doi:10.1016/j.lfs.2008.11.017.

[208] S. Feil, F. Hofmann, R. Feil, SM22 Modulates Vascular Smooth Muscle Cell Phenotype During Atherogenesis, Circ. Res. 94 (2004) 863–865. doi:10.1161/01.RES.0000126417.38728.F6.

[209] S. a Fisher, Vascular smooth muscle phenotypic diversity and function, Physiol. Genomics. 42A (2010) 169–187. doi:10.1152/physiolgenomics.00111.2010.

[210] K. Hayashi, Y. Fujio, I. Kato, K. Sobue, Structural and functional relationships between h- and l-Caldesmons, J. Biol. Chem. 266 (1991) 355–361.

[211] M. Gimona, I. Kaverina, G.P. Resch, E. Vignal, G. Burgstaller, Calponin repeats regulate actin filament stability and formation of podosomes in smooth muscle cells, Mol. Biol. Cell. 14 (2003) 2482–2491. doi:10.1091/mbc.E02-11-0743.

[212] R. Liu, J.-P. Jin, Calponin isoforms CNN 1, CNN 2 and CNN 3: Regulators for actin cytoskeleton functions in smooth muscle and non-muscle cells, Gene. 585 (2016) 143–153. doi:10.1016/j.gene.2016.02.040.

[213] G.J. van Eys, P.M. Niessen, S.S. Rensen, Smoothelin in Vascular Smooth Muscle Cells, Trends Cardiovasc. Med. 17 (2007) 26–30. doi:10.1016/j.tcm.2006.11.001.

[214] D. PAULIN, Z. LI, Desmin: a major intermediate filament protein essential for the structural integrity and function of muscle, Exp. Cell Res. 301 (2004) 1–7. doi:10.1016/j.yexcr.2004.08.004.

[215] I. Vukovic, N. Arsenijevic, V. Lackovic, V. Todorovic, The origin and differentiation potential of

smooth muscle cells in coronary atherosclerosis., Exp. Clin. Cardiol. 11 (2006) 123–128. http://www.ncbi.nlm.nih.gov/pubmed/18651048.

[216] S. Sakurai, T. Fukasawa, J.M. Chong, A. Tanaka, M. Fukayama, Embryonic form of smooth muscle myosin heavy chain (SMemb/MHC-B) in gastrointestinal stromal tumor and interstitial cells of Cajal, Am. J. Pathol. 154 (1999) 23–28. doi:10.1016/S0002-9440(10)65246-7.

[217] J. Vandesompele, K. De Preter, F. Pattyn, B. Poppe, N. Van Roy, A. De Paepe, F. Speleman, Accurate normalization of real-time quantitative RT-PCR data by geometric averaging of multiple internal control genes, Genome Biol. 3 (2002) research0034.1. doi:10.1186/gb-2002-3-7-research0034.

[218] T.D. Schmittgen, K.J. Livak, Analyzing real-time PCR data by the comparative CT method, Nat. Protoc. 3 (2008) 1101–1108. doi:10.1038/nprot.2008.73.

[219] R. Lozano, M. Naghavi, K. Foreman, S. Lim, K. Shibuya, V. Aboyans, J. Abraham, T. Adair, R. Aggarwal, S.Y. Ahn, M.A. AlMazroa, M. Alvarado, H.R. Anderson, L.M. Anderson, K.G. Andrews, C. Atkinson, L.M. Baddour, S. Barker-Collo, D.H. Bartels, M.L. Bell, E.J. Benjamin, D. Bennett, K. Bhalla, B. Bikbov, A. Bin Abdulhak, G. Birbeck, F. Blyth, I. Bolliger, S. Boufous, C. Bucello, M. Burch, P. Burney, J. Carapetis, H. Chen, D. Chou, S.S. Chugh, L.E. Coffeng, S.D. Colan, S. Colquhoun, K.E. Colson, J. Condon, M.D. Connor, L.T. Cooper, M. Corriere, M. Cortinovis, K. Courville De Vaccaro, W. Couser, B.C. Cowie, M.H. Criqui, M. Cross, K.C. Dabhadkar, N. Dahodwala, D. De Leo, L. Degenhardt, A. Delossantos, J. Denenberg, D.C. Des Jarlais, S.D. Dharmaratne, E.R. Dorsey, T. Driscoll, H. Duber, B. Ebel, P.J. Erwin, P. Espindola, M. Ezzati, V. Feigin, A.D. Flaxman, M.H. Forouzanfar, F.G.R. Fowkes, R. Franklin, M. Fransen, M.K. Freeman, S.E. Gabriel, E. Gakidou, F. Gaspari, R.F. Gillum, D. Gonzalez-Medina, Y.A. Halasa, D. Haring, J.E. Harrison, R. Havmoeller, R.J. Hay, B. Hoen, P.J. Hotez, D. Hoy, K.H. Jacobsen, S.L. James, R. Jasrasaria, S. Jayaraman, N. Johns, G. Karthikeyan, N. Kassebaum, A. Keren, J.P. Khoo, L.M. Knowlton, O. Kobusingye, A. Koranteng, R. Krishnamurthi, M. Lipnick, S.E. Lipshultz, S. Lockett Ohno, J. Mabweijano, M.F. MacIntyre, L. Mallinger, L. March, G.B. Marks, R. Marks, A. Matsumori, R. Matzopoulos, B.M. Mayosi, J.H. McAnulty, M.M. McDermott, J. McGrath, Z.A. Memish, G.A. Mensah, T.R. Merriman, C. Michaud, M. Miller, T.R. Miller, C. Mock, A.O. Mocumbi, A.A. Mokdad, A. Moran, K. Mulholland, M.N. Nair, L. Naldi, K.M.V. Narayan, K. Nasseri, P. Norman, M. O'Donnell, S.B. Omer, K. Ortblad, R. Osborne, D. Ozgediz, B. Pahari, J.D. Pandian, A. Panozo Rivero, R. Perez Padilla, F. Perez-Ruiz, N. Perico, D. Phillips, K. Pierce, C.A. Pope, E. Porrini, F. Pourmalek, M. Raju, D. Ranganathan, J.T. Rehm, D.B. Rein, G. Remuzzi, F.P. Rivara, T. Roberts, F. Rodriguez De León, L.C. Rosenfeld, L. Rushton, R.L. Sacco, J.A. Salomon, U. Sampson, E. Sanman, D.C. Schwebel, M. Segui-Gomez, D.S. Shepard, D. Singh, J. Singleton, K. Sliwa, E. Smith, A. Steer, J.A. Taylor, B. Thomas, I.M. Tleyjeh, J.A. Towbin, T. Truelsen, E.A. Undurraga, N. Venketasubramanian, L. Vijayakumar, T. Vos, G.R. Wagner, M. Wang, W. Wang, K. Watt, M.A. Weinstock, R. Weintraub, J.D. Wilkinson, A.D. Woolf, S. Wulf, P.H. Yeh, P. Yip, A. Zabetian, Z.J. Zheng, A.D. Lopez, C.J.L. Murray, Global and regional mortality from 235 causes of death for 20 age

groups in 1990 and 2010: A systematic analysis for the Global Burden of Disease Study 2010, Lancet. 380 (2012) 2095–2128. doi:10.1016/S0140-6736(12)61728-0.

[220] D. Kim, G. Pertea, C. Trapnell, H. Pimentel, R. Kelley, S.L. Salzberg, TopHat2: accurate alignment of transcriptomes in the presence of insertions, deletions and gene fusions, Genome Biol. 14 (2013) R36. doi:10.1186/gb-2013-14-4-r36.

[221] C. Trapnell, B. a Williams, G. Pertea, A. Mortazavi, G. Kwan, M.J. van Baren, S.L. Salzberg, B.J. Wold, L. Pachter, Transcript assembly and quantification by RNA-Seq reveals unannotated transcripts and isoform switching during cell differentiation, Nat. Biotechnol. 28 (2010) 511–515. doi:10.1038/nbt.1621.

[222] M.I. Love, W. Huber, S. Anders, Moderated estimation of fold change and dispersion for RNA-seq data with DESeq2, Genome Biol. 15 (2014) 550. doi:10.1186/s13059-014-0550-8.

[223] Y. Benjamini, Y. Hochberg, Controlling the False Discovery Rate: a practical and powerful approach to multiple testing, J. R. Stat. Soc. Ser. B. 57 (1995) 289–300. doi:10.2307/2346101.

[224] G. Yu, L.-G. Wang, Y. Han, Q.-Y. He, clusterProfiler: an R Package for Comparing Biological Themes Among Gene Clusters, Omi. A J. Integr. Biol. 16 (2012) 284–287. doi:10.1089/omi.2011.0118.

[225] C. V Remillard, A. Makino, J.X. Yuan, Textbook of Pulmonary Vascular Disease, Springer US, Boston, MA, 2011. doi:10.1007/978-0-387-87429-6.

[226] A.T. Churchman, R.C.M. Siow, Isolation, Culture and Characterisation of Vascular Smooth Muscle Cells, in: Angiogenes. Protoc., 2009: pp. 127–138. doi:10.1007/978-1-59745-241-0_7.

[227] GeneCards, CXCL9, GeneCards - Hum. Gene Database. (2014). http://www.genecards.org/cgi-bin/carddisp.pl?gene=CXCL9&keywords=cxcl9.

[228] GeneCards, CXCL10, GeneCards - Hum. Gene Database. (2010). http://www.genecards.org/cgi-bin/carddisp.pl?gene=CXCL10&keywords=cxcl10.

[229] GeneCards, CD5L, GeneCards - Hum. Gene Database. (n.d.). http://www.genecards.org/cgi-bin/carddisp.pl?gene=CD5L&keywords=cd5L.

[230] S. Arai, J.M. Shelton, M. Chen, M.N. Bradley, A. Castrillo, A.L. Bookout, P.A. Mak, P.A. Edwards, D.J. Mangelsdorf, P. Tontonoz, T. Miyazaki, A role for the apoptosis inhibitory factor AIM/Spα/Api6 in atherosclerosis development, Cell Metab. 1 (2005) 201–213. doi:10.1016/j.cmet.2005.02.002.

[231] I. Alloza, H. Goikuria, J.L. Idro, J.C. Triviño, J.M. Fernández Velasco, E. Elizagaray, M. García-Barcina, G. Montoya-Murillo, E. Sarasola, R. Vega Manrique, M. del M. Freijo, K. Vandenbroeck, RNAseq based transcriptomics study of SMCs from carotid atherosclerotic plaque: BMP2 and IDs proteins are crucial regulators of plaque stability, Sci. Rep. 7 (2017) 3470. doi:10.1038/s41598-017-03687-9.

[232] S. Feil, B. Fehrenbacher, R. Lukowski, F. Essmann, K. Schulze-Osthoff, M. Schaller, R. Feil,

Transdifferentiation of Vascular Smooth Muscle Cells to Macrophage-Like Cells During Atherogenesis, Circ. Res. 115 (2014) 662–667. doi:10.1161/CIRCRESAHA.115.304634.

[233] J. Song, N.F. Worth, B.E. Rolfe, G.R. Campbell, J.H. Campbell, Heterogeneous distribution of isoactins in cultured vascular smooth muscle cells does not reflect segregation of contractile and cytoskeletal domains, J. Histochem. Cytochem. 48 (2000) 1441–1452. doi:10.1177/002215540004801101.

[234] D. Sims, I. Sudbery, N.E. Ilott, A. Heger, C.P. Ponting, Sequencing depth and coverage: key considerations in genomic analyses, Nat. Rev. Genet. 15 (2014) 121–132. doi:10.1038/nrg3642.

[235] Y. Liu, J. Zhou, K.P. White, RNA-seq differential expression studies: more sequence or more replication?, Bioinformatics. 30 (2014) 301–304. doi:10.1093/bioinformatics/btt688.

[236] D. Risso, K. Schwartz, G. Sherlock, S. Dudoit, GC-Content Normalization for RNA-Seq Data, BMC Bioinformatics. 12 (2011) 480. doi:10.1186/1471-2105-12-480.

[237] K.D. Hansen, R.A. Irizarry, Z. WU, Removing technical variability in RNA-seq data using conditional quantile normalization, Biostatistics. 13 (2012) 204–216. doi:10.1093/biostatistics/kxr054.

[238] R.C. Team, R: A language and environment for statistical computing, (2013). http://www.r-project.org/.

[239] W. Stacklies, H. Redestig, M. Scholz, D. Walther, J. Selbig, pcaMethods a bioconductor package providing PCA methods for incomplete data, Bioinformatics. 23 (2007) 1164–1167. doi:10.1093/bioinformatics/btm069.

[240] S. Anders, W. Huber, Differential expression analysis for sequence count data, Genome Biol. 11 (2010) R106. doi:10.1186/gb-2010-11-10-r106.

[241] C. Trapnell, A. Roberts, L. Goff, G. Pertea, D. Kim, D.R. Kelley, H. Pimentel, S.L. Salzberg, J.L. Rinn, L. Pachter, Differential gene and transcript expression analysis of RNA-seq experiments with TopHat and Cufflinks, Nat. Protoc. 7 (2012) 562–578. doi:10.1038/nprot.2012.016.

[242] J.A. Blake, K.R. Christie, M.E. Dolan, H.J. Drabkin, D.P. Hill, L. Ni, D. Sitnikov, S. Burgess, T. Buza, C. Gresham, F. McCarthy, L. Pillai, H. Wang, S. Carbon, H. Dietze, S.E. Lewis, C.J. Mungall, M.C. Munoz-Torres, M. Feuermann, P. Gaudet, S. Basu, R.L. Chisholm, R.J. Dodson, P. Fey, H. Mi, P.D. Thomas, A. Muruganujan, S. Poudel, J.C. Hu, S.A. Aleksander, B.K. McIntosh, D.P. Renfro, D.A. Siegele, H. Attrill, N.H. Brown, S. Tweedie, J. Lomax, D. Osumi-Sutherland, H. Parkinson, P. Roncaglia, R.C. Lovering, P.J. Talmud, S.E. Humphries, P. Denny, N.H. Campbell, R.E. Foulger, M.C. Chibucos, M.G. Giglio, H.Y. Chang, R. Finn, M. Fraser, A. Mitchell, G. Nuka, S. Pesseat, A. Sangrador, M. Scheremetjew, S.Y. Young, R. Stephan, M.A. Harris, S.G. Oliver, K. Rutherford, V. Wood, J. Bahler, A. Lock, P.J. Kersey, M.D. McDowall, D.M. Staines, M. Dwinell, M. Shimoyama, S. Laulederkind, G.T. Hayman, S.J. Wang, V. Petri, P. D'Eustachio, L. Matthews, R. Balakrishnan, G. Binkley, J.M. Cherry, M.C. Costanzo, J. Demeter, S.S. Dwight, S.R. Engel, B.C. Hitz, D.O. Inglis, P. Lloyd, S.R. Miyasato, K. Paskov, G.

Roe, M. Simison, R.S. Nash, M.S. Skrzypek, S. Weng, E.D. Wong, T.Z. Berardini, D. Li, E. Huala, J. Argasinska, C. Arighi, A. Auchincloss, K. Axelsen, G. Argoud-Puy, A. Bateman, B. Bely, M.C. Blatter, C. Bonilla, L. Bougueleret, E. Boutet, L. Breuza, A. Bridge, R. Britto, C. Casals, E. Cibrian-Uhalte, E. Coudert, I. Cusin, P. Duek-Roggli, A. Estreicher, L. Famiglietti, P. Gane, P. Garmiri, A. Gos, N. Gruaz-Gumowski, E. Hatton-Ellis, U. Hinz, C. Hulo, R. Huntley, F. Jungo, G. Keller, K. Laiho, P. Lemercier, D. Lieberherr, A. Macdougall, M. Magrane, M. Martin, P. Masson, P. Mutowo, C. O'Donovan, I. Pedruzzi, K. Pichler, D. Poggioli, S. Poux, C. Rivoire, B. Roechert, T. Sawford, M. Schneider, A. Shypitsyna, A. Stutz, S. Sundaram, M. Tognolli, C. Wu, I. Xenarios, J. Chan, R. Kishore, P.W. Sternberg, K. Van Auken, H.M. Muller, J. Done, Y. Li, D. Howe, M. Westerfeld, Gene Ontology Consortium: going forward, Nucleic Acids Res. 43 (2015) D1049–D1056. doi:10.1093/nar/gku1179.

[243] M. Kanehisa, S. Goto, KEGG: Kyoto Encyclopedia of Genes and Genomes, Nucleic Acids Res. 28 (2000) 27–30. doi:10.1093/nar/28.1.27.

[244] A. Fabregat, K. Sidiropoulos, P. Garapati, M. Gillespie, K. Hausmann, R. Haw, B. Jassal, S. Jupe, F. Korninger, S. McKay, L. Matthews, B. May, M. Milacic, K. Rothfels, V. Shamovsky, M. Webber, J. Weiser, M. Williams, G. Wu, L. Stein, H. Hermjakob, P. D'Eustachio, The Reactome pathway Knowledgebase, Nucleic Acids Res. 44 (2016) D481–D487. doi:10.1093/nar/gkv1351.

[245] G. Yu, L.-G. Wang, G.-R. Yan, Q.-Y. He, DOSE: an R/Bioconductor package for disease ontology semantic and enrichment analysis, Bioinformatics. 31 (2015) 608–609. doi:10.1093/bioinformatics/btu684.

[246] J. Montojo, K. Zuberi, H. Rodriguez, G.D. Bader, Q. Morris, GeneMANIA: Fast gene network construction and function prediction for Cytoscape, F1000Research. 153 (2014) 1–7. doi:10.12688/f1000research.4572.1.

[247] R. Saito, M.E. Smoot, K. Ono, J. Ruscheinski, P.-L. Wang, S. Lotia, A.R. Pico, G.D. Bader, T. Ideker, A travel guide to Cytoscape plugins, Nat. Methods. 9 (2012) 1069–1076. doi:10.1038/nmeth.2212.

[248] A.R. Wu, N.F. Neff, T. Kalisky, P. Dalerba, B. Treutlein, M.E. Rothenberg, F.M. Mburu, G.L. Mantalas, S. Sim, M.F. Clarke, S.R. Quake, Quantitative assessment of single-cell RNA-sequencing methods, Nat. Methods. 11 (2014) 41–46. doi:10.1038/nmeth.2694.

[249] P.C. HEINRICH, I. BEHRMANN, S. HAAN, H.M. HERMANNS, G. MÜLLER-NEWEN, F. SCHAPER, Principles of interleukin (IL)-6-type cytokine signalling and its regulation, Biochem. J. 374 (2003) 1–20. doi:10.1042/bj20030407.

[250] G.W. Jones, L. McLeod, C.L. Kennedy, S. Bozinovski, M. Najdovska, B.J. Jenkins, Imbalanced gp130 signalling in ApoE-deficient mice protects against atherosclerosis, Atherosclerosis. 238 (2015) 321–328. doi:10.1016/j.atherosclerosis.2014.12.037.

[251] M. Klouche, S. Bhakdi, M. Hemmes, S. Rose-John, Novel path to activation of vascular smooth muscle cells: up-regulation of gp130 creates an autocrine activation loop by IL-6 and its soluble

receptor., J. Immunol. 163 (1999) 4583–4589.

[252] V.L. King, Atherosclerosis: should we stop TWEAKing it?, Arterioscler. Thromb. Vasc. Biol. 29 (2009) 1982–1983. doi:10.1161/ATVBAHA.109.197228.

[253] G. Straface, F. Biscetti, D. Pitocco, G. Bertoletti, M. Misuraca, C. Vincenzoni, F. Snider, V. Arena, E. Stigliano, F. Angelini, L. Iuliano, S. Boccia, C. De Waure, F. Giacchi, G. Ghirlanda, A. Flex, Assessment of the genetic effects of polymorphisms in the osteoprotegerin gene, TNFRSF11B, on serum osteoprotegerin levels and carotid plaque vulnerability, Stroke. 42 (2011) 3022–3028. doi:10.1161/STROKEAHA.111.619288.

[254] J.G. Emery, P. McDonnell, M.B. Burke, K.C. Deen, S. Lyn, C. Silverman, E. Dul, E.R. Appelbaum, C. Eichman, R. DiPrinzio, R.A. Dodds, I.E. James, M. Rosenberg, J.C. Lee, P.R. Young, Osteoprotegerin is a receptor for the cytotoxic ligand TRAIL, J. Biol. Chem. 273 (1998) 14363–14367. doi:10.1074/jbc.273.23.14363.

[255] L. O'Leary, a M. van der Sloot, C.R. Reis, S. Deegan, a E. Ryan, S.P.S. Dhami, L.S. Murillo, R.H. Cool, P.C. de Sampaio, K. Thompson, G. Murphy, W.J. Quax, L. Serrano, A. Samali, E. Szegezdi, Decoy receptors block TRAIL sensitivity at a supracellular level: the role of stromal cells in controlling tumour TRAIL sensitivity, Oncogene. 35 (2016) 1261–1270. doi:10.1038/onc.2015.180.

[256] E.P.C. van der Vorst, Y. Döring, C. Weber, Chemokines and their receptors in atherosclerosis, J. Mol. Med. 93 (2015) 963–971. doi:10.1007/s00109-015-1317-8.

[257] Genecards - Human Genes. Gene Database. Gene Search., (1980). http://www.genecards.org/cgi-bin/carddisp.pl?gene=TNFAIP1&keywords=TNFAIP1 (accessed July 28, 2017).

[258] I.E. Wertz, K.M. O'Rourke, H. Zhou, M. Eby, L. Aravind, S. Seshagiri, P. Wu, C. Wiesmann, R. Baker, D.L. Boone, A. Ma, E. V Koonin, V.M. Dixit, De-ubiquitination and ubiquitin ligase domains of A20 downregulate NF-kB signalling, Nature. 430 (2004) 694–699. doi:10.1038/nature02794.

[259] M. Mellett, P. Atzei, A. Horgan, E. Hams, T. Floss, W. Wurst, P.G. Fallon, P.N. Moynagh, Orphan receptor IL-17RD tunes IL-17A signalling and is required for neutrophilia, Nat. Commun. 3 (2012) 1119. doi:10.1038/ncomms2127.

[260] C.C. Wei, Y.H. Hsu, H.H. Li, Y.C. Wang, M.Y. Hsieh, W.Y. Chen, C.H. Hsing, M.S. Chang, IL-20: biological functions and clinical implications, J. Biomed. Sci. 13 (2006) 601–612. doi:10.1007/s11373-006-9087-5.

[261] T. Tamiya, I. Kashiwagi, R. Takahashi, H. Yasukawa, A. Yoshimura, Suppressors of cytokine signaling (SOCS) proteins and JAK/STAT pathways: Regulation of T-cell inflammation by SOCS1 and SOCS3, Arterioscler. Thromb. Vasc. Biol. 31 (2011) 980–985. doi:10.1161/ATVBAHA.110.207464.

[262] O.J. de Boer, J.J. van der Meer, P. Teeling, C.M. van der Loos, M.M. Idu, F. Van Maldegem, J. Aten, A.C. van der Wal, Differential expression of interleukin-17 family cytokines in intact and

complicated human atherosclerotic plaques, J. Pathol. 220 (2010) 499–508. doi:10.1002/path.2667.

[263] B. Carow, M.E. Rottenberg, SOCS3, a major regulator of infection and inflammation, Front. Immunol. 5 (2014) 1–13. doi:10.3389/fimmu.2014.00058.

[264] H. Taki, T. Sakai, E. Sugiyama, T. Mino, A. Kuroda, K. Taki, T. Hamazaki, H. Koizumi, M. Kobayashi, Monokine stimulation of interleukin-11 production by human vascular smooth muscle cells in vitro, Atheroscler. 144 (1999) 375–380.

[265] J.C. Kovacic, R. Gupta, A.C. Lee, M. Ma, F. Fang, C.N. Tolbert, A.D. Walts, L.E. Beltran, H. San, G. Chen, C.S. Hilaire, M. Boehm, Stat3-dependent acute Rantes production in vascular smooth muscle cells modulates inflammation following arterial injury in mice, J. Clin. Invest. 120 (2010) 303–314. doi:10.1172/JCI40364.

[266] N.R. Veillard, B. Kwak, G. Pelli, F. Mulhaupt, R.W. James, A.E.I. Proudfoot, F. Mach, Antagonism of RANTES receptors reduces atherosclerotic plaque formation in mice, Circ. Res. 94 (2004) 253–261. doi:10.1161/01.RES.0000109793.17591.4E.

[267] J.R. Goldsmith, Y.H. Chen, Regulation of inflammation and tumorigenesis by the TIPE family of phospholipid transfer proteins, Cell. Mol. Immunol. 14 (2017) 482–487. doi:10.1038/cmi.2017.4.

[268] G.C.T. Pipes, E.E. Creemers, E.N. Olson, The myocardin family of transcriptional coactivators: versatile regulators of cell growth, migration, and myogenesis., Genes Dev. 20 (2006) 1545–56. doi:10.1101/gad.1428006.

[269] R. Ross, J.A. Glomset, Atherosclerosis and the arterial smooth muscle cell: Proliferation of smooth muscle is a key event in the genesis of the lesions of atherosclerosis, Science (80-.). 180 (1973) 1332–1339. doi:10.1172/JCI200215686.9.

[270] Y. Liu, S. Sinha, O.G. McDonald, Y. Shang, M.H. Hoofnagle, G.K. Owens, Kruppel-like Factor 4 Abrogates Myocardin-induced Activation of Smooth Muscle Gene Expression, J. Biol. Chem. 280 (2005) 9719–9727. doi:10.1074/jbc.M412862200.

[271] E.K. Arkenbout, R.J. Dekker, C.J.M. de Vries, A.J.G. Horrevoets, H. Pannekoek, Focusing on transcription factor families in atherogenesis: the function of LKLF and TR3., Thromb. Haemost. 89 (2003) 522–529. doi:10.1055/s-0037-1613383.

[272] B. Zheng, M. Han, J.-K. Wen, Role of Krüppel-like factor 4 in phenotypic switching and proliferation of vascular smooth muscle cells, IUBMB Life. 62 (2010) 132–139. doi:10.1002/iub.298.

[273] H. Iwata, I. Manabe, K. Fujiu, T. Yamamoto, N. Takeda, K. Eguchi, A. Furuya, M. Kuro-o, M. Sata, R. Nagai, Bone marrow-derived cells contribute to vascular inflammation but do not differentiate into smooth muscle cell lineages, Circulation. 122 (2010) 2048–2057. doi:10.1161/CIRCULATIONAHA.110.965202.

[274] Y. Liu, B. Deng, Y. Zhao, S. Xie, R. Nie, Differentiated markers in undifferentiated cells:

Expression of smooth muscle contractile proteins in multipotent bone marrow mesenchymal stem cells, Dev. Growth Differ. 55 (2013) 591–605. doi:10.1111/dgd.12052.

[275] N.F. Worth, B.E. Rolfe, J. Song, G.R. Campbell, Vascular smooth muscle cell phenotypic modulation in culture is associated with reorganisation of contractile and cytoskeletal proteins, Cell Motil. Cytoskeleton. 49 (2001) 130–145. doi:10.1002/cm.1027.

[276] J. Song, B.E. Rolfe, J.H. Campbell, G.R. Campbell, Changes in three-dimensional architecture of microfilaments in cultured vascular smooth muscle cells during phenotypic modulation, Tissue Cell. 30 (1998) 324–333. doi:10.1016/S0040-8166(98)80045-1.

[277] J. Saltis, A.C. Thomasb, A. Agrotis, J.H. Campbellb, G.R. Campbellb, A. Bobik, Expression of growth factor receptors on arterial smooth muscle cells . Dependency on cell phenotype and serum factors, Methods. 118 (1995) 77–87.

[278] S. Allahverdian, A.C. Chehroudi, B.M. McManus, T. Abraham, G.A. Francis, Contribution of intimal smooth muscle cells to cholesterol accumulation and macrophage-like cells in human atherosclerosis, Circulation. 129 (2014) 1551–1559. doi:10.1161/CIRCULATIONAHA.113.005015.

[279] J.K. Salabei, B.G. Hill, Autophagic regulation of smooth muscle cell biology, Redox Biol. (2015). doi:10.1016/j.redox.2014.12.007.

[280] B. Swaminathan, H. Goikuria, R. Vega, A. Rodríguez-Antigüedad, A. López Medina, M. Del Mar Freijo, K. Vandenbroeck, I. Alloza, Autophagic marker MAP1LC3B expression levels are associated with carotid atherosclerosis symptomatology, PLoS One. 9 (2014). doi:10.1371/journal.pone.0115176.

[281] Y. Vengrenyuk, H. Nishi, X. Long, M. Ouimet, N. Savji, F.O. Martinez, C.P. Cassella, K.J. Moore, S.A. Ramsey, J.M. Miano, E.A. Fisher, Cholesterol Loading Reprograms the MicroRNA-143/145–Myocardin Axis to Convert Aortic Smooth Muscle Cells to a Dysfunctional Macrophage-Like Phenotype, Arterioscler. Thromb. Vasc. Biol. 35 (2015) 535–546. doi:10.1161/ATVBAHA.114.304029.

[282] M.W. Huff, J.G. Pickering, Can a vascular smooth muscle-derived foam-cell really change its spots?, Arterioscler. Thromb. Vasc. Biol. 35 (2015) 492–495. doi:10.1161/ATVBAHA.115.305225.

[283] S. Shukla, X. Zhang, Y.S. Niknafs, L. Xiao, R. Mehra, M. Cieślik, A. Ross, E. Schaeffer, B. Malik, S. Guo, S.M. Freier, H.-H. Bui, J. Siddiqui, X. Jing, X. Cao, S.M. Dhanasekaran, F.Y. Feng, A.M. Chinnaiyan, R. Malik, Identification and Validation of PCAT14 as Prognostic Biomarker in Prostate Cancer, Neoplasia. 18 (2016) 489–499. doi:10.1016/j.neo.2016.07.001.

[284] R. Miao, H. Luo, H. Zhou, G. Li, D. Bu, X. Yang, X. Zhao, H. Zhang, S. Liu, Y. Zhong, Z. Zou, Y. Zhao, K. Yu, L. He, X. Sang, S. Zhong, J. Huang, Y. Wu, R.A. Miksad, S.C. Robson, C. Jiang, Y. Zhao, H. Zhao, Identification of prognostic biomarkers in hepatitis B virus-related hepatocellular carcinoma and stratification by integrative multi-omics analysis, J. Hepatol. 61

(2014) 840–849. doi:10.1016/j.jhep.2014.05.025.

[285] S. Goodwin, J.D. McPherson, W.R. McCombie, Coming of age: ten years of next-generation sequencing technologies, Nat. Rev. Genet. 17 (2016) 333–351. doi:10.1038/nrg.2016.49.

[286] G.C. Jickling, F.R. Sharp, Biomarker Panels in Ischemic Stroke, Stroke. 46 (2015) 915–920. doi:10.1161/STROKEAHA.114.005604.

[287] K. Miyazono, K. Kusanagi, H. Inoue, Divergence and convergence of TGF-beta/BMP signaling., J. Cell. Physiol. 187 (2001) 265–276. doi:10.1002/jcp.1080.

[288] S. Tsukamoto, T. Mizuta, M. Fujimoto, S. Ohte, K. Osawa, A. Miyamoto, K. Yoneyama, E. Murata, A. Machiya, E. Jimi, S. Kokabu, T. Katagiri, Smad9 is a new type of transcriptional regulator in bone morphogenetic protein signaling, Sci. Rep. 4 (2014) 7596. doi:10.1038/srep07596.

[289] T. Katagiri, M. Imada, T. Yanai, T. Suda, N. Takahashi, R. Kamijo, Identification of a BMP-responsive element in Id1, the gene for inhibition of myogenesis, Genes to Cells. 7 (2002) 949–960. doi:10.1046/j.1365-2443.2002.00573.x.

[290] N.W. Morrell, D.B. Bloch, P. ten Dijke, M.-J.T.H. Goumans, A. Hata, J. Smith, P.B. Yu, K.D. Bloch, Targeting BMP signalling in cardiovascular disease and anaemia, Nat. Rev. Cardiol. 13 (2016) 106–120. doi:10.1038/nrcardio.2015.156.

[291] A.Y. Simões Sato, G.L. Bub, A.H. Campos, BMP-2 and -4 produced by vascular smooth muscle cells from atherosclerotic lesions induce monocyte chemotaxis through direct BMPRII activation, Atherosclerosis. 235 (2014) 45–55. doi:10.1016/j.atherosclerosis.2014.03.030.

[292] M. Zhang, J. Sara, F. Wang, L.-P. Liu, L.-X. Su, J. Zhe, X. Wu, J. Liu, Increased plasma BMP-2 levels are associated with atherosclerosis burden and coronary calcification in type 2 diabetic patients, Cardiovasc. Diabetol. 14 (2015) 64. doi:10.1186/s12933-015-0214-3.

[293] Y. YAO, A. ZEBBOUDJ, A. TORRES, E. SHAO, K. BOSTROM, Activin-like kinase receptor 1 (ALK1) in atherosclerotic lesions and vascular mesenchymal cells, Cardiovasc. Res. 74 (2007) 279–289. doi:10.1016/j.cardiores.2006.09.014.

[294] A. Weiss, L. Attisano, The TGFbeta Superfamily Signaling Pathway, Wiley Interdiscip. Rev. Dev. Biol. 2 (2013) 47–63. doi:10.1002/wdev.86.

[295] R.N. Wang, J. Green, Z. Wang, Y. Deng, M. Qiao, M. Peabody, Q. Zhang, J. Ye, Z. Yan, S. Denduluri, O. Idowu, M. Li, C. Shen, A. Hu, R.C. Haydon, R. Kang, J. Mok, M.J. Lee, H.L. Luu, L.L. Shi, Bone Morphogenetic Protein (BMP) signaling in development and human diseases, Genes Dis. 1 (2014) 87–105. doi:10.1016/j.gendis.2014.07.005.

[296] J. Yang, X. Li, Y. Li, M. Southwood, L. Ye, L. Long, R.S. Al-Lamki, N.W. Morrell, Id proteins are critical downstream effectors of BMP signaling in human pulmonary arterial smooth muscle cells, Am. J. Physiol. Cell. Mol. Physiol. 305 (2013) L312–L321. doi:10.1152/ajplung.00054.2013.

[297] J. Yang, X. Li, N.W. Morrell, Id proteins in the vasculature: from molecular biology to cardiopulmonary medicine, Cardiovasc. Res. 104 (2014) 388–398. doi:10.1093/cvr/cvu215.

[298] K. Miyazono, K. Miyazawa, Id: A Target of BMP Signaling, Sci. Signal. 2002 (2002) pe40-pe40. doi:10.1126/stke.2002.151.pe40.

[299] K. Nishiyama, Id1 Gene Transfer Confers Angiogenic Property on Fully Differentiated Endothelial Cells and Contributes to Therapeutic Angiogenesis, Circulation. 112 (2005) 2840–2850. doi:10.1161/CIRCULATIONAHA.104.516898.

[300] F. Kyei, D.-B. Asante, J. Edekor, E. Sarpong, E. Gavor, D. Konja, Down-regulation of Id1 and Id3 genes affects growth and survival of Human Umbilical Vein Endothelial Cells (HUVECs), J. Appl. Biol. Biotechnol. 4 (2016) 023–029. doi:10.7324/JABB.2016.40204.

[301] I. Gorenne, M. Kavurma, S. Scott, M. Bennett, Vascular smooth muscle cell senescence in atherosclerosis., Cardiovasc. Res. 72 (2006) 9–17. doi:10.1016/j.cardiores.2006.06.004.

[302] Y. Jen, K. Manova, R. Benezra, Expression patterns of Id1, Id2, and Id3 are highly related but distinct from that of Id4 during mouse embryogenesis, Dev. Dyn. 207 (1996) 235–252. doi:10.1002/(SICI)1097-0177(199611)207:3<235::AID-AJA1>3.0.CO;2-I.

[303] P.J. Andres-Barquin, M.-C. Hernandez, M. a Israel, Id4 Expression Induces Apoptosis in Astrocytic Cultures and Is Down-regulated by Activation of the cAMP-Dependent Signal Transduction Pathway, Exp. Cell Res. 247 (1999) 347–355. doi:10.1006/excr.1998.4360.

[304] R. Bouchareb, N. Côté, Marie-Chloé-Boulanger, K. Le Quang, D. El Husseini, J. Asselin, F. Hadji, D. Lachance, E.E. Shayhidin, A. Mahmut, P. Pibarot, Y. Bossé, Y. Messaddeq, D. Boudreau, A. Marette, P. Mathieu, Carbonic anhydrase XII in valve interstitial cells promotes the regression of calcific aortic valve stenosis, J. Mol. Cell. Cardiol. 82 (2015) 104–15. doi:10.1016/j.yjmcc.2015.03.002.

[305] L.F. de Castro, D. Lozano, S. Portal-Núñez, M. Maycas, M. De la Fuente, J.R. Caeiro, P. Esbrit, Comparison of the skeletal effects induced by daily administration of PTHrP (1-36) and PTHrP (107-139) to ovariectomized mice, J. Cell. Physiol. 227 (2012) 1752–1760. doi:10.1002/jcp.22902.

[306] P. Hu, B.Y. Huang, X. Xia, Q. Xuan, B. Hu, Y.H. Qin, Therapeutic effect of CNP on renal osteodystrophy by antagonizing the FGF-23/MAPK pathway, J. Recept. Signal Transduct. 36 (2016) 213–219. doi:10.3109/10799893.2015.1075041.

[307] J.-M. Zhang, J. An, Cytokines, inflammation and pain, Int Anesth. Clin. 45 (2007) 27–37. doi:10.1097/AIA.0b013e318034194e.

[308] J.-I. Koga, M. Aikawa, Crosstalk between macrophages and smooth muscle cells in atherosclerotic vascular diseases, Vascul. Pharmacol. 57 (2012) 24–28. doi:10.1016/j.vph.2012.02.011.

[309] S.A. Jones, Directing transition from innate to acquired immunity: defining a role for IL-6, J.

Immunol. 175 (2005) 3463–3468. doi:10.4049/jimmunol.175.6.3463.

[310] T. Kishimoto, IL-6: from its discovery to clinical applications, Int. Immunol. 22 (2010) 347–352. doi:10.1093/intimm/dxq030.

[311] D.G. Hildebrand, E. Alexander, S. Horber, S. Lehle, K. Obermayer, N.-A. Munck, O. Rothfuss, J.-S. Frick, M. Morimatsu, I. Schmitz, J. Roth, J.M. Ehrchen, F. Essmann, K. Schulze-Osthoff, IκBζ is a transcriptional key regulator of CCL2/MCP-1, J. Immunol. 190 (2013) 4812–4820. doi:10.4049/jimmunol.1300089.

[312] S. Watanabe, W. Mu, A. Kahn, N. Jing, J.H. Li, H.Y. Lan, T. Nakagawa, R. Ohashi, R.J. Johnson, Role of JAK/STAT pathway in IL-6-induced activation of vascular smooth muscle cells, Am. J. Nephrol. 24 (2004) 387–392. doi:10.1159/000079706.

[313] S. Akhtar, F. Gremse, F. Kiessling, C. Weber, A. Schober, CXCL12 promotes the stabilization of atherosclerotic lesions mediated by smooth muscle progenitor cells in apoe-deficient mice, Arterioscler. Thromb. Vasc. Biol. 33 (2013) 679–686. doi:10.1161/ATVBAHA.112.301162.

[314] F. Guo, Y. Wang, J. Liu, S. Mok, F. Xue, W. Zhang, CXCL12/CXCR4: a symbiotic bridge linking cancer cells and their stromal neighbors in oncogenic communication networks, Oncogene. 35 (2015) 816–826. doi:10.1038/onc.2015.139.

[315] S. Abi-Younes, A. Sauty, F. Mach, G.K. Sukhova, P. Libby, A.D. Luster, The stromal cell-derived factor-1 chemokine is a potent platelet agonist highly expressed in atherosclerotic plaques, Circ. Res. 86 (2000) 131–138. doi:10.1161/01.RES.86.2.131.

[316] C. Weber, Platelets and Chemokines in Atherosclerosis: Partners in Crime, Circ. Res. 96 (2005) 612–616. doi:10.1161/01.RES.0000160077.17427.57.

[317] K. Yokota, K. Sato, T. Miyazaki, H. Kitaura, H. Kayama, F. Miyoshi, Y. Araki, Y. Akiyama, K. Takeda, T. Mimura, Combination of tumor necrosis factor α and interleukin-6 induces mouse osteoclast-like cells with bone resorption activity both in vitro and in vivo, Arthritis Rheumatol. 66 (2014) 121–129. doi:10.1002/art.38218.

[318] N.P.E. Kadoglou, T. Gerasimidis, S. Golemati, A. Kapelouzou, P.E. Karayannacos, C.D. Liapis, The relationship between serum levels of vascular calcification inhibitors and carotid plaque vulnerability, J. Vasc. Surg. 47 (2008) 55–62. doi:http://dx.doi.org/10.1016/j.jvs.2007.09.058.

[319] S. Kiechl, G. Schett, G. Wenning, K. Redlich, M. Oberhollenzer, A. Mayr, P. Santer, J. Smolen, W. Poewe, J. Willeit, Osteoprotegerin is a risk factor for progressive atherosclerosis and cardiovascular disease, Circulation. 109 (2004) 2175–2180. doi:10.1161/01.CIR.0000127957.43874.BB.

[320] Y. Feng, A.J. Sanders, F. Ruge, C.A. Morris, K.G. Harding, W.G. Jiang, Expression of the SOCS family in human chronic wound tissues: Potential implications for SOCS in chronic wound healing, Int. J. Mol. Med. 38 (2016) 1349–1358. doi:10.3892/ijmm.2016.2733.

[321] Y. Tian, L.J. Sommerville, A. Cuneo, S.E. Kelemen, M. V Autieri, Expression and suppressive

effects of interleukin-19 on vascular smooth muscle cell pathophysiology and development of intimal hyperplasia, Am. J. Pathol. 173 (2008) 901–909. doi:10.2353/ajpath.2008.080163.

[322] M.C. Trengove, A.C. Ward, SOCS proteins in development and disease, Am. J. Clin. Exp. Immunol. 2 (2013) 1–29.

[323] M. Fujimoto, T. Naka, Regulation of cytokine signaling by SOCS family molecules, Trends Immunol. 24 (2003) 659–666. doi:10.1016/j.it.2003.10.008.

[324] J.J. Babon, L.N. Varghese, N.A. Nicola, Inhibition of IL-6 family cytokines by SOCS3, Semin. Immunol. 26 (2014) 13–19. doi:10.1016/j.smim.2013.12.004.

[325] F. Seif, M. Khoshmirsafa, H. Aazami, M. Mohsenzadegan, G. Sedighi, M. Bahar, The role of JAK-STAT signaling pathway and its regulators in the fate of T helper cells, Cell Commun. Signal. 15 (2017) 23. doi:10.1186/s12964-017-0177-y.

[326] S. Taleb, A. Tedgui, Z. Mallat, IL-17 and Th17 cells in atherosclerosis: Subtle and contextual roles, Arterioscler. Thromb. Vasc. Biol. 35 (2015) 258–264. doi:10.1161/ATVBAHA.114.303567.

[327] F. Ilhan, S.T. Kalkanli, Atherosclerosis and the role of immune cells, World J. Clin. Cases. 3 (2015) 345–352. doi:10.12998/wjcc.v3.i4.345.

[328] Y. Fuchs, M. Brunwasser, S. Haif, J. Haddad, B. Shneyer, O. Goldshmidt-Tran, L. Korsensky, M. Abed, S. Zisman-Rozen, L. Koren, Y. Carmi, R. Apte, R.B. Yang, A. Orian, J. Bejar, D. Ron, Sef is an inhibitor of proinflammatory cytokine signaling, acting by cytoplasmic sequestration of NF-κB, Dev. Cell. 23 (2012) 611–623. doi:10.1016/j.devcel.2012.07.013.

[329] M. Mellett, P. Atzei, R. Bergin, A. Horgan, T. Floss, W. Wurst, J.J. Callanan, P.N. Moynagh, Orphan receptor IL-17RD regulates Toll-like receptor signalling via SEFIR/TIR interactions, Nat. Commun. 6 (2015) 6669. doi:10.1038/ncomms7669.

[330] Y. Hsu, W. Chen, C. Chan, C. Wu, Z. Sun, M. Chang, Anti – IL-20 monoclonal antibody inhibits the differentiation of osteoclasts and protects against osteoporotic bone loss, J. Exp. Med. 208 (2011) 1849–1861. doi:10.1084/jem.20102234.

[331] N.J. Logsdon, A. Deshpande, B.D. Harris, K.R. Rajashankar, M.R. Walter, Structural basis for receptor sharing and activation by interleukin-20 receptor-2 (IL-20R2) binding cytokines, Proc. Natl. Acad. Sci. 109 (2012) 12704–12709. doi:10.1073/pnas.1117551109.

[332] A. Sahoo, S.-H. Im, Molecular mechanisms governing IL-24 gene expression, Immune Netw. 12 (2012) 1–7. doi:10.4110/in.2012.12.1.1.

[333] C. Wahl, W. Müller, F. Leithäuser, G. Adler, F. Oswald, J. Reimann, R. Schirmbeck, A. Seier, J.M. Weiss, B. Prochnow, U.M. Wegenka, IL-20 receptor 2 signaling down-regulates antigen-specific T cell responses, J. Immunol. 182 (2009) 802–810. doi:10.4049/jimmunol.182.2.802.

[334] K.-M. Lee, H.-A. Kang, M. Park, H.-Y. Lee, M.-J. Song, K. Ko, J.-W. Oh, H.-S. Kang, Interleukin-24 suppresses the growth of vascular smooth muscle cells by inhibiting H(2)O(2)-

induced reactive oxygen species production, Pharmacology. 90 (2012) 332–41. doi:10.1159/000343242.

[335] K. Gabunia, A.B. Herman, M. Ray, S.E. Kelemen, R.N. England, R.D. La Cadena, W.J. Foster, K.J. Elliott, S. Eguchi, M. V. Autieri, Induction of MiR133a expression by IL-19 targets LDLRAP1 and reduces oxLDL uptake in VSMC, J. Mol. Cell. Cardiol. 105 (2017) 38–48. doi:10.1016/j.yjmcc.2017.02.005.

[336] A.A. Cuneo, D. Herrick, M. V. Autieri, Il-19 reduces VSMC activation by regulation of mRNA regulatory factor HuR and reduction of mRNA stability, J. Mol. Cell. Cardiol. 49 (2010) 647–654. doi:10.1016/j.yjmcc.2010.04.016.

[337] R. Maier, V. Ganu, M. Lotz, Interleukin-11, an inducible cytokine in human articular chondrocytes and synoviocytes, stimulates the production of the tissue inhibitor of metalloproteinases, J. Biol. Chem. 268 (1993) 21527–21532.

[338] M. Abdelnaseer, N. Elfayomi, E.H. Esmail, M.M. Kamal, A. Hamdy, R.M.A. Samie, E. Elsawy, Relationship between matrix metalloproteinase-9 and common carotid artery intima media thickness, Neurol. Sci. 37 (2016) 117–122. doi:10.1007/s10072-015-2358-z.

[339] Y. Takeuchi, S. Watanabe, G. Ishii, S. Takeda, K. Nakayama, S. Fukumoto, Y. Kaneta, D. Inoue, T. Matsumoto, K. Harigaya, T. Fujita, Interleukin-11 as a stimulatory factor for bone formation prevents bone loss with advancing age in mice, J. Biol. Chem. 277 (2002) 49011–49018. doi:10.1074/jbc.M207804200.

[340] K. Lian, C. Ma, C. Hao, Y. Li, N. Zhang, Y.H. Chen, S. Liu, TIPE3 protein promotes breast cancer metastasis through activating AKT and NF-κB signaling pathways, Oncotarget. 8 (2017) 48889–48904. doi:10.18632/oncotarget.16522.

[341] A.O. Kraaijeveld, S.C.A. de Jager, T.J.C. van Berkel, E.A.L. Biessen, J.W. Jukema, Chemokines and atherosclerotic plaque progression: towards therapeutic targeting?, Curr. Pharm. Des. 13 (2007) 1039–52. doi:10.2174/138161207780487584.

[342] E. Galkina, K. Ley, Immune and inflammatory mechanisms of atherosclerosis, Annu. Rev. Immunol. 27 (2009) 165–197. doi:10.1146/annurev.immunol.021908.132620.

[343] A. Schober, Chemokines in vascular dysfunction and remodeling, Arterioscler. Thromb. Vasc. Biol. 28 (2008) 1950–1959. doi:10.1161/ATVBAHA.107.161224.

[344] T.J. Schall, K. Bacon, K.J. Toy, D. V Goeddel, Selective attraction of monocytes and T lymphocytes of the memory phenotype by cytokine RANTES, Nature. 347 (1990) 669–671. doi:10.1038/347669a0.

[345] A.O. Kraaijeveld, S.C.A. De Jager, W.J. De Jager, B.J. Prakken, S.R. McColl, I. Haspels, H. Putter, T.J.C. Van Berkel, L. Nagelkerken, J.W. Jukema, E.A.L. Biessen, CC chemokine ligand-5 (CCL5/RANTES) and CC chemokine ligand-18 (CCL18/PARC) are specific markers of refractory unstable angina pectoris and are transiently raised during severe ischemic symptoms, Circulation. 116 (2007) 1931–1941. doi:10.1161/CIRCULATIONAHA.107.706986.

[346] R.R. Koenen, C. Weber, Therapeutic targeting of chemokine interactions in atherosclerosis, Nat. Rev. Drug Discov. 9 (2010) 141–153. doi:10.1038/nrd3048.

[347] X. Yu, Y. Huang, P. Collin-Osdoby, P. Osdoby, CCR1 chemokines promote the chemotactic recruitment, RANKL development, and motility of osteoclasts and are induced by inflammatory cytokines in osteoblasts, J Bone Min. Res. 19 (2004) 2065–2077. doi:10.1359/JBMR.040910.

[348] B. Peruzzi, A. Teti, The physiology and pathophysiology of the osteoclast, Clin. Rev. Bone Miner. Metab. 10 (2012) 71–97. doi:10.1007/s12018-011-9086-6.

[349] F.J. Mendoza, I. Lopez, A.M. De Oca, J. Perez, M. Rodriguez, E. Aguilera-Tejero, Metabolic acidosis inhibits soft tissue calcification in uremic rats, Kidney Int. 73 (2008) 407–414. doi:10.1038/sj.ki.5002646.